Thermoconvective Eddies in Air

Application to Meteorology

by

Dusan Avsec Ph.D.

Translated from the French by Carl A. Rönne.

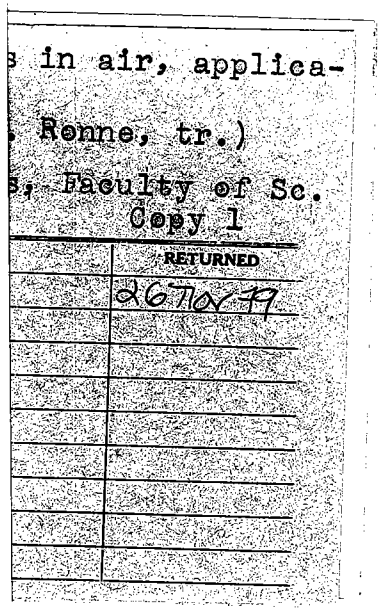

Scientific and Technical Publications of the Air Ministry

Works of the Institute of Fluid Mechanics

of the Faculty of Sciences at Paris

No. 155

Thermoconvective Eddies in Air

Application to Meteorology

by

Dusan Avsec Ph.D.

Preface by M. A. Foch

Professor at the Sorbonne

Director of the Fluid Mechanics Laboratory

This work obtainable in French at:

Ed. Blondel la Rougery
7, Rue Saint Lazare
Paris

Gauthier-Villars
55 Quaides
Grands-Augustins
Paris

1939

Translated by Carl A. Ronne

Preface

The work of Mr. D. Avsec relates to the ensemble of researches inaugurated in 1899 by H. Bénard, with his thesis on cellular eddies. Consecrated to a phenomenon which appeared to arise solely from the laboratory, this thesis has assumed in the space of twenty years an unquestioned importance for geophysics. The thermoconvective eddies which the young physicist discovered in liquid layers whose thickness was approximately a millimeter have been recognised by P. Idrac, reproduced in a scale almost one million times larger, in the foggy formations that render visible atmospheric movements. To be sure, the extrapolation has appeared justified; but it is precisely for the purpose of founding it upon an unquestionable basis that upon the request of H. Bénard, Mr. Avsec undertook the realization and study of eddies in bands in a scale one hundred times - (for want of better) - larger than that obtained in the researches of 1899.

The reader will appreciate the ingenuity and the patience of the experimenter which succeeded in obtaining organized circulations, the dimensions of which reach the decimeter; he will follow the mechanism of their appearing, their development and their evolution; he will see how, under the action of kinematic or of thermic perturbations there appear the instabilities of form which undulate and wind up the boundaries; finally, he will be able to consider the fashion in which the diverse hydrodynamic theories render account of experimental particulars.

In relation to the original edition, I must formulate a reproach: conceived under the form of a systematic exposé of the application of convective currents to phenomena in free atmosphere, it did

not make sufficiently evident all that the original work boasted of originality, as much in the experimental domain as in theoretical synthesis. I had to insist to Mr. Avsec that the chapter of conclusions be added where is found precisely set forth the personal contribution that the young and modest Yugoslavic savant was able to bring to the problem of cloud forms, that curious meteorological enigma wherein the laboratory reproduces so faithfully and so precisely all the appearances of reality.

A. Foch

Professor at the Sorbonne

Director of the Fluid Mechanics Laboratory

INTRODUCTION

The object of the present work is a study on thermoconvective eddies in a layer of air heated uniformly from below. Being given the importance that these eddies present in meteorological phenomena, we have tried to attain three principal objectives:

1 To realize systematic experiments on thermoconvective eddies in air under thicknesses exceeding considerably the scale generally employed by preceding experimenters;

2 To verify experimentally the practical value of the numerical results deriving from the theory of thermoconvective eddies;

3 To complete, by the results acquired in the course of

our researches in the laboratory, the theory of thermo-convective eddies in the free atmosphere.

Many experimenters have been concerned with the production of cellular eddies in a layer of air. Being given that in general the thickness of this layer did not exceed one centimeter, their researches related solely to the study of the geometric forms of the cellules as a function of the speed of translation and to the study of a few interesting transformations.

In order to deepen the study of these eddies, on the one hand, by observations of the mechanism of their appearing and of their development, and, on the other, by systematic measurements on the dimensions of the cellules and on the distribution of temperature, we have undertaken new researches at the Laboratory of Fluid Mechanics of the University of Paris, under the personal direction of Mr. Henri Bénard, and under the auspices of the Commission of Atmospheric Turbulence, presided over by Mr. Philippe Wehrlé, Director of the National Meteorological Office.

The execution of this program of work has necessitated the production of eddies of the largest size obtainable; the experiment has shown us that the uniformity of the general current in the experimental chamber and the uniformity of heating are the fundamental conditions for the production of big eddies.

Thanks to the careful and perfected construction of the eddy-producing apparatus, we have arrived at some handsome results,

the most interesting of which relate to the formation of eddies in longitudinal bands; we have obtained some using depths varying from 1 to 8 centimeters. But, if one wished to exceed the thinkness of 8 centimeters one would need to use a longer canal to improve the uniformity of the general current and to assure a sufficiently long duration of flow, indispensable to the complete development of large rolls.

Here now is the resumé of acquired results.
Having first succeeded in producing regular eddies in a layer of air several centimeters thick, we undertook the observation of the mechanism whereby the organized convective currents appear, and develop. Now - each one of the three principal species of eddies, that is, the polygonal cellular eddies, the eddies in longitudinal bands, and the eddies in transversal bands, has specific characteristics; the study of these characteristics has permitted us to make precise the classification, and to set forth in relief certain particularities.

For example, we have corrected the earlier conception on the origin of eddies in bands perpendicular to the general current. We think we have established that these bands result from two successive phenomena: first, formation of Helmholtz waves on the surface of the denser fluid layer; in the second place, appearance of convective currents that form in the hollow of two consecutive waves.

In the same category of researches lie the investigations on the intermediary forms and on the mutual transformations

of thermoconvective eddies. We have demonstrated by experiment that the polygonal cellules do not attain the hexagonal form except in a steady state and in a fluid layer the surface of which is, whether free (liquid), or whether easily deformable (a layer of air above a layer of dense smoke). If the fluid layer is limited by two plane and rigid sides the polygonal cellules arrange themselves in chains and finally transform themselves into vermicular bands.

It results from these same experiments that the criteria usually given as marking the transitions from one to the other type of eddy are not perfectly defined. That is the reason why it is not rare that two or three species of eddy appear simultaneously.

We have consecrated a special study to eddies in longitudinal bands with wavy sides. We have found that several distinct causes can contribute to provoke this undulation - as for instance:

1 The slowing up of the movement of translation of the ensemble of eddies in bands with rectilinear sides;

2 The interpolation of supplementary rolls provoked by an accidental or artificial perturbation;

3 The considerable augmentation of the difference of the extreme temperatures of the two surfaces.

For the sake of deepening the study of organized thermoconvective currents, it was indispensable to submit the theoretical results to the experimental control. We have thus studied:

1 The numerical value of the Rayleigh-Bénard criterion.

2 The distribution of temperature with the thickness and width of the fluid layer.

3 The thermic field following the rectangular section of the eddies in longitudinal bands.

4 The dimensions of polygonal eddies in bands.

5 The lines of flow inside the eddies.

As respects the Rayleigh-Bénard criterion, we have confirmed that the regime of thermoconvective currents is preceded by a stable preconvective regime. This fundamental result is in entire agreement with the previsions of the theory.

The conditions to the limits realized in our experiments not having been rigorously the same as those assumed, whether in the problem of Rayleigh, or in the problem of Jeffreys, the numerical value of this criterion differs from corresponding theoretical values. But it is necessary to underline that the numerical results of this class of experiment are not absolutely independent of the judgment of the experimenter who must decide on the moment when he determines the first ascending currents.

Thanks to the largeness of the eddies in longitudinal bands, we have been able to realize systematic measures of the distribution of temperature with the thickness and width of the ensemble of the rolls. Thus we give several characteristic diagrams which represent the temperature as a function of the side Z and of the abscissa X, the first directed vertically and the other perpendicular to the longitudinal bands. We have likewise managed to establish several varieties of the thermic field in the rectangular section of the eddies in longitudinal bands.

After having reduced the problem of the eddies in bands to

the study of the problem in two dimensions, we have undertaken a mathematical analysis of the distribution of temperatures. The confrontation between the theoretic results and the experimental measures makes proof of a quite complete agreement.

At the time of his first researches on cellular eddies in liquids, H. Bénard had shown that the ratio of the transversal dimensions and of the thickness h of the cellules is an essential characteristic of their geometric properties. That is the reason why we have undertaken an analogous work on eddies in gasses and in particular on the eddies in longitudinal bands, which constitute the most stable of all the classes.

The ratio λ/h has been in general, but not always, superior to 2. However, we have observed that the number of rolls has varied a bit from one experiment to another, and - in consequence, λ/h likewise. We have made a determined effort to seek to explain this variation of the number of the rolls in conditions apparently identical. We have demonstrated experimentally that these variations have been provoked by initial accidental perturbations. By provoking regular perturbations artificially whose amplitude exceeded the little accidental perturbations, we have obtained at will a number determined in advance of rolls, which enabled us to make the ratio λ/h vary from 1.25 to 5. But one should remark that the formations which correspond to the extreme values are not very stable. We have terminated this experimental study by a theoretical analysis of the variation of the ratio λ/h. From it, there has been shown that it is useless to search for a very great precision in geometric measures.

The study on the stream lines of the flow has also been conducted at the same time on the theoretical plane and on the experimental plane. Since the flow in the interiors of the eddies can be clarified by the study of the movement in two dimensions, we have been able to resolve analytically several particular cases.

In order to facilitate the study of the internal movement, we have completed the experiments realized in our big apparatus by a series of experiments upon two-dimensional cellular eddies contained in a flat vat with walls of glass very close together. This arrangement permitted us to observe and photograph the partitioning and the trajectories in the vertical plane.

A. R. Low, author of a mathematical analysis more general than the theory of Lord Rayleigh, has found that along with the simple solution admitting a single stage of eddies, there exist solutions which correspond to two or to several stages. We have shown that starting from the original theory of Jeffires one can arrive at the same result. We have developed the calculation of the Rayleigh-Bénard criterion for any number of superposed circulations, and finally we have calculated the values for the criterion Λ , as a function of perturbation Z and as a function of ψ for one and two stages of eddies.

To verify the practical value of this theoretic result, we have proceeded to the necessary experiments. In using the same flat vat, we have succeeded in producing two stages of eddies: the first constituted by the dense smoke, and the second by the pure air. If one could avoid the progressive diffusion of the

smoke, the staging of the cells (in layers) would be possible thanks to the different density of the two layers. But, one can never hope that permanent movements in two or even more stages can establish themselves practically, in a fluid homogeneous layer.

The practical interest in the cellular eddies of Bénard increased as soon as it was perceived that one could explain by their mechanism, different natural phenomena pertaining to the domains of metallurgy, chrystallography, structural geology (columns of basalt, structural soils of Northern and Alpine regions) oceanography (convective currents in the upper layer of the sea, rendered visible by algae gathered together in polygonal networks), astrophysics (lunar circles, granulations of the solar photosphere) etc. and also, meteorology.

Also we have been keeping as a special goal in our researches the object of contributing to the theory of convective organized currents in free air. One frequently observes in the sky superb cloud formations, representing all the geometric characteristics of thermoconvective eddies. It is to P. Idrac that the credit belongs of having demonstrated the existence in the atmosphere of organized thermoconvective currents, and, of having explained the large cloud rolls by the eddies in bands. This theory has been favorably received in the domain of meteorology: the English meteorologists were the first to contribute greatly to its development and its affirmation. In France, the Commission of Atmospheric Turbulence is actively pursuing

researches of that order and Mr. H. Bénard, who was directing the work concerning convective organized currents was good enough to confide to us a part of the researches.

In keeping account of all the preceding work and of the results acquired from our own experiments, we have consecrated Chapter XII entirely to the systematic exposition of the existing state of the theory of convective eddies in the terrestrial atmosphere.

One finds again in the category of the clouds in fragmented layers all the geometric forms of thermoconvective eddies. The clouds in polygonal and rectangular cellules do not permit the slightest doubt: both are of convective origin. On the contrary, if it is a question of clouds in transversal bands, one must not lose sight of a second theory, giving to this form of clouds a dynamic origin, seeing there the result of Helmholtz's atmospheric waves, which produced themselves at the separation-surface of two layers of air, each of them animated with a different speed.

But Sir G. T. Walker and A. C. Philipps have succeeded, in their experiments in the laboratory, in producing eddies in bands disposed perpendicularly to the speed of translation. That is why Walker considers that Helmholtz's clouds are produced very rarely, and, consequently, that the transversal bands must themselves be of thermoconvective origin. However, our experiments on eddies in bands give certain essential observations that can lead to the reconciliation of the theory of atmospheric waves, and of the

thermoconvective theory. We have, in effect, shown that the eddies in transversal bands are intimately bound to the simultaneous formation of waves of dynamic origin. In these conditions, the wave theory remains always valid, but one must complete it by the thermoconvective theory, should the call arise.

By the experiments on thermoconvective eddies in air saturated with water-vapor, we have thrown light on several facts in the study of compartmented clouds. We believe we can explain the mechanism whereby the compartmented clouds transform themselves into an extended cloudy layer and conversely. On the other hand, they show that the clouds in longitudinal bands are the result of the condensation of water-vapor between two eddying rolls, turning contrary to each other: hence, they place themselves in the regions where ascending currents are produced. As for the thickness of the cloudy layer, it is not necessarily equal to that occupied by the thermoconvective currents. In general it is smaller. Hence, the ratio of the distance of two cloudy bands and their thickness will exceed more or less the same ratio applied to the eddying rolls.

Since the Commission of Atmospheric Turbulence proposes likewise to undertake researches in flight on the convective currents, we thought it useful to give, at the end of Chap. XII, several directives which could guide future explorations in the free atmosphere.

To conclude, we remark that in the course of our researches on thermoconvective currents in a gas, it has appeared to us that

the physical causes of the formation of organized currents are not found to be defined exclusively by the thermic state of the atmosphere, but that it is equally possible to envisage movements having an electrical origin.

In 1936-37 we undertook in collaboration with Mr. Luntz, a series of experiments that have fully confirmed the presumed existence of cellular eddies of electrical origin. We have named them electroconvective eddies. The existence in the atmosphere of movements of electroconvective origin is, hence, very probable together with thermoconvective currents. It is legitimate to foresee equally the superposition of thermic convection and of electric convection. Meteorology will be led surely to orient its explorations towards this second domain.

*
* *

In terminating this work my greatest pleasure would be to be able to thank my regretted teacher, Mr. Henri Bénard, Director of the Laboratory of Fluid Mechanics and Professor at the Sorbonne, for the benevolent reception that he reserved for me in 1934 among his collaborators, and for his enlightened direction up to the beginning of 1939, when an unexpected death interrupted his scientific activity. In evoking his memory I must express to him under posthumous title, my most profound thanks for having signalized to me all the interest of this study and for having encouraged me tirelessly by his precious advices.

After the premature loss of Mr. Bénard, this could not be terminated but thanks to the support of Mr. Adrien Foch, present

Director of the Mechanical Laboratory of Fluids, and Professor at the Sorbonne, who has been good enough to take to his charge the scientific direction of my researches. I offer to him for his benevolence, and his aid in the perfecting of the present memorandum my most sincere thanks.

I owe the same respectful gratitude to Mr. Henri Villat, Member of the Institute and Director of the Mechanical Institute of the University of Paris, who kindly took interest in my researches and presented in my name several notes to the Academy of Sciences.

On another hand I must express all my gratitude to the Commission of Atmospheric Turbulence and in particular to its President, Mr. Philippe Wherlé, Director of the National Meteorological Office, and to Mr. Georges Dedebant, Chief of the Scientific Service of that office, to whom I am indebted that I have become Science Collaborator of the Air Ministry, and who have kindly placed upon the program of works that the Turbulence Commission pursues, my researches on the organized thermoconvective currents.

Be it also allowed me to tell all my gratitude to the Technical Service of Scientific Aeronautical Researches, and specially, to Mr. Paul Jouglard, Director of this service, and to Messrs. Paul Dupont and Pierre Vernotte, Chief Aeronautic Engineers who accorded to me the printing of this memoire in "Publications Scientifiques et Techniques du Ministère de l'Air".

Lastly, I must thank Messrs. E. Drussy, Laboratory Mechanician, and R. Fabre for the numerous services they rendered me during my sojourn at the Laboratory.

Chapter One (Sec.1)

Generalities on Convection Currents

Historical Outline

1. - Definition of Convection. Thermoconvective and Electroconvective Eddies. Work of Mr. H. Bénard.

One understands generally by convection the transmission of heat through a fluid mass by movements that present an appearance of organization, this word being taken in a very general sense. The notion of convection is, in reality, more general, for the object of the transport can as well be some form of energy, and even of matter. The most interesting category of convection is represented by the convective currents, where a part of the transported energy serves for their own maintenance. The convection of heat and electricity come in first place.

If certain conditions are realized, these currents manifest an admirable organization. The thermoconvective currents in a horizontal fluid layer heated uniformly from beneath, and the electroconvective currents in a fluid layer submitted to a very intense electrostatic field afford the two principal examples. The elements of organized convection, having the form of cellules, are named according to their physical origin: thermoconvective cellular eddies, christened briefly cellular eddies by H. Bénard (1) at the time of his first researches, and electroconvective cellular eddies, which we have recently discovered and described in collaboration with Mr. Luntz (2). Despite their similar morphologic and cinematic

characters, these two species of eddies have a profoundly different origin.

Only thermoconvective currents will be studied here, and quite particularly the cellular eddies in air.

The instabilities produced by differences of temperature in fluids when the lower layers are lighter than the upper layers, give rise in these latter, to particular movements which depend upon external conditions and interior properties of the fluids.

The simplest example of an organized circulation in water under the action of heat from beneath is given by the experiment of the English physicist James Tyndall, (1820 - 1893). When the water contained in a cylindrical container is heated from below, a permanent circulation is established. The hot water, being lighter, rises vertically, then it grows colder at the free surface, and becoming dense, descends along the sidewalls of the container. The behaviour of the trajectories, schematically represented by Fig. 1, depends principally upon the form of the container used.

We find a particularly interesting case when the fluid forms a thin layer unlimited in the horizontal, or at least, a layer of such an extent that the influence of the sidewalls no longer intervenes.

The first complete experimental study of this problem is due to Henri Bénard (1), who in 1899 - 1900 carried out researches, since become classic, upon thermoconvective currents in a layer of melted spermacetti oil. He worked out all the experimental and recording

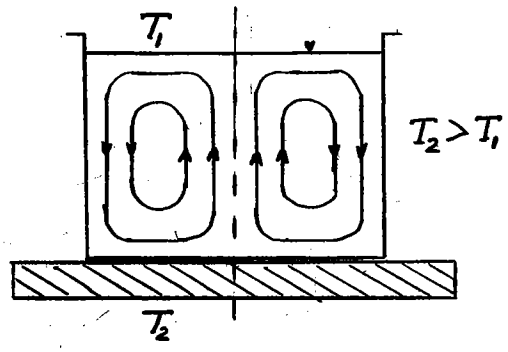

Fig. 1 - Circulation of liquid in a cylindrical receptable heated from beneath. (Tyndall, 1863)

techniques and he created the needed terminology. The christening of the phenominon "cellular eddies" has been most happy. The description of these eddies in a liquid layer propagating heat by convection, in a permanent regime, was so perfect that the ideas on this subject have not changed since. It is fitting, hence, to recount the principal results of these experiments, which are basic to all succeeding work.

When one heats uniformly from beneath a liquid layer, where one has incorporated aluminum powder, for instance, one observes the appearance on the free surface of a network of more or less regular polygones (Fig. 2 - see back) which tend toward the hexagonal form as to a regime-limit (Fig. 3 - see back).

In observing closely the particles of aluminum, one perceives the existence of a superficial movement, schematized by Figure 4. This movement is directed from the center of each polygon towards its contour. From this one deduces that the circulation and the surface polygonal division continue in depth. The vertical section

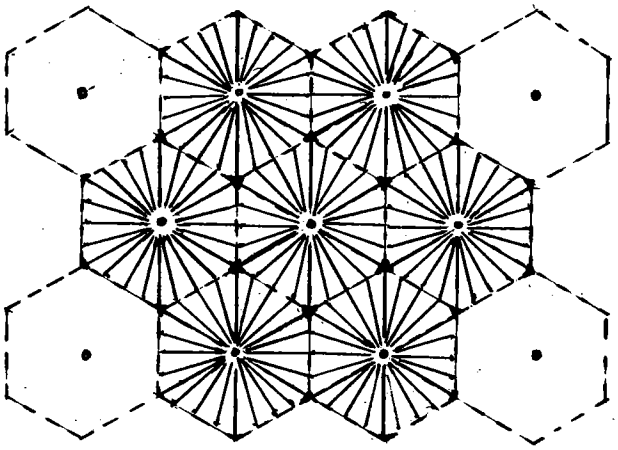

Fig. 4 Surface currents going from the center of each polygon (hexagon) towards its contour. Bénard.

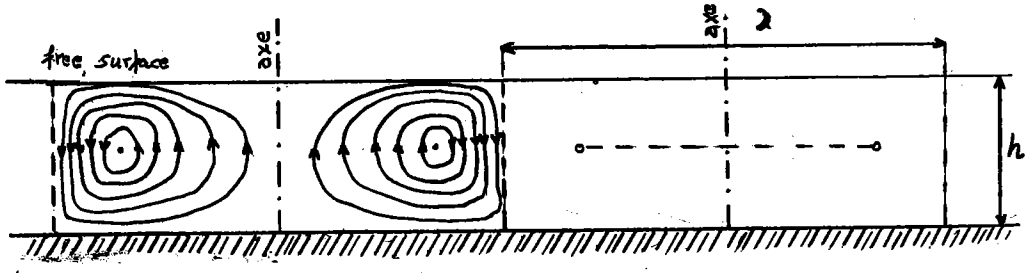

Fig. 4 Vertical section of Bénard's cellular eddies.

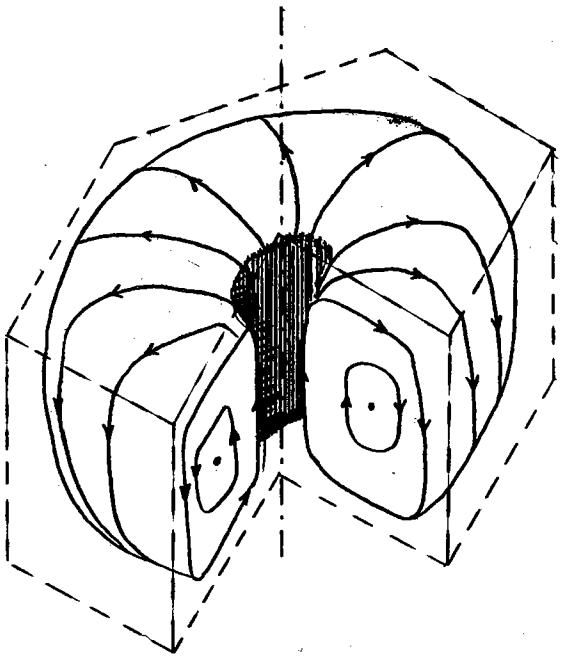

Fig. 5 Vertical section of Bénard's cellular eddies.

of the polygonal elements, that Bénard called cellules, is shown schematically on Figure 5. The internal circulation of a hexagonal cellule is given in perspective on Fig. 6.

To sum up, when a liquid layer is heated from below, it divides itself spontaneously into a great number of polygonal cellules, in the interior of which a permanent toroidal circulation establishes itself. This organization of the motion favors the transport of heat, which would be very weak if the propagation were carried out simply by conduction.

Experimental Researches Subsequent to the Work of H. Bénard

The experimental researches on cellular eddies of Mr. Bénard were actively pursued by C. Dauzère (3). He studied particularly the solidification of thermoconvective eddies, and its application to the cellular structure frequently realized in solid bodies. Using an amorphous material, for instance, white beeswax (pure or mixed with stearic acid or paraffine), he has shown that the solid plaque conserved, after solidification, the cellular structure. Each eddy leaves on the free surface a trace in the form of a circular relief. We reproduce in Fig. 7 (back) the photograph of the solidified cellules.

H. Bénard noted the great resemblance of the solidified eddies to lunar circles, and he suggested the idea that they would be the result of the solidification of gigantic eddies in the primitive lava. The mechanism of solidification becomes more complex when it is a question of crystallizable substances (nitrate of soda), for the currents of convection are disturbed by the formation of crystals. For details one should consult several notes by C. Dauzère to the C. R. of the Academy of Sciences and his thesis on Cellular Solidification (3-h).

Let us go on to the work of P. Idrac (4). During his numerous programs dedicated to the study of vertical atmospheric currents, he was led to express the hypothesis that the currents ascending and descending could be due to vertical instability, like the cellular eddies studied by H. Bénard.

To explain in detail the spatial periodicity of the ascending and descending currents, which manifest a sharply defined organization in gigantic rolls oriented in the direction of the general wind, he performed an experiment as simple as it was ingenious (4-C,e).

A layer of air, limited by two horizontal metal plaques close together and by two lateral sidewalls, is drawn along by a ventilator. The lower plaque rests on a bed of sand heated uniformly by rows of gas burners. The upper plaque is chilled by a bath of water. The injection of light smoke in the air in longitudinal movement makes visible the convective currents, which appear under the quite novel form of bands, with almost square section, stretched in the direction of the general current. The trajectories are a sort of screw. The direction of rotation in the interior of two adjacent bands is alternatively to right and to left. Consequently, if one traverses at right angles across the eddies in bands, one passes periodically through banks with currents ascending and descending. The mechanism of these eddies can, hence, account for the phenomenon observed in the atmosphere.

Several years after the fine experiment of P. Idrac, the Japanese physicists undertook the research of thermoconvective eddies. Certain experiments have been very original. T. Terada and his students (5) have produced in liquids eddies in bands having the same form as the eddies of Idrac in air. For their experiments they used pure alcohol, mixtures of alcohol and glycerine in various proportions, ether and water. In volatile

liquids, the vertical instabilities were provoked by the chilling of the surface of the layer slipping along a plaque slightly inclined. With liquids where the effect of evaporation did not suffice to produce vertical instability, the layer was heated from below.

Let us remember right now that experiments where one used a liquid layer in motion are not without precedent. In fact, H. Bénard (1-a) had observed a species of eddies intermediary between the polygonal cellules and the longitudinal bands: these are the eddies in chains. He obtained them by rocking lightly the rectangular vat containing melted spermaceti where the polygonal eddies formed themselves previously. The polygonal cellules take rectangular shape and align themselves in chains directed along the direction of the slope. (Fig. 8 - back).

A year after the experiments on eddies in bands in liquids, T. Terada and M. Tamano, undertook an analogous work with a layer of air (6). Their memorandum is very interesting, as it contains the description of the method of operation, a description neglected entirely by P. Idrac.

The exploration of thermoconvective eddies and the different phenomena that can be explained by their mechanism passed next to English meteorologists, physicists and mathematicians.

A. R. Low and D. Brunt in 1925 published an article (7) on the instability of the movements of viscous fluids. The first declares the hypothesis that the polygonal networks formed by rocks,

- a phenomenon widely distributed in northern regions, would be of convective origin. The author offers very sound reasons that could affirm the theory of cellular eddies for structural soils.

D. Brunt, for his part, evokes the special interest of Bénard for meteorology. The instabilities, analogous to those realized in a liquid layer less dense in its lower part, are frequently produced in the terrestrial atmosphere and can occasion the formation of little clouds, of a form comparable to that of the eddies of Bénard.

Low and Brunt completed their first communication by several articles (8, 15) in which, by reasoning and without recourse to personal experiment, the two authors have contributed largely to affirm the eddy theory in certain atmospheric phenomena.

Mr. S. Mal in 1930 published an important work upon segmented clouds (9). In comparing certain cloudy formations with the similar forms of thermoconvective eddies, the observer is tempted to suppose that the two phenomena have the same origin. In view of confirming this idea, S. Mal repeated the experiments of Benard and Terada in liquids. He found some intermediate forms between the polygonal cellules and the longitudinal bands. They resemble tiles and rectangles, structures equally observable in clouds. S. Mal next gave the analysis of the direct measures of the temperature, of the pressure and of the humidity, obtained by the aid of sounding-balloons and in the course of several airplane ascents at the moment when the clouds in question were present. We leave the examination of these results for the end of our

memorandum (Chap. XII: Application to Meteorology).

Sir G. T. Walker in collaboration with A. C. Phillips continued the investigations (10). His work had as its object to show that the clouds in bands perpendicular to the wind-direction could be also of thermoconvective origin, a cloud-formation explained up to that time as Helmholtz's Atmospheric Waves. The two authors re-undertook the experiments of S. Mal, using a paraffine solution in automobile oil in equal proportions. They rediscovered the forms already known. All attempts to produce transversal bands having remained vain, they proceeded to experiments with air, in an apparatus similar to that of P. Idrac. The maximum thickness of the layer of air was fixed at 6 mm. Attempts with tobacco smoke having given negative results, tetracloride of titanium was selected as indicator of the convective currents. The results were conclusive. One obtained eddies in transversal bands together with all the other usual forms in liquids. Sir G. T. Walker draws from it the conclusion that the clouds in transversal bands can as well be of thermal convective origin as can the clouds in longitudinal bands. Hence, the theory of atmospheric waves can not be applied without precautions. One must examine each case in particular to know to what category it belongs.

Sir G. T. Walker points out at the end of the memorandum that the conditions realized in the experiments have not been identical with those realized in free air. The sidewalls of the experimental chamber being fixed, the current of air is reined in by the two horizontal plaques, in such fashion that the distribution

of horizontal speeds along the vertical is parabolic (it is the problem of the flow of viscous fluids between two parallel plaques in close proximity to each other). On the contrary, in free atmosphere (as well as in the experiments done in liquids whose surface may remain free) it is a question of a single surface of contact which divides the layer of air from the cloud layer. The distribution of speeds along the vertical would be approximately linear. This author has hence suggested to A. Graham (11) to undertake experiments in a layer of air where the distribution of speeds along the vertical line would be linear. To realize this essential condition, A. Graham constructed an experimental chamber of which the upper wall, consisting of a long glass plaque, was movable. He reproduced all the forms that Walker and Phillips had obtained in a chamber with fixed walls.

Sir G. I. Walker (12) has resumed and analyzed over and again all the analogous work carried out by the researchers belonging to the English school, adding also the needed supplements.

The works that we have just enumerated above pertain, of course, to two categories. In the first are laboratory experiments studying the phenomenon from a purely physical viewpoint, in the second are the works seeking to explain the different natural phenomina by the mechanism of cellular eddies. Amongst these last the works that interest meteorology are the most numerous.

The present memo being in the first place a contribution to the question of vertical instabilities in the atmosphere, we have not shown the numerous works relating to crystallography and

metallography, to geology, oceanography and astrophysics.

Together with the experimental researches there exist the mathematical studies of Lord Rayleigh (13), of H. Jeffries (14), of A. R. Low (15), and of P. Vernotte (16). For the moment, we omit their analyses because we shall discuss the principles of the theory in Chapter VI.

In France, since 1935, a great activity reigns to try to elucidate the origin of the different atmospheric phenomena. For the sake of actively pushing the study of these problems, a special commission entitled Commission of Atmospheric Turbulence was created at the Air Ministry under the presidency of Mr. Ph. Wehrlé, Director of the National Meteorological Office. In the vast general program, elaborated by this Commission, figure in particular the researches on organized convective currents, the direction of which had been confided to Mr. H. Bénard, Director of the Laboratory of Fluid Mechanics of the U. of Paris, a savant renowned for his works on cellular eddies of thermoconvective origin. Mr. Bénard was good enough to do us the honor of charging us with the execution of part of the laboratory researches on thermoconvective eddies in a layer of air heated from below.

Before beginning the exposé of our results, we think we should point out that during the period when we carried out the present work, several of our colleagues at the Laboratory of Fluid Mechanics have either completed or are still pursuing very interesting works pertaining to the domain of convection currents.

Let us mention first the work of Mr. V. Volkovisky (17-b,c,d)

on thermoconvective eddies in liquids. In the theoretical part, the author studies convection in a viscous fluid by the aid of Boussinesq equations. In particular, he develops the case of steady movement in two dimensions and treats the problem of vertical trajectories by giving a formula for the speed for the whole length of such a jet. The author insists that the method employed by Lord Rayleigh, H. Jeffries, and A. R. Low in the study of fluid layer subjected to a reversed gradient of temperature has a too specialized character, and he gives a generalization of the notion of the criterion of stability. In the experimental part, Volkovisky communicates a great number of quantitative data on the secondary phenomena of convection, accompanying the formation of eddies in bands in liquids. His study on the influence of the viscosity and speed of the liquid layer on the ratio λ/h is carefully developed. As for the other interesting questions, we can do no better than to direct the reader to the original work of Mr. Volkovisky.

Mr. G. Sartory (18) is now at work on the thermoconvective currents that produce themselves above a region uniformly heated by radiation. These experiments interest particularly the meteorologist, for on one hand, heating by radiation reproduces faithfully what happens in the free air, and, on the other hand, the phenomenon is studied on a very large scale. (The experimental chamber is one meter high.)

Mr. V. Romanovsky (19), on his part, is busy upon thermoconvective eddies in muds. This experimental work is a development of the experiments initiated in 1933 by the Japanese physicist

Y. Hudino (1) and German geologist K. Gripp. Its object would be to buttress solidly the thermoconvective theory of structural soils, quite common in northern regions and in alpine sites, a theory first advanced by A. R. Low and D. Brunt (7).

Finally, along with these principal works, we must point out two isolated experiments, one, that of V. Volkovisky (17-a) on eddies in festoons in liquids, the other that of Mr. Luntz (20) on alternating thermoconvective eddies in a thin liquid layer.

Chapter II

Vertical Instabilities in Fluid Layers: Onset of Organized Motions

1. Fluid layers of different densities superposed one over the other.

Vertical Instability. - The simplest example of vertical instability is furnished by a system of two fluid layers the denser of which is placed above the other. To fix our ideas, let us consider a layer of water of thickness h_1, superposed on a layer of oil of thickness h_2. This system, which we will designate by I, is found to be in unstable equilibrium, for the density of the water ρ_1 is greater than that of the oil ρ_2. But since the resultant of external forces acting upon the volume of the lighter liquid is nulle, the system I could continue indefinitely if exterior perturbations could be avoided.

One determines immediately that the lower layer is not submitted to a vertical force. Let us define the resultant of the surface and volume forces that acts upon a cylindrical volume cut in the layer of oil, the circular section of which is equal to unity and of which the height is h_2. The horizontal components X and Y, which result uniquely from the surface forces, are nulle. Consequently, the resultant of the forces to which the considered volume is submitted is identical to the vertical component Z.

In designating by p_1 the pressure at the surface of separation of the two fluid layers and by p_2 the pressure on the bottom, this resultant is expressed by:

$$R = Z = p_2 - p_1 - g \rho_2 h_2,$$

where

$$p_2 = p_1 + g \rho_2 h_2,$$

and in consequence:

$$R = 0, \quad \text{q.e.d.}$$

One demonstrates equally that system I is in unstable equilibrium. The potential energy accumulated in the vertical column having a height $h_1 + h_2$ and whose section is equal to unity, and calculated in relation to the bottom of the container, is equal to:

$$\mathcal{P}_I = g \rho_1 h_1 (\tfrac{1}{2} h_1 + h_2) + \tfrac{1}{2} g \rho_2 h_2^2 = g(\tfrac{1}{2} \rho_1 h_1^2 + \rho_1 h_1 h_2 + \tfrac{1}{2} \rho_2 h_2^2).$$

If the two liquids interchange their places, the potential energy of the new system II becomes:

$$\mathcal{P}_{II} = g(\tfrac{1}{2} \rho_2 h_2^2 + \rho_2 h_1 h_2 + \tfrac{1}{2} \rho_1 h_1^2).$$

The density ρ_1 is by definition greater than ρ_2, hence the difference:

$$\mathcal{P}_I - \mathcal{P}_{II} = g\, h_1\, h_2 (\rho_1 - \rho_2) > 0,$$

and:

$$\mathcal{P}_I > \mathcal{P}_{II}.$$

System II is in stable equilibrium, for the potential energy $\mathcal{P}_{II}$ is minimum. All the others, and in particular system I where $\mathcal{P}_I$ is maximum, are in unstable equilibrium.

The onset of the motion - A perturbation of some sort is needed if the two liquids of system I are to change their positions. But, it is impossible to foresee the kinematic mechanism by which a movement once released comes to rest at its steadiest state of equilibrium. We had recourse to an experiment the initial conditions of which are the simplest.

A flat container whose sidewalls are composed of two sheets of glass 15 mm apart, contains in equal proportions water and oil called Spidoléine B.R. These two liquids are cleanly separated and are found in stable equilibrium. The container being sealed hermetically, one can revolve it brusquely on its longitudinal axis: the oil takes its place on top of the water. Fig. 9.

This system which we have designated by I, persists in unstable equilibrium for a few instants. Soon after, the surface of separation of the two liquids becomes lightly undulated Fig. 9-b. The amplitude of undulation increases rapidly, and the two liquids bury themselves progressively the one into the other Fig. 9-c. There comes a moment when the tops of the waves of the layer of oil touch the ceiling: the mass of water is cut into isolated compartments, which take the form of large drops Fig. 9-d. Once they reach the bottom of the container they flatten themselves and push up the threads of oil towards the top, Fig. 9-e. Finally, all the mass of the oil has passed into the upper level and the system of superposed layers has become stable, Fig. 9-f. One will notice that in general the volume occupied by the water is not superposable upon the volume occupied by the oil at the same instant.

This example gives a preliminary idea of the organization of the motions released in the fluids as a consequence of vertical instability. One understands, of course, that the movement halts as soon as the layers have changed their positions.

A more detailed study would be very interesting. It would be fitting to try different liquids that do not mix, for it is certain that the form of the surface of discontinuity depends essentially on

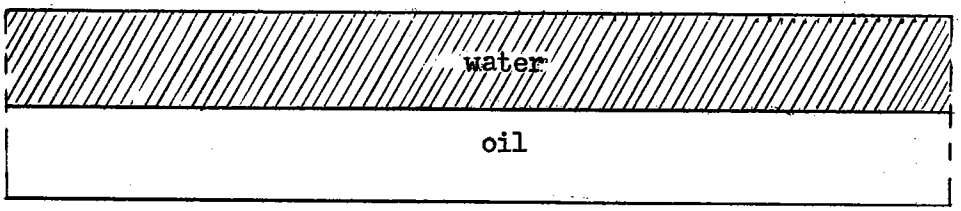

Fig. 9-a

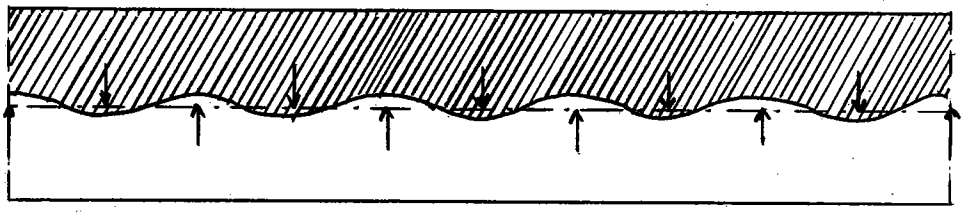

Fig. 9-b

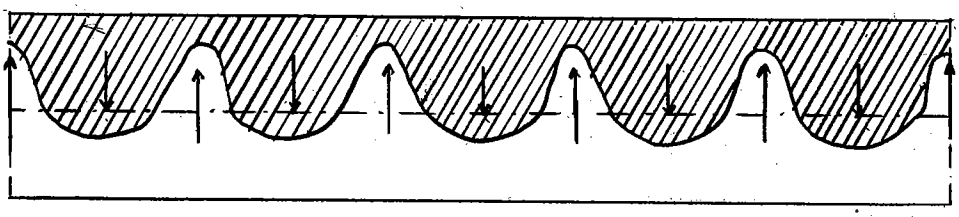

Fig. 9-c

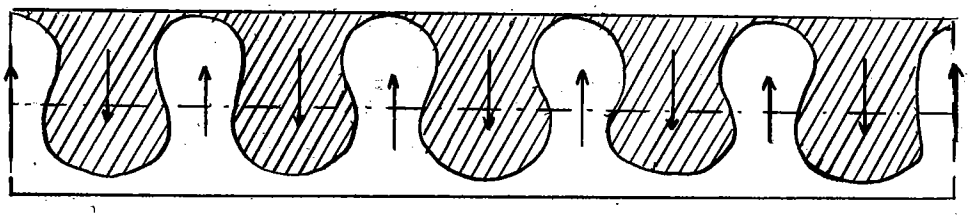

Fig. 9-d

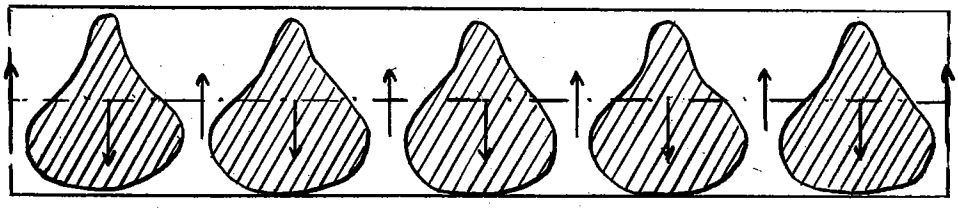

Fig. 9-e

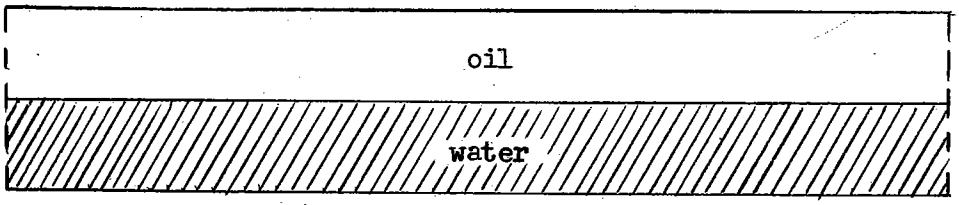

Fig. 9-f

Figs. 9-a, 9-b, 9-c, 9-d, 9-e, 9-f. A few characteristic phases in the overturn of a double layer of oil and water.

the viscosity and surface tension of the liquids employed. In fact, if one could find two liquids of equal viscosity and of different densities, it would not be impossible that at any instant the volume occupied by the water is exactly superposable upon the volume occupied by the oil. Next, one could envisage the same experiments with the liquids in different proportions, and above all, experiments in extended horizontal layers.

2. Fluid layer the density of which varies continually in the vertical.

This is the case of a horizontal fluid layer whose limiting surfaces are maintained at two constant temperatures, the higher temperature being beneath. Let us suppose that the temperature diminishes linearly with the depth of the layer. The corresponding distribution of densities, hence, is inverse: the denser layers are overlain upon the less dense ones. If the isotherms coincide with the equipotential surfaces, the system finds itself in unstable equilibrium. The demonstration that the vertical force is nulle, is the same as in the preceding case for two liquid layers of unequal densities.

Let us calculate the difference of energies of the two systems I and II, accumulated in the vertical fluid column the height of which h is equal to the thickness of the layer and of which the section is unity.

The elementary energy in the system I is written:

$$d\mathfrak{T}_1 = gzdm = gz\rho_1 dz,$$

where: $$\rho_1 = f(z) = \rho_2 + \frac{\rho_1 - \rho_2}{h} z;$$

by integration one obtains the total energy:

$$\mathcal{T}_1 = g\int^h z(\rho_2 + \frac{\rho_1-\rho_2}{h} z)dz = gh^2(\frac{1}{3}\rho_1 + \frac{1}{6}\rho_2).$$

If one changes the indices, one finds the potential energy of the stable regime, calculated relative to the bottom:

$$\mathcal{T}_{II} = gh^2(\frac{1}{3}\rho_2 + \frac{1}{6}\rho_1).$$

The difference:

$$\mathcal{T} = \mathcal{T}_1 - \mathcal{T}_{II} = \frac{1}{6} gh^2(\rho_1 - \rho_2) > 0,$$

is hence the usable energy: it can be transformed partially into kinetic energy. In fact, an accidental disturbance releases motions impossible to predict in advance and which assure the exchange of places between the warm and the cold masses.

If the sidewalls were not conductors, these motions would die away after the less dense layers were on top. On the contrary, the motion does not stop if the bottom is a good conductor and uniformly heated, for the descending cold mass reheats itaelf and the ascending warm mass rechills itself continually. Hence, it is the source of heat that furnishes the energy necessary to the maintenance of the motions.

The forms of the thermoconvective currents, whose appearance is evident, can not be established except experimentally. We shall see that they are very various and that they depend essentially on the conditions at the boundaries.

Let us commence by the case of two-dimensional eddies which is the basis for all the others (21-e).

3. Thermoconvective currents of two dimensions in a layer of air.

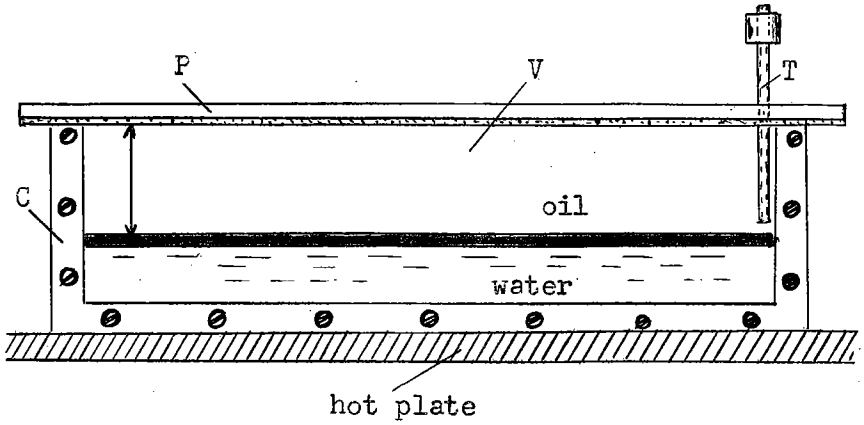

Fig. 10 Narrow tank for spontaneous production of cellular eddies of two dimensions.

A flat container (Fig. 10) (320x83x15 mm) in a vertical position, consists of a metal frame C in the shape of a U, and two sidewalls V of glass, 15 mm apart. One pours to the bottom of the container a layer of water. Another thin layer of oil prevents the evaporation of the water. The level of this layer fixes the height h of the upper air layer. The container is sealed hermetically by the ceiling P and placed on a uniformly heated plaque.

Next, one introduces by the tube T, which traverses the lid and comes down almost to the level of the layer of oil, a small amount of tobacco smoke. It fills the bottom and remains several moments cleanly separated from the layer of pure air above it Fig. 11a (back). A little later one observes slight depressions

on the surface of the layer of smoke. That indicates that the thermoconvective currents are developing in the midst of the layer of air. These currents accumulate the smoke in crests with sharp points that coincide with the centers of ascension Fig. 11-b (back). This smoke is drawn by the eddy-movement. The filament of smoke makes visible the currents that are particularly organized. The ascending currents, distributed at the moment of their birth somewhat haphazardly, bump themselves against the ceiling of the container where they bifurcate and redescend. One obtains in this way permanent organized currents in fictitious compartments called cellules. Each cellule carries an eddy-core whose axis is perpendicular to the sidewalls of the container. The direction of rotation of the eddies is alternatively to left and to right.

The ascending currents oscillate and seek a more stable position. The Figure 11-c, taken a few instants after Figure 11-b, represents a more stable phase. The smoke diffuses itself progressively in the cellules. On the Figure 11-d, one sees only a few traces of concentrated smoke, which soon disappear entirely. This final phase is reproduced in Figure 11-e. The cellules are completely rectangular. The six cellular eddies at the center are almost equal; the two lateral ones are wider by reason of special conditions occasioned by the sidewalls.

Knowledge of thermoconvective eddies in two dimensions will facilitate the description of other forms that are produced in a horizontal sheet of air.

4. Experiments in humid air.

We have also undertaken a series of experiments on thermo-convective eddies the conditions of which more closely approach those frequently realized in free air: instead of operating in dry air, we have had recourse to air saturated with water vapor (21-g).

These experiments were done with the flat container which served for the experiments in dry air. But the surface of the layer of water was left free so that evaporation could come about. After closing the cover of the container hermetically, we put it on a heating surface.

In a few moments little foggy smudges, regularly spaced, appeared on the glass. The first photograph, Fig. 12-a, taken during an experiment when the height of the layer of air was 62 mm, represents such a formation. One sees there three lenticular smudges, disposed on the upper half of the container along a horizontal line. The island in the centre is prolonged towards the base by a transparent trace, the origin of which we will presently show.

If the heat is moderate, the smudges reach a size-limit that can maintain itself for hours. On the contrary, with more active heat, they grow progressively larger and finish by uniting themselves in a single opaque band.

The second photograph, Fig. 12-b, taken 30 minutes after the first, gives the final phase. One still sees the three lenticular elements. (Fig. 12 in back).

The explanation of this phenomenon is as follows: In the

layer of air there form cellular eddies of two dimensions the description of which has been already given. The ascending currents carry off the water vapor which comes by evaporation from the surface of the liquid. The upper portion of the chamber being colder, the water vapor condenses in fine droplets. Those which circulate close to the walls of the container cling to them and form opaque smudges (see Fig. 12-a). Thanks to the continual eddy-movement, the deposits of condensed vapor accumulate. The droplets grow larger by coalescence. The strongest condensation is produced at the places that coincide with the ascending currents, where the air in eddy-movement is the wettest. It becomes dry progressively in the course of its circulation. When it returns to the surface of the water, it recharges itself with vapor.

Figure 12-b shows that the largest drops are formed in the midst of the central smudge. As soon as the drops are heavy enough, they slip towards the base. (The two lateral smudges have a special character, due to the presence of metal sidewalls left and right.

We have drawn on the same photograph the eddy-cellules and shown the direction of circulation. The two cellules at the center are perfectly square ($\lambda/h = 2$).

Two series of photographs reproduce the development of the foggy smudges. The first series corresponds to an experiment where the thickness h of the layer of air was 49 mm and the difference of the two extreme temperatures 4.6°C (T_1 = 38.2°C; T_2 = 33.6°C), and the second (corresponds) to an experiment where h was fixed at 41 mm and the difference of the temperatures at 11.9°C (T_1=48.5°C; T_2=36.6°C).

(Figs. 13 and 14 in back).

First experiment with Moderate Heat. (Fig. 13)

First phase (2 minutes after setting the experiment in operation): Four smudges slightly foggy appear. The two at the centre have the form of a mushroom, and the two at the sides the form of a lentil.

Second phase (8 minutes after the first phase): The lateral lentils and the mushrooms in the middle have developed considerably.

Third phase (20 minutes after the second phase): The contours of vapor condensation have become very neat and the caps of the mushrooms have attained the size of the lateral lentils. Also, the structure has changed: one sees the appearance of droplets resulting from the incessant condensation of the vapor.

Fourth phase (25 minutes after the third phase): The shape and size of the condensations have not changed, but the droplets have grown bigger, especially in the regions forming the nodes of these condensations.

Fifth phase (1 hour and ten minutes after the fourth phase): The condensations of vapor have visibly reached the limit of their development. The drops are heavy and they slide towards the base.

One remarks on the three last photographs that the surfaces wetted by the condensed vapor are superposable to the surface that remained dry (with the exception of a part at the left and right, influenced by the edges of the container).

Second Experiment with stronger heating (Fig. 14).

First phase (1 minute after setting the experiment in operation): Two small foggy smudges appear in the central region. There are also scarcely visible traces of two lateral smudges.

Second phase (10 minutes after the first phase): The four lenticular smudges occupying the upper half of the container are much larger. The two central lentils have reached out towards the base by less foggy traces.

Third phase (15 minutes after the second phase): The opaque smudges have become larger and more defined. One sees that the two central smudges take successively the form of a mushroom, a shape, by the way, that was neater in the preceding experiment.

Fourth phase (20 minutes after the third phase): The lentils have reached out. They are separated one from the other by very narrow spaces. The structure of the droplets reappears, especially at the places that coincide with ascending currents.

Fifth phase (20 minutes after the fourth phase): The individual smudges have run together in a single opaque band occupying the upper half of the container. However, one can still detect the eddy-elements. The ascending currents are marked by vertical regions, rich in thick drops of condensed vapor.

One hour afterward, the form has in nowise changed. The fifth phase constitutes the final phase.

The method of visualization by condensation of water vapor allows one to establish the centers of the ascending currents (concentration of drops) and descending (currents) (spaces separating the individual foggy smudges). It gives hence the number and the transversal dimensions of cellules.

Moreover, the results that arise from these experiments clarify certain essential facts in the phenomenon of compartmented clouds. But this method and the conclusions derived from it are recounted at the end of this memo, where we will speak of the applications of the theory of convective currents to meteorology.

Chapter III

Description of Apparatus used in Production of Thermoconvective Eddies in a Horizontal Layer of Air. Method of Operation.

1. Preliminary Remarks

The greater part of the experiments on convection currents in air had been carried out by meteorologists. Their work had for its unique object, to show the geometric similitude of thermoconvective eddies obtained in laboratory experiments, with certain cloud formations, and to conclude from them that compartmented clouds are of the same physical origin as cellular eddies. In these conditions, a vast domain of investigations remained still open to physicists and meteorologists.

One might first complete the observations and the qualitative results by varying the thickness of the layer of air by the largest interval possible and by going on to quantitative measures, which, it seems, have been completely neglected.

All the experimenters noted that the regular forms ceased to appear as soon as they attempted to give the layer of air a thickness exceeding 1 cm. But in a layer of too small a thickness, the distribution of temperature becomes hard to determine, because the introduction of an instrument, however small, risks disturbing or even destroying the regular internal movements of the cellular eddies.

It is principally for this reason that from the start we determined to produce thermoconvective eddies in a layer of air having a thickness of several centimeters - an attempt that proved quite successful (21-a).

It first was necessary to determine the causes potentially able to prevent the production of large cellular eddies in thick layers.

According to the general theory on thermoconvective currents in a horizontal fluid layer, a theory we shall set forth further on, the difference of extreme temperatures needed for the release and maintenance of the eddy-currents varies inversely with the third power (cube) of the thickness h. In other words, when the fluid layer becomes thick, a very slight difference of extreme densities (which is to say, a very slight difference of temperatures) suffices to maintain the system of cellular eddies.

A quite uniform heating and chilling of the two limiting surfaces is the essential condition if the cellules are to be regular. It is very hard to bring about this uniformity when we deal with a thick layer, because the slightest local excess of temperature can provoke considerable irregularities. Production of big eddies, then, depends on the precision of the construction of the apparatus. It is needful, hence, to assure there, (in the apparatus) the uniformity of temperatures of the two limiting plaques and the uniformity of the general movement of the fluid sheet.

2. Description of apparatus used in production of thermoconvective eddies in air.

The greatest care was exercised in constructing the apparatus for producing thermoconvective eddies in a horizontal layer of air.

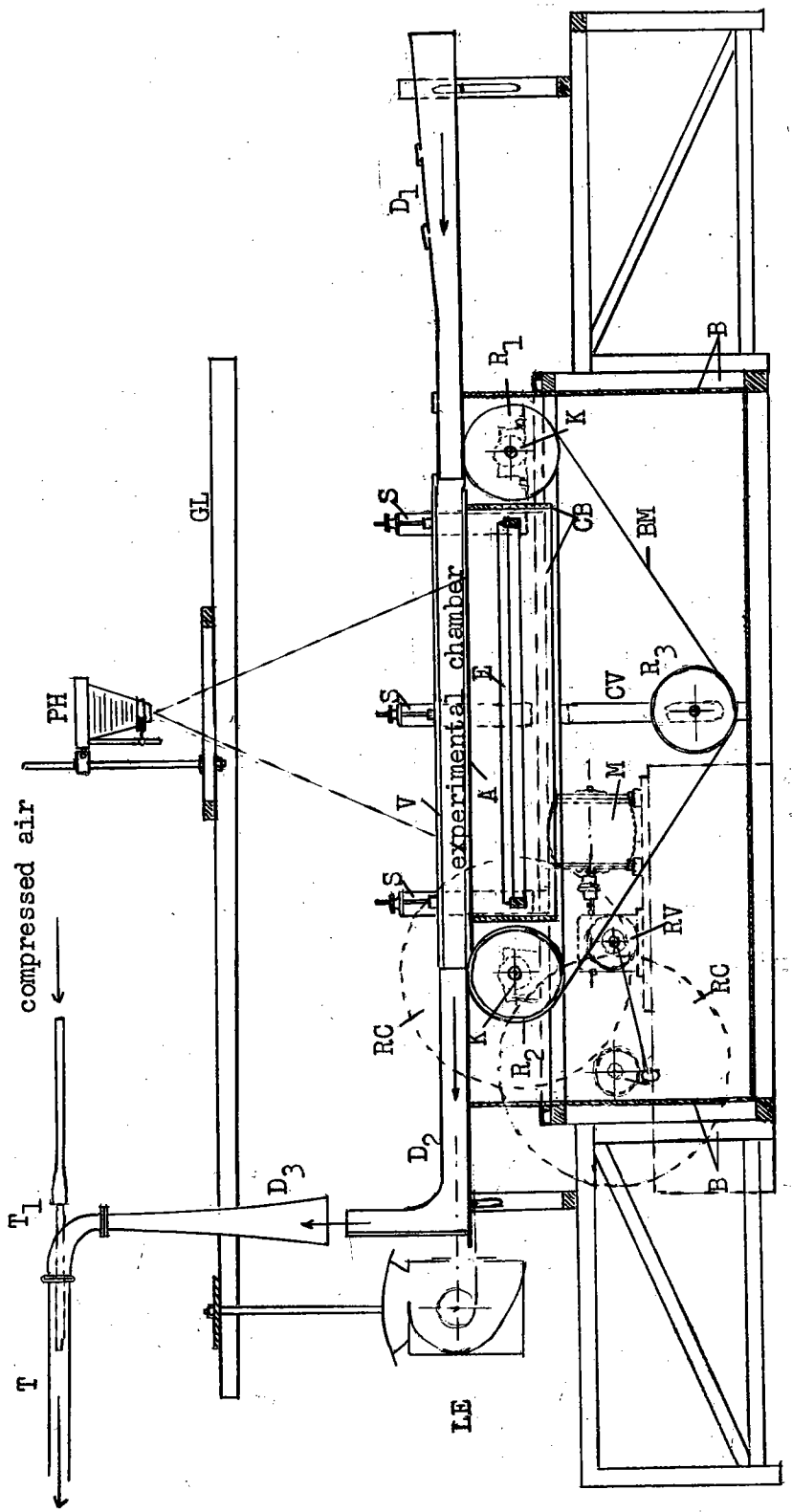

Fig. 15 Longitudinal cut of apparatus producing thermoconvective eddies in gasses.

Two principal cuts (longitudinal and transversal) and a plane view shown in Figs. 15, 16, and 17, represent a construction offering notable improvements upon the invention of A. Graham(11). A steel plate A (length 130 cm; width 50 cm; thickness 1 cm) constitutes the lower heating surface of the experimental chamber. This plate rests on a frame of wood CB that surrounds the electric heater E. The inside of this frame is sheathed with asbestos and one of its sides is removable, so as to give easy access to the heater. The entire thing is placed on a framework of wood B, x-framed and of plywood.

At each end of the steel plate, two rollers R_1 and R_2, of a diameter of 20 cm and a length of 50 cm, are mounted on the four bolted arborbearing plates K. The common tangent of the two cylinders which are coated with soft rubber touches exactly the surface of the steel plate. The rollers R_1 and R_2 serve for the transmission of a metal band BM, which then slides very exactly over the steel plate. This band, with a thickness 0.2 mm, in duraluminum, is actually hooked into an endless metal ribbon 3.8 m long. To keep the tension up on this ribbon, there is a third roller of 50 kg, R_3, the axle of which is guided by two vertical slides CV.

A metal frame, self-soldered (welded) is fixed by bolts to the upper part of the wood framework. It is provided to receive the four arborbearing plates. Fig. 16. The method of fastening the arborplates allows an adjustment of the rollers R_1 and R_2, so as to obtain both parallelism of their axes and their horizontality.

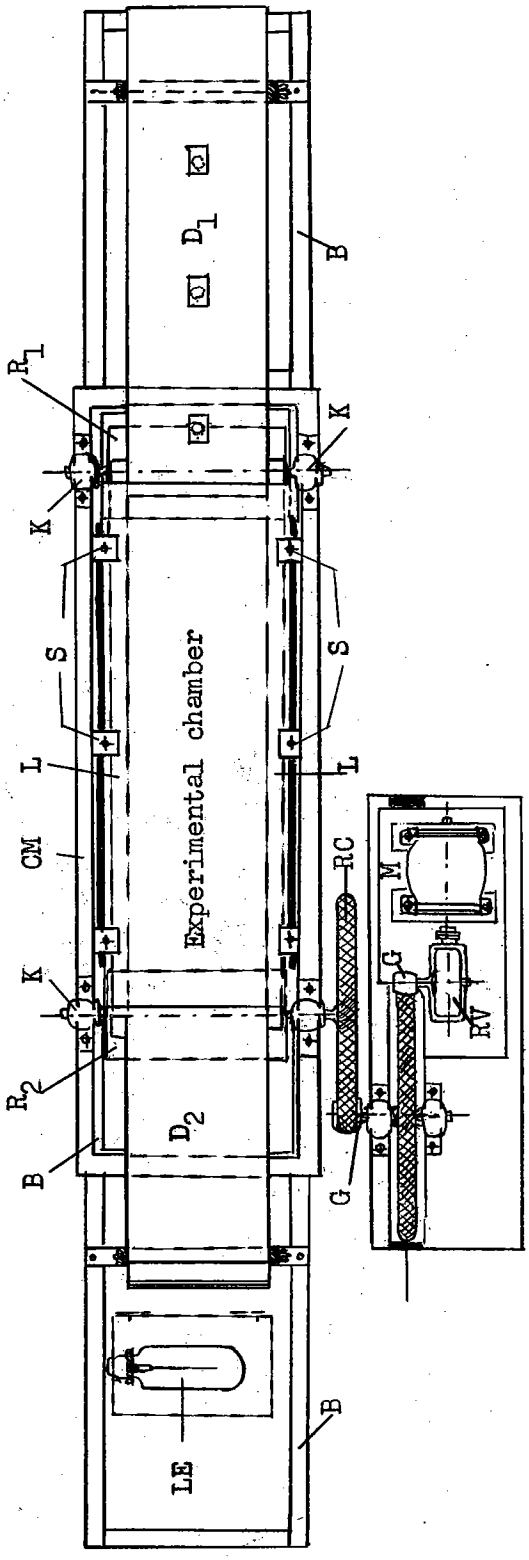

Fig. 16. View from above of apparatus producing thermoconvective eddies in gasses.

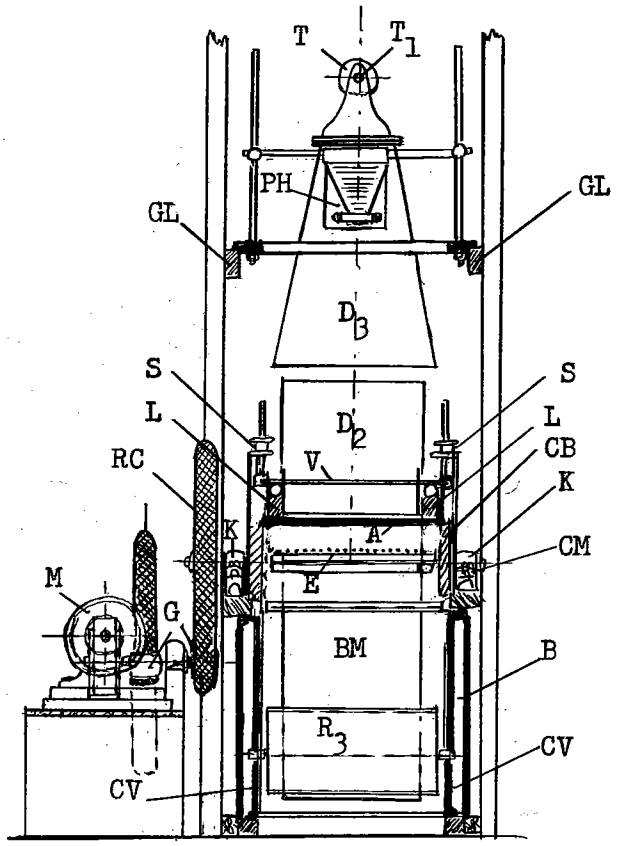

Fig. 17 Transverse cut of apparatus producing thermoconvective eddies in gasses.

The ceiling of the experiment-chamber is made of a plate of glass V of dimensions equal to those of the steel plate. By displacing the ceiling V by means of six supports S placed at each side of the experiment chamber, one can create various thickness for the layer of air from 3 to 180 mm. The sidewalls of the canal are made of two bands of wood L. Two long rubber tubes engaged between these sidebands and the ceiling assure hermetic closure. By pumping up the tubes as desired the system adapts

itself to all thicknesses, and also permits one to vary the width of the canal. The tubes alone (empty) were utilized for thickness less than 2 cm. To assure in the canal the regularity of the general movement, and to avoid perturbations at the moment of injection of the smoke, destined to make visible the eddy-movements, the experimental chamber is prolonged fore and aft by the canals D_1 and D_2, built of plywood. Their extremities can easily be accomodated to the section of the experimental chamber. The canal D_2 is turned up. A window fitted in the elbow of canal D_2, permits illuminating the experimental chamber in the direction of its longitudinal axis.

The general drawing-along of the layer of air is assured whether by the metal band BM in motion, or by the aspirator at the mouth of canal D_2. The aspirating arrangement is made of a collector D_3, mounted in a vertical position. Its end, near the mouth of the canal, has a width of 50 cm which diminishes towards the top. A flexible tube T adapts itself to the square section of the collector by means of a suitably fitted metal piece. The other rubber tube T_1, ending inside tube T, brings compressed air. One obtains a uniform and adjustable flow of the air in the canal by simple throttle adjustment of the compressed air, or by adjusting the position of the collector D_3.

A direct-current motor whose speed is reduced by a speed reducer RV and a combination of friction drive pulleys G, and rubber-covered wheels RC, assures the movement of the metal band BM. To make this band keep its direction without getting out of line laterally, it is necessary to put all wheels in perfect parallel.

For this reason, the rollers R_1, R_2 and R_3 have been tired with soft rubber 1 cm thick which smoothes all troublesome inequalities. Different combinations of interchangeable friction drive wheels, mentioned above, allow us to vary in a cascading series of changes in the speed of the band. By varying the motor speed we create a continuous variation of the speed between the cascades. And so, we can produce every speed of movement comprised between 1.5 mm/s and 250 mm/s in two opposite directions.

The lighting is made in the direction of the longitudinal axis of the canal. A 1500 watt lamp with straight filament ("Linea") type, is placed beside the exit end. It is protected by a tin box having a horizontal slot that can be regulated and a brilliant cylindrical parabolic reflector.

Above the experimental chamber a photo apparatus PH is mounted on a special support guided in the horizontal plane by two trackways GL. This allows the camera to be brought instantly over the place where the phenomena most favorable to be photographed appear.

The electric heating arrangement, E, suspended below the steel plate at a regulatable distance, is formed by a network of 50 steel wires (d = 0.2 mm). A metal frame provides the needed rigidity. The maximum power of 3 kw corresponding to heat required to turn the wires red, can be reduced to 60 watts by a big rheostat. The wires being subject to considerable increase in length when they are so heated, tension on them is kept up by a system of coil springs.

To avoid annoying reflections on the glass plate covering the experimental chamber, the whole eddy-producing apparatus is protected by black curtains.

3. Method of Operation

Visualization of eddy motions. Eddy motions produced in the layer of pure air are not visible except by artificial means. After numerous attempts, we have come in most cases to rely on tobacco smoke as an indicator of thermoconvective currents.

For the production of tobacco smoke we made a little generator of brass, very convenient, Fig. 18.

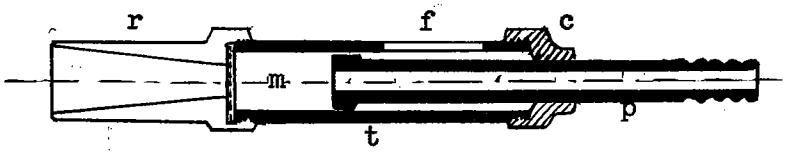

Fig. 18 Generator of tobacco smoke.

It comprises: 1st, a tube t filled with cut cigarette tobacco; 2nd, a hollow piston p which compresses the tobacco and brings the air needed for combustion; 3rd, a cover c screwed to the end of the tube to guide the piston; 4th, a piece r screwed to the other end of the tube and pierced with a conical hole to give off the tobacco smoke. A disk of screen wire m seized between the piece r and the tube, maintains the chopped tobacco in place. A lengthwise slot in the tube permits the lighting.

One governs the production of smoke by varying the flow of air, derived from the compressed air lines in the laboratory. The

little generator can be disconnected instantly to be filled or cleaned.

The introduction of the smoke into the experimental chamber is by way of holes provided in the ceiling of the canal D_1. The shock of the smoke that escapes from the mouth of the generator dies away against the bottom. The smoke fills the floor of the canal and then penetrates to the experiment chamber, drawn along by the air current. This procedure is particularly convenient for producing eddies in longitudinal bands. For producing cellular eddies it is better to introduce the smoke directly into the chamber by means of a long tube.

The tobacco smoke stays white and dense several minutes after combustion. Although a bit heavier than pure air, it is drawn along by the thermoconvective eddies as soon as these have established themselves in the pure air, and it then renders visible the internal movements.

Repose and translation of the layer of air. - The experiments on thermoconvective currents are divided in two groups: (a) Experiments on a layer of air in repose (speed of translation null); (b) Experiments on a layer of air in movement of translation.

a) Layer of air in repose: To avoid external perturbations, we close carefully the inlet and outlet of the canal, for instance, with two plugs of cotton. The smoke can still be let in to the chamber by a long tube passed through the plug in the entrance end. Once the tube has been withdrawn, calm is reestablished in the gaseous layer.

b) Layer of air in translational motion: It is necessary to distinguish two possible cases; in the first, the layer of air is submitted to a bilateral rubbing or frictional drag and in the second case, to a unilateral frictional drag.

In the first case the two horizontal walls (the heating plaque and the chilling plaque) are fixed, and the movement of translation of the fluid layer is provoked by the aspiration of the compressed air system described above. The speed of translation V can be easily regulated by the amount of compressed air and by the position of the collector D_3, as we have said before. For slow speeds, the simple natural aspiration produced by the warm air that rises above the electric lamp placed at the outlet of the canal suffices entirely (one obtains speeds up to 2 to 6 cm/s). To further diminish the speed, it is necessary to reduce the section of the canal at the inlet and outlet.

The distribution of speeds in the vertical between the two immobile sidewalls is approximately parabolic, Fig. 19. The speed is null in contact with the limiting plaques and maximum in the median plane. The vertical gradient of speed, undergoes, hence, an inversion in consequence of the bi-lateral frictional drag.

Let us go on to the second case, that where the general movement is communicated to the gaseous layer by the translation of one of the two horizontal walls of the experiment-chamber.

In our apparatus, it is the metal band constituting the lower surface of the canal that communicates its speed to the gaseous sheet contained between it and the glass plate above. The layer adhering

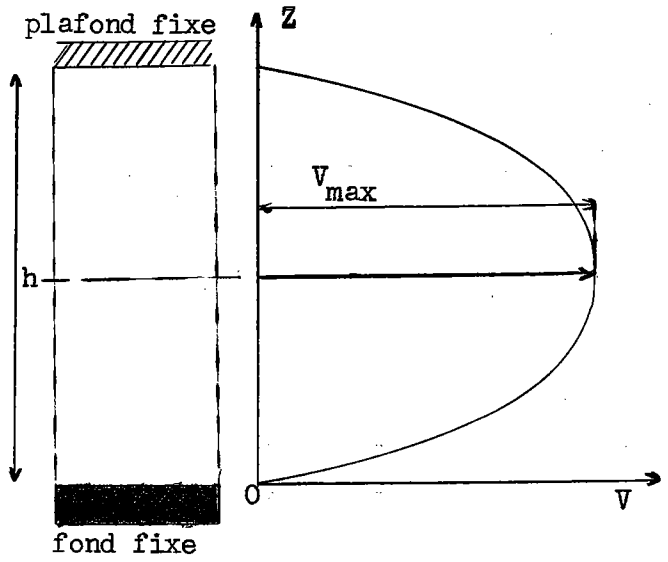

Fig. 19 Vertical distribution of speeds of translation in a rectangular canal with two fixed indefinite sidewalls. "Plafond" is ceiling, fond = floor, h = hauteur, height, V + vitesse, speed.

to the moving band has the speed of this band, while the speed of the superposed layers decreases with height and becomes null at contact with the upper plate. The vertical distribution of speeds corresponds approximately to the diagram of Fig. 20. By varying the speed of the electric motor M and the combinations of friction drive wheels and wheels that put the metal band in motion, one obtains different values for the average gradient of the function $V = V(Z)$.

It is this distribution of speeds resulting from the unilateral friction that corresponds more exactly to conditions realized in the free atmosphere. For, as Sir G. T. Walker had remarked, there also, there is only one single surface of friction situated in the plane of discontinuity between the cloudy layer and the clear air.

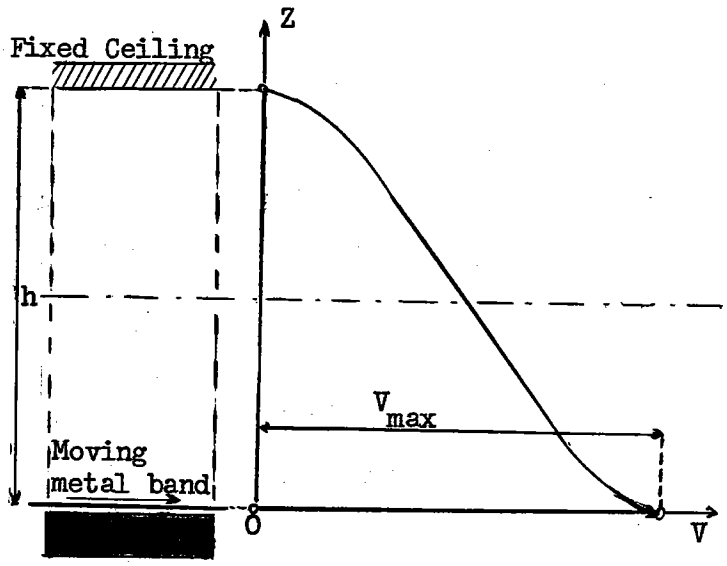

Fig. 20 Vertical distribution of speeds of translation in a rectangular canal whose ceiling is fixed and bottom in uniform movement.

Certain summary experiments have shown us that all the principal forms of thermoconvective eddies appear in a layer submitted to the bilateral friction as well as in a layer submitted to the unilateral friction, and that they present no essential morphological difference. In these circumstances, we have carried out experiments systematically only in a layer of air contained between immobile walls, for the maneuver by aspiration is much more convenient than by the employment of the endless metal band.[1]

[1]However, the circulating band apparatus seems to be immediately usable in cases where it is necessary to drag by friction the lower layer of gas, for example in the study of waves at the surface of separation between the layer of dense smoke and of pure air. We propose to continue this study later on.)

Heating. - We have already described the electric heating apparatus and its control. For an experiment one starts with an intense heating. When the bottom of the canal reaches a temperature convenient to the given thickness of the layer of air to be studied, one reduces the electric current to the value that suffices to keep this temperature constant.

A certain number of experiments have likewise been done with the temperature at first increasing and then decreasing.

The heat source being closed within heat-proof insulation, one can trust that the heat produced is transmitted in large part to the steel plate and next to the layer air where the eddy movements occur.

Lighting. - One obtains best results with a lighting in the horizontal plane of the fluid layer under experiment. The pencil of light is directed and diaphragmmed in such fashion that the black bottom of the experiment chamber remains in the shadow and only the smoke-filled layer is lighted up. The tobacco smoke being white and the bottom of the canal black, one obtains some very intense luminous contrasts. This mode of lighting is applicable when the density of smoke is not great. It is particularly easy to photograph the eddies in longitudinal bands. If the smoke is dense this lighting is not penetrating enough; then, it is better to illuminate obliquely the surface of the layer charged with tobacco smoke.

Photography. - The photographic apparatus is mounted on a support with trackways which allow it to be moved in the horizontal plane parallel to the layer of air under experiment. One can easily explore, either the whole of the field on which the phenomena appear, or only a part of it. A graduated rule in fixed union with the camera apparatus, moves along the whole length of the plate of glass and can be photographed in conjunction with the phenomena observed, which facilitates all geometric measurements below.

Chapter IV

Thermoconvective Eddies in a Motionless Layer of Air or One in Movement of Translation
Principal Forms and Mechanism of their Development

In this chapter we study the mechanism of the appearance and of the development of thermoconvective eddies in a horizontal layer of air whose thickness is small compared to its transversal dimensions. These experiments have been carried out with the apparatus described in the preceding chapter.

The mechanism is the same in principle for the three principal forms of thermoconvective eddies, i.e. polygonal cellular eddies, eddies in transversal bands and eddies in longitudinal bands.

We obtain polygonal cellules when the fluid layer stands in absolute repose; transversal bands if the layer of air is submitted to a general small movement and if other supplementary conditions are realized; longitudinal bands always appear if the speed of

translation is great enough.

In any case, these eddies have certain specific characteristics which require that each case be examined separately.

1. - Polygonal cellular eddies.
Eddies in worm-shaped bands.

Polygonal cellular eddies appear spontaneously in a layer at rest, uniformly heated from below. These eddies, produced in a liquid sheet, have been known since the classic labors of H. Bénard (1). We have already noted in the historical summary in Chap. 1, the essential characteristics of this species of eddies.

If the surface of the liquid sheet is free, it cannot stay perfectly smooth in the presence of movements in the interior of the cellules. In fact, the centers of the cellules are concave umbilici, and the edges are summits; the lines that join two neighboring summits are crests slightly prominent.

These differences of level, extremely small, moreover (of the order of 1 micron for cellules of 1 mm size), have been used to advantage by H. Bénard for the optical recording of the polygonal network. The photograph chosen from the collection of Mr. H. Bénard already reproduced Fig. 3, is evidence of the admirable precision of this method.

Figure 21 also borrowed from Mr. Bénard, gives the vertical section of certain polygonal cellules where surface irregularities are shown on an exaggerated scale.

H. Bénard also suggested for the study of cellular eddies in a liquid sheet, an apparatus with two metal plaques which could assure

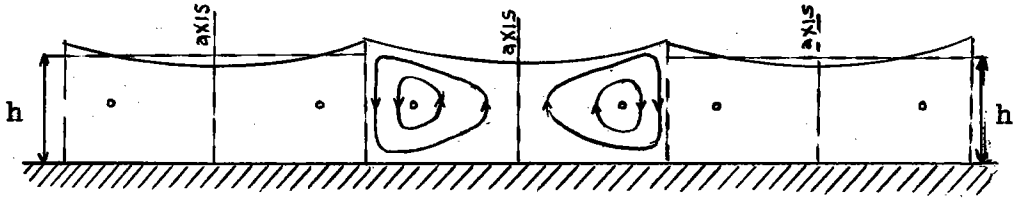

Fig. 21 Dislevelments at the free surface of a sheet of liquid, the seat of Bénard's cellular eddies.

the good conductivity of the two limiting sidewalls. Direct observation in these conditions being impossible, the author has not developed this class of experiment.

C. Dauzère (3-c) has signalized an intermediate case, realized in his experiments on isolated eddies. Using colored stearic acid, the whole surface of the melted sheet covers itself with a thin superficial skin formed by the tiny grains of the coloring material. Hence one has not a "free" surface in the capillary sense, but a veritable crust that exercises a considerable influence on the form of cellular eddies. The polygonal cellules are replaced by very elongated eddies that we call "eddies in wormshaped bands". Fig. 22 from a photograph by Mr. C. Dauzère, shows that the wormshaped bands result from the enchainment of successive polygonal cellules.

Cellular eddies in Gas. - When one makes researches in a layer of gas, the layer must be limited by two horizontal plaques. The plaques being flat, no relief can produce itself on the surfaces of the fluid sheet. This fact is full of consequences relative to the form of the cellules, which has already been demonstrated in fluids by C. Dauzère.

One introduces tobacco smoke into the experimental chamber, whose metal bottom has been evenly heated. Immediately thereafter

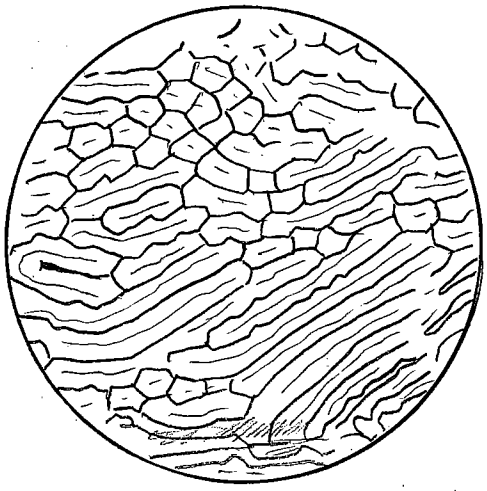

Fig. 22 Spontaneous eddies in vermiculated bands in a layer of melted wax heated from below.

one seals hermetically all the sides of the chamber. The smoke, thick and white, having a density greater than air, spreads out upon the bottom. The lower layer of smoke is neatly separated from the upper layer of air.

A few instants later, slight depressions in the form of concave umbilici are seen in the layer of smoke, Fig. 23-a. These depressions apparently arise without any governing law. They move about and seek the stablest position. This displacement and enlargement of the concave umbilici cease as soon as the whole surface is occupied by them. The cavities bump one another and their edges become polygonal (Fig. 23-6). The depressions grow deeper: the smoke is pushed from the center towards the edges. The black bottom of the canal appears in the central shoals disengaged from the smoke. One sees in the same figure the quincuncial assemblage of black holes surrounded by crests of white smoke. The crests in their turn, constitute a network of polygons (both Fig. 23-a and Fig. 23-b in back).

This network is the exact image of the cellular eddies that are formed spontaneously in the layer of pure air. And so it is under the action of these organized thermoconvective currents that the cavities at the surface of the smoke layer produced themselves. The same currents have cleaned the central shoals, and accumulated the smoke in sharp crests. These indicate infallibly the direction of circulation inside the polygonal eddies: the descent is produced in the central part and the ascent following the vertical sidewalls of the prismatic compartmentations. In consequence, the direction of circulation in gas is the inverse of what one observes in the greater part of liquids.

The continued eddy movement entrains, by friction, the accumulated smoke into crests. The cellules clothe themselves with a thin sheath of smoke which shows up the internal movement whose direction of circulation is that just now indicated. The reserves of smoke are soon drawn off: they pass entirely into the cellules which then become opaque. One will find in the four, drawn, vertical cuts, Fig. 24, the most distinguishable phases in the development of cellular eddies.

From the moment when all smoke has diffused in the polygonal cellules, these undergo a profound transformation not seen in liquids with free surface. One knows that in this last case the semi-regular cellular system (the surfaces of the cellules are more or less equal, but the form of the polygons still varies) is followed by the final system where all the cellules equalize themselves and tend to the form of regular hexagons.

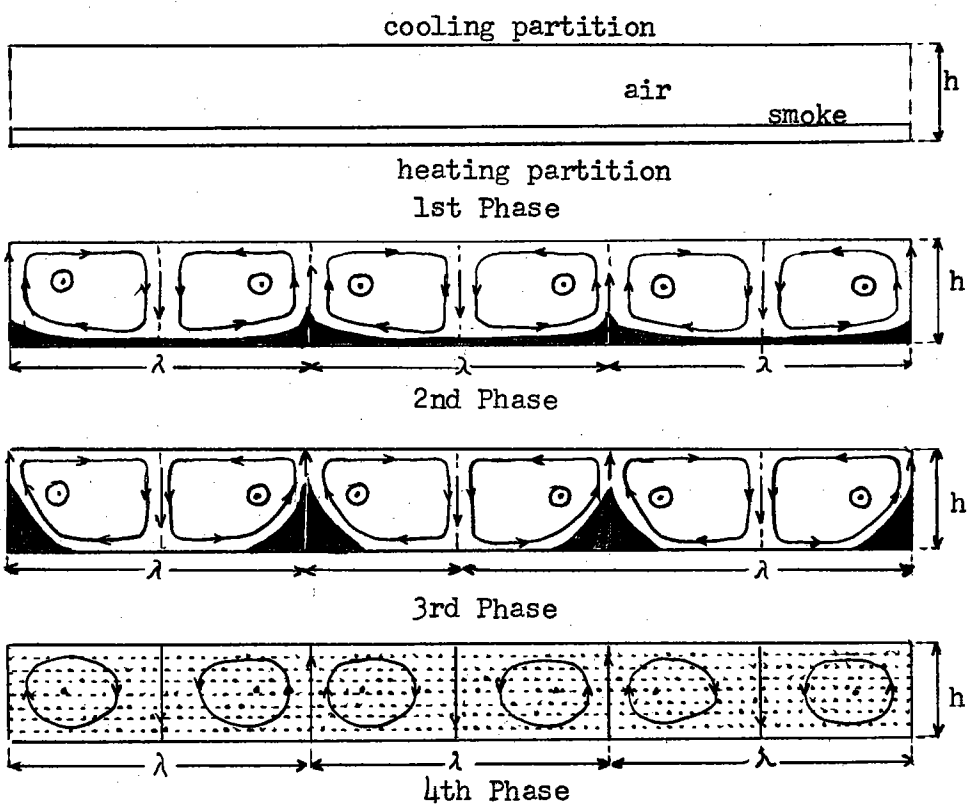

Fig. 24 Schematic development of cellular eddies in a layer of air (made visible by tobacco smoke)

However - with a gaseous layer limited by two rigid, plane-surfaced sidewalls, there constitute themselves, in a second phase, polygonal cellules that in general are very unequal. These cellules align themselves then the one after the other. The separating sidewalls vanish: the chain of cellules transforms itself into two wormshaped bands. All trajectories are brought into the planes perpendicular to the axes of these bands. The direction of rotation of two adjacent rolls is necessarily inverse: the current arises following exterior walls, and descends along the wall that separates each pair of twin bands. The zigzag form of

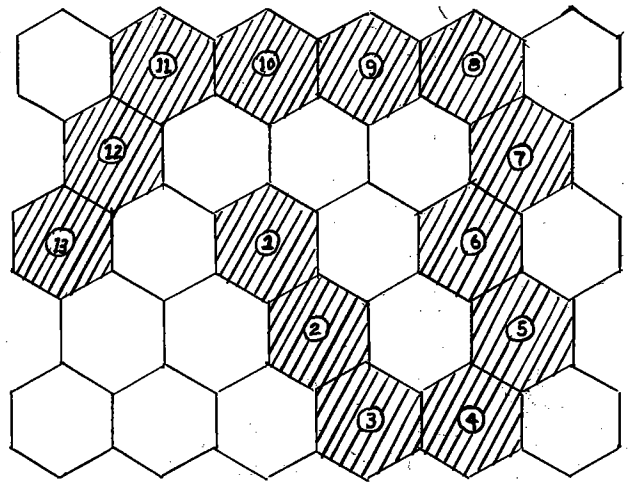

1st phase

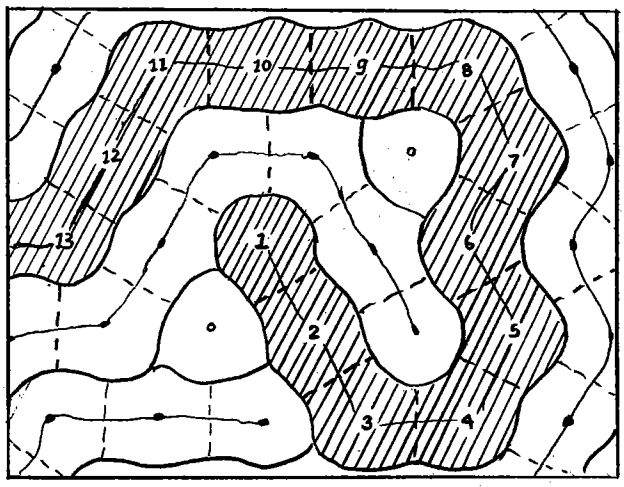

2nd phase

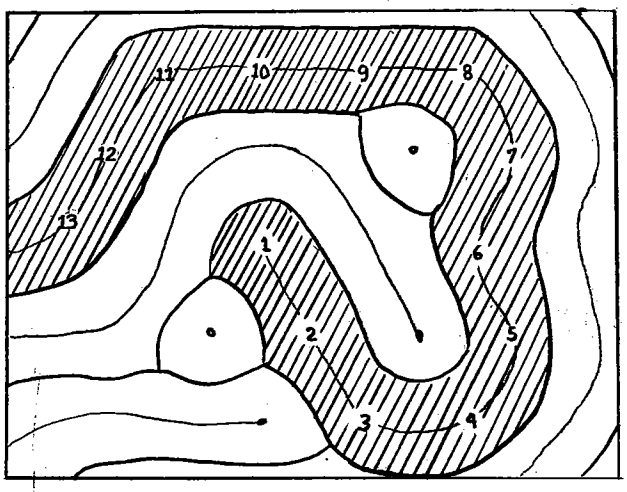

3rd phase

Fig. 25 Schematic transformation of hexagonal eddies into eddies in vermiculated bands in a layer of air heated from below.

their external convolutions, arising from the sidewalls of polygonal cellules, stretches and smoothes itself out.

The final aspects of eddies in wormshaped bands are very various, for the order of enchainment of the cellules is altogether accidental. One very often sees, among these formations, polygonal cellules enrolled by spiral bands. (Fig.26, and Fig. 27, back).

The transformation of the polygonal network into a vermicular, or wormshaped network is schematically represented by Fig. 25. Elsewhere, in Figures 26, 27, 28, photographs of a number of characteristic aspects are reproduced.

Conclusion - The polygonal cellules that in the permanent régime tend towards regular hexagonal prisms can develop only in a fluid sheet one of the two horizontal faces of which is free, or at least easily deformable. (Fig. 28 and Fig. 29 back).

It is in this way that polygonal eddies are produced in a liquid sheet whose surface may remain free, and also in a layer of air lying upon a layer of heavier smoke, because its surface adapts itself very readily to the eddy-movements in the upper layer of air. On the contrary, if the fluid sheet is comprised between two rigid, flat sidewalls, the stablest formation is constituted by the eddies in worm-shaped bands. (Fig.30 and Fig. 31 back).

In the above experiments the little quantity of tobacco smoke plays the same rôle as do the solid particles denser than the liquid in the essays of H. Bénard. Being given that the

direction of circulation in the two cases is inverse, the deposits of solid particles form themselves in the centers of the liquid cellules, whereas the tobacco smoke is drawn by the centrifugal currents towards the polygonal contour. Hence, the little powdery heapings from a quincunx, Fig. 29, while the concentrated smoke forms a network reticulated with lacunae. (Fig. 23-b, 26, etc.)

A special case is presented if one introduces into the chamber a quantity of smoke sufficient to fill the entire space right from the start. Thermoconvective eddies then produce themselves in the midst of the smokey mass. Each cellule has within it an opaque nodule surrounded by an envelope of purified air. Figures 30 and 31 give the impression of floating blisters. The opacity of the nodules disappears progressively and the mass constituting the cellules becomes more homogeneous. From then on, one observes the same transformation of the polygonal cellules in worm-shaped bands which we have already described.

2. - Eddies in Transversal Bands in the Air.

One calls "eddies in transversal bands" the thermoconvective currents spontaneously organized in rolls that are equidistant and perpendicular to the general current of the fluid layer. This formation is not very frequent because, for the appearance of the transversal rolls, several conditions must be realized at the same time.

Figure 32 represents several eddies in transversal bands, drawn in perspective. The section of the equidistant rolls is

approximately square. The whole ensemble of rolls turning alternatively to left and right, moves itself along the canal with a relatively small speed of translation (in general it is less than 2 cm/s).

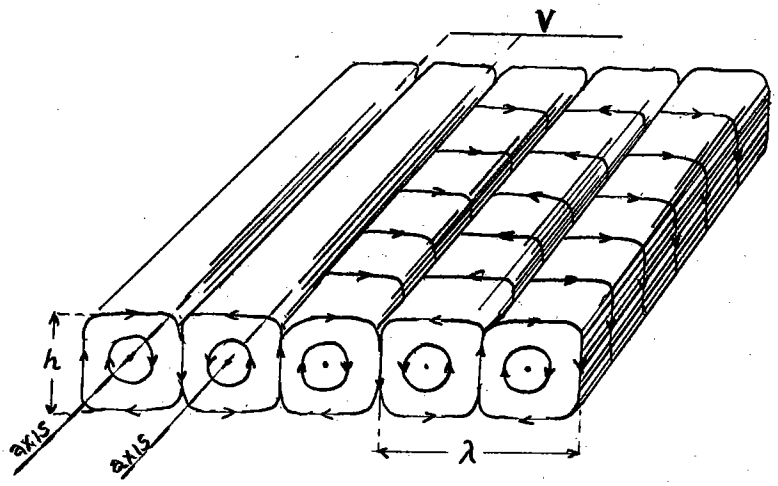

Fig. 32 Schema of eddies in transversal bands, seen in perspective.

This form was obtained for the first time by A. C. Philipps and Sir G. T. Walker (10) for a layer of air 6 mm thick. Because of the small thickness, the two authors were not able to give a sure explanation of the origin of the transversal bands.

Our experiments (21-f) effectuated on a larger scale, permitted us to observe that these eddies resulted from the superposition of the two following phenomena:

1st. Spontaneous formation of transversal waves at the surface of separation between the lower layer of smoke and the upper layer of air, being animated in different speeds;

2nd. Development of transversal rolls of thermoconvective origin,

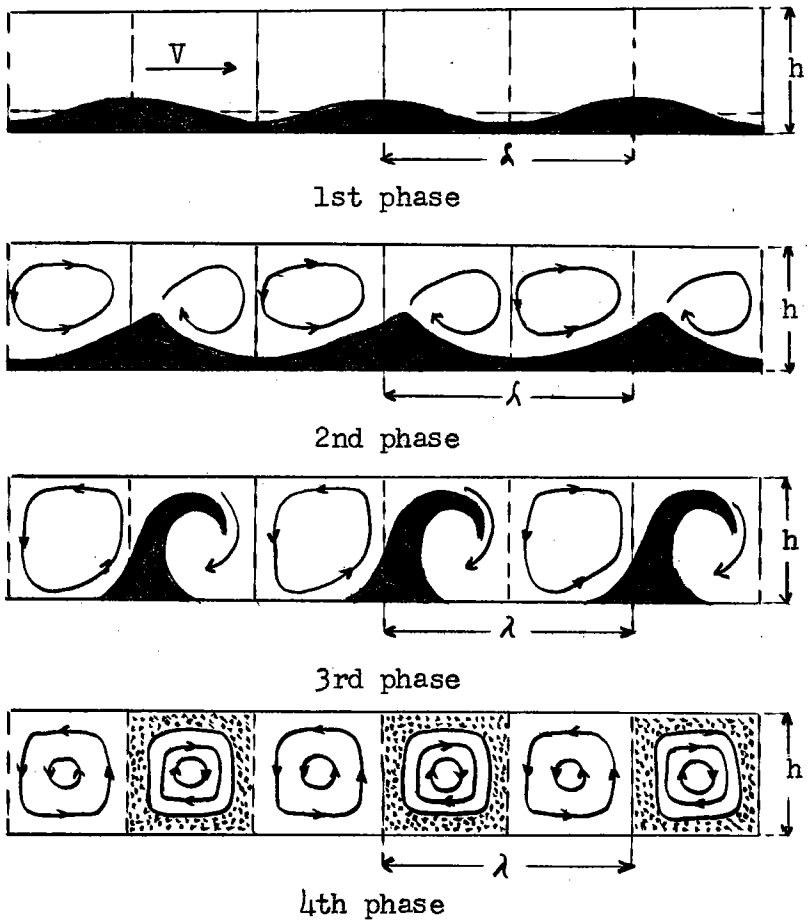

Fig. 33. Schematic development of eddies in transversal bands in a layer of air. Dense smoke shown black, diffused smoke is dotted.

each pair of rolls being placed in the hollow formed by the crests of two successive waves.

The four designed cuts (Fig. 33) reproduce the principal phases of the development of eddies in transversal bands, just as our experiments have revealed it (this development) to us.

First phase: One introduces into the canal some tobacco smoke. Two separate layers establish themselves: the lower layer of smoke and the upper layer of air. The outlet of the canal, whose bottom

has first been heated is merely half-open, to assure a small speed of translation. At once one perceives that the surface of the smoke layer becomes lightly undulated. The wave-length is marked by lambda, λ, and the arrow shows the direction of the general current (Fig. 34, back).

Second phase: In the hollow between two crests of successive waves, appear the thermoconvective currents having the form of two rolls turning in opposite directions. The smoke, pushed towards the periphery of the eddies in a state of growth, accumulates in crests that point out the centers of rising currents.

Third phase: The crests of smoke then lean over in the direction of the current and envelop the rolls immediately in front of them.

Fourth phase: The smoke is entirely absorbed by the system of transversal rolls rolling downstream in the canal, whereas the complimentary system of rolls has to remain transparent for lack of smoke.

The origin of the two systems of rolls, the one opaque, the other transparent, is thus explained in a simple fashion.

The production of eddies in transversal bands is extremely delicate. It is especially the friction of the sidewalls of the canal that prevents their production on a vaster surface. Here are two photos, taken one after the other of transversal rolls formed in a layer of 12 mm thickness and 260 mm width. One sees

on the first (Fig. 34) the appearance of waves that do not stay rectilinear. Being given that the fluid is braked by the side-walls, the mass in the centre of the canal flows with greater speed, which occasions the more and more pronounced deformation of the transversal waves. The second photo (Fig. 35) shows a more advanced phase: twelve rolls, (six of white smoke and six of pure air) are well developed. They occupy only the upper part (near the inlet) of the canal, whereas the rest is occupied by the worm-shaped bands. (Fig. 35, back).

3. Eddies in Longitudinal Bands

The handsomest results are associated with the formation of eddies in longitudinal bands, that is to say, with axes parallel to the general direction of flow. We obtained some with thicknesses varying from 1 to 8 cm (21-a). It is a very stable formation, that one can produce easily whether in liquids (as has been shown in experiments of Japanese physicists and English meteorologists) - or in gasses.

For reasons set forth in Chapter V, we consider a whirl in longitudinal bands as constituted by a pair of contiguous symmetrical rolls oriented in the direction of the general current. Figure 36 gives the scheme of this type of eddies. The section of the individual rolls is, in the first approximation, square. Each roll turns around its axis: the first to the right, the second to the left, and so forth. The vertical planes separating the rolls coincide alternatively with the centers of the ascending and descending currents.

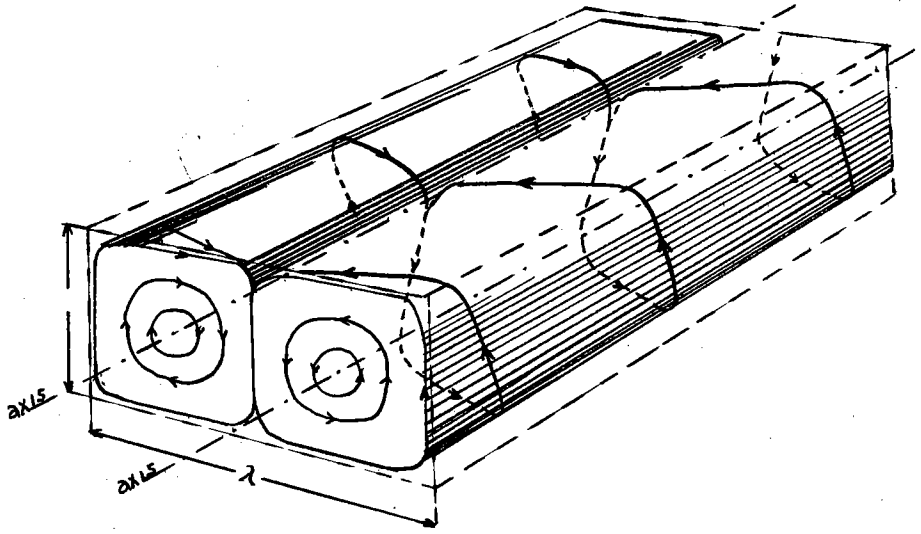

Fig. 36 Schema of eddies in longitudinal bands seen in perspective (two rolls, twins, forming one eddy in longitudinal bands).

The whole ensemble of the fluid moves along the canal with a speed of translation that in general is more than 2 cm/s. The trajectories, that result from the translation and the rotation inside the rolls, constitute a sort of helix. We will give the details in Chapter X devoted to speeds and to trajectories of thermoconvective eddies. In the diagrams we have designated by λ the width of two twin rolls and by h their height which is that of the fluid layer under experiment. (Fig. 37, back).

To produce eddies in longitudinal bands in a layer of air, we establish by aspiration the general current in the experiment chamber whose metal bottom is suitably heated. One introduces tobacco smoke by the hole in the prolonged canal D_1. The smoke, carried by the current, penetrates the experiment chamber in the form of a thin layer with a rectilinear front. Fig. 37a, which in a few instants becomes regularly indented (Fig. 37-b,c). The indented front develops finally into eddy or whirl-rolls (Fig. 37-d).

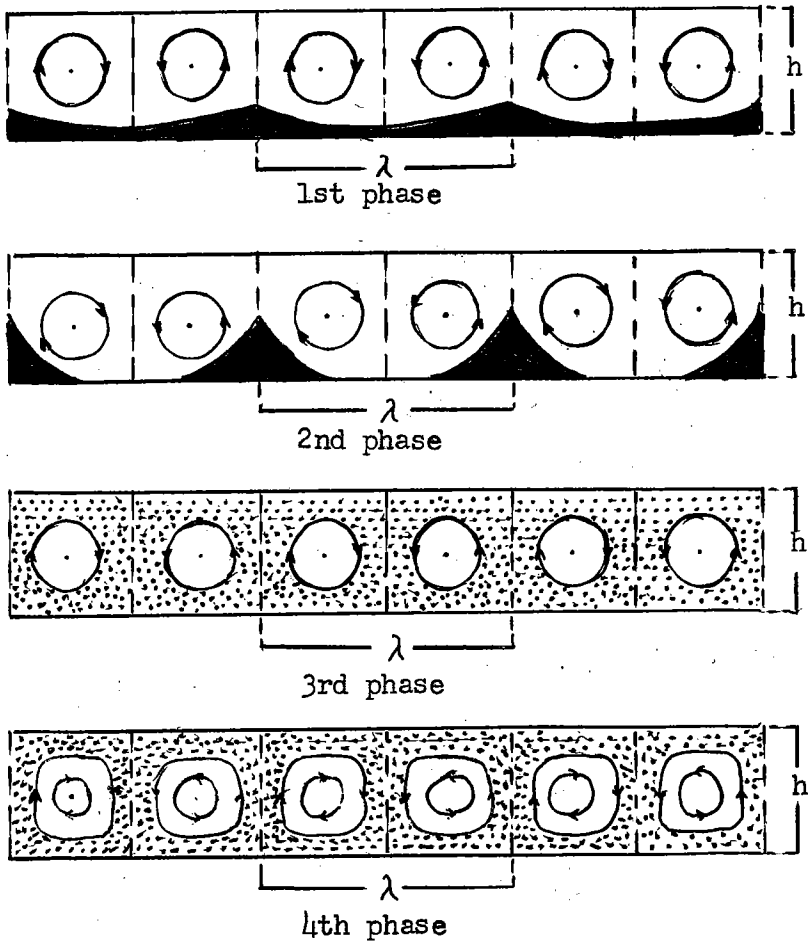

Fig. 38 Schematic development of eddies in longitudinal bands in a layer of air. Dense smoke in black; diffused in dottings.

Let us follow on Figure 38 the four successive phases in the development of longitudinal bands when the layer of smoke covers the entire bottom of the chamber, the plane of observation being placed in the transversal section of the canal. (Figs. 39, 40, 41, 42, back).

First phase: One notices that the surface of the layer of smoke (drawn in black) becomes slightly wavy. These depressions oriented in the direction of the general current, indicate that the eddies in bands form themselves spontaneously in the midst of the layer of pure air.

Second phase: The depressions grow deeper. The dense smoke is pushed towards the edges of the growing eddies. It accumulates in sharp crests which indicate the centers of rising currents. The smoke concentrated thus in elongated crests, is drawn along by the eddy-movement. The rolls clothe themselves in a thin sheath of smoke.

Third phase: The reserves of smoke are used up. It has passed entirely to the interior of the rolls which become regularly opaque.

Fourth phase: The central mass of the rolls flows off more rapidly than the peripheral mass, for this last is braked by the enclosing walls. The centres purify themselves little by little and the rolls become transparent.

We show likewise four photographs that correspond to the principal phases, described and represented schematically above.

Fig. 39: The layer of dense smoke divides itself under action of the eddie-whorls coming to life in the midst of the layer of air into parallel bands elongated in the direction of the general current.

Fig. 40: One or two minutes afterwards, the greatest part of the smoke has passed off. What remains is accumulated in sharp crests. These last are sure indicators of ascending currents. Two longitudinal rolls are then placed between two successive crests. The smoke which has been drawn along by the movement of rotation, envelopes the rolls. The thin sheath of diffused smoke,

seen in projection, indicates by a fine line the central plane of descending currents.

Fig. 41: The reserves of smoke are used up. One can no longer discern on the photographs the ascending and descending currents: all the plans of separation between the rolls present themselves in projection under the same aspect of fine lines.

Fig. 42: The visibility of the rolls vanishes in proportion as the smoke passes off, but the eddy-whorls in longitudinal bands still persist in the pure air. They are perfectly rectilinear and regular.

A new injection of smoke, operated with the necessary precautions, permits us to re-materialize the eddies. This operation is reproduced in Fig. 43. The white smoke penetrates exactly in the preceding rolls. The number of tendrils is then that of the preceding rolls in pure air. One also notices the helicoid character of the internal movement.

This method, which one might call the "method of visualization by incorporation", is profoundly different from the preceding one where the smoke, forming a particular layer, has been progressively drawn along by the eddy movement. (Figs. 43, 44, back).

Figure 44 shows a system of eddies in opaque bands enveloped by sheathes of pure air (through the spaces separating the neighboring rolls, one sees the floor of the canal in the form of black lines).

If we check the feeding of the smoke, the centers of the rolls

purify themselves and the rolls take again the aspect already known, by Fig. 42.

Besides the three principal forms of thermoconvective eddies, there exist other intermediate ones. We will speak of them in Chapter V, where we study the mutual transformations and intermediary forms of cellular eddies.

Chapter V.

Transformations between the Principal Forms and Intermediary Forms of Thermoconvective Eddies

1. Polygonal cellules transforming themselves into vermicular bands.

It has been shown by experiment that the polygonal cellules tending towards the hexagonal form, develop and remain stable only in a fluid layer whose surface is free (liquids) or at least easily deformable (gas with a layer below of dense smoke). By contrast, between two plane and rigid surfaces, the cellules, polygonal at first, align themselves bit by bit in chains and at last transform themselves into vermicular (worm-shaped) bands.

For details of this transformation, see the preceding Chapter (paragraph 1: Polygonal cellular eddies. Eddies in vermicular bands.)

2. Polygonal cellules at first at rest transforming themselves into longitudinal bands.

First, one lets the polygonal cellules develop in the layer of air at rest superposed upon the layer of smoke below also at rest.

Then, without waiting for the second phase where the cellules would arrange themselves as we know, in vermicular bands, we open the outlet of the experiment chamber: the ensemble puts itself progressively in a movement of translation. The cellules enchain each other then. The alignment finishes itself effectively in the sense and direction of the speed of translation. The compartment-walls of the aligned cellules vanish: the cells are replaced by eddies in longitudinal bands. Their characteristic is exactly the same as that we gave for eddies in bands producing themselves in a layer of air subjected from the start to the movement of translation.

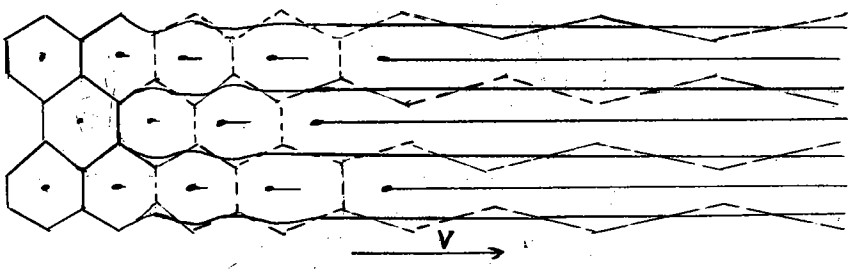

Fig. 45. Schematic transformation of hexagonal cellules into longitudinal bands.

Figure 45 gives the scheme of this transformation. The inner walls like zigzags, resulting from the polygonal contour of the original cellules, stretch out and straighten out. One finds on the photo, Figure 46 all the characters of the preceding schema. (Fig.46, 47, back)

Another photograph (Fig. 47) taken at the moment when the reserves of smoke are not yet exhausted, reproduces also the trajectories inside

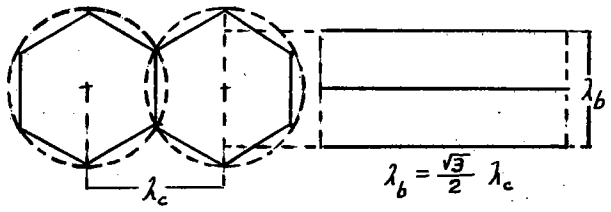

Fig. 48 Geometric relation of the transversal dimensions of hexagonal cellules and longitudinal bands.

the rolls. One sees there also that each pair of rolls derives from one polygonal cellule. Hence, it is legitimate to consider a pair of bands as an inseparable unity, constituting an eddy in bands, or now, a whorl in bands. Being given that the eddies in bands derive from the hexagonal cellules, the total width of the two twin bands λ_b is directly bound to the distance λ_c of the centers of the preceding cellules. One sees on Figure 48, where one has designed on one hand the hexagonal cellules and on the other the longitudinal bands, that:

$$\lambda_b = \frac{\sqrt{3}}{2} \lambda_c = 0.865 \lambda_c,$$

a result to which we will return in Chapter VIII on Dimensions of Eddies.

3. Polygonal cellules in translation and their transformation into longitudinal bands.

In the foregoing experiments, the eddies in longitudinal bands appear rapidly if the gaseous layer is animated by a significant speed. If, on the contrary, the translation speed of the gaseous layer is very small, the polygonal cellules produce themselves there still, but their form is more or less modified.

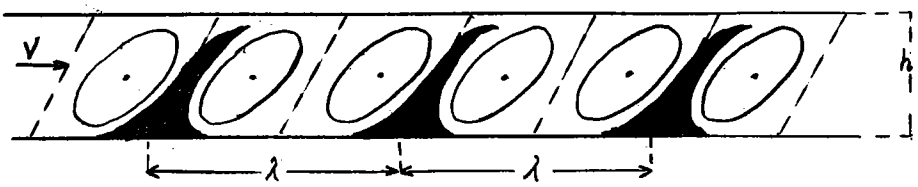

Fig. 49 Schema of cellular eddies in very slow movement of translation; the crests of smoke slope forward under action of the general current.

Figure 49 gives the longitudinal cut of the canal. The smoke-crests (drawn in black) that indicate the centers of rising currents, are sloped ahead under the action of the general current; hence the lines of the current inside the cellular eddies must adapt themselves to the form of the inclined partitions; the sharp angles of the polygonal prisms round themselves off, as seen in Figure 50. But there is a case of an intermediary from not very durable. In general it transforms itself quickly enough into longitudinal bands. Figure 51 reproduces this transition. (Figs. 50, 51, 52, back).

4. Accidental transformation of the polygonal cellules into transversal bands.

It sometimes happens, that by chance, the cellules are aligned perpendicularly to the general current. Then they lose progressively, under the thrust of the current, their individuality, and melt into two transversal bands, each one turning inversely (see Chap. IV).

Two photographs (Fig. 52 and Fig. 53), the one corresponding to the thickness (h = 20 mm) and the other (h = 25 mm), give the aspects of eddies in transversal bands just on the point of forming themselves. The bands, slightly oblique, occupy only a small part

of the field of observation. The character of the individual cellules is not yet effaced.

5. Coexistence of eddies of different forms.

The criteria of transition from one to the other type of eddies studied up to this point, have not been determined perfectly. And so one observes from time to time the appearance simultaneously of two or three forms. Such formations do not persist indefinitely. The less stable make place finally for the more stable. In a layer brought to rest, the worm-shaped bands represent the final régime: but on the contrary, the longitudinal bands prevail almost always in the layer in movement of translation, even for speeds that are very slow.

The coexistence of eddies both cellular and in longitudinal bands seems to be the most frequent state. Simply consider the preceding figures, 46, 47, and 51, where the system of longitudinal bands is followed by a layer of thick smoke, the seat of the cellular eddies.

The formation of a few transversal bands in presence of the cellules is sometimes seen. Such a formation is reproduced in Figs. 52 and 53. (Figs. 53 and 54 back). Finally, as an exception one sees the coexistence of longitudinal bands with transversal bands, or, more exactly, with oblique bands. These last arise from the perfectly perpendicular bands that transform themselves by oblique positions into longitudinal rolls. A fine example is given in Fig. 54.

Let us point out finally a disposition of transversal and longitudinal rolls according to the pattern of Fig. 55, which we have also observed but not photographed.

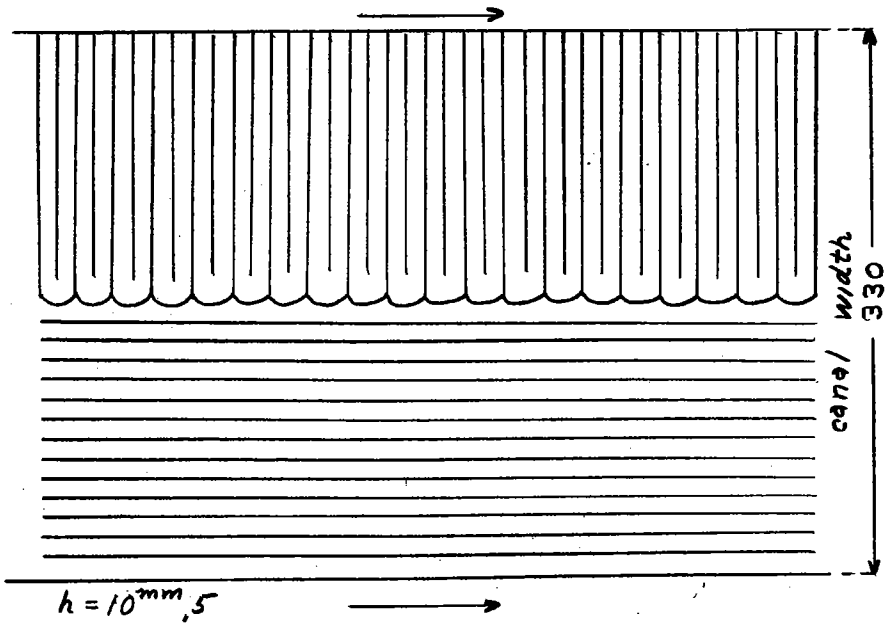

Fig. 55 Coexistence of longitudinal bands and transversal bands. Schematic figure from an effective observation.

6. Eddies in undulated longitudinal bands.

Eddies in longitudinal bands are generally perfectly rectilinear; but there are cases where the partition walls separating the contiguous rolls take on an undulated form (21-d).

Several distinct causes can contribute to provoke this undulation:

a) Slowing up of the movement of translation of the ensemble of eddies in bands with rectilinear sidewalls;

b) Intercalation of supplementary rolls provoked by accidental perturbation or some artifice;

c) Considerable increase of the difference of extreme temperatures on the two limiting walls (this case will be separately examined in Paragraph 7 of this same Chapter).

a) Undulation of the bands caused by a slowing up of the speed of translation.- When we slow up the movement of translation of the eddies in rectilinear bands (by reducing the aspiration or the section at the outlet of the canal), we observe that their sidewalls take very various undulated forms. Two of the most characteristic are represented by the Figures 56 and 57. (Figs. 56 and 57, back).

On the first photograph (number of rolls $n = 8$; width of canal $L = 350$ mm; and thickness $h = 40$ mm), the partitions 1, 3, 5, 7, 9 stay straight: these are the partitions of ascending currents. As for the partitions of descending currents (2, 4, 6, 8) they show an undulation that dies away towards the head (upstream).

The second photograph ($n = 10$; $L = 300$ mm; $h = 30$ mm) represents a variant where the sinusoidal bands having a constant breadth (4 and 7) intercalate themselves between the rolls of the preceding case.

No forwarning can be offered as to which of these two formations will be able to appear: it is all subject to hazard.

The undulated bands persist only a short time after the slow-up. In fact, when the speed of translation re-established itself, the rolls become once more rectilinear, being understood that the

new speed V remains greater than the critical value necessary for the maintenance of eddies in longitudinal bands.

One recognises easily in Fig. 56 that the undulated bands tend to transform themselves into hexagonal cellules. That would come about if the current of air were entirely cut off, and if this form could persist between two plane, rigid sidewalls. This transformation is the inverse of that one where the hexagonal cellules changed themselves into longitudinal bands. Consequently, knowing the breadth of two twin rolls λ_b, one may calculate the periodicity of the resulting hexagonal cellules.

$$\lambda_c = \frac{2}{\sqrt{3}} \lambda_b = 1.15 \lambda_b.$$

b) Eddies in undulated bands following accidental or artificial perturbations. - One very frequently observes the eddies in undulated bands for quite a long time of duration in experiments where the characteristic λ/h is less than 2. That comes about above all when one imposes a number of rolls greater than that which would produce itself in normal conditions. (c.f. Chap. IX, Parag. I).

Here is an example of this last case. At the time of an experiment with h = 30 mm and L = 280 mm, the number of rolls most frequent was 8 (hence, $\lambda/h = 2.34$). One then put at the entry of the canal a distributor (guide vane apparatus) with five cellules, to bring the number of rolls to 10 and reduce the ratio λ/h to 1.87. The ten rolls forseen were not slow to appear, but their partitions

were particularly wavy. One sees in the photo, Fig. 58, the alternative succession of two types of rolls: the first is constituted of sinusoidal bands of equal width, and the second of the bands which consist of an alternated suite of distended regions and restricted regions. (Figs. 58, 59 back).

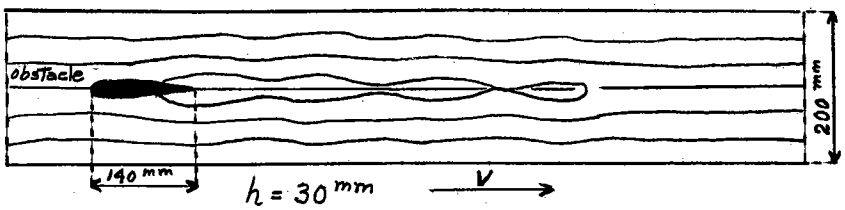

Fig. 60 In the wake of an obstacle with profile like a wing, two rolls with undulated partitions take shape. Schematic figure from an effective observation.

These undulated bands do not persist, either: little by little, they rectify themselves and reoccupy the entire space. This form, hence, is only transitory. Here, moreover, are two experiments proving that the eddies in undulated bands are the exterior manifestation of perturbations in the normal equilibrium.

We divided the layer of air, of a total width L = 400 mm and of a thickness h = 30 mm, in eight sections, of which four had a width, each one, λ_1 = 40 mm, and the others λ_2 = 60 mm. One sees on the photo, Fig. 59, sixteen rolls entirely developed. In view of the feeble ratio of the rolls proceeding from the narrow trenches or cuts ($\lambda_1/h = 1.35$), they cannot find final equilibrium except through the intermediary of oscillations of their sidewalls. On the contrary, the second group of rolls ($\lambda_2/h = 2$)

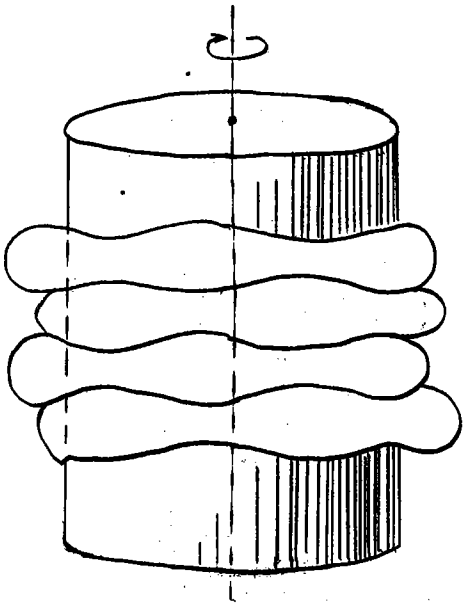

Fig. 61 Special toroidal eddies with undulated partitions, in a layer of liquid contained between two coaxial cylinders turning with different angular speeds.

is constituted of eight rectilinear rolls, which proves their perfect equilibruim.

Here is the second experiment. We placed in the center of the canal (h = 30 mm, L = 200 mm) an obstacle with the profile of a wing, occupying all the height h, as we have drawn it in Fig. 60. Upstream of the obstacle, six rectilinear rolls ($\lambda/h = 2.22$) formed themselves. But downstream, in the wake of the obstacle, two new rolls with undulated edges suddenly appeared. The form of the neighboring bands was likewise modified in proportion. Whatever it was that was causing it, the two new rolls could not develop. They were annihilated, and the preceding system of six rolls was re-established entirely in the lower part of the canal.

Remark - There is an evident similitude between these undulated forms and the toroidal eddies that G.I. Taylor (22) observed

in his experiments with a liquid comprised between two coaxial cylinders turning opposite to each other. The sketch of undulated toroidal eddies, reproduced from the memoir of G.I. Taylor in Fig. 61, is witness of this.

7. Influence exercised on thermoconvective currents by the difference of extreme temperatures between the limiting surfaces.

We have described in the preceding chapters the mechanism of thermoconvective eddies. It has been demonstrated that their forms depend especially upon the speed of translation to which the fluid layer is submitted.

Another factor just as important as the speed of translation, to modify the geometric forms of the thermoconvective eddies, is the difference of extreme temperatures.

The eddies in longitudinal bands furnish an excellent example. One sees there three characteristic phases.

a) When the general movement of the layer of air is uniform and the difference of extreme temperatures moderate, the eddies in longitudinal bands are perfectly rectilinear (cf. Fig. 42, 70, 71, 72, etc.)

The interval of temperatures considered as moderate has as a lower limit the critical value ΔT_c (appearance of the first thermoconvective currents) for which we have reserved all of Chap. VII, and for upper limit, another value, which comes close to being an integral multiple of ΔT_c. Writing:

$$\Delta T_c < \Delta T_1 < m \Delta T_c,$$

we have discovered that the multiple m was in the order of 5.

b) If one raises the heat still higher, the internal movement (speed of rotation) becomes more lively. It brings on an undulation of the vertical partitions of the rolls.

Fig. 62 shows a fine formation of six rolls regularly undulated obtained in the canal with 30 mm thickness and 300 mm width. The contours of the undulated partitions are effectively parallel. One ascertains likewise that the trajectories of internal motion adapt themselves to the exterior form of undulated bands (more exactly, it is the internal movement that requires the undulated form). (Fig. 62 back)

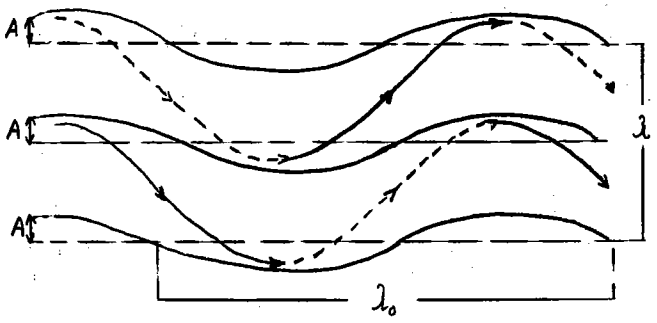

Fig. 63 Design of eddies in twisted columns. Wave-length λ_o and amplitude A of the undulated bands.

The wavelength λ_o (Fig. 63) depends upon the speed of translation, whereas the amplitude of undulation A is a function of the difference of extreme temperatures ΔT. It is evident that λ_o stretches itself out if the speed of translation keeps on increasing, and that A increases with the increase of ΔT.

The temperature interval ΔT where one sees the eddies in regular undulated bands, extends from the greater preceding value

$m\Delta T_c$, to a value $n\Delta T_c$, where the multiple n is considerably greater than m (it is in the order of 10 to 15):

$$m\Delta T_c < \Delta T_{II} < n\Delta T_c.$$

(Figs. 64, 65, back).

Another photograph (Fig. 64) reproduces eight rolls (h = 3 mm; L = 330 mm) with the partitions slightly undulated. The picture was taken at the moment when the smoke had been greatly exhausted.

The third photograph (Fig. 65) made under similar conditions, relates to an experiment with h = 35 mm, when the translation speed was small and the heat more active than in the preceding case. Consequently, the oscillations have a very short wavelength and an amplitude relatively great.

c) The amplitude of the oscillations augments with the difference of extreme temperatures. One can make it increase to the point where the particles of the fluid do not follow regular trajectories any longer. They pass, without apparent law, from one compartment to another: the organized régime of cellular eddies is destroyed in favor of disorganized turbulence.

Chapter VI

Review of the Theory of Thermoconvective Eddies

The theory of thermoconvective eddies has revealed certain interesting facts that had escaped hitherto the attention of experi-

mentors. In these conditions, we proposed to verify them experimentally. This verification holds particular reference to:

a) the value of the Rayleigh-Bénard criterion;

b) the distribution of temperature with depth in the fluid layer;

c) the thermal field following the rectangular sections of the eddies and longitudinal bands;

d) the dimensions of the cellular eddies;

e) the lines of flow inside cellular eddies.

It is, hence, indispensable to give a brief outline of the classic, theoretical works that served as a basis for our experimental labors.

1. - Historical outline of theoretical works.

The first mathematical study of Bénard's cellular eddies was presented in 1916 by Lord Rayleigh (13). The problem appears very complicated because the density ρ that figures in the Euler equations, and which is intimately bound to the variation of temperature, is no longer a constant. Thanks to Boussinesq's analytical method, (23), which replaces the effect of the variation of temperature by a little force proportional to the temperature T, one is led to the equations of motion where the density ρ is considered as constant, and consequently, the equation of continuity becomes once more that of an incompressible fluid. It is necessary to add to these equations, the equation of thermal conductivity established, likewise, by Boussinesq:

$$\frac{DT}{Dt} = \varkappa\left(\frac{\partial^2 T}{\partial x^2} + \frac{\partial^2 T}{\partial y^2} + \frac{\partial^2 T}{\partial z^2}\right),$$

where $\frac{D}{Dt}$ designates the Stokes operator:

$$\frac{\partial}{\partial t} + u\frac{\partial}{\partial x} + v\frac{\partial}{\partial y} + w\frac{\partial}{\partial z},$$

and $\varkappa$ the coefficient of thermal diffusion. See definition of $\varkappa$ in Chapter VII, page 116.

To simplify the problem, Lord Rayleigh takes the boundary conditions that are not the same as those realized in Bénard's experiments. He assumes that the two faces of the fluid sheet are free, and good heat conductors.

In the first part of his memoir the author examines the conditions of the instabilities in a fluid layer the bottom of which is less dense than the upper part. The principal result of this analysis is as follows:

If the fluid is hypothetically perfect, - non viscous - the least perturbation must provoke thermoconvective movements; if, on the contrary, the fluid is real, it is possible that the fluid sheet can remain in stable equilibrium even if the denser layers (cold) are above the lighter layers (hot).

Hence, according to Rayleigh, there is a stable preconvective régime that precedes the régime of the thermoconvective currents. The two régimes are separated by the criterion*:

$$\frac{\rho_1 - \rho_2}{\rho_2} \leqslant \frac{27\pi^4 \varkappa\nu}{4 g h^3},$$

*The numerical value of this criterion relates solely to the case where the boundary conditions are those superposed by Rayleigh.

where ρ_1 is the density of the fluid at the upper surface, ρ_2 that at the lower surface, ν the kinematic viscosity, α the coefficient of thermic diffusion, h the thickness of the fluid sheet, and g the acceleration of gravity.

If the left hand member of this inequality is smaller than the right hand one, the little accidental perturbations die away: hence the fluid remains in stable equilibrium. In the contrary case, these perturbations keep on increasing with time, and the thermoconvective currents release themselves into action.

In the second part, less developed than the first, Lord Rayleigh gives several partial solutions which satisfy the differential equations. The simplest case of the eddies with three dimensions is represented by the fractionation of the fluid layer into square cellules. The cases of the triangular and hexagonal cellules have not been resolved analytically. However, the author gives an approximate solution for hexagonal cellules, in considering them as circular cellules.

The case of the two-dimensional cellular eddies, analytically still simpler, has been treated likewise. This form presents for us a particular interest, for it can be considered as the transversal section of eddies in bands.

In 1926 H. Jeffreys (14-a) published a new mathematical study on the stability of a fluid layer heated from beneath. This work is an extension of the Lord Rayleigh theory to certain cases where the boundary conditions approximate more nearly those realized in the experiments - that is:

α) The fluid layer is contained between two rigid partitions that are good conductors, Jeffries finds the same value for the criterion as Lord Rayleigh;

β) The fluid sheet is limited beneath by a rigid partition that conducts well, whereas the surface stays free and non-conductive (conditions found in most experiments in liquids);

γ) The fluid layer is contained between two rigid partitions that are non-conductors;

δ) For the problem of a fluid sheet with two surfaces free and good conductors, Jeffries finds the same value for the criterion as Lord Rayleigh.

To abridge, we will now set forth the following designation:

Problems of Jeffreys I and II, the cases α) and γ);

Problem of Bénard, case β);

Problem of Rayleigh, case δ).

A. R. Low (7) showed in 1925 the analogy between the instability of a fluid layer heated from beneath and that of a fluid layer between two coaxial cylinders turning in opposite directions, a problem studied mathematically and experimentally in 1923 by G. I. Taylor (22).

The conditions of Jeffreys' problem I are analogous to those of the problem of G. I. Taylor. In spite of this perfect analogy, the value of the criterion of instability found by H. Jeffreys in 1926, was no more than two thirds the value indicated by Taylor. To clear up this disagreement, A. R. Low (15-a) undertook in 1929 a work suggested by G. I. Taylor. He examined notably the problems

of Rayleigh, Jeffreys and Bénard. He found for the problem of Jeffreys a new value that agrees perfectly with that of Taylor.

H. Jeffreys(14-b) had moreover indicated in 1928 an inexactitude of his criterion given in 1926, and had indicated the new value which conforms to the result found by Low, and consequently to the criterion of the problem of G. I. Taylor. In 1930, A. R. Low (15-b) completed his work of 1929 by researches on the multiple modes of instability, from which it results that one can look at the formation of cellular eddies in superposed layers. We have shown that the same result can be obtained starting from the theory of Jeffreys. Also, we submitted this theoretical result to experimental verification that has not proved entirely conclusive.

The most recent theoretical work is due to P. Vernotte (16). This author makes several objections of principle to the Rayleigh theory, and in particular to the numerical value of the criterion; the order of magnitude of this criterion would be one hundred times smaller than that calculated by Rayleigh. The part relating to dimensions of cellular eddies and to eddies in bands is very developed and offers some particularly interesting results. In fact, P. Vernotte demonstrated that the size of the eddies can take different values for a given thickness, and that all these possible systems are quite stable. Our own researches have confirmed incontestably the exactitude of this theoretical result.

Finally we must point out the work of C. Woronetz (24) on perturbations in the motion of a fluid submitted to variations of

temperature. The author gives a generalization of the theory of Boussinesq and applies it to some cases where not only gravity intervenes, but also the forces of inertia. He next studies two particular problems of instability: lst the one in a fluid layer between two coaxial cylinders that turn at different angular speeds (problem of G. I. Taylor) and which are maintained each at a different constant temperature from the other; the other in the case of two concentric spheres. Woronetz does not treat cellular eddies specially, but one finds in his memoir some elements that may concern this problem.

What follows is an exposé, in part personal, of the principles of the theory of thermoconvective eddies. We complete the results of H. Jeffreys, in showing that they likewise contain the multiple solutions obtained by A. R. Low following another method. We then carry out the formal solution of the problem into numerical results for the purpose of confronting them with the results obtained by experiment.

2. Development of the theory of H. Jeffreys.

The formulation of the general equations. - Let us designate by x, y, z the coordinates of a viscous, fluid element, the axes x and y being placed in the horizontal plane, and the axis z vertical. Let u, v, w be its components of speeds; p, ρ and v the pressure, density and kinematic viscosity respectively, and g be the acceleration of gravity.

The general equations of motion of viscous fluids are written:

$$(1)\qquad \begin{cases} \rho \dfrac{Du}{Dt} = -\dfrac{\partial p}{\partial x} + \nu \rho \nabla^2 u \\ \rho \dfrac{Dv}{Dt} = -\dfrac{\partial p}{\partial y} + \nu \rho \nabla^2 v \\ \rho \dfrac{Dw}{Dt} = -\dfrac{\partial p}{\partial z} + \nu \rho \nabla^2 w - g\rho \ , \end{cases}$$

where ∇^2 is the La Placien (N.B. As we have taken Δ to designate the finite differences, we have designated by exception the La Placian by ∇^2):

$$\frac{\partial^2}{\partial x^2} + \frac{\partial^2}{\partial y^2} + \frac{\partial^2}{\partial z^2} \ ,$$

and where $\frac{D}{Dt}$ represents the Stokes operator*, and the equation of continuity:

$$(2)\qquad \frac{D\rho}{Dt} = -\rho\left(\frac{\partial u}{\partial x} + \frac{\partial v}{\partial y} + \frac{\partial w}{\partial z}\right).$$

Let us add the equation of heat:

$$(3)\qquad \frac{DT}{Dt} = x \nabla^2 T,$$

where x is the coefficient of thermal diffusion, and the characteristic equation that connects the density ρ to the temperature T:

$$(4)\qquad \rho = \rho_0 (1 - \alpha T),$$

where ρ_0 is the density at temperature zero and α the coefficient of thermal expansion.

Let p_s be the static pressure of the system at rest. The equations (1) reduce themselves in this case to:

$$(5)\qquad -\frac{\partial p_s}{\partial x} = 0, \quad -\frac{\partial p_s}{\partial y} = 0, \quad -\frac{\partial p_s}{\partial z} - g\rho_s = 0.$$

Let us write in the case of a movement:

$$p = p_s + \Delta p, \quad \rho = \rho_s + \Delta\rho \ , \quad T = T_s + \Delta T,$$

*loc. cit.

where Δp, $\Delta \rho$ and ΔT are the perturbations occurring to p_s, ρ_s and T_s following the movement.

Let us substitute these expressions in the equations (1), let us take account of the expressions (5) and let us omit all the squares of the small quantities proceeding from the perturbation. In these conditions, the operator $\frac{D}{Dt}$ reduces itself to $\frac{\partial}{\partial t}$, and the equations (1) become, consequently:

$$\rho_s \frac{\partial u}{\partial t} = - \frac{\partial \Delta p}{\partial x} + \nu \rho_s \nabla^2 u$$

$$\rho_s \frac{\partial v}{\partial t} = - \frac{\partial \Delta p}{\partial y} + \nu \rho_s \nabla^2 v$$

$$\rho_s \frac{\partial w}{\partial t} = - \frac{\partial \Delta p}{\partial z} + \nu \rho_s \nabla^2 w - g \Delta \rho,$$

or, again, in abbreviated notation:

$$(6) \qquad \rho_s \left(\frac{\partial}{\partial t} - \nu \nabla^2 \right) (u, v, w) = - \left(\frac{\partial}{\partial x}, \frac{\partial}{\partial y}, \frac{\partial}{\partial z} \right) \Delta p - (0, 0, g \Delta \rho).$$

In a steady regime, we can readily eliminate all the functions, except temperature T, in the following manner. If we form the divergence of the left and right part of (6), we can replace ρ_s by ρ_0 without committing any appreciable error, for ρ_0 is multiplied by a very small quantity. That leads to:

$$(7) \qquad \rho_0 \left(\frac{\partial}{\partial t} - \nu \nabla^2 \right) \left(\frac{\partial u}{\partial x} + \frac{\partial v}{\partial y} + \frac{\partial w}{\partial z} \right) = - \nabla^2 \Delta p - g \frac{\partial \Delta \rho}{\partial z} .$$

The differentiation of the equation characteristic (4) with respect to time gives with (3):

$$\frac{D\rho}{Dt} = - \rho_0 \alpha \frac{DT}{Dt} = - \rho_0 \alpha \chi \nabla^2 T.$$

Being given that $T = T_s + \Delta T$, one demonstrates the identity:

$$\nabla^2 T = \nabla^2 \Delta T.$$

Let us utilize these last relations and let us suppose that the difference of the extreme densities be small, in such fashion that the ratio ρ_0 / ρ should be sensibly equal to 1. Then the equation of continuity (2) becomes:

$$\frac{\partial u}{\partial x} + \frac{\partial v}{\partial y} + \frac{\partial w}{\partial z} = \alpha \chi \nabla^2 \Delta T. \tag{8}$$

Let us substitute the expression (8) into equation (7) by expressing $\Delta \rho$ in function of ΔT:

$$\alpha \chi \left(\frac{\partial}{\partial t} - \nu \nabla^2 \right) \nabla^2 \Delta T = - \frac{1}{\rho_0} \nabla^2 \Delta p + \alpha g \frac{\partial \Delta T}{\partial z}. \tag{9}$$

Let us do the operation

$$\frac{DT}{Dt} = \frac{DT_s}{Dt} + \frac{D\Delta T}{Dt} = \frac{\partial T_s}{\partial t} + u \frac{\partial T_s}{\partial x} + v \frac{\partial T_s}{\partial y} + w \frac{\partial T_s}{\partial z} + \frac{D\Delta T}{Dt},$$

where

$$\frac{\partial T_s}{\partial t} = \frac{\partial T_s}{\partial x} = \frac{\partial T_s}{\partial y} = 0,$$

and where the gradient of temperature following the vertical is a constant:

$$\frac{\partial T_s}{\partial z} = \beta .$$

Being given that the derivative $\frac{D\Delta T}{Dt}$ reduces itself to $\frac{\partial \Delta T}{\partial t}$, we obtain:

$$\frac{DT}{Dt} = \chi \nabla^2 \Delta T = \beta w + \frac{\partial \Delta T}{\partial t},$$

or again:

$$\left(\frac{\partial}{\partial t} - \chi \nabla^2 \right) (\Delta T) + \beta w = 0. \tag{10}$$

In expressing w by (10), the vertical equation of motion (6), where

we replace ρ_s by ρ_0, becomes:

$$(11) \qquad \left(\frac{\partial}{\partial t} - \chi\nabla^2\right)\left(\frac{\partial}{\partial t} - \nu\nabla^2\right)(\Delta T) = \frac{\beta}{\rho_0}\frac{\partial \Delta p}{\partial z} - g\alpha\beta\Delta T.$$

Let us eliminate Δp between (9) and (11). Let us apply first the operator ∇^2 to (11):

$$\left(\frac{\partial}{\partial t} - \chi\nabla^2\right)\left(\frac{\partial}{\partial t} - \nu\nabla^2\right)(\nabla^2\Delta T) = \frac{\beta}{\rho_0}\nabla^2\left(\frac{\partial \Delta p}{\partial z}\right) - g\alpha\beta\nabla^2\Delta T,$$

and let us take the derivative with respect to z of equation (9):

$$\alpha\chi\frac{\partial}{\partial z}\left(\frac{\partial}{\partial t} - \nu\nabla^2\right)(\nabla^2\Delta T) = -\frac{1}{\rho_0}\frac{\partial}{\partial z}(\nabla^2\Delta p) + g\alpha\frac{\partial^2\Delta T}{\partial z^2}.$$

In view of the identity

$$\frac{\partial}{\partial z}\left(\nabla^2\Delta p\right) = \nabla^2\left(\frac{\partial \Delta p}{\partial z}\right),$$

we find:

$$(12) \left[\alpha\chi\frac{\partial}{\partial z} + \frac{1}{\beta}\left(\frac{\partial}{\partial t} - \chi\nabla^2\right)\right]\left(\frac{\partial}{\partial t} - \nu\nabla^2\right)(\nabla^2\Delta T) = -g\alpha\left(\frac{\partial^2\Delta T}{\partial x^2} + \frac{\partial^2\Delta T}{\partial y^2}\right).$$

The product $\alpha\chi$ is very small, which allows us to neglect the term $\alpha\chi\frac{\partial}{\partial z}$. If the régime is steady the partial derivative $\frac{\partial}{\partial t}$ does not appear either, and (12) reduces itself to:

$$(13) \qquad \boxed{\nabla^6\Delta T = -\frac{g\alpha\beta}{\chi\nu}\left(\frac{\partial^2\Delta T}{\partial x^2} + \frac{\partial^2\Delta T}{\partial y^2}\right).}$$

Particular Integral - Let us now essay the solution of the type:

$$(14) \qquad \Delta T = \Delta T_0 \sin lx \sin my\, Z,$$

where Z is a function of direction z only.

Let us take the second derivative of ΔT with respect to x, y and z and let us substitute them in equation (13). We obtain:

$$(15) \qquad \left[\frac{\partial^2}{\partial z^2} - (l^2+m^2)\right]^3(\Delta T) = \frac{g\alpha\beta}{\chi\nu}(l^2+m^2)\Delta T.$$

In putting:

$$z = h\zeta, \tag{16}$$

where h is the thickness of the fluid layer under experiment,

$$(l^2 + m^2)h^2 = a^2, \tag{17}$$

and

$$\frac{g\alpha\beta h^4}{\varkappa\nu} = -\Lambda, \tag{18}$$

the equation (15) is finally written:

$$\left[\frac{\partial^2}{\partial\zeta^2} - a^2\right]^3(\Delta T) = -\Lambda a^2 \Delta T. \tag{19}$$

In this differential equation of the sixth order, there enters solely the partial derivative of ΔT according to ζ ; one can see, moreover, at once that with the form (14) for particular integral, the equation (19) comes to:

$$\left[\frac{d^2}{d\zeta^2} - a^2\right]^3(Z) = -\Lambda a^2 Z \text{ (*)}. \tag{20}$$

*For the sake of documentary interest, this fundamental equation is written in developed notation:

$$\frac{d^6Z}{d\zeta^6} - 3a^2\frac{d^4Z}{d\zeta^4} + 3a^4\frac{d^2Z}{d\zeta^2} - a^6Z = -\Lambda a^2 Z$$

Solution of the differential equation (20). Let us pass from the variable ζ to the variable ξ such that

$$\xi = \pi\zeta = \pi\frac{z}{h}, \tag{21}$$

and let us write

$$\frac{a^2}{\pi^2} = b^2 \quad \text{and} \quad \Lambda = M\pi^4. \tag{22}$$

The differential equation (20) then becomes:

$$\left(\frac{d^2}{d\xi^2} - b^2\right)^3(Z) + Mb^2Z = 0. \tag{23}$$

Guided by the presence of the sixth derivative in (23), let us try an integral Z satisfying the following relationship:

$$\frac{d^6 Z}{d\xi^6} = \sum_{r=1}^{\infty} A_r \sin r\xi. \tag{24}$$

The integration of (24) gives the function:

$$\begin{cases} Z = B_o + B_1\left(\frac{\pi}{2} - \xi\right) + \frac{B_2}{2!}\left(\frac{\pi}{2} - \xi\right)^2 + \frac{B_3}{3!}\left(\frac{\pi}{2} - \xi\right)^3 \\ \quad + \frac{B_4}{4!}\left(\frac{\pi}{2} - \xi\right)^4 + \frac{B_5}{5!}\left(\frac{\pi}{2} - \xi\right)^5 - \sum_{r=1}^{\infty} \frac{A_r}{r^6} \sin r\xi, \end{cases} \tag{25}$$

where $B_o \ldots\ldots B_5$ and A_r (r being all the integers) are arbitrary constants.

If we designate the polynomial in (25) by P, the equation (23) takes the form:

$$\sum_{r=1}^{\infty}\left[(r^2 + b^2)^3 - Mb^2\right]\frac{A_r}{r^6} \sin r\xi + \left[\left(\frac{d}{d\xi^2} - b^2\right)^3 + Mb^2\right]P = 0. \tag{26}$$

Let us put:

$$\left(\frac{\pi}{2} - \xi\right) = \eta,$$

and:

$$\frac{(r^2 + b^2)^3 - Mb^2}{r^6} A_r = \Lambda_r, \tag{27}$$

let us develop the operation:

$$\left[\left(\frac{d}{d\xi^2} - b^2\right)^3 + Mb^2\right]P,$$

and let us substitute the result in (26). We get:

$$\begin{cases} \sum_{r=1}^{\infty} \Lambda_r \sin r\xi = 3b^2\left(B_4 + B_5\eta\right) - 3b^4\left(B_2 + B_3\eta + \frac{B_4}{2!}\eta^2 + \frac{B_5}{3!}\eta^3\right) \\ \quad + \left(b^6 - Mb^2\right)\left(B_o + B_1\eta + \frac{B_2}{2!}\eta^2 + \frac{B_3}{3!}\eta^3 + \frac{B_4}{4!}\eta^4 + \frac{B_5}{5!}\eta^5\right) = Q. \end{cases} \tag{28}$$

To determine Λ_r, let us multiply the two members of (28) by sin r ξ and let us integrate them from 0 to π :

$$(29) \qquad \int_0^\pi \left[\sum_{r=1}^{\infty} \Lambda_r \sin r\xi\right] \sin r\xi \, d\xi = \int_0^\pi Q \sin r\xi \, d\xi .$$

The integral of the sum Σ reduces itself to the integral of a single member, whose value is known, to wit:

$$\int_0^\pi \Lambda_r \sin^2 r\xi \, d\xi = \frac{\pi}{2} \Lambda_r ,$$

for all the others are identically zero. (29) then becomes:

$$(29 \text{ bis}) \qquad \frac{\pi}{2} \Lambda_r = \int_0^\pi Q \sin r\xi \, d\xi .$$

In arranging in (28) the polynomial Q according to the powers of η , (29 again) takes the form:

$$(30) \quad \left\{ \begin{aligned} \frac{\pi}{2}\Lambda_r &= \left[3\,b^2 B_4 - 3\,b^4 B_2 + (b^6 - Mb^2) B_0\right] \int_0^\pi \sin r\xi \, d\xi \\ &+ \left[3\,b^2 B_5 - 3\,b^4 B_3 + (b^6 - Mb^2) B_1\right] \int_0^\pi \eta \sin r\xi \, d\xi \\ &- \left[3\,b^4 \frac{B_4}{2!} - (b^6 - Mb^2) \frac{B_2}{2!}\right] \int_0^\pi \eta^2 \sin r\xi \, d\xi \\ &- \left[3\,b^4 \frac{B_5}{3!} - (b^6 - Mb^2) \frac{B_3}{3!}\right] \int_0^\pi \eta^3 \sin r\xi \, d\xi \\ &+ (b^6 - Mb^2) \frac{B_4}{4!} \int_0^\pi \eta^4 \sin r\xi \, d\xi \\ &+ (b^6 - Mb^2) \frac{B_5}{5!} \int_0^\pi \eta^5 \sin r\xi \, d\xi . \end{aligned} \right.$$

When the power p of η , going from 0 to 5, and r are simultaneously equal or unequal, (even or odd), the integral

$$\int_0^\pi \eta^p \sin r\xi \, d\xi = 0 .$$

On the contrary, when one of the two numbers p and r is even and the other odd, and vice versa, one has in the two cases:

$$(31)\quad \begin{cases} \int_0^{\pi} \eta^p \sin r\xi \, d\xi = \\ \frac{2}{r}\left(\frac{\pi}{2}\right)^p \left[1 - \frac{p(p-1)}{r^2}\left(\frac{2}{\pi}\right)^2 + \frac{p(p-1)(p-2)(p-3)}{r^4}\left(\frac{2}{\pi}\right)^4 \right. \\ \qquad \left. - \frac{p(p-1)(p-2)(p-3)(p-4)(p-5)}{r^6}\left(\frac{2}{\pi}\right)^6 + \ldots\ldots\right]. \end{cases}$$

If p is even and r uneven, the relation (30) becomes with (31):

$$(32)\quad \begin{cases} \frac{1}{4}\pi r \Lambda_r = \left[3b^2 B_4 - 3b^4 B_2 + (b^6 - Mb^2)B_0\right] \\ \qquad - \left[3b^4 \frac{B_4}{2} - (b^6 - Mb^2)\frac{B_2}{2}\right]\left[1 - \frac{2}{r^2}\left(\frac{2}{\pi}\right)\right]\left(\frac{\pi}{2}\right)^2 \\ \qquad + (b^6 - Mb^2)\left[1 - \frac{12}{r^2}\left(\frac{2}{\pi}\right)^2 + \frac{24}{r^4}\left(\frac{2}{\pi}\right)^4\right]\frac{B_4}{24}\left(\frac{\pi}{2}\right)^4. \end{cases}$$

In the contrary case, where r is even and p odd, we obtain:

$$(33)\quad \begin{cases} \frac{1}{4}\pi r \Lambda_r = \left[3b^2 B_5 - 3b^4 B_3 + (b^6 - Mb^2)B_1\right]\frac{\pi}{2} \\ \qquad - \left[b^4 \frac{B_5}{2} - (b^6 - Mb^2)\frac{B_3}{6}\right]\left[1 - \frac{6}{r^2}\left(\frac{2}{\pi}\right)^2\right]\left(\frac{\pi}{2}\right)^3 \\ \qquad + \left[b^6 - Mb^2\right]\left[1 - \frac{20}{r^2}\left(\frac{2}{\pi}\right)^2 + \frac{120}{r^4}\left(\frac{2}{\pi}\right)^4\right]\frac{B_5}{120}\left(\frac{\pi}{2}\right)^5. \end{cases}$$

The coefficients A_r of the trigonometric series of the equation (25), connected to Λ_r by the relation (27), are determined as functions of the constants B_p and the differential equation (23) is formally resolved by (25).

From the fact that A_r diminishes like r^{-1}, the members of the trigonometric series of the solution (25) diminish like r^{-7}. The

series converges very rapidly, and as a consequence, the solution (25) has a practical value.

The numerical determination of the coefficients B_p depends on the boundary conditions to which the fluid is submitted.

Boundary Conditions - The general integral of the problem contains six arbitrary constants which we are going to be able to determine by six boundary conditions (three for each one of the two surfaces). These conditions are naturally different in the case of each physical problem of thermoconvection that one will have to consider.

a) Fixity of the temperatures on the two extreme surfaces - One supposes that the temperatures T_1 and T_2 of the two surfaces of the fluid sheet are maintained constant. Hence, the thermal perturbation in these localities:

$$\Delta T = 0$$

or again by virtue of (14):

(34) $$z = 0$$

b) Planeity of the two extreme surfaces - If the two limiting surfaces are plane, then the vertical component of speed in contact with the partitions is null:

$$w = 0.$$

Being given that the equation (10) reduces itself in a steady state to:

(35) $$w = \frac{\chi}{\beta} \nabla^2 \Delta T,$$

it results therefrom that also:

(36) $$\nabla^2 \Delta T = 0.$$

Let us carry out the operation $\nabla^2\Delta T$. The condition of the horizontality of the two surfaces then presents itself under the form:

$$\frac{d^2Z}{dz^2} - (l^2 + m^2)Z = 0,$$

or again with the variable ζ and by virtue of (16) and (17):

(37) $$\frac{d^2Z}{d\zeta^2} - a^2Z = 0.$$

The condition (37) combined with the condition (34), reduces itself on the two extreme surfaces to:

(38) $$Z'' = 0$$

c) Surfaces with friction. - If the walls exercise a rubbing on the fluid, which is always the case when they are solid, the two other components u and v, are also equal to zero. It follows therefrom that the divergence:

$$\frac{\partial u}{\partial x} + \frac{\partial v}{\partial y} = 0.$$

Let us take then equation (8), which yields with (36):

(39) $$\frac{\partial w}{\partial z} = \alpha\chi\nabla^2\Delta T = 0$$

The partial derivative of w with respect to z, hence is proportional to $\nabla^2\Delta T$, and by the intermediary of (35), to w also.

If one carries out the operation $\frac{\partial w}{\partial z}$, w being defined by (35), and if one considers the expression (39), then the condition sought acquires the form:

$$\frac{d^3Z}{dz^3} - (l^2 + m^2)\frac{dZ}{dz} = 0,$$

and with the variable ζ :

(40) $$\frac{d^3Z}{d\zeta^3} - a^2 \frac{dZ}{d\zeta} = 0.$$

d) Free surfaces without friction. - If we consider the other case where the surfaces remain free, the two speeds u and v have surely finite values. But, the value of w is very small, relatively, and such that one may suppose still that:

$$w = 0.$$

We can hence treat a free surface as a surface limited by a solid, plane, wall - considered always as without any friction. In consequence, condition (36) still obtains.

To find the new condition due to the absence of friction, let us differentiate (8) with respect to z:

$$\frac{\partial^2 u}{\partial x \partial z} + \frac{\partial^2 v}{\partial y \partial z} + \frac{\partial^2 w}{\partial z^2} = \alpha \chi \frac{\partial}{\partial z} \nabla^2 \Delta T.$$

Again, the derivatives $\frac{\partial^2 u}{\partial x \partial z}$ and $\frac{\partial^2 v}{\partial y \partial z}$ are null; from that:

$$\frac{\partial^2 w}{\partial z^2} = \alpha \chi \frac{\partial}{\partial z} \nabla^2 \Delta T.$$

α and χ being both very small, we commit a negligible error if we put:

$$\frac{\partial^2 w}{\partial z^2} = 0$$

In carrying out this double differentiation, we obtain by (35) and (14) the condition that the wall does not exert any friction, in the form:

$$\frac{d^4Z}{dz^4} - (l^2 + m^2) \frac{d^2Z}{dz^2} = 0,$$

or with the variable ζ :

(41) $$\frac{d^4 z}{d\zeta^4} - a^2 \frac{d^2 z}{d\zeta^2} = 0.$$

In presence of the condition (38), the expression (41) reduces itself to:

(42) $$Z^{IV} = 0.$$

In all cases, one supposes on the one hand that the temperature of both surfaces are fixed, and on the other hand that these two same surfaces are perfectly plane - which gives the first four conditions. As to the fifth and sixth conditions, they may be, according to the case, either identical - (for example: the fluid sheet is limited by two rough-surfaced walls, or the two surfaces are free and without any friction) -, or, they may be different - (for example: one of the two surfaces is free and without any friction, and the other is limited by a partition that is rough and creates friction).

In the following chapters, we take up only two cases. The first case approximates the conditions realized in our laboratory experiments (fluid sheet contained between two plane-surfaced walls, with friction and good conductors of heat - a case we have designated Problem I of Jeffreys). The second case corresponds rather to certain facts of the free atmosphere, for one can consider a layer of humid air limited by layers of dry air as a fluid sheet whose surfaces are almost free (fluid sheet with two surfaces free without friction - a case previously designated as Problem of Rayleigh).

Being given that in our problems studied the boundary conditions are the same for the two surfaces, the constants B_0, B_2, B_4 and B_1, B_3,

B_5 come in separately. That is as much as to say that there are two solutions in Z possible: the one symmetric and the other anti-symmetric about the one median plane ($z = h/2$).

Chapter VII

Determination in Certain Particular Cases of the Rayleigh-Bénard Criterion.

A. - Theoretical Section

Lord Rayleigh (13) has demonstrated that if thermoconvective currents are to be able to appear in a viscous fluid sheet, the difference of the extreme densities must attain a sufficient value.

In a problem that he had studied (fluid sheet with two free surfaces that are good conductors of heat), he found a characteristic inequality:

$$g\alpha\beta' \leqslant \frac{27\pi^4}{4}\frac{\chi\nu}{h^4},$$

which decides between the stable preconvective régime, and the convective régime.

If we put this inequality into the form:

$$\frac{g\alpha\beta' h^4}{\chi\nu} \leqslant \frac{27\pi^4}{4} \tag{43}$$

we recognize there the character of equation (18) of the preceding chapter. In considering that in the equation (18) the vertical gradients of temperature β is, by definition, negative, we find that the characteristic number (dimensionless) is

$$\Lambda = \frac{27\pi^4}{4} = 657.5$$

We shall see by what follows that Λ has a more general significance.

Its value depends upon the boundary conditions, amongst which also is found the particular problem of Lord Rayleigh.

Be it as it may, from now on we will call the number Λ the criterion of Rayleigh-Bénard, to memorialize the fact that Lord Rayleigh was the first to indicate the existence of the stable preconvective régime in the phenomenon of the cellular eddies of Bénard.

After having set forth in the previous chapter the principles of the Jeffreys theory (14), we can pass on to the numerical determination of the criterion Λ in certain interesting cases. In his theoretical memorandum, Jeffreys unhappily confined himself to the simple solution of the problem. His method, however, is more powerful: we have shown, in effect, that it contains the multiple solutions which A.R. Low (15) signalized in his analogous work, and for which solutions we give further on a generalization of the calculation of the corresponding Λs.

1. - Fluid sheet with two free surfaces that are good heat-conductors (Lord Rayleigh Problem).

In this problem, the conditions are the same for the two surfaces. Each surface being a good conductor, plane and without friction, the boundary conditions are expressed by (34), (38) and (42):

$$Z = 0, \quad Z'' = 0, \quad Z^{IV} = 0. \tag{44}$$

Symmetric solution.- p being even and r odd, one obtains for $\xi_1 = 0$ or $\xi_1 = \pi$:

$$Z = B_0 + \frac{B_2}{2!}\left(\frac{\pi}{2}\right)^2 + \frac{B_4}{4!}\left(\frac{\pi}{2}\right)^4 ,$$

$$Z'' = B_2 + \frac{B_4}{2}\left(\frac{\pi}{2}\right)^2 ,$$

$$Z^{IV} = B_4$$

In virtue of the boundary conditions, (44), one finds:

$$B_4 = B_2 = B_0 = 0$$

But, by (32), all Λ_r simultaneously vanish. The sole solution different from zero is this one when the numerator of (27) vanishes:

$$(r^2 + b^2)^3 - Mb^2 = 0,$$

whence, with (22) that connects M to Λ :

$$(r^2 + b^2)^3 = Mb^2 = \frac{\Lambda}{\pi^4} b^2,$$

or again:

(45) $$\Lambda = \frac{(r^2 + b^2)^3 \pi^4}{b^2} .$$

Let us study the variation of Λ as a function of the constant b. For:

(45') $$b = \frac{r}{\sqrt{2}} ,$$

Λ attains its relative minimum:

(46) $$\Lambda = r^4 \frac{27\,\pi^4}{4} ,$$

and for r = 1, its absolute minimum:

(46a) $$\Lambda_{min} = \frac{27\,\pi^4}{4} = 657.5$$

The value obtained is exactly the same that Lord Rayleigh also found.

Asymmetric solution. - r is even and p, odd. One obtains, as before, in the symmetric solution:

$$B_5 = B_3 = B_1 = 0.$$

The relative minimum of Λ_r is represented also in the form of (46). This relation, hence, has a general validity, for r even and odd.

We shall later see that the criteria (46) correspond to the eddies in superposed layers, r being the number of modes contained in the total thickness h of the fluid layer.

2. Fluid sheet contained between two rigid walls that are good heat conductors (Problem of H. Jeffreys).

This is the case that interests us first, as it approximates conditions realized during our experiments in a layer of air.

Let us suppose that the conditions are the same for the two surfaces. If the walls are good conductors of heat, plane and rough (with friction), one expresses these conditions by (34), (38) and (40). In choosing the variable ξ defined by (21), the group of the three conditions presents itself by:

$$Z = 0, \quad Z'' = 0, \quad Z''' - b^2 Z' = 0. \tag{47}$$

Symmetric solution for any number of modes piled up.- r odd and p even. The conditions (47) give us for $\xi = 0$ or π :

$$B_0 + \frac{B_2}{2}\left(\frac{\pi}{2}\right)^2 + \frac{B_4}{24}\left(\frac{\pi}{2}\right)^4 = 0,$$

$$B_2 + \frac{B_4}{2}\left(\frac{\pi}{2}\right)^2 = 0,$$

(48)

$$-\frac{\pi^2}{8}\left(1 + \frac{b^2\pi^2}{12}\right) + \sum_n^\infty \frac{1}{r^2} + b^2 \sum_n^\infty \frac{1}{r^4} - \sum_n^\infty \frac{r^2(r^2+b^2)}{(r^2+b^2)^3 - Mb^2} = 0,$$

where n signifies the number of modes piled up.

If we write:

$$\sum_n^\infty = \sum_1^\infty - \sum_1^{n-2},$$

we obtain:

$$\sum_n^\infty \frac{1}{r^2} + b^2 \sum_n^\infty \frac{1}{r^4} = \sum_1^\infty \frac{1}{r^2} + b^2 \sum_1^\infty \frac{1}{r^4} - \left[\sum_1^{n-2} \frac{1}{r^2} + b^2 \sum_1^{n-2} \frac{1}{r^4}\right],$$

where:

$$\sum_1^\infty \frac{1}{r^2} = \frac{\pi^2}{8} \quad \text{and} \quad \sum_1^\infty \frac{1}{r^4} = \frac{\pi^4}{96}.$$

With that, the third condition of (48) takes the form:

$$-\sum_n^\infty \frac{r^2(r^2+b^2)}{(r^2+b^2)^3 - Mb^2} - \left[\sum_1^{n-2} \frac{1}{r^2} + b^2 \sum_1^{n-2} \frac{1}{r^4}\right] = 0,$$

or again, if we replace b^2 by $\frac{a^2}{\pi^2}$ and M by $\frac{\Lambda}{\pi^4}$:

$$(49) \quad \sum_n^\infty \frac{r^2\pi^2(r^2+a^2)}{(r^2+a^2)^3 - \Lambda a^2} + \frac{1}{\pi^2}\left[\sum_1^{n-2} \frac{1}{r^2} + \frac{a^2}{\pi^2} \sum_1^{n-2} \frac{1}{r^4}\right] = 0.$$

Let us now consider the sum:

$$(50) \quad \sum_n^\infty \frac{r^2\pi^2}{(r^2\pi^2+a^2)^2} = \sum_1^\infty \frac{r^2\pi^2}{(r^2\pi^2+a^2)^2} - \sum_1^{n-2} \frac{r^2\pi^2}{(r^2\pi^2+a^2)^2}.$$

Being given that:

$$\sum_1^\infty \frac{4a}{r^2\pi^2+a^2} = \operatorname{tgh} \frac{a}{2},$$

it is easy to show that:

$$(51)\quad \sum_{1}^{\infty} \frac{r^2\pi^2}{(r^2\pi^2 + a^2)^2} = \frac{1}{8}\left(\frac{1}{a} + \frac{d}{da}\right) \operatorname{tgh} \frac{a}{2} = \frac{1}{8a} \operatorname{tgh} \frac{a}{2} + \frac{1}{16} \operatorname{sech}^2 \frac{a}{2} = K.$$

Let us subtract the expression (50) from (49). We get, after reduction:

$$(52)\quad \sum_{n}^{\infty} \frac{r^2\pi^2 a^2 \Lambda}{\left[(r^2\pi^2 + a^2)^3 - \Lambda a^2\right](r^2\pi^2 + a^2)^2} + H = 0,$$

where:

$$(53)\quad H = K - \sum_{1}^{n-2} \frac{r^2\pi^2}{(r^2\pi^2+a^2)^2} + \frac{1}{\pi^2}\left[\sum_{1}^{n-2} \frac{1}{r^2} + \frac{a^2}{\pi^2} \sum_{1}^{n-2} \frac{1}{r^4}\right].$$

Let us extract from (52) the first term. Then (52) is written:

$$(54)\quad \left\{ \begin{array}{l} \dfrac{n^2\pi^2 a^2 \Lambda}{\left[(n^2\pi^2+a^2)^3 - \Lambda a^2\right](n^2\pi^2+a^2)^2} \\ \\ + \displaystyle\sum_{n+2}^{\infty} \dfrac{r^2\pi^2 a^2 \Lambda}{\left[(r^2\pi^2+a^2)^3 - \Lambda a^2\right](r^2\pi^2+a^2)^2} + H = 0 \end{array} \right.$$

One determines the value of Λ by successive approximation. By neglecting the sum $\sum_{n+2}^{\infty}$, one obtains the first approximation, which gives, after a few transformations:

$$(55)\quad a^2\Lambda = \frac{(n^2\pi^2+a^2)^3}{1 - \dfrac{n^2\pi^2}{H(n^2\pi^2+a^2)^2}}.$$

What interests us the most is the minimum of Λ in function of a. We obtain it very easily if we choose for a several values and we calculate the corresponding Λs. We carry this first approximation for Λ in the sum of the equation (54). We repeat the same operation enough times until the value of Λ approaches a limit.

When the number of modes n is very large, and above all when it

becomes infinite, equation (53) tends towards a limit:

$$H = \frac{1}{8} + \frac{a^2}{96},$$

which, moreover, is infinite because a is infinite. In fact, for $n = \infty$, the term as denominator of (55)

$$\frac{n^2\pi^2}{H(n^2\pi^2+a^2)^2} = 0,$$

and the equation (55) reduces itself to:

$$a^2\Lambda = (n^2\pi^2+a^2)^3$$

For:

$$a = n\frac{\pi}{\sqrt{2}}$$

Λ becomes minimum:

$$\Lambda = n^4\frac{27\pi^4}{4}.$$

This result is interesting, for we find thus the same expression of Λ minimum, as in the problem of Rayleigh treating piled-up eddies (see equation (46)). This proves that the influence of the walls disappears when the number of piled-up modes is sufficiently great, and that then we can treat this case like the problem of Lord Rayleigh.

Solution for a single vertical mode of eddies. - The most important case, of them all, is that one where the number of vertical modes of eddies reduces itself to one alone: a problem already calculated by H. Jeffreys, and, by a different approach, by A. R. Low.

In placing in our previous equations n = 1, we discover at once the equations that figure in the memorandum of H. Jeffreys. In fact, the equation (53) reduces itself to identity:

$$H = K,$$

and the equation (54) to:

$$(56)\quad \left\{ \begin{array}{l} \dfrac{\pi^2 a^2 \Lambda}{[(\pi^2+a^2)^3 - \Lambda a^2](\pi^2+a^2)^2} \\ + \sum_3^\infty \dfrac{r^2\pi^2 a^2 \Lambda}{[(r^2\pi^2+a^2)^3 - \Lambda a^2](r^2\pi^2+a^2)^2} + K = 0, \end{array} \right.$$

and in like fashion, the equation (55) reduces itself to:

$$(57)\quad a^2\Lambda = \frac{(\pi^2+a^2)^3}{1 - \dfrac{\pi^2}{K(\pi^2+a^2)^2}}.$$

In utilizing (56) and (57), we have found, by a first and second approximation, (a third would be useless), the results contained in the following table:

a		$\frac{\pi}{2}$	2.4	2.6	3	3.1	3.2	3.7	4
Λ	1st approx.	2910	1880	1790	1718.4	1714.9	1716.7	1794	1890
	2nd approx.	2890	1870	1780	1711	1707.5	1709.3	1785	1880

Λ takes the minimum value for a = 3.1; it is equal to 1707.5. These values differ slightly from those given by Jeffreys (Λ = 1709.5; a = 3.17), and they more nearly approach those of A.R. Low (Λ = 1704.4; a = 3.09).

Asymmetric solution for any number of piled-up modes. - Here, r is even and p odd. The conditions (47) applied to the equation (25) and to its derivatives, give for $\xi_0 = 0$ or π :

$$(58)\quad \left\{ \begin{array}{l} B_1 + \dfrac{B_3}{6}\left(\dfrac{\pi}{2}\right)^2 + \dfrac{B_5}{120}\left(\dfrac{\pi}{2}\right)^4 = 0, \\ B_3 + \dfrac{B_5}{6}\left(\dfrac{\pi}{2}\right)^2 = 0, \\ -\dfrac{b^2}{90}\left(\dfrac{\pi}{2}\right)^4 - \dfrac{1}{6}\left(\dfrac{\pi}{2}\right)^2 + \sum_n^\infty \dfrac{1}{r^2} + b^2 \sum_n^\infty \dfrac{1}{r^4} - \sum_n^\infty \dfrac{r^2(r^2+b^2)}{(r^2+b^2)^3 - Mb^2} = 0, \end{array} \right.$$

where n is an even number of modes piled up.

By putting:

$$\sum_{n}^{\infty} = \sum_{2}^{\infty} - \sum_{2}^{n-2}$$

one obtains

$$\sum_{n}^{\infty} \frac{1}{r^2} + b^2 \sum_{n}^{\infty} \frac{1}{r^4} = \sum_{2}^{\infty} \frac{1}{r^2} + b^2 \sum_{2}^{\infty} \frac{1}{r^4} - \left[\sum_{2}^{n-2} \frac{1}{r^2} + b^2 \sum_{2}^{n-2} \frac{1}{r^4} \right],$$

where:

$$\sum_{2}^{\infty} \frac{1}{r^2} = \frac{\pi^2}{24} \quad \text{and} \quad \sum_{2}^{\infty} \frac{1}{r^4} = \frac{\pi^4}{1440} ;$$

the third condition of (58) reduces itself to:

$$- \sum_{n}^{\infty} \frac{r^2(r^2+b^2)}{(r^2+b^2)^3 - Mb^2} - \left[\sum_{2}^{n-2} \frac{1}{r^2} + b^2 \sum_{2}^{n-2} \frac{1}{r^4} \right] = 0$$

It becomes, by replacing b^2 by $\frac{a^2}{\pi^2}$ and M by $\frac{\Lambda}{\pi^4}$:

$$\sum_{n}^{\infty} \frac{r^2\pi^2(r^2+a^2)}{(r^2\pi^2+a^2)^3 - \Lambda a^2} + \frac{1}{\pi^2} \left[\sum_{2}^{n-2} \frac{1}{r^2} + \frac{a^2}{\pi^2} \sum_{2}^{n-2} \frac{1}{r^4} \right] = 0$$

By carrying out the same operations as in the symmetric problem, we find an expression analogous to (54):

$$(59) \quad \left\{ \frac{n^2\pi^2 a^2 \Lambda}{\left[(n^2\pi^2+a^2)^3 - \Lambda a^2\right](n^2\pi^2+a^2)^2} + \sum_{n+2}^{\infty} \frac{r^2\pi^2 a^2 \Lambda}{\left[(r^2\pi^2+a^2)^3 - \Lambda a^2\right](r^2\pi^2+a^2)^2} + H' = 0, \right.$$

where:

$$(60) \quad H' = \sum_{2}^{\infty} \frac{r^2\pi^2}{(r^2\pi^2+a^2)^2} - \sum_{2}^{n-2} \frac{r^2\pi^2}{(r^2\pi^2+a^2)^2} + \frac{1}{\pi^2} \left[\sum_{2}^{n-2} \frac{1}{r^2} + \frac{a^2}{\pi^2} \sum_{2}^{n-2} \frac{1}{r^4} \right].$$

By utilizing the identity:

$$\operatorname{ctgh} \frac{a}{2} = \frac{2}{a} + \sum_{r=2}^{\infty} \frac{4a}{r^2\pi^2 + a^2} ,$$

we obtain:

$$\sum_{r=2}^{\infty} \frac{r^2\pi^2}{(r^2\pi^2+a^2)^2} = \frac{1}{8}\left(\frac{1}{a}+\frac{d}{da}\right)\left(\text{ctgh}\,\frac{a}{2}-\frac{2}{a}\right)$$

$$= \frac{1}{8a}\,\text{ctgh}\,\frac{a}{2} - \frac{1}{16}\,\text{cosecant}^2\,\frac{a}{2} = K'.$$

If we omit in (59) the sum $\sum_{n+2}^{\infty}$, we obtain a formula analogous to (55):

$$a^2\Lambda = \frac{(n^2\pi^2+a^2)^3}{1-\frac{n^2\pi^2}{H'(n^2\pi^2+a^2)^2}}. \tag{61}$$

It is evident that (61) leads to the same result as (55) when the number of modes piled up, n, is large. In fact, for:

$$a = n\frac{\pi}{\sqrt{2}},$$

Λ becomes minimum and takes the form:

$$\Lambda = n^4\frac{27\pi^4}{4}.$$

We have likewise obtained this result in the problem of Lord Rayleigh.

Solution for two stages of eddies. - The smallest number of the vertical mode in the antisymmetric solution is equal to 2. The equation (60) reduces itself to:

$$H' = K',$$

and the formula (61) becomes for n = 2:

$$a^2\Lambda = \frac{(4\pi^2+a^2)^3}{1-\frac{4\pi^2}{K'(4\pi^2+a^2)^2}}. \tag{62}$$

By choosing different values for a, one obtains from (62) the corresponding values for Λ, as here:

a	4	4.8	5.4	5.45	5.5	6.1	6.5
Λ	19,900	18,135	17,805	17,809	17,812	18,235	18,775

The minimum value of Λ is, in first approximation, equal to 17,805 for a = 5.4. The second approximation, which suffices entirely, gives:

$$\Lambda = 17,650 \text{ for } a = 5.4$$

B. - Experimental Section

In 1934, when our experiments began, the existence of a stable, preconvective régime in a fluid layer heated from beneath had not been as yet confirmed by experiment. In these circumstances, the experimental proof of the criterion Λ constituted, in the views of Mr. H. Bénard, an essential part of the labors in view. However, in the course of our own researches, R. J. Schmidt and S. W. Milverton (31), made similar experiments in a layer of water contained between two metal plaques (good conductors), and from 4 to 5.5 mm thick. The two authors found that the value of Λ that H. Jeffreys had taken for such boundary conditions, namely $\Lambda = 1,709.5$, was well confirmed under test.

In these conditions, we have tried to approach solely the case of a layer of air limited by two rigid walls. In 1936, we published in the Comptes Rendus de l'Académie des Sciences (21-b) the first results confirming the existence of a stable preconvective régime. We will give hereafter the description of the method employed in our researches on the Rayleigh-Bénard criterion and the results

that we have obtained. Let us point out again that, during this time a similar work has been executed by K. Chandra (25). His results, published in 1938 in the "Proceedings of the Royal Society", are in full agreement with our own in the interval where comparison is possible.

1. Some supplementary remarks relative to the Rayleigh-Bénard criterion.

If we replace in the characteristic inequality of Lord Rayleigh (43) the numerical term $\frac{27\pi^4}{4}$ by Λ, the value of which depends, as we have seen, on boundary conditions, we obtain the generalized inequality:

$$\frac{g\alpha\beta' h^4}{\chi\nu} \leqslant \Lambda \tag{63}$$

For the experimental verification of this inequality, it is necessary to produce either extreme density or temperature differences.

On the one hand the vertical gradient of temperature is expressed by:

$$\beta' = \frac{T_2 - T_1}{h} \tag{64}$$

and on the other hand, it is easy to find for the coefficient of thermal expansion:*

$$\alpha = \frac{\rho_1 - \rho_2}{\rho_2 (T_2 - T_1)}, \tag{65}$$

ρ_1 and ρ_2 being the densities of the fluid at the upper surface and

*By definition:

$$= \rho_0 + \Delta\rho = \rho_0 \left(1 + \frac{\Delta\rho}{\rho_0}\right) = \rho_0 (1 - \alpha\Delta T);$$

then:

$$\alpha = \frac{\rho_0 - \rho}{\rho_0 \Delta T} = \frac{\rho - \rho_0}{\rho_0 (T_0 - T)}$$

on the bottom, and T_1 and T_2 the corresponding temperatures. By carrying (64) and (65) in the inequality (63) this last becomes:

(66) $$\frac{\rho_1 - \rho_2}{\rho_2} \frac{gh^3}{\varkappa \nu} \leqslant \Lambda$$

If the fluid is a gas it is fitting to introduce in (66) the extreme temperatures T_1 and T_2.

The characteristic equation for perfect gasses is written:

$$pv = R(273 + T)$$

In our problem, we can suppose that the pressure p is constant, and that the whole of specific volume v depends on the temperature T; in these conditions:

$$\frac{v_1}{v_2} = \frac{\rho_2}{\rho_1} = \frac{273 + T_1}{273 + T_2};$$

in fine, the inequality of Rayleigh presents itself under the form:

(66 bis) $$\frac{T_2 - T_1}{T_1 + 273} \frac{gh^3}{\varkappa \nu} \leqslant \Lambda ,$$

which lends itself readily to interpretation.

Λ being a constant without dimensions, defined entirely in each individual problem, it hence results that the difference of temperatures $T_2 - T_1$, necessary to release the thermoconvective currents, must be higher in proportion as the temperature T_1 and the coefficients of kinematic viscosity ν and heat diffusion $\varkappa$ are the greater, but it (the difference of temperatures) must diminish in inverse ratio to the third power of the thickness h of the fluid layer.

2. Numerical evaluations. Delimitation of the interval of the thicknesses where Λ might be experimentally defined.

Certain numerical evaluations are needed for the execution of the experiments. Let us first examine what is the order of magnitude of the critical difference of temperatures as a function of the average temperature of the fluid. To fix the ideas, let us take a layer of air with thickness 1 cm, and calculate $(T_2 - T_1)$ critical for the problems of Rayleigh and Jeffreys, when Λ is equal to 657.5 and 1,707.5 respectively.

h being equal to 1 cm, one obtains from the inequality (66 bis) the critical difference of temperatures:

$$(67) \qquad T_2 - T_1 = \frac{\Lambda}{g} \varkappa \nu \ (T_1 + 273) \simeq \frac{\Lambda}{g} \varkappa \nu (T_m + 273),$$

where $\varkappa$ and ν are two functions of the average temperature $T_m = \frac{T_1 + T_2}{2}$ of the gas.*

By definition:

$$\nu = \frac{\mu}{\rho} \text{ and } \varkappa = \frac{\lambda}{C_p \rho}.$$

where we designate by μ the viscosity, by λ the thermal conductibility, and by C_p the specific heat at atmospheric pressure.

These four quantities have for respective expressions as a

*The temperature differences needed to release the convective currents are very small when the thickness of the gaseous layer is larger than 1 cm; so, it is reasonable to consider $\varkappa$ and ν as two functions of the initial temperature T_1, or even to replace T_1 in the second member of (67) by T_m.

function of the average temperature:

$$\mu = 0.000,1824 - 0.000,000,493(23° - T_m),$$

$$\rho = \frac{1.2927 \cdot 10^{-3}}{(1 + 0.00367\ T_m)} \ \frac{gr}{cm^3} \ ,$$

$$\lambda = 0.0000568(1 + 0.0026\ T_m) \ \frac{cal}{cm\ s\ °C} \ ,$$

$$C_p = 0.2405 + 0.0000095\ T_m \ \frac{cal}{gr} \ .$$

In choosing for T_m 0°, 20° and 50°C, we obtain for χ and the following values:

T_m	0°	20°	50°
χ	0.1826	0.2060	0.2446
ν	0.1323	0.1525	0.1792

If we carry these values in the expression (67) we find the table that we give below:

T_m (°C)	$(T_2 - T_1)$ critical (°C)	
	$\Lambda = 657.5$ (Rayleigh)	$\Lambda = 1707.5$ (Jeffreys)
0	4.42	11.5
20	6.16	16.1
50	9.5	24.7

We see that the average temperature exercises a considerable influence on the value of the critical difference of temperatures.

The results of the preceding table have been transferred onto Figure 66, where we have carried as abscissa the average temperature T_m and as ordinate the critical difference of the temperatures.

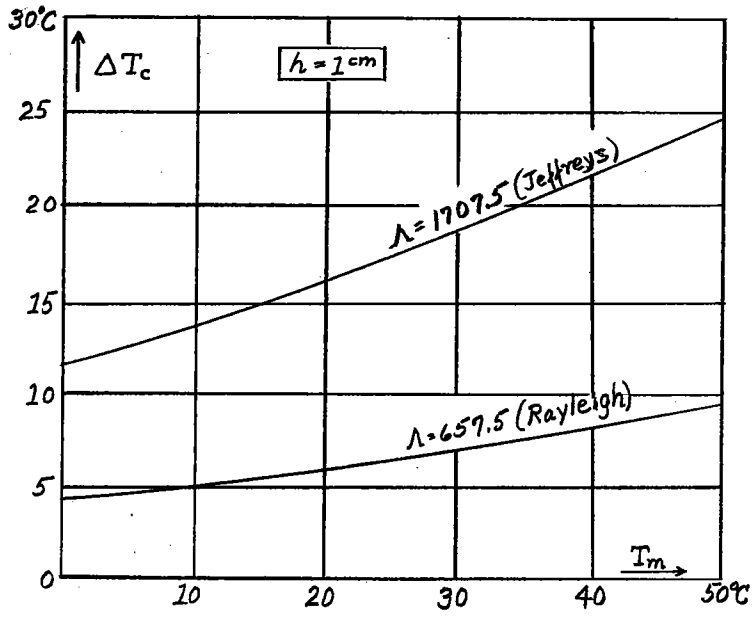

Fig. 66 Critical difference of stability of extreme temperatures as a function of the average temperature of the air, for h = 1 cm.

The interval of thickness in which the experimental verification of Λ has meaning is very restricted. The lower limit is imposed by the fact that the study theoretically supposes weak the difference of the two extreme densities, and by consequence, the two temperatures. In fact, the disagreement becomes very important as soon as the thickness of the layer of air is less than 1 cm. As for the upper limit, it depends on the precision of measuring instruments and the producing apparatus of the eddies. In supposing it possible to measure the temperature to 1/20°C, about, ($T_2 - T_1 = 0.05$), one can calculate the maximum thickness from the formula drawn from the inequality (66 bis):

$$h \leq \sqrt[3]{\frac{\chi \nu}{g} \frac{T_1 + 273}{T_2 - T_1} \Lambda} .$$

One finds, with average temperature 20°C and for $\Lambda = 1{,}707.5$ (problem of Jeffreys), $h_{max} = 6.8$ cm.

In reality, the experiment showed that results were uncertain - starting at a thickness of 6 cm. In these conditions, the interval of thickness explored has been contained between 1 and 6 cm.

3. Execution of experiments. Results.

The measures and the observations have been made in a layer of air in translational motion. This method appears to be more advantageous than when the gas is at rest; the in-coming air actually retains a very constant temperature, and by sweeping continually the two limiting plaques, it assures a more uniform distribution of the two extreme temperatures.

By the aid of a precise mercury thermometer, reading to 1/20°C, we have measured the temperature of the metal bottom T_2, the temperature below the ceiling of glass plate T_1, and the temperature of the air arriving in the experiment chamber T_A. This last can be identified with the average temperature $T_m = \frac{1}{2}(T_1 + T_2)$.

The operative manual goes as follows: One heats progressively the layer of air, and one watches the appearance of the first ascending currents, rendered visible by successive injections of smoke.

It is easy to show qualitatively that a fluid layer can stay stable, even if the denser (cold) layers are above the less dense (hot) layers. But, the precise determination of the critical moment when one passes from the stable preconvective regime to the thermo-

convective régime is more difficult.

One begins by determining a sufficiently small interval of temperatures comprising the critical value of the difference of the two extreme temperatures. For instance, in a layer of air 15 mm thick, a temperature difference of 1.5°C occasions no ascending movement, whereas - the eddies in longitudinal bands develop themselves entirely when this difference of temperatures is equal to 3°C. To find the exact critical value of $(T_2 - T_1)$, we examine only the restricted interval.

It is evident that this class of experiments depends somewhat too much on the judgment of the experimenter. Only a great number of trials, carried out by a number of operators could erase the subjective character.

To give more certitude to our experimental results, we repeated the experiments several times for each thickness. The observations were taken in two senses, to wit: 1 Observation of appearance of ascending currents during the period of progressive heating; 2 Observation of the disappearance of these currents during the period when the metal bottom was being allowed to cool slowly.

We have determined the criterion for thicknesses of 11, 22, 30, 40 and 63 mm. The results are shown in the following table, Page 121.

To facilitate the interpretation, let us write the inequality (66 bis) under the form:

$$(68) \qquad \frac{T_2 - T_1}{(T_m + 273)\chi\nu} \leqslant \frac{\Lambda}{gh^3} \quad *$$

*See note on page 116.

h (mm)	T_2 (°C)	T_1 (°C)	ΔT_c (°C)	T_m (°C)	$\varkappa$ (CGS)	ν (CGS)	$\frac{\Delta T_c}{(T_m+273)\varkappa\nu}$	$\frac{657.5}{gh^3}$	$\frac{1707.5}{gh^3}$	Λ (experiments)
11	36.1	26.6	9.5	31.35	0.1626	0.2207	0.872	0.525	1.364	1,140
	30.5	20.6	9.9	25.55	0.1575	0.2132	0.990			1,292
22	23.7	22.85	0.85	23.28	0.1554	0.2102	0.088	0.063	0.1635	920
	24.3	23.2	1.1	23.75	0.1558	0.2108	0.113			1,180
	22.8	21.9	0.9	22.35	0.1546	0.209	0.095			993
30	19.05	18.85	0.2	18.95	0.1516	0.2047	0.022	0.0248	0.0645	583
	21.01	20.80	0.21	20.9	0.1533	0.2072	0.0225			596
	19.00	18.84	0.16	18.92	0.1515	0.2046	0.018			477
40	19.70	19.65	0.05	19.67	0.1522	0.2056	0.0055	0.0105	0.0272	345
	21.26	21.36	0.10	21.31	0.1537	0.2077	0.0106			665
	20.63	20.54	0.09	20.59	0.1530	0.2068	0.0097			608
	19.66	19.60	0.06	19.63	0.1522	0.2055	0.0066			414
63	18.00	17.95	0.05	17.97	0.1507	0.2034	0.0056	0.0027	0.007	1,373
	18.10	18.08	0.02	18.09	0.1508	0.2035	0.0022			540

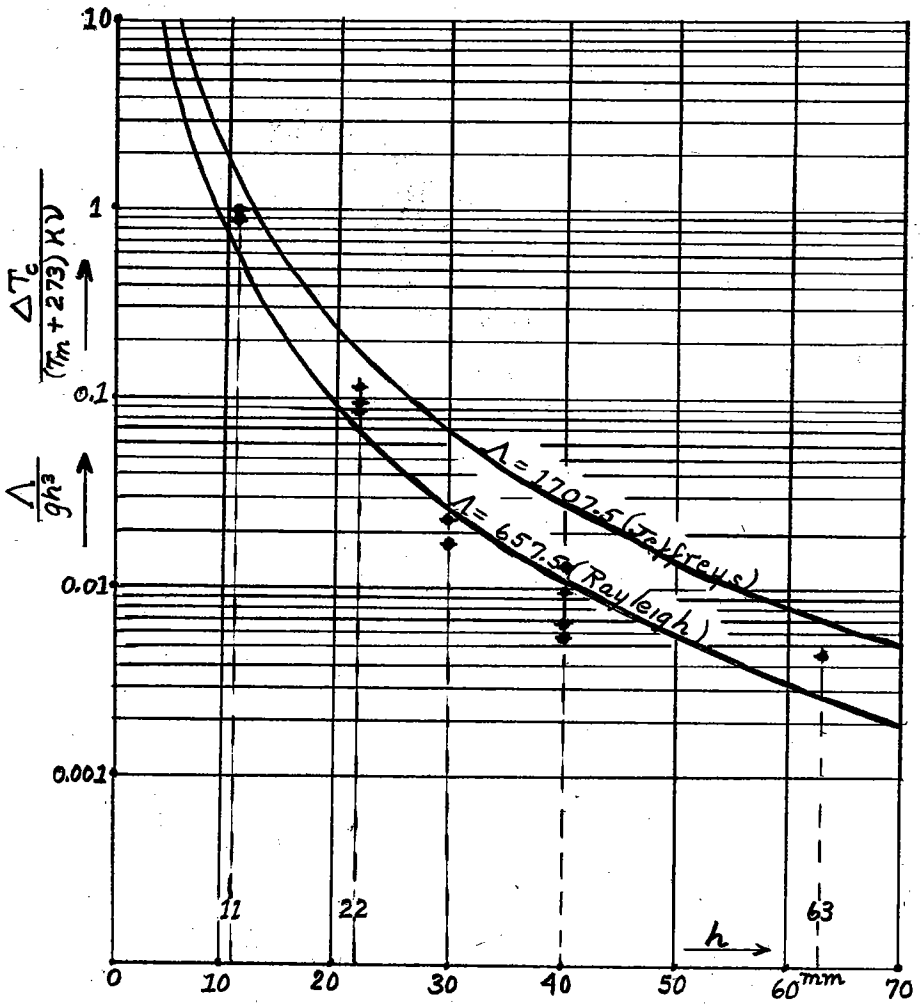

Fig. 67. Criteria of Rayleigh and Jeffreys and the experiment in air.

The first member of this inequality contains the terms to be determined experimentally (χ and ν are functions of the average temperature T_m), while the second member is calculable if the boundary conditions are determined.

We have calculated the second member of (68) for $\Lambda = 657.5$, and for $\Lambda = 1707.5$ (problems of Rayleigh and of Jeffreys) as a function of the thickness h. One finds these values in the columns (9) and (10) of the table. Column (8) contains the experimental values, calculated according to the first member of (68). One can see that

these last place themselves for h = 11, 22, and 63 mm, between the cases $\Lambda = 657.5$ and $\Lambda = 1707.5$ while for h = 30 and 40 mm, they place themselves below the case $\Lambda = 657.5$.

The diagram, Figure 67, represents these experimental results, and compares them to the theoretical results. In this diagram we have carried as the abscissa the thickness h, and as the ordinate, on a logarithmic scale, the function, on the one hand, $\frac{\Lambda}{gh^3}$, for two theoretical criteria, 657.5 and 1,707.5, and on the other hand, the values of $\frac{(T_2 - T_1)_c}{(T_m + 273)\chi\nu}$, obtained experimentally.

4. - Conclusions

We have confirmed experimentally that the regime of thermoconvective currents is actually preceded by a stable preconvective régime. This fundamental result, found in the particular problem of a layer of air, is applicable to all the other problems that one could imagine.

The experiments were done in a range of thicknesses going from 11 to 63 mm. We have shown that the thickness of 6 cm would be, in the case of gasses, the upper limit where one can practically establish the existence of any stable, preconvective régime. This limit depends on the precision of measurement of temperature and of function of the apparatus producing the thermoconvective eddies. When the thickness of the air layer exceeds the value of 6 cm, the thermoconvective currents there release themselves spontaneously in presence of the slightest difference of temperatures.

Being given that the boundary conditions realized in our experiments are not exactly the same as one supposes in the problem of Jeffreys (the glass plate forming the ceiling is not a good heat-conductor), the criterion Λ differs greatly from the theoretical value 1705.5. On the other hand, Λ varies in our experiments from 345 to 1,373 (cf. column 11 of the table), for, just as we have stated, the determination of the moment when the first ascending currents manifest themselves, depends entirely upon the judgment of the experimenter.

Chapter VIII Part 1.

Dimensions of thermoconvective eddies.

A. Theoretical Section

1. - Definitions.

The relation of the transversal dimensions and of the thickness h of the cellular eddies is an essential characteristic of their geometric properties.

In the case of two-dimensional cellular eddies and of eddies in bands, either longitudinal or transversal, one takes by preference for transversal dimension the distance λ between two eddy centers having the same direction of rotation (Fig. 68-a). At the same time, λ is the total width of two rectangular cellules (eddies with two dimensions) or of two twin rolls (longitudinal or transverse), constituting by definition an eddy unit.

When it is a question of regular polygonal eddies, it is fitting to take for λ the shortest distance between the vertical axes of two

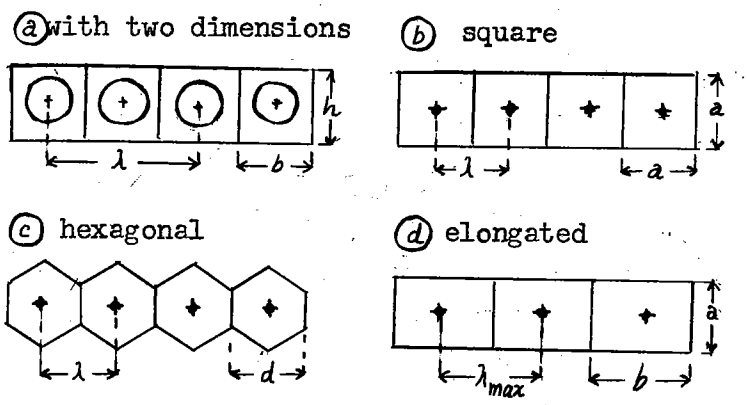

Fig.68. Transversal dimensions of the principal forms of cellular eddies.

adjacent eddies. If the cellules are square or hexagonal in form, the distance λ expresses equally their widths (Fig. 68 - b,c).

Finally, if the cellules have the elongated form, one should indicate two relationships, λ/h, the one for λ minimum, and the other for λ maximum (Fig. 68-d).

2. Theoretical values of the relationship λ/h in a few simple cases.

The theory of thermoconvective eddies (cf. Chaps. VI and VII) supposes that all the perturbations that enter this problem (pressure, velocity, temperature) are proportional to sine lx sine my Z [cf.(14)], where:

$$(l^2 + m^2)h^2 = a^2 \quad \text{(cf.(17))}.$$

The constant a depends upon boundary conditions. This applies equally well to the problem of a layer with two free surfaces and for a single stage of eddies (cf. relations (22) and (45') where r = 1) where the constant:

(69a) $$a = \pi b = \frac{\pi}{\sqrt{2}} = 2.22 \quad ,$$

In the problem of two walls with friction (cf. Chap.VII, Paragraph 2, Solution for a single stage of eddies):

(69b) $$a = \pi b = 3.1$$

Eddies of two dimensions and eddies in bands.- m being equal to zero, the relation (17) simplifies to

(70) $$l^2h^2 = a^2$$

which gives the wave length following the x-axis:

(71) $$\lambda = \frac{2\pi}{a} h.$$

In utilizing the values of a (69a) and (69b), one finds for the relationships λ/h respectively:

(72a) $$\frac{\lambda}{h} = 2\sqrt{2} = 2.83 ,$$

and

(72b) $$\frac{\lambda}{h} = 2.03$$

Then, in the problem of Lord Rayleigh, the width of the cellules (demi-eddies) is greater by 40% than their height h, while in the problem of Jeffreys the cellules are almost square.

These results apply entirely to eddies in bands, whose transversal section is identical to that of two-dimensional cellules.

Polygonal cellular eddies. - Among regular equilateral polygons, the triangles, the squares, and the hexagons are the only ones that can fill up all the surface without gaps anywhere between them.

The square cellules are, moreover, the only form that are analytically simple. In that case, the wave lengths λ and μ following the two coordinate axes are equal. The relation (17) then gives:

$$2\, l^2h^2 = 2\, m^2h^2 = a^2 ,$$

or again

(73) $$\lambda = \mu = \frac{2\sqrt{2}\,\pi}{a}\,h \quad .$$

It is easy to demonstrate that the wave length so defined is not the shortest distance between the vertical axes of two contiguous eddies.

To fix the ideas, let us consider the cellular eddies in a gaseous layer where the ascending currents are found at the vertical cell walls and the descent occurs at the axes of the cellules. In consequence, the square partitioning must coincide with the places with currents directed essentially towards the top.

To this condition corresponds two families of straight lines, defined respectively by:

(a) $$y = x - n\lambda \quad ,$$

(straight lines forming an angle of 45° with the x-axis) and by:

(b) $$y = -x + \frac{1 + 2n}{2}\,\lambda \quad ,$$

(straight lines forming an angle of 135° with the x-axis).

Being given that the vertical component of speed w is proportional to the product sine lx sine my (see Chap. X, equation (90)), one can verify that it stays positive if conditions (a) and (b) are realized. In fact, one has the equations:

$$\text{sine } lx \text{ sine } ly = \text{sine } lx \text{ sine } l(x - n\lambda) = \text{sine } lx \text{ sine}(lx - 2n\pi) = \text{sine}^2 lx \geq 0,$$

and

$$\text{sine } lx \text{ sine } ly = \text{sine } lx \text{ sine } l\left(-x + \frac{1 + 2n}{2}\,\lambda\right)$$

$$= \text{sine } lx \text{ sine } \left[-lx + (1 + 2n)\pi\right] = \text{sine}^2\, lx \geqq 0.$$

In these conditions, the network of the square cellules presents itself as it is drawn in Fig. 69. One sees there that λ $(=\mu)$ is the diagonal of the square. The shortest distance between the centers of two neighboring cellules is, hence, equal to the side of the square, which we will designate by λ^*. With:

$$\lambda^* = \frac{\lambda}{\sqrt{2}} ,$$

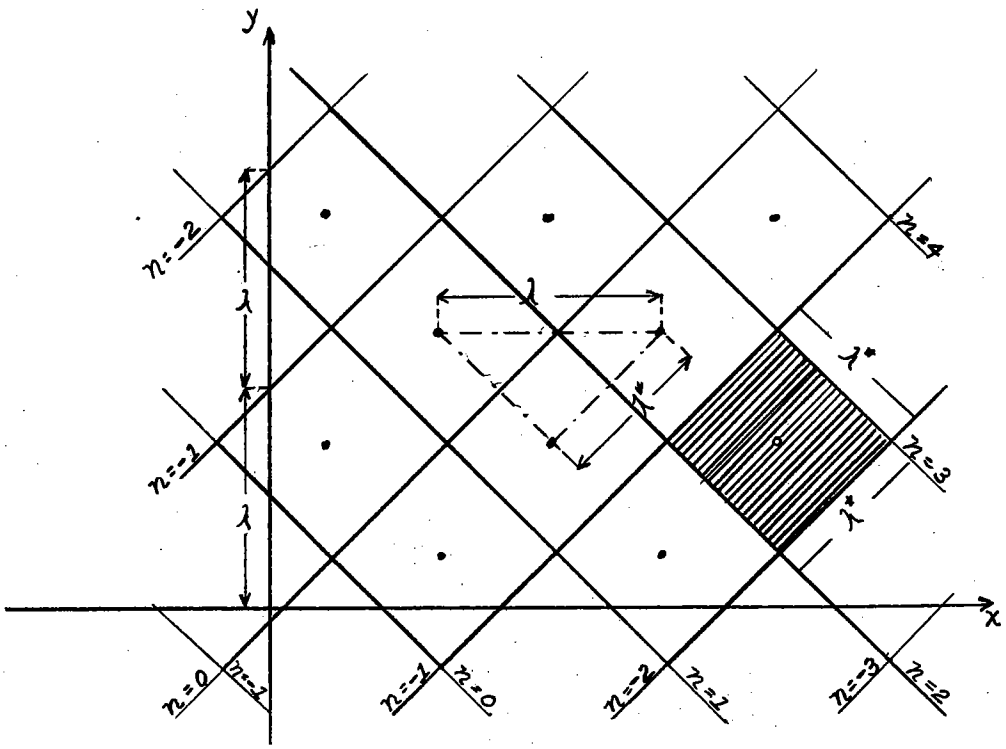

Fig. 69 Network of square cellules and their dimensions.

The characteristic relationship becomes:

$$\frac{\lambda^*}{h} = \frac{2\pi}{a}$$

In the problem of Rayleigh $\left(a = \frac{\pi}{\sqrt{2}} = 2.22\right)$:

$$\frac{\lambda^*}{h} = 2\sqrt{2} = 2.83$$

and in the problem of Jeffreys (a = 3.1):

$$\frac{\lambda^*}{h} = 2.03 .$$

As for the hexagonal cellules, Rayleigh (13) has indicated an approximate solution, based on Bessel's functions, in considering them as cylindrical cellules whose circular section would be equal to the surface area of the hexagon. H. Bénard, who finished the calculation (1-d), found:

$$\left(\frac{\lambda}{h}\right)_{min.} = \frac{2\, z_1}{\sqrt{\pi}\sqrt{3}} = 3.29 ,$$

z_1 being the first positive root of the equation

$$J'_0(z) = 0$$

Chapter VIII Part 2.

B. - Experimental Part

1. - Analysis of previous works.

H. Bénard (1-a,b,d) made a complete study of the λ/h relationship relative to hexagonal cellules in a sheet of melted spermaceti.

He found that the λ/h ratio is constant on first approximation. But precise measurements demonstrated that this ratio varied as a function of the thickness h and of the average temperature of the liquid - to wit:

1. At a given average temperature, λ/h increases with thickness; or in other words, the cellules flatten in proportion as the thickness

is greater;

2. For a pre-determined thickness, he finds between 50° and 100°C a temperature where λ/h is a minimum which varied in his experiments from 3.27 to 3.34. This value accords fully with Reyleigh's theoretical value, 3.29.

Mr. Bénard (1-d,e,f) completed the measurements on hexagonal cellules by measurements relative to square cellules, with straight-line bands, and with worm-shaped, vermicular bands. The results of these measurements which the author carried out either on his own photographs or on the photographs placed at his disposal by C. Dauzère, are assembled in the following table.

Liquid	Form of the Cellules	Temperature Avg. °C	h mm	λ/h	Author
Melted Spermaceti	hexagons	50-100	0.495-1	3.21-4.05	H. Bénard
	squares	50-100	0.5-1	2.95-3.57	
White Bees Wax	hexagons	128	0.69	3.17	H. Bénard and C. Dauzère
	squares	128	0.69	2.83	
Stearic acid (impure)	worm-shaped bands	87-119	2.44	1.95-2.29	
Development bath	rectilinear bands	18	1	1.96	H. Bénard
Pure Alcohol		ambient	0.14-0.35	3.7-5.9	T. Terada
Water		?	4.5-14	1.5-1.09	

On the other hand, Terada (5) and his students carried out an analogous work on eddies in longitudinal bands in liquids. The first series of experiments was done with volatile liquids, (pure alcohol,

mixture of alcohol and glycerine in different proportions), flowing down an inclined plane and becoming chilled at their surface by evaporation, and the second series with water heated from beneath.

When we examine their results, we see at once (see table above) that the λ/h ratio varies within very wide limits. Besides, we glimpse the following facts:

1. λ/h varies with the thickness of the fluid sheet;

2. λ/h depends equally on the physical nature of the fluid; for example, in volatile liquids, λ/h increases as a function of h, and in water, λ/h diminishes.

According to the theory we have set forth, λ/h would be equal to $2\sqrt{2}$ for a fluid layer with two free surfaces, and to 2 for a layer between two rigid walls. It is very likely that one would find, for the case of a liquid sheet whose surface remains free, a theoretical value which would fall between 2 and $2\sqrt{2}$. But the experimental results of the Japanese are very remote from all that. On the other hand, the λ/h ratio (= 1.96) that H. Bénard found in the developing bath (liquid contained between two solid plaques) is in excellent agreement with the theoretical value. It is the same way with the measurements of vermicular bands in impure stearic acid (see the same tabulation).

2. Dimensions of thermoconvective eddies in gasses.

No analogous work having been done in gasses, we proposed to measure the dimensions of thermoconvective eddies in air. Systematic experiments have been carried out in a layer of air whose thickness h varied from 10.5 to 50 mm. Several other individual experiments have also been done with thicknesses of 63 and 80 mm.

Eddies in longitudinal bands (21-c). This formation, in comparison with all the rest, presents the greatest stability. Also, measurements relating to longitudinal bands are precise and easy to make.

The results obtained may be summarized as follows:

1. λ/h is generally but not always greater than 2;

2. There is a tendency toward increase of this ratio when the thickness h increases: the rolls, that is, flatten themselves out more and more;

3. The number of rolls varies a little from one experiment to another, and, in consequence, the ratio λ/h likewise;

4. The number of rolls in permanent régime is always even; when there is an odd number, one can observe either the appearing of another complementary roll, or the disappearance of a superfluous roll;

5. The number of rolls possible for a given width of the canal appears to be independent of the difference of extreme temperatures, on condition that this last remains smaller than that value at which the eddy-movement commences to affect the exterior form of the rolls (see Chap. V, Paragraph 7);

6. The number of rolls depends but little upon the speed of translation, being understood that it remains larger than a minimum value necessary for the formation of longitudinal bands; however, one can testify that these rolls tend to enlarge themselves when the speeds are low;

7. The physical constituency of the eddies has a certain influence on their dimensions; in particular, the rolls constituted of thick smoke are wider than the rolls in purified air.

Let us pass now to the detailed analysis of other particulars that accompany the problem under study, in referring to a series of photographs reproduced either heretofore or hereafter.

Examining these photographic reproductions, one notes that in all cases the longitudinal rolls are perfectly developed. Their rectilinear form, and the parallelism of the lateral partitions are particularly remarkable.

On the other hand, the width of the different rolls of a single experiment is not always constant. The presence of the lateral partitions plays a big rôle. They modify the conditions of the translation (via friction) and of the thermic conductivity. One constantly observes that the rolls that touch the lateral partitions are wider than the ones in the center. Figures 70, 71, 72 and 73 are typical cases, and notably figure 73 where the two marginal rolls are extremely developed at the expense of the central bands.

To show the importance of the difference of the individual widths, we have composed the following table which contains the numerical values of the average λ/h ratios, maximum and minimum taken from the same snapshots:

FIGURE	h mm	L mm	n	$\frac{\lambda \text{average}}{h}$	$\frac{\lambda \text{max}}{h}$	$\frac{\lambda \text{min}}{h}$
70	20	352	16	2.2	2.5	2
71	30	308	10	2.05	2.54	1.74
72	40	335	6	2.8	3.85	2.5
73	50	285	4	2.85	3.7	2.2

We have noted that the number of rolls that can form themselves in the canal of a finite width is, in steady flow, always even, and

that the system progressively becomes even when there is an uneven number in the first place.
(Figs. 70, 71, 72, 73 in back).

Here is one striking example, taken from an experiment with a layer of air 15 mm thick and 330 mm wide.

The first attempt gave twenty-one longitudinal bands (Fig.74). One of the two marginal rolls, having a structure significant of progressive disappearance, is very narrow. A few minutes later, it became entirely suppressed. On Fig. 75 one may still distinguish the last trace of the superfluous roll which in an instant or two is going to disappear: the system of twenty rolls is going to establish itself definitely.

On the other hand, a second trial gave nineteen rolls strongly developed. Little by little, the twentieth roll formed itself (Fig. 76), and later on, the system of twenty rolls was established. In these conditions, the ratio λ/h relative to the nineteen rolls and the twenty-one rolls (2.32, and 2.1 respectively) is not stable. And so it is only the formation of twenty rolls that must be taken into consideration, and for which $\lambda/h = 2.2$.

We have likewise observed in a steady régime some systems of eighteen and 22 rolls. So the ratio λ/h varied from 2 to 2.44. But these systems are less frequent than that of $n = 20$.

We have observed the same variation of the number of rolls for all the other thicknesses. However, we have arrived in each case at an average value of λ/h, by repeating each experiment ten to thirty times.

(Figs. 74, 75, 76, in back).

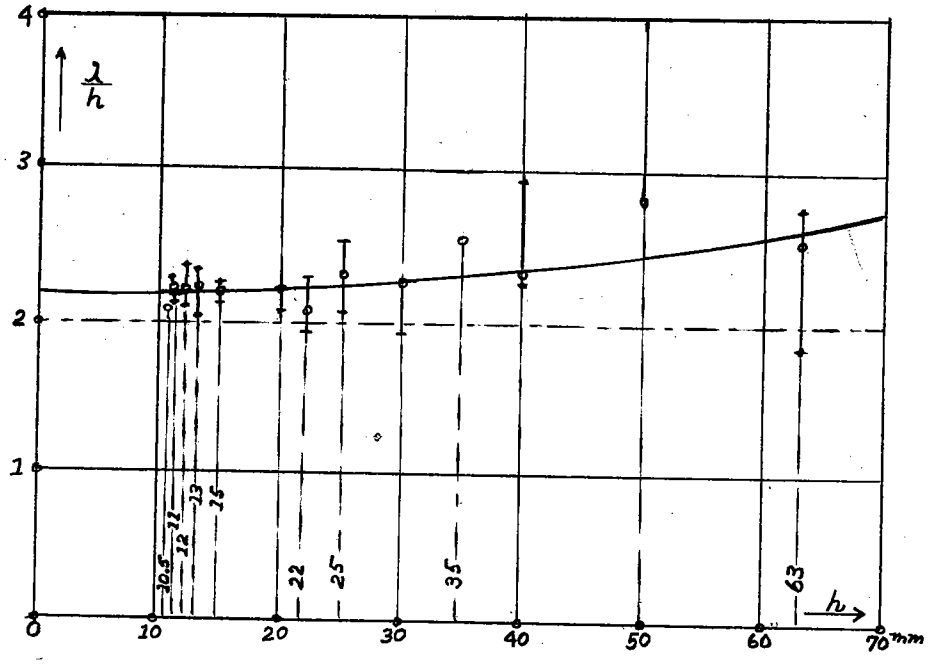

Fig. 77 Experimental relationship-ratio λ/h of the eddies in longitudinal bands in function of their thickness h.

The tables(in back) reproduce the assembly of average values of λ/h as a function of the thickness h. It is clarified by the diagram (Fig. 77) where we have carried as abscissa the thickness h and as ordinate the ratio λ/h. To the side of the average value, we have marked the extreme values (maxima and minima) and the intermediate (values). The dispersion of the points is very strong for thicknesses above 4 cm, because the number of rolls diminishes necessarily in presence of the width of the canal which can not much exceed 40 cm; in consequence, the eventual variation of the number of rolls brings on with it variations in steps of λ/h. None the less, there is a number, very small, of experiments where the value of λ/h

is below 2, the theoretical minimum. Also, one notes that the average value of λ/h tends to increase when h increases.

The problem of the accidental variation of the number of rolls (of the ratio λ/h), along with the study of the stability of these formations will form the subject of Chapter IX.

Eddies in transversal bands. - This formation is less stable and consequently less frequent than the longitudinal eddies. The results of measuring their dimensions from certain photos among our collection, are given in the following table. The ratio λ/h is essentially equal to 2 when the rolls are entirely developed. During their development, λ/h is less than 2. It is to be noted that the width of the rolls containing smoke is less than that of the rolls constituted from pure air. To say it in a word, the demi-unit eddy (one roll) has an almost square section.

Eddies in Transversal Bands

FIGURE	h mm	L mm	n	λ/h	REMARKS
34	12	160	15	1.78	In development
35	12	120	10	2	
52	20	160	8	2	
53	25	140	6	1.87	In development
54	10.5	105	10	2	
-	12	144	12	2	Photo 18 A not reproduced in this report

Polygonal cellular eddies. We have shown (cf. Chap. IV, Parag. 1) that in presence of two limiting partitions, the polygonal cellules finally give way to eddies in vermicular bands. The polygonal cellules persist for only a very short time; their duration

is too short for the size and the form of the cellules to equalize themselves. This is why we can establish only the average value of the ratio λ/h.

We have employed the following method. The characteristic transversal dimension λ is, in the case of the polygonal cellules, the shortest distance between their contiguous centers. So we mark on the photograph the centers of the cellules and we connect them. The sum of all these distances, divided by the number N of lines of connection, gives the average value of λ:

$$\lambda_{average} = \frac{\Sigma\lambda}{N}.$$

In the case of hexagons, granted that each cellule be connected to the group by <u>at least</u> two sides, the number $N = (2n-3)$, where one designates by n the number of cellules, (of centers, that is) hence:

$$\lambda_{average} = \frac{\Sigma\lambda}{2n - 3}$$

Be it understood, for these measurements we have eliminated those cellules whose dimensions were visibly aberrant.

The following table shows the results obtained upon a dozen photographs: (Eddies in polygonal cellules, p.138)

The values of λ/h proceeding from these experiments are much lower than the theoretical value given by Lord Rayleigh ($\lambda/h = 3.29$). This comes about on one hand by reason of the fact that the final régime has not been attained, far from it, and on the other hand from the fact that the boundary conditions for a gaseous layer (two rigid partitions) are essentially different from those governing Rayleigh's

Eddies in Polygonal Cellules

FIGURE	h mm	N	$\Sigma \lambda$ mm	λ average	$\frac{\lambda \text{ average}}{h}$	REMARKS
26	20	4	176	44	2.20	
27	30	4	314	79.4	2.61	
30	20	26	1370	52.8	2.64	
31	20	56	2300	41	2.05	In growing state
46	20	46	2090	45.4	2.27	
47	20	22	1008	45.8	2.29	
50	20	23	988	43	2.15	travelling cellules
51	30	8	500	62.5	2.08	travelling cellules
-	12	16	417	26.1	2.17	Photo 22 A, not reproduced in this report

problem (two surfaces without friction). Let us also say that λ/h is excessively small when the cellular eddies are just commencing to appear (see Fig. 31). Their transversal dimensions also diminish if the cellules displace themselves like the ensemble, which has been the case in the experiments reproduced in Figures 50 and 51.

Chapter IX

Variation of the ratio λ/h for Eddies in Longitudinal Bands and Their Stability

1. Production of eddies in bands of predetermined dimensions

We indicated in the previous chapter that the number of longitudinal rolls varied a bit from one experiment to the next, or, in other words, that their λ/h characteristic was not constant.

We have been insistent in seeking an explanation for this variation in the number of rolls producing themselves in apparently identical

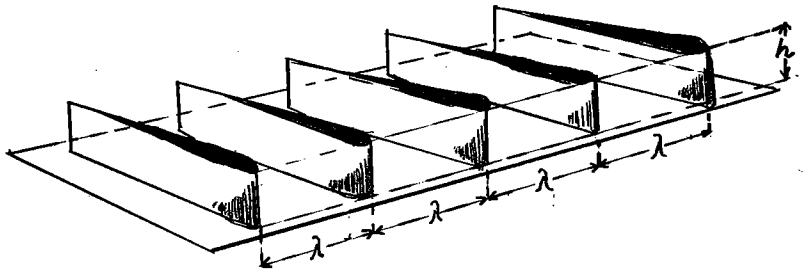

Fig. 78 Smoke-distributor, set up at the entrance of the experiment chamber.

conditions. It seemed to us that we would need to introduce the role of initial accidental perturbations. We have demonstrated experimentally the exactitude of this hypothesis, by artificially provoking regular perturbations whose amplitude exceeded the little accidental perturbations. To assure a predetermined number of rolls, it was sufficient to put a cardboard distributor at the entry of the canal. This last (see Fig. 78) is divided by vertical partitions into little compartments the size of which can be fixed arbitrarily. The tobacco smoke must traverse this obstacle before entering the experiment chamber. The smoke-layer is cut by these partitions into parallel slices.

Each compartment of the distributor determines the origin of two twin rolls, constituting by definition an eddy in longitudinal bands. The eddies that it produces are perfectly regular, and their width λ (width of two rolls) is that of the distance of separation between the partitions. In these conditions, we can produce a number of rolls that can very between very wide limits.

The employment of such a distributor is not necessary to produce an arbitrary number of rolls. If one places at the entry of the canal very small solid obstacles, having the form of little cylinders

of 1 cm diameter and 1 cm in height, one obtains the same result. (Fig. 79 in back).

Behind each obstacle there forms a sort of wake or furrow marked by white crests of tobacco smoke. They propagate themselves the full length of the canal and determine the partitions of separation of two consecutive pairs of rolls. The mechanism of the development, (exhaustion of the smoke accumulated in elongated crests) is such as we described in Chap. IV and drew in Fig. 38.

Here is a concrete example, in which the height h of the canal was 40 mm and its width L 200 mm. Four rolls took shape immediately (Fig. 79) when the conditions were normal (no obstacle at the entry of the canal). The λ/h ratio is hence equal to 2.5.

In order to increase the number of rolls to six, we placed two cylindrical obstacles at the entry of the canal, that cut the air-layer into three slices, each having 1/3 of the total width L. The six rolls produced themselves without any difficulty (Fig. 80). Hence, the λ/h relationship diminished from 2.5 to 1.67, and consequently, the thickness of the rolls is greater than their width. (Figs. 80, 81 in back).

Finally, we tried to produce eight rolls, by putting three obstacles at the entry (Fig. 81). The layer divided itself into four slices. They are separated by three crests of thick smoke placed in the wake of these obstacles. Each of the two lateral slices gives rise to two twin rolls. Four other rolls likewise attempt a beginning in the central space, but their number does not conserve itself, for the center slices are very much jammed together to the profit of the marginal rolls. The two rolls in the center are progressively absorbed

by their neighbors. One sees by the figure that the median crest of smoke, indicator of rising currents, is suppressed further downstream.

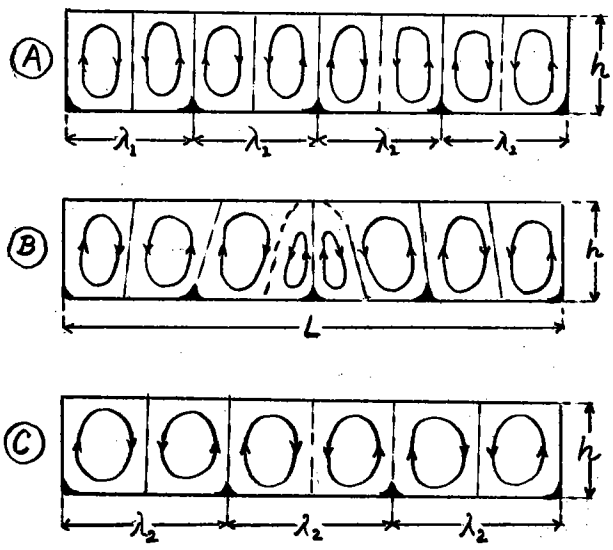

Fig. 82 Schematic representation of the preceding experiment - progressive transformation of 8 rolls into 6.

(Fig. 83 in back). That proves that the four rolls that started to take shape have been replaced by two wider rolls. In sum, the system of six rolls reestablishes itself.

The three transversal cuts A, B, and C (Fig. 82), taken at separate points in the length of the canal, represent schematically the mechanism of progressive transformation from eight rolls to six.

Endeavors were undertaken also in the way of reducing the number of rolls. Without going into detail concerning the artifice employed, we can state that in the same canal we managed to reduce the number of rolls to two only, and to attain thereby the ratio $\lambda/h = 5$ (Fig. 83).

We carried out a great number of experiments of like kind by making the thickness h vary. The values obtained of the λ/h ratio vary from 1.25 to 5.

It is necessary to remark that the formations corresponding to the extreme values, and notably to the lower values, are not very stable. A little, accidental perturbation in the field of observation can provoke, according to circumstances, either an increase or a decrease in the number of rolls.

2. Mechanisms of reduction of the number of rolls.

We have already described one mode of reduction of the number of rolls. Here is a second mechanism of transition that we have observed very frequently.

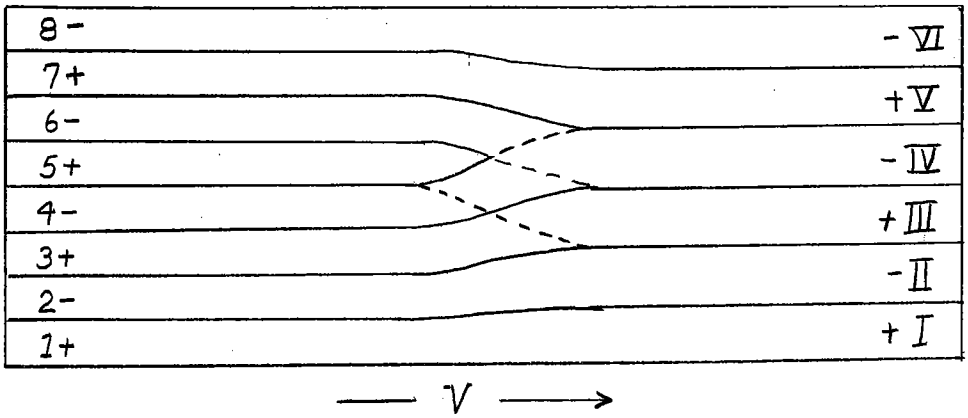

Fig. 84 Schematic reduction of the number of rolls by splicing.

During an experiment (h = 30 mm, L = 200 mm), where the most probable number of rolls would be equal to six ($\lambda/h = 2.22$), eight rolls formed themselves in the upstream region of the canal. Further downstream they were reduced to six by the mechanism drawn in Fig. 84.

We designate the initial rolls by 1, 2, ... 8, the resulting

rolls by I, II, ...VI, and by the signs + and - the rotation from right to left, and conversely.

Roll 3 and roll 5 twist themselves into one single roll III, all having the same direction of rotation. Similarly, 4 and 6 twist themselves into IV. Rolls 4 and 5 have to cross each other before penetrating the resultant rolls III and IV.

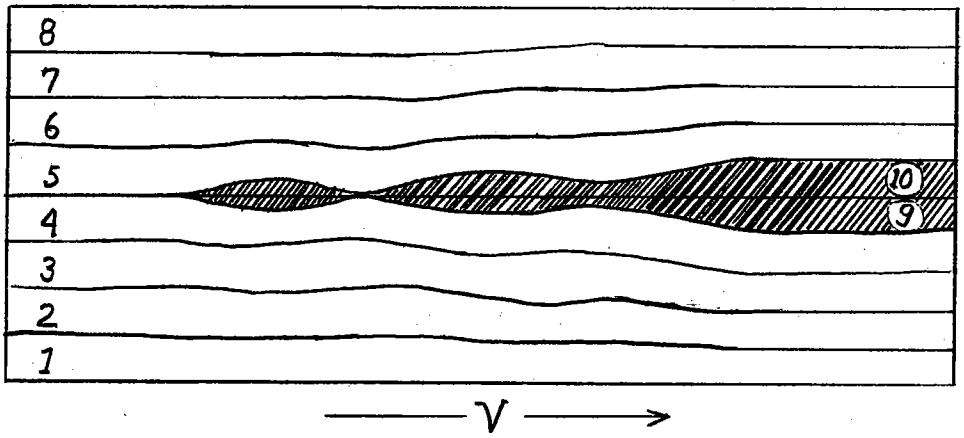

Fig. 85 Schematic suppression of two undulated rolls: the 8 roll system succeeds the 6 roll system.

Let us pass to the third example. In an experiment, the width and thickness of the canal were 360 and 30 mm respectively. The eight-roll system produced itself most frequently ($\lambda/h = 3$). Notwithstanding, ten rolls also did appear ($\lambda/h = 2.4$), but this system did not endure: two center rolls were suppressed by the neighbors. One sees the mechanism of their annihilation in Fig. 85. The two rolls with undulating partitions were simultaneously "ground in" and pushed towards the outlet of the canal. The whole field is progressively invaded by the stabler system of eight rolls.

3. Mechanisms of increasing the number of rolls

Augmentation of the number of rolls by bifurcation. We have observed this particular case in the course of an experiment ($h = 40$ mm, $L = 335$ mm) where we predetermined the production of six rolls ($\lambda/h = 2.8$). They took perfect shape. Nevertheless, further downstream a little accidental perturbation provoked the bifurcation of two crests: two new pairs of rolls were now created (Fig. 86). The accident was evidently of a transitory nature, because the system of ten rolls ($\lambda/h = 1.67$) was soon after replaced by the six predetermined rolls.

Augmentation of the number of rolls by interpolation. - Let us take as example one of our experiments where $h = 30$ mm and $L = 308$ mm. These conditions have been favorable to the formation of ten rolls ($\lambda/h = 2$). By placing at the entry of the canal a distributor with six compartments, twelve rolls were incited to take shape (Fig. 87). But for all that, one pair of rolls could not develop itself at once: it got squeezed together like a narrow sharp wedge. It was but very slowly that the two supplementary rolls interpolated themselves amongst the others and that the system of twelve rolls filled up all the space. (Figs. 86 and 87 in back).

Another aspect of penetrating rolls is drawn on Figure 88. The undulating partitions recall the analogous formation cited among the examples of the diminution of the number of rolls.

Conclusion. - Experience shows that a fluid layer in translation can divide itself spontaneously into a number of rolls that varies within

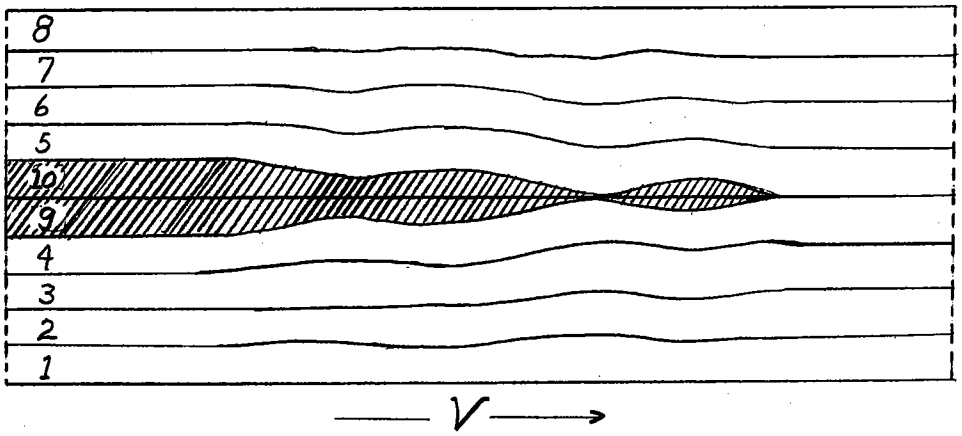

Fig. 88 Schematic augmentation of the number of rolls by undulated interpolation of a pair of supplementary rolls. The system of 10 rolls has succeeded that of 8 rolls.

certain limits. Their interval can be considerably widened if we take recourse to perturbations artificially provoked. Each one of these formations, once established, is stable. As for the degree of their stability, it is evident that it is variable. It is very probable that the stablest formation will be the most frequent, on condition that all the perturbations and irregularities be avoided as far as possible.

By analogy, one could apply the same conclusion to all other forms of thermoconvective eddies.

4. Theoretical Considerations.

To terminate this chapter, a short mathematical analysis relative to eddies in bands, (eddies with two dimensions) with the conditions of Jeffreys, would be very useful.

According to theory, the dimensions of the eddies are in direct correlation with the number Λ, which is by definition (18) proportional

to the linear gradient of temperature β, and to the fourth power of thickness h.

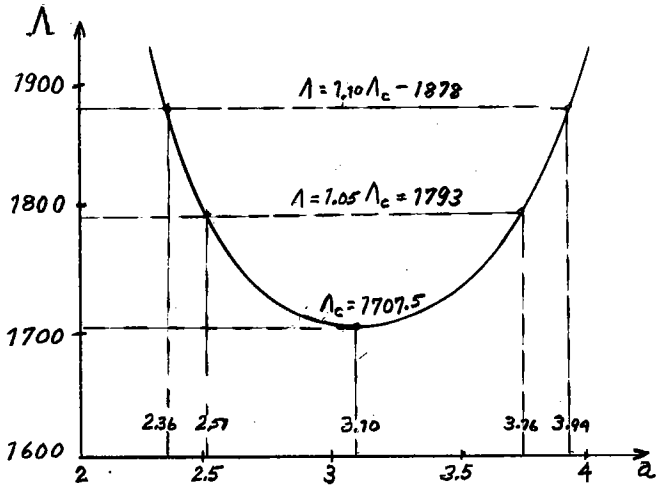

Fig. 89 Jeffreys' criterion as a function of the pure number a.

Being granted that, in the system of two dimensions, the wave length λ is defined by (71), one finds, according to relation (57) (which gives Λ as function of a) for each value of Λ two values of a, and thus also two values of λ. In the particular case where Λ passes through its minimum, a takes a single value. We know (cf. Chap. VII, Theoretical Part) that at this critical moment when the first thermo-convective currents can release themselves, $\Lambda = 1707.5$, $a = 3.1$ and in consequence $\lambda/h = 2.03$ (cf. (72b)). Let us suppose that these theoretical values are rigorously exact. It can happen, none the less in the experiments that the release of the motions is retarded by one reason or another. When that happens, the value of Λ_c (the index c should indicate that Λ_c is the actual critical value, λ_c the corresponding wave length) - is more or less passed by.

The numerical calculation shows that that is full of consequences for the wave length λ. For example, if Λ is greater than Λ_c by only 5%, the ratio λ/h diminishes by 20% or augments by 25% in relation to the critical value λ_c/h.

Λ in function of a, constructed according to (57), is graphically represented in Fig. 89. We have marked the four values of a corresponding to: $\Lambda = 1.05\ \Lambda_c = 1793$ and to: $\Lambda = 1.10\ \Lambda_c = 1878$.

Furthermore, we have carried in the table given below the values of λ/h calculated for the same Λ's.

Λ	a_1	$\lambda_1/h = \frac{2\pi}{a_1}$	a_2	$\lambda_2/h = \frac{2\pi}{a_2}$
$1.05\,\Lambda_c = 1793$	2.51	2.5 (25% above the critical value)	3.76	1.67 (20% above the critical value)
$1.10\,\Lambda_c = 1878$	2.36	2.66 (33% above the critical value)	2.94	1.6 (25% above the critical value)

This theoretical analysis of the simple case that we have just carried out, gives a clear explanation of the origin of the variation of the ratio λ/h. It results therefrom likewise that precision in geometric measures is not useful because the dimensions fluctuate too much.

Chapter X

Streamlines

A. Theoretical Section

1. Stream function in the problem of eddies of two dimensions.

The study of the motions in the midst of the convective eddies

may be reduced as often as we choose to the study of motions in two dimensions, which lends itself readily to mathematical analysis.

Let us take in the vertical plane the orthogonal axes x and z, z being vertical and directed straight upward. We can suppose, without committing any appreciable error, that the divergence is null (according to (8) it is equal to $\alpha \chi \nabla^2 \Delta T$); and so, in the problem with two dimensions:

$$\frac{\partial u}{\partial x} + \frac{\partial w}{\partial z} = 0 \tag{74}$$

The equation of continuity (74) entails the existence of the stream function ψ such that:

$$u = \frac{\partial \psi}{\partial z} \qquad \text{and} \qquad w = -\frac{\partial \psi}{\partial x} \tag{75}$$

is a function of the coordinates x and z and of the time t. Then, the total differential $d\psi$ is written:

$$d\psi = \frac{\partial \psi}{\partial x} dx + \frac{\partial \psi}{\partial z} dz + \frac{\partial \psi}{\partial t} dt \tag{76}$$

If the motion is steady, time does not intervene. In these circumstances, and in virtue of (75), the integration of (76) gives us, except for a constant:

$$\psi = -\int w\, dx + \int u\, dz \tag{77}$$

We have found before that the vertical component of velocity w is equal to (35). On the other hand, re-introducing the relationship (14), the perturbation of the thermal field in the two-dimensional system reduces itself to

$$\Delta T = \Delta T_o \sin lxZ.$$

With this expression, (35) becomes:

$$(78) \qquad w = \frac{\chi}{\beta} \sin lx \left[\frac{d^2Z}{dz^2} - l^2 Z\right].$$

By using the equation of continuity (74) and the expression (78), we obtain:

$$(79) \qquad u = \frac{\chi}{\beta}\frac{1}{l}\cos lx \left[\frac{d^3Z}{dz^3} - l^2\frac{dZ}{dz}\right].$$

The two components u and w being determined by (79) and (78), the stream function (77) becomes, after integration:

$$\psi = 2\frac{\chi}{\beta}\frac{1}{l}\cos lx \left[\frac{d^2Z}{dz^2} - l^2 Z\right]$$

Omitting the constant factor, this function is written in the ξ system, with (70):

$$(80) \qquad \psi = \cos a\frac{x}{h}\left[Z - \frac{\pi^2}{a^2}\frac{d^2Z}{d\xi^2}\right].$$

Before we apply this result to a number of particular cases, we must determine the corresponding functions of Z.

2. Determination of the Z function in a number of particular cases.

The general solution of the differential equation of the sixth order (24) has been given by the expression (25). It divides itself into two independent parts in the problems where the conditions at the two surfaces are identical. There results from this one symmetric solution and the other anti-symmetric with respect to the median plane of the fluid sheet. The symmetric solution (p are even and r odd) is written then:

$$(81) \qquad Z = B_0 + \frac{B_2}{2!}\left(\frac{\pi}{2} - \xi\right)^2 + \frac{B_4}{4!}\left(\frac{\pi}{2} - \xi\right)^4 - \sum_{r=1}^{\infty}\frac{A_r}{r^6}\sin r\xi,$$

and the antisymmetric solution (p are odd and r even):

$$(82)\quad Z = B_1\left(\frac{\pi}{2}-\xi\right)+\frac{B_3}{3!}\left(\frac{\pi}{2}-\xi\right)^3+\frac{B_5}{5!}\left(\frac{\pi}{2}-\xi\right)^5-\sum_{r=2}^{\infty}\frac{A_r}{r^6}\sin r\xi.$$

Problem of Lord Rayleigh. We found in Chapter VII that all the constants of the two possible solutions vanished. In these conditions, the function Z is null. However, there exists a solution that is different from zero. That comes when the denominator of the relationship (cf. (27)):

$$A_r = \frac{r^6}{(r^2+b^2)^3 - Mb^2}\Lambda_r,$$

is equal to zero simultaneously with Λ_r. We hence can attribute to the constant A_r, which figures in the trigonometric series, a finite value of some sort. If we suppose that:

$$A_r = -r^6,$$

we obtain:

$$(83)\qquad Z = \sin r\xi,$$

where r is a whole number, even or odd. This function corresponds to the eddies in layers piled one on the other, whose number is equal to r.

The function (83) simplifies itself in the case of a single stage of eddies to

$$(83a)\qquad Z = \sin \xi.$$

Problem of Jeffreys. The symmetric solution and the antisymmetric solution differ one from the other. We shall determine the function Z only for <u>one</u> and <u>two</u> stages of eddies.

a) Symmetric solution (one single stage of eddies). Let us take again the boundary conditions (48) that we established for the problem

of Jeffreys, and the equation (32) that gives Λ_r as a function of the constants B_0, B_2 and B_4. By utilizing the two first conditions of (48), (32) reduces itself to:

$$(84) \qquad \Lambda_r = \frac{4}{\pi r}\left[3b^2\left(1+\frac{b^2}{r^2}\right)+\frac{b^6-Mb^2}{r^4}\right]B_4$$

In the particular case of a single stage of eddies (r = 1) (cf. Chap. VII, p.95):

$$\Lambda_{r=1} = 1707.5 \qquad \text{and} \qquad b = \frac{a}{\pi} = \frac{3.1}{\pi} = 0.987.$$

With that, the equation (84) gives at once the constant B_4. B_4 being known, B_2 and B_0 are likewise defined. Finally, one calculates with (27) and (84) the constants A_r.

We have found the following values:

$B_0 = -164$, $B_2 = 160$, $B_4 = -129.6$,

$A_1 = -181.7$, $A_3 = -124.6$, $A_5 = -88.6$.

With these values, (81) becomes:

$$(85) \qquad Z = -164 + 80\left(\frac{\pi}{2}-\xi\right)^2 - 5.4\left(\frac{\pi}{2}-\xi\right)^4$$

$$+ 181.7 \sin \xi + 0.17 \sin 3\xi + 0.0057 \sin 5\xi + \ldots$$

We have calculated only three terms of the trigonometric series, because they converge rapidly towards zero.

The function Z, represented in Fig. 90, is very close to the sinusoidal curve, which is, as one knows, the function Z of the problem of Lord Rayleigh. It is understood, of course, that the maxima of the two curves have been made equal.

b) Antisymmetric solution (two stages of eddies). Substituting the first two conditions of (58), the equation (33), is reduced to:

(86) $$\Lambda_r = \frac{2}{r}\left[3b^2\left(1+\frac{b^2}{r^2}\right) + \frac{b^6 - Mb^2}{r^4}\right] B_5 .$$

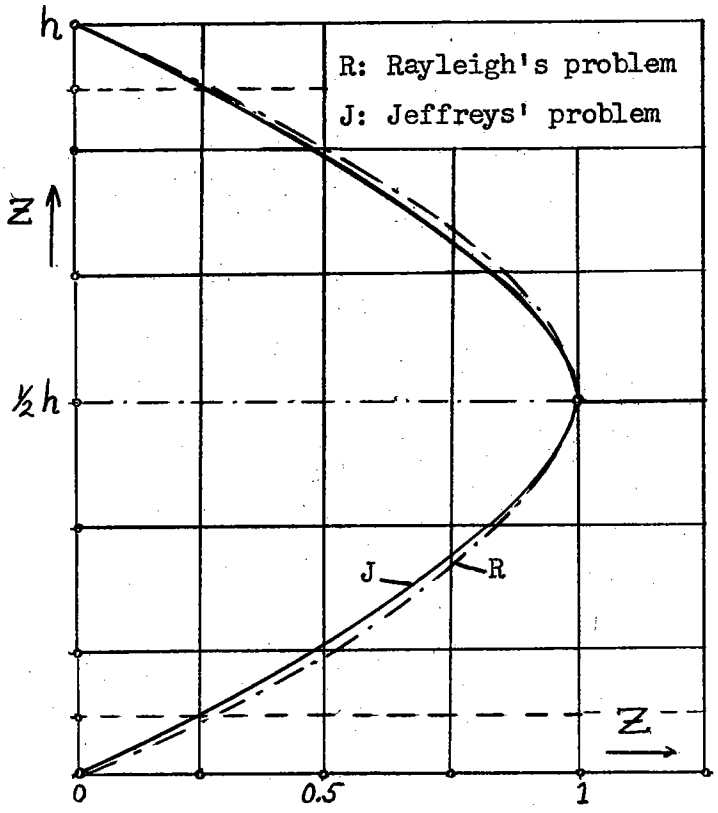

Fig. 90 Function Z in the problems of Rayleigh and Jeffreys for one single stage of eddies.

This relationship gives the numerical value of B_5 if we put there $\Lambda_{r=2} = 17{,}650$ and $b = 1.72$, values found in Chapter VII when r was equal to 2. The equations (27), (58), (86) furnish all the other constants. Here they are:

$$B_1 = -127.2, \qquad B_3 = 441, \qquad B_5 = -1073,$$
$$A_2 = -5650, \qquad A_4 = -2920, \qquad A_6 = -2635.$$

The solution (82) takes the form:

$$(87) \qquad Z = -127.2\left(\frac{\pi}{2} - \xi\right) + 73.5\left(\frac{\pi}{2} - \xi\right)^3 - 8.94\left(\frac{\pi}{2} - \xi\right)^5 + 88.3 \sin 2\xi + 0.7125 \sin 4\xi + \ldots,$$

which is graphically represented by Fig. 91. We have likewise traced the simusoidal curve corresponding to the problem of Rayleigh. The maxima of the two curves compared do not coincide: those of the Jeffreys problem are pushed towards the interior; this fact is brought about by the presence of the rigid walls.

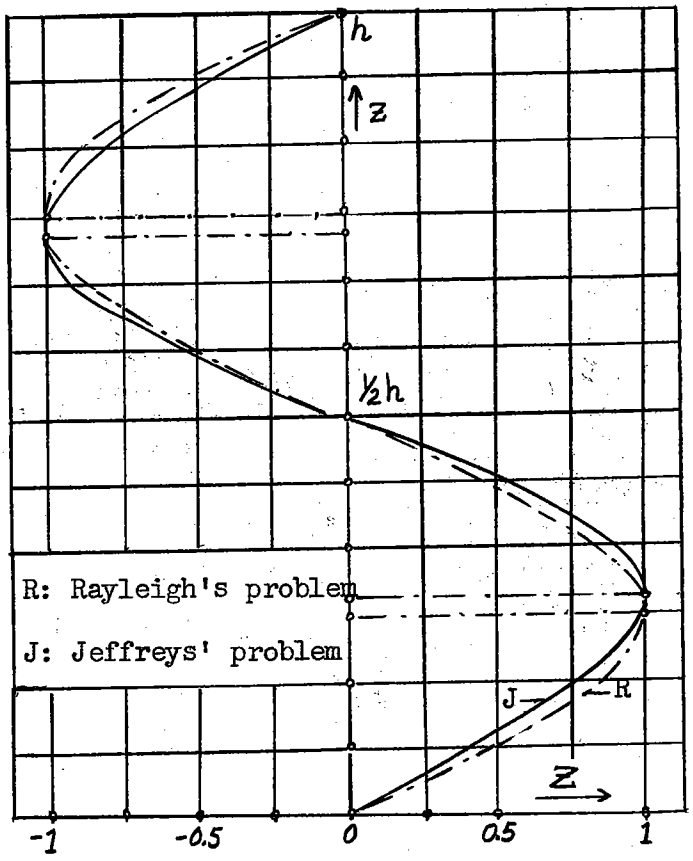

Fig. 91 Function Z in the problems of Rayleigh and Jeffreys for two stages of eddies.

3. Determination of the stream function in certain particular cases.

Fluid sheet with two free surfaces (problem of Lord Rayleigh).

The function Z has taken in this problem the form (83), which is a simple sinusoidal curve. In virtue of (22) and (45'), the stream function (80) becomes:

$$\psi = \cos\left(\frac{r\pi}{\sqrt{2}}\frac{x}{h}\right)\sin\left(r\pi\frac{z}{h}\right).$$

For each value of ψ , one finds a closed stream line. It becomes, for $\psi = 0$, a rectangle whose width is equal to $\frac{\sqrt{2}h}{r}$ and the height to $\frac{h}{r}$. It reduces itself to a central point when $\psi = 1$. The two figures 92 and 93 reproduce the stream lines, corresponding

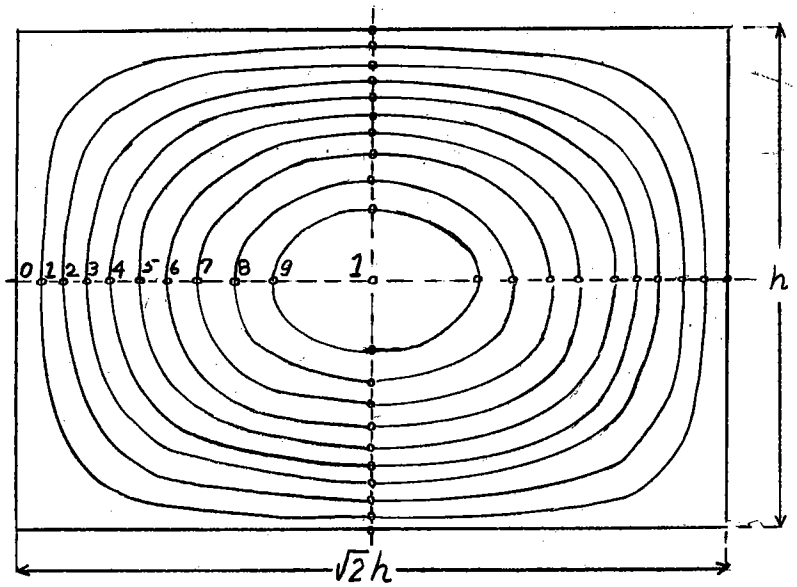

Fig. 92 Stream lines in the problem of Rayleigh for one single stage of eddies.

respectively to <u>one</u> and to <u>two</u> stages of eddies (r = 1 and 2). The behaviour pattern of the stream lines in the two cases is exactly the same, with this difference that in the first case the rectangle $\sqrt{2}$ hxh is engendered by a single cellule, and in the second case by

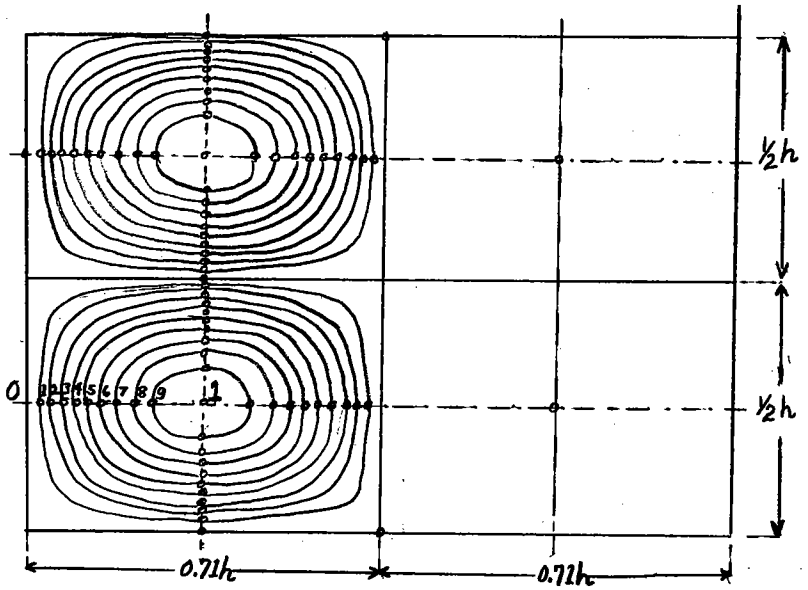

Fig. 93 Stream lines in the problem of Rayleigh for two stages of eddies.

four cellules (each one occupies a surface $\frac{\sqrt{2}h}{2} \times \frac{h}{2}$).

Fluid sheet between two rigid partitions (problem of Jeffreys) - symmetrical solution (one single stage of eddies). In this problem, the function Z presents itself under the form (85). Elsewhere one has had $a = 3.1$ (cf. p.110). With these values, the function:

$$(88) \quad Z \frac{\pi^2}{a^2} \frac{d^2Z}{d\xi^2} = -328.3 + 146.5 \left(\frac{\pi}{2} - \xi\right)^2 - 5.4 \left(\frac{\pi}{2} - \xi\right)^4 + 368.4 \sin \xi + 1.74 \sin 3\xi + 0.15 \sin 5\xi + \ldots$$

This function, which, in the problem of two free surfaces, was a simple sinusoidal curve, has become more complex. One sees in Figure 94 that the curves $(Z - \frac{\pi^2}{a^2} Z'')$, corresponding to the two cases under consideration become considerably separated.

When we divide the expression (88) by its maximum value (=38.5),

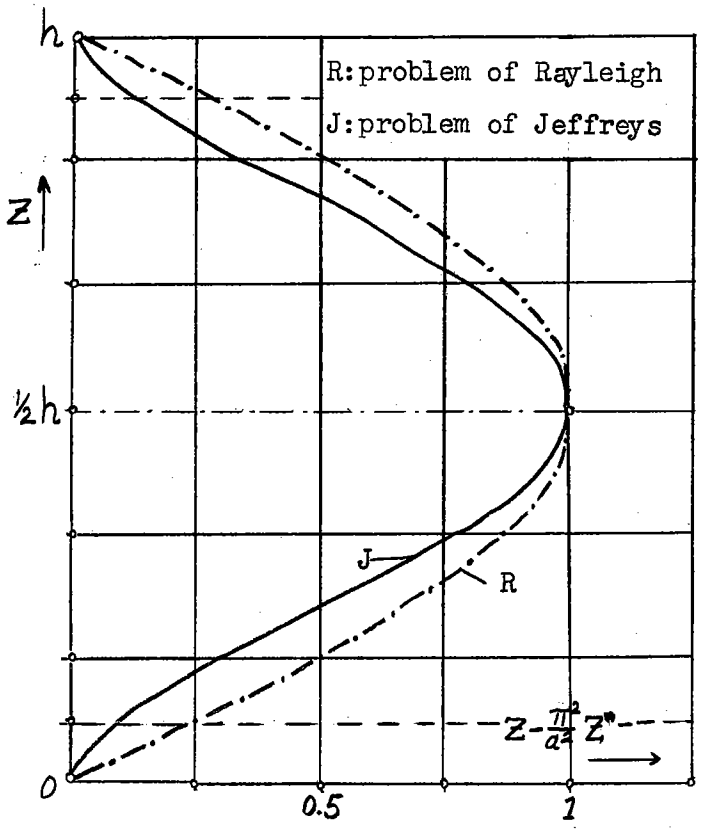

Fig. 94 Function $Z - \frac{\pi^2}{a^2} Z''$ in the problems of Rayleigh and Jeffreys for two stages of eddies.

the function of current (80) becomes:

$$\psi = \cos 3.1 \frac{x}{h} \left[- 8.53 + 3.81 \left(\frac{\pi}{2} - \xi \right)^2 - 0.14 \left(\frac{\pi}{2} - \xi \right)^4 + 9.67 \sin \xi + 0.045 \sin 3\xi + 0.004 \sin 5\xi + \ldots \right].$$

When $\psi = 0$, the stream line equals a square with sides = h. It reduces itself to a central point for $\psi = 1$. The stream line field ($\psi = 0$, 0.1, 0.2 .... 0.9 and 1) is represented in Fig. 95.

Fluid sheet between two rigid walls (problem of Jeffreys) - antisymmetric solution (two stages of eddies). Let us take up again the function Z drawn from the antisymmetric solution (87), where the

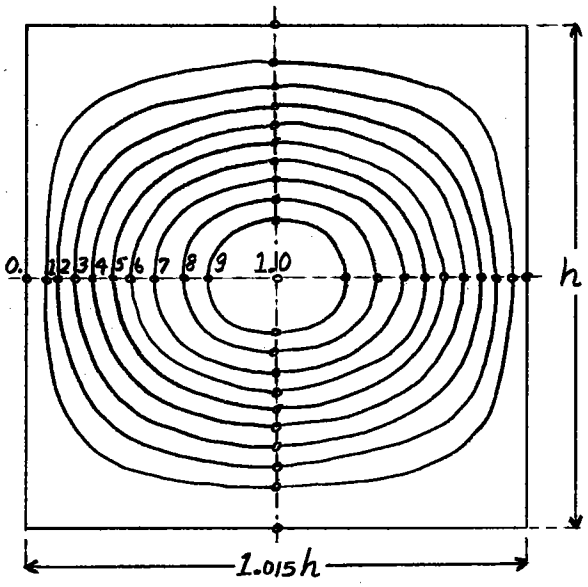

Fig. 95 Stream lines in the problem of Jeffreys for a single stage of eddies.

number $a = 5.4$ (cf. p. 113). Using these values, we obtain:

$$(89) \quad z - \frac{\pi^2}{a^2}\frac{d^2z}{d\xi^2} = -277\left(\frac{\pi}{2} - \xi\right) + 134\left(\frac{\pi}{2} - \xi\right)^3 - 8.9\left(\frac{\pi}{2} - \xi\right)^5 + 208 \sin 2\xi + 4.6 \sin 4\xi + \ldots$$

This function is outlined in Fig. 96 beside the analogous function in the problem of Lord Rayleigh. The separation of the curves is very accentuated.

If we divide here again the function (89) by its maximum value (=43.4), we obtain for the stream function (80):

$$\psi = \cos 5.4\,\frac{x}{h}\left[-6.4\left(\frac{\pi}{2} - \xi\right) + 3.1\left(\frac{\pi}{2} - \xi\right)^3 - 0.2\left(\frac{\pi}{2} - \xi\right)^5 + 4.8 \sin 2\xi + 0.1 \sin 4\xi + \ldots\right].$$

In putting $\psi = 0$, the stream lines become rectangular. The individual rectangles, ranged in two stages, have width 0.58 h and their height h/2. Elsewhere, when $\psi = 1$, the stream lines reduce

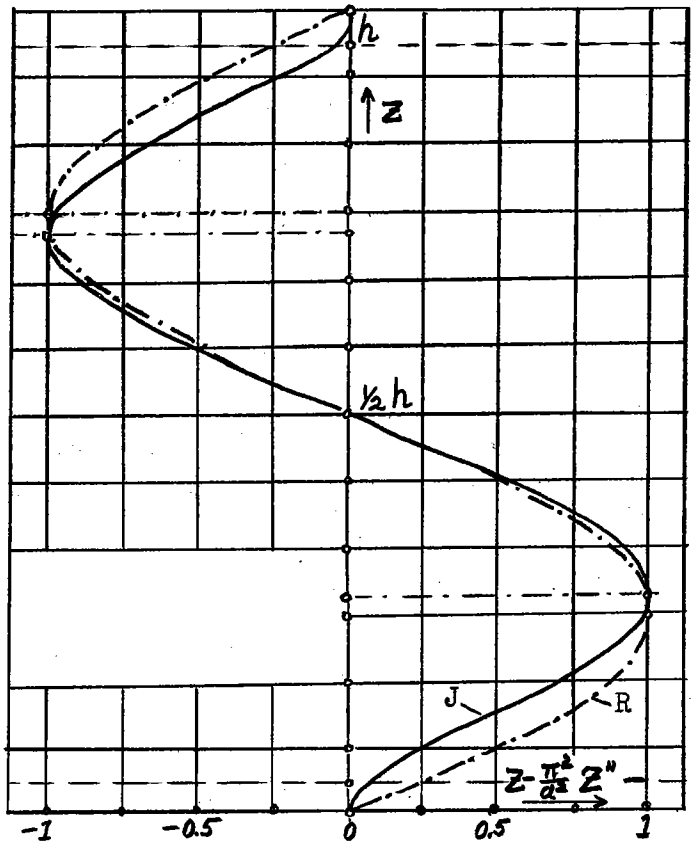

Fig. 96 Function $(Z - \frac{\pi^2}{d^2} Z'')$ in the problems of Rayleigh and Jeffreys for two stages of eddies.

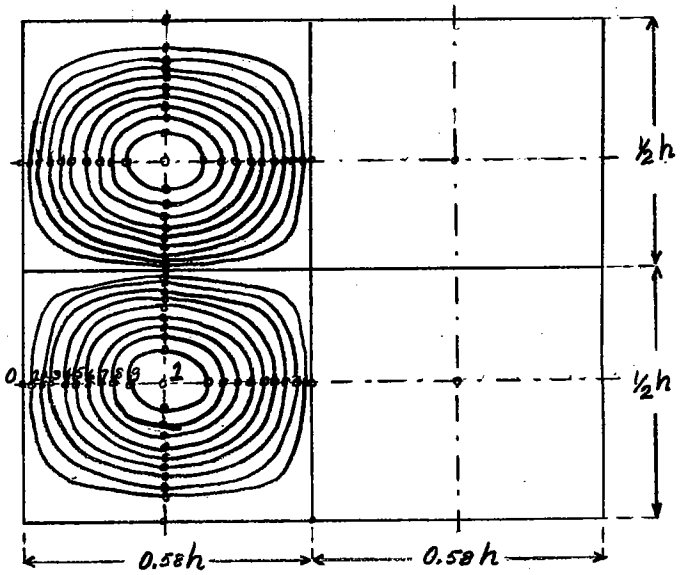

Fig. 97 Stream lines in the problem of Jeffreys for two stages of eddies.

themselves to isolated points, separated along two horizontal lines. Figure 97 reproduces the stream lines of two superposed cellules, calculated for the values $\psi = 0,\ 0.1,\ 0.2,\ \ldots\ 0.9$ and 1.

4. Vertical velocity w in the problem of the square cellules.

Hereafter, in the Experimental Section, we shall need to know the distribution of velocities in the median horizontal plane ($z = h/2$) of a layer of air divided into square cellules, a distribution that we shall now proceed to determine.

The median plane being the plane of symmetry, (because we take the same conditions for the two limiting surfaces), it is evident that the components of velocity u and v vanish, and that the vertical component w, defined by (35) alone remains.

If we reintroduce the supposition (14), the relationship (35) gives us, after the operation with ∇^2:

$$w = \frac{x}{\beta}\,\Delta T_0 \left[Z'' - (l^2 + m^2)Z \right] \sin lx \sin my.$$

In the median plane, the last relationship can be written under the form:

$$w = w_0 \sin lx \sin my, \tag{90}$$

where w_0 is a constant which depends only on the boundary conditions and on the form of the cellules. It is to this expression precisely that we shall return later on.

B - Experimental Section

1. Two-dimensional cellular eddies.

The two-dimensional cellular eddies, contained in a slender

tank with glass walls very close together (cf. Chap. II), are the only ones allowing the direct observation and photographing of the trajectories and of the partitioning in the vertical plane.

One single stage of eddies. - The photographs taken during the phase where the smoke is still sufficiently concentrated (see Figs. 11-b and c, Chap. II and Fig. 98), show that the actual trajectories resemble, on first approximation, those which result from mathematical analysis. Bear in mind, however, the dimensions of the cellules do not enter into the discussion.

None the less, when we examine the photos relating to a more advanced phase in the regularization of the cellules(diffused smoke), we find out that the centers of rotation C_r do not coincide with the geometric centers C_g of the rectangular partitions. For one thing, they are pushed toward the top, and for another, they draw nearer to the centers of descending currents (hence, they draw away from the centers of ascending currents, as shown in Figs. 99 and 100. By designating e_h the horizontal elongation of the center of rotation from the geometric center (Fig. 101), one becomes aware that the average speed of the descending currents W_d is necessarily greater than the average speed of the ascending currents W_a by reason of the relationship:

$$W_a : W_d = b_2 : b_1 ,$$

where

$$b_1 = \frac{1}{2}\lambda + 2\ e_h \qquad \text{and} \quad b_2 = \frac{1}{2}\lambda - 2\ e_h,$$

λ being the width of the two twin cells.

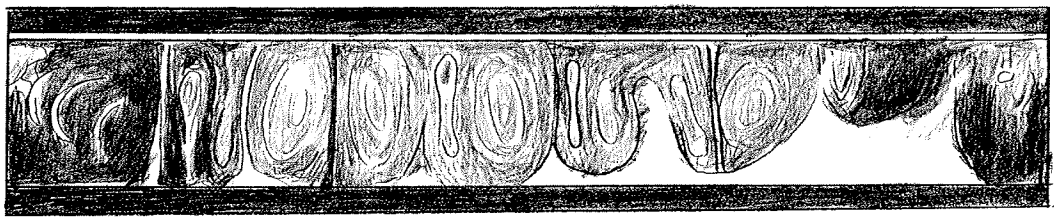

Fig. 98 Experimental eddies of two dimensions in a layer of air; trajectories made visible by tobacco smoke. Height of layer h = 65 mm.

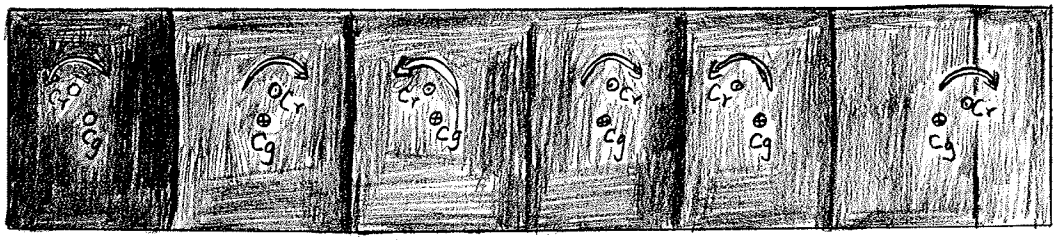

Fig. 99 Experimental eddies of two dimensions in a layer of air with diffused tobacco smoke. The geometric centers C_g of the cellules do not coincide with the centers of rotation C_r. h = 65 mm.

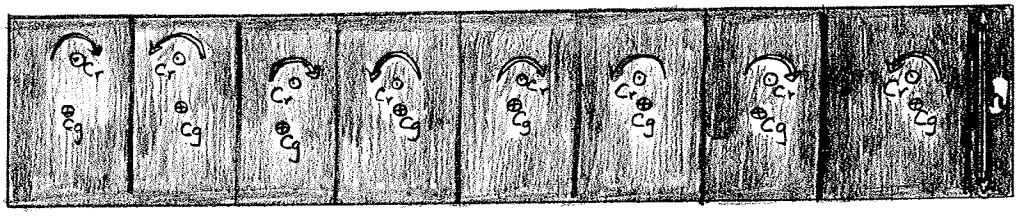

Fig. 100 Experimental eddies of two dimensions in a layer of air with diffused tobacco smoke. The geometric centers C_g do not coincide with the centers of rotation C_r. h = 85 mm.

It results likewise from the measurements taken on the photographs (Fig. 99 and 100), where we have marked the centers C_r and C_g, that the vertical displacement e_v is very much greater than the horizontal displacement e_h; and in consequence, the difference of the average

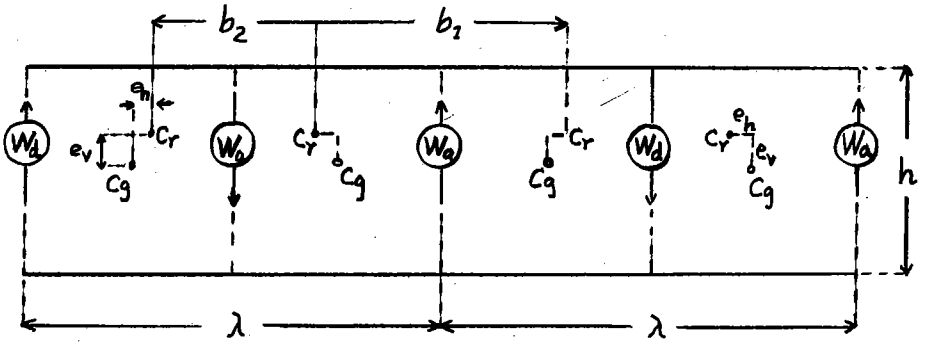

Fig. 101 Schematic eccentricity of the geometric centers C_g and of the centers of rotation C_r of the cellules.

horizontal speeds above and below the line of the centers of rotation is again more accentuated.

Two stages of eddies. - The first mathematical analysis of cellular eddies, given by Lord Rayleigh, revealed the existence of the stable preconvective regime , a problem which we have submitted to experimental verification with full success (cf. Chap. VII). A second fact, arising likewise from the mathematical analysis, has been indicated by A.R. Low (15-b). This author resumed the theory of Rayleigh and Jeffreys and he found that besides the simple solution, admitting one single stage of cellular eddies, there exist multiple solutions which correspond to numbers of stages greater than one. He also carried out the calculations and the drawings of the stream lines for the cases of convective eddies with one, two, three and four stages.

We have shown, withal, that in starting from the original theory of Jeffreys one can arrive at the same result. In particular, we have developed the calculation of the Rayleigh-Bénard criterion for a given number of piled-up modes, and that equally well for the conditions of the problem of Rayleigh as for those of the problem of

Jeffreys (cf. Chap. VII, Theoretical Section).

More especially still, we have treated the antisymmetric problem with two stages of eddies. We have determined numerically the criterion $\Lambda_{r=2}$, the function Z and the stream function ψ, and all that for the two aforementioned problems. For all the details, the reader should refer directly to the corresponding chapter.

Multiple modes have never been seen by the experimenters. In view of confirming or rejecting the practical value of this theoretical result we have proceeded to the necessary experiments (21-e) using the same slender tank that served us before in producing cellular

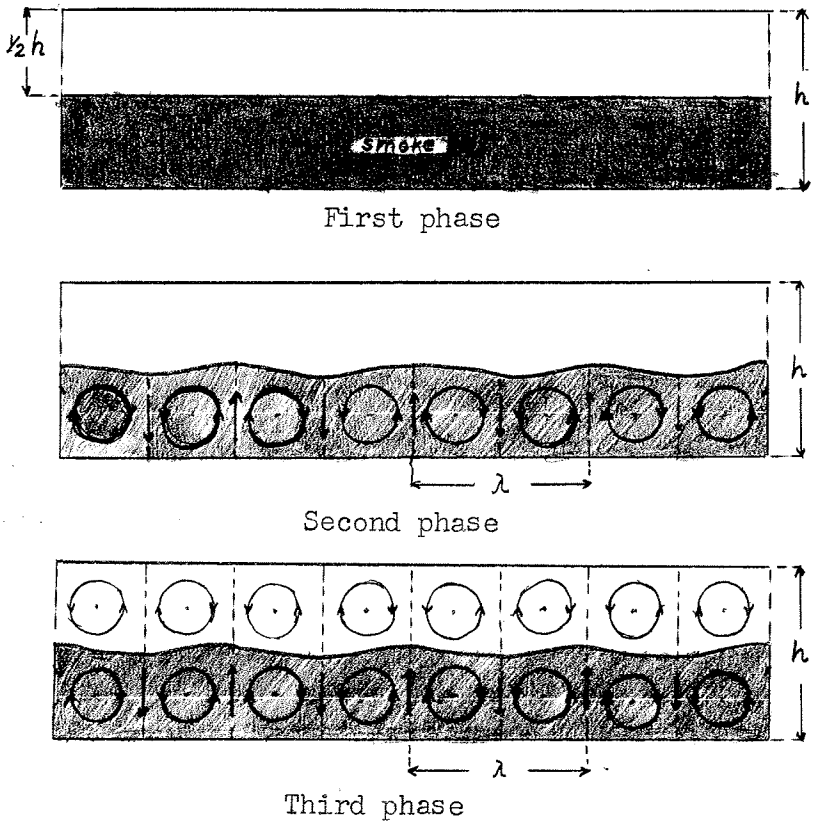

Fig. 102 Schematic development of eddies of two dimensions in two superposed layers, one formed of dense smoke, the other of pure air.

eddies in two dimensions (cf. Chap II).

As soon as the thickness h of the gaseous layer is determined by the level of the layer of water covered by a thin sheet of oil, one allows tobacco smoke to flow in sufficient quantity to fill up the lower half of the hermetically sealed tank. The layer of thick smoke (Fig. 102: First phase) stays horizontal some time and cleanly separated from the upper layer of pure air.

One readily perceives that in the smokey layer the thermo-convective eddies establish themselves (Fig. 102: Second phase). The interior motion provokes a very strong undulation of the surface of separation.

Soon, a filament of smoke indicates that eddies, superimposed upon the preceding ones, have likewise formed in the upper layer. (Fig. 102: Third phase).

After the establishment of currents in two stages, the surface of separation remains in undulatory movement. This proves that this formation is not very stable, even if it is only a matter of two stages and despite the fact that the densities of the thick smoke and pure air differ perceptibly. The bringing about of regular currents of several stages, would be, then, in the case of gasses, almost impossible, even if we could avoid the diffusion of the gasses. On the contrary, no difficulty presents itself if one operates with liquids that are different and do not mix.

The phenomenon of diffusion also intervenes in our experiment made with two superposed layers. In the upper layer, the eddy-motion progressively absorbs the tobacco smoke at the expense of the lower layer.

At last, all the smoke diffuses and a single layer of eddies is established, a form described from the beginning in Chapter II.

Analogous experiments in an indefinite horizontal layer would be very interesting, but as one can see, they would be delicate to realize.

To sum up, if superposed eddy-currents are to come about, it is needful that the empiled layers be sufficiently heterogeneous. Moreover, in the case of gasses, the diffusion must be avoided, or at least slowed up. As a consequence, one can never hope that motions in two or even several stages can establish themselves practically in a layer constituted of a homogeneous fluid. And so, the result of Mr. A.R. Low has only a mathematical interest for us.

2. Eddies in transversal bands.

The longitudinal section of the ensemble of transversal rolls gives the exact aspect of cellular eddies of two dimensions. Hence,

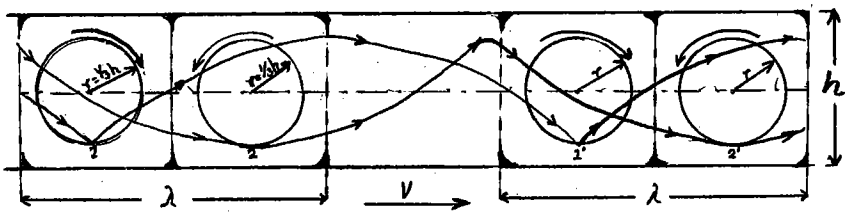

Fig. 103 Schematic trajectories in form of a shortened cycloid, described by the particles constituting the eddies in transversal bands.

the theoretical results relative to the problem in two dimensions apply just as well to eddies in transversal bands. In these conditions, the stream lines inside the rolls are rectangles whose angles

become the more rounded in proportion as they are nearer to the center of rotation (see Fig. 33: Fourth phase). These lines are curves situated entirely in the vertical planes oriented in the direction of the general current.

Being given that the ensemble of rolls moves with a rate of translation V, it results therefrom that the trajectories resemble shortened cycloids. These pseudo-cycloids appertain to two different families, for the ensemble of rolls is composed of two groups, of which the first turns to the right and the other to the left. The two types of trajectories can be compared with the shortened cycloids we have constructed on Figure 103, taking circles of diameter 2/3 h for the stream lines inside the rolls.

3. Eddies in longitudinal bands.

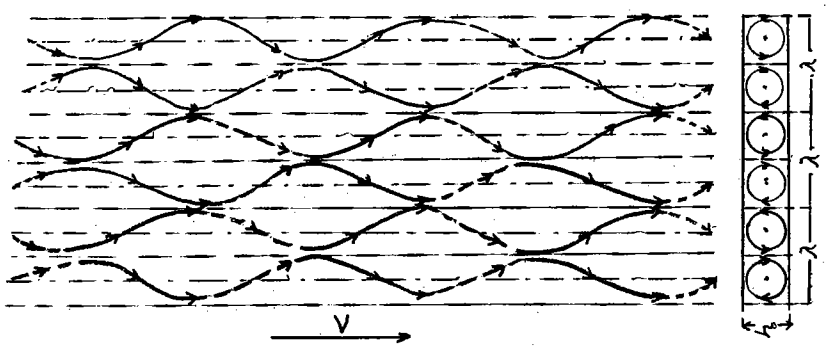

Fig. 104 Schematic helicoidal trajectories described by the particles forming eddies in longitudinal bands.

The considerations relating to the longitudinal section of transversal rolls apply integrally to the transversal section of eddies in longitudinal bands. We can therefor consider them as the same problem in two dimensions.

The speed of translation being perpendicular to the plane of rotation, the trajectories that result from it are pseudo-helicoidal curves. A view from above the longitudinal rolls and their transversal section are sketched in Fig. 104. The helicoidal trajectories, seen in projection, have a nearly sinusoidal form.

As regards photographic recording of internal motions, let us recall first the penetration of the concentrated smoke in the rolls already formed in the midst of the layer of pure air. The twist-drills (see Fig. 43) reveal very well the helicoidal character of the movement inside the longitudinal rolls.

The phase of penetration of the twist-drills is particularly favorable to the realization of quantitative measurements concerning the distribution of the component of axial speed with respect to the rectangular section of the rolls. Here is the principle of the method: We photograph at two well-determined instants, t_1 and t_2, the ensemble of penetrating twist-drills. Their form has elongated itself following the approximately parabolic distribution of the translation velocity in relation to the cross section of the rolls, as this is schematically represented in Fig. 105. The distance, s between points 1 and 2, situated on the two contours A and B (the one registered at instant t_1, and the other at instant t_2) is the direct measure of the lengthwise speed at the considered point. In fact, the longitudinal speed, in the permanent régime is expressed by:

$$V = \frac{s}{t_2 - t_1} = V(x,z).$$

It attains its maximum in the axis of the roll.

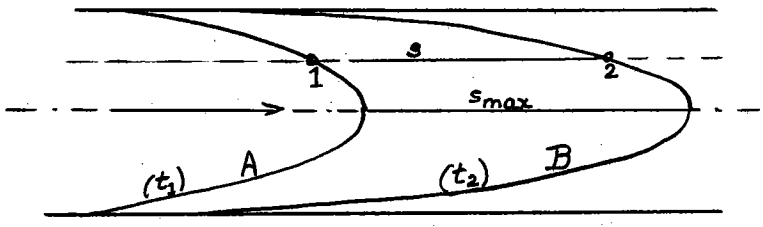

Fig. 105 Schematic distribution of speeds of translation along the longitudinal section of a roll.

Being given that the photographs are made in vertical projection, only the distribution of speeds in the median horizontal plane ($Z = 1/2$ h) can be established with exactitude. However, the gyratory character of the rolls allows us, with all necessary reserves, to apply the distribution of speeds of the median plane to other azimuthal planes.

Let us go on to the second means of visualization of the internal motions. It is the method of materializing individual helicoidal trajectories by means of the filament of smoke, an operation that is particularly successful when the thickness h is in excess of 20 mm.

The first photograph (Fig. 106) reproduces eight longitudinal rolls ($h = 35$ mm, $L = 345$ mm, $\lambda/h = 2.46$). The filament of smoke, injected in little doses in the individual rolls reproduces exactly the internal trajectories. These last, seen in projection, have sinusoidal form. Their wave-length is a function of the speed of translation and the angular speed. In turn, the speed of translation depends on the force of aspiration and on the friction of the gaseous mass in the canal, and the angular speed depends upon the difference of extreme temperatures and also on the friction. If the aspiration and the extreme temperatures are constant, the wave-length is only a

function of the spatial coordinates: it is short near the partitions and longer inside the rolls. The schema (Fig. 107) reproduces two twin rolls only. We have drawn for each roll three coaxial trajectories. The form of the peripheral trajectories is considerably influenced by the friction against the limiting plates. On the contrary,

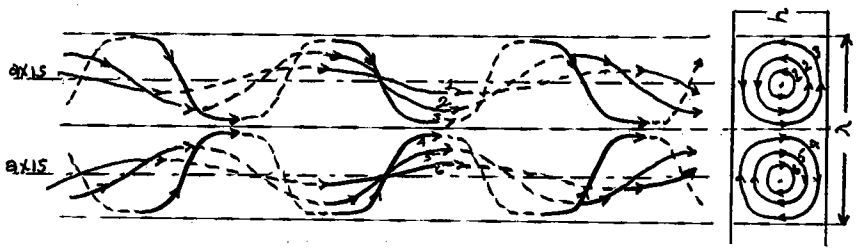

Fig. 107 Schematic helicoidal trajectories as a function of their elongation starting from the axis of longitudinal rolls.

the central trajectories reproduce very nicely perfect helices. These are the more elongated as they are nearer the central axis of the roll. The axis itself is a trajectory upon which the speed of translation attains its maximum value. (Figs. 106, 108, 109 back).

The second photograph (Fig. 108), relating to a layer of air 50 mm thick and 345 mm wide with eight rolls imposed, proves that the helicoidal trajectories remain always perfect, as they are in the case shown by Fig. 106.

Finally, the third photograph (Fig. 109) taken likewise for h = 50 mm, is interesting by its lateral rolls, where the peripheral trajectories are particularly deformed in consequence of the presence of the lateral walls of the canal.

As the translation and the rotation of the longitudinal rolls are rapid, the quantitative measurements would seem to require the use

of the cinema. The material means actually placed at our disposal have not permitted the realization of this interesting part. Their execution had to be adjourned until a later date.

4. Polygonal Cellular Eddies.

Hexagonal cellules. - Let us suppose that the gaseous layer be divided into hexagonal cellules whose principal dimensions conform to the result that one deduces easily from the theory of Lord Rayleigh (horizontal distance of two centers of contiguous hexagons $\lambda = 3.29h$). The trajectories of the steady circulation are closed curves situated in the vertical planes passing through the axes of the cellules.

It is easy to determine approximately the central line of the eddy around which all the threads of the fluid turn, by supposing that the average vertical ascending and descending speeds in the median horizontal plane ($Z = h/2$) are equal. In these conditions, the central portion (face where currents descend) and the peripheral portion (face where currents ascend) of the hexagon must have the same surface areas. If we admit that the central eddy line separating the two faces is a regular hexagon (in reality, its summits are rounded off) and concentric with the hexagon of the cellule, we find, according to Figure 110 that its side b, expressed by λ and h, is equal to:

$$b = \frac{\lambda}{\sqrt{6}} = \frac{3.29h}{\sqrt{6}} = 1.34\ h.$$

Hence if we make a vertical cut perpendicular to the sides of the

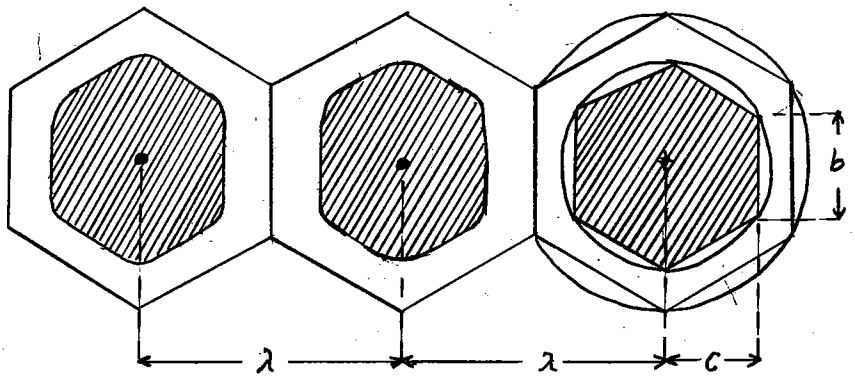

Fig. 110 Hexagonal cellular eddies in gasses: schematic separation of areas of ascending currents (white) and areas of descending currents (hatchings).

hexagons and passing through their axes, we obtain a series of rectangles each one having a height h and width $\lambda/2 = 1.65$ h (Fig. 111). The

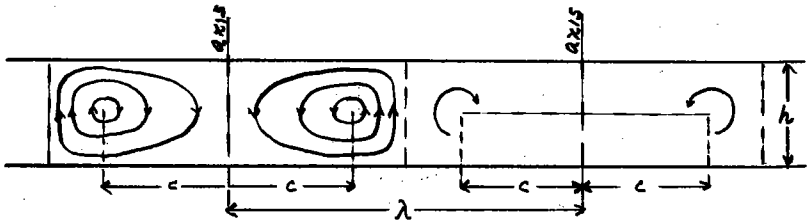

Fig. 111 Vertical section of hexagonal cellules in gasses with some trajectories around the line of rotation. The rotation is the reverse of that observed in liquids; ascent along lateral walls, descent along the axis.

central points about which the circulation occurs are defined equally. They are found on the horizontal line $z = h/2$, symmetrically separated with respect to the vertical axes at the distance c which is equal to:

$$c = \frac{\sqrt{3}}{2} b = \frac{\lambda}{2\sqrt{2}} = 1.16 \text{ h.}$$

Guided by the rectangular contour of the vertical section of a hexagonal cellule and by the position of the two central points of the

circulation, we have designed upon the same Figure 111 several intermediary trajectories (see also Fig. 5 relative to eddies in liquids).

Square cellules. - The reasoning we have just applied to hexagonal cellules can be entirely applied to square cellules, it being understood that the central eddy-line would be here a square with rounded summits with the side:

$$b = \frac{\lambda}{\sqrt{2}},$$

where λ is the distance of the centers of two contiguous cellules (or again the side of the square cellule).

If we mark in black the regions with descending currents and leave white the regions with ascending currents, we obtain the characteristic distribution shown in Fig. 112. Let us make the same design using the analytic solution (90) for the component of vertical velocity w, relative to square cellules, where the wave-lengths λ and μ are equal and defined by (73).

It is needed to determine the places with rising currents ($w > 0$) and descending, ($w < 0$). It is evident that one must pass from the places of one given sign to those of the opposite sign by $w = 0$. The geometric spot where $w = 0$ (cf. (90)) is defined by:

$$lx = \pm n\pi \qquad \text{and} \qquad ly = \pm n\pi ,$$

where $n = 0, 1, 2, \ldots$, which gives two systems of straight lines. The first ($lx = \pm n\pi$) is parallel to the y-axis, and the other ($ly = \pm n\pi$) to the x-axis.

We can check easily that the quadratic surfaces occupied by the ascending and descending currents are disposed in a checkerboard,

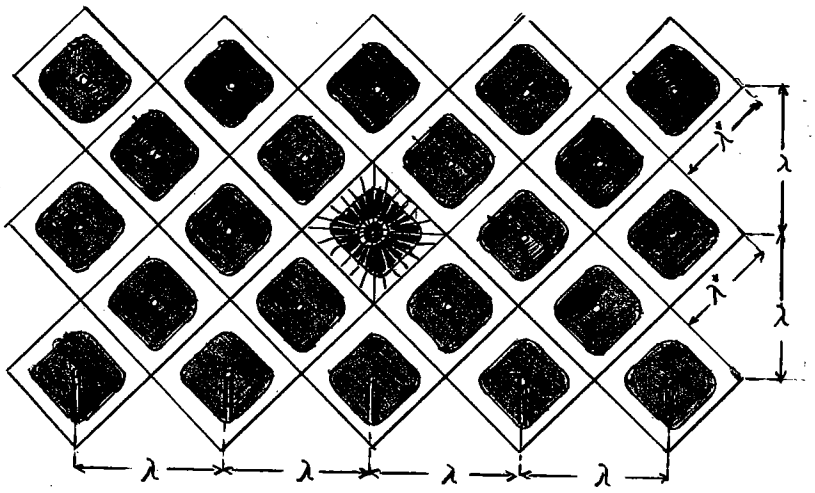

Fig. 112 Schematic square cellular eddies; surface motion and separation of areas of ascending currents (white) and places of descending currents (black) as seen in the experiments.

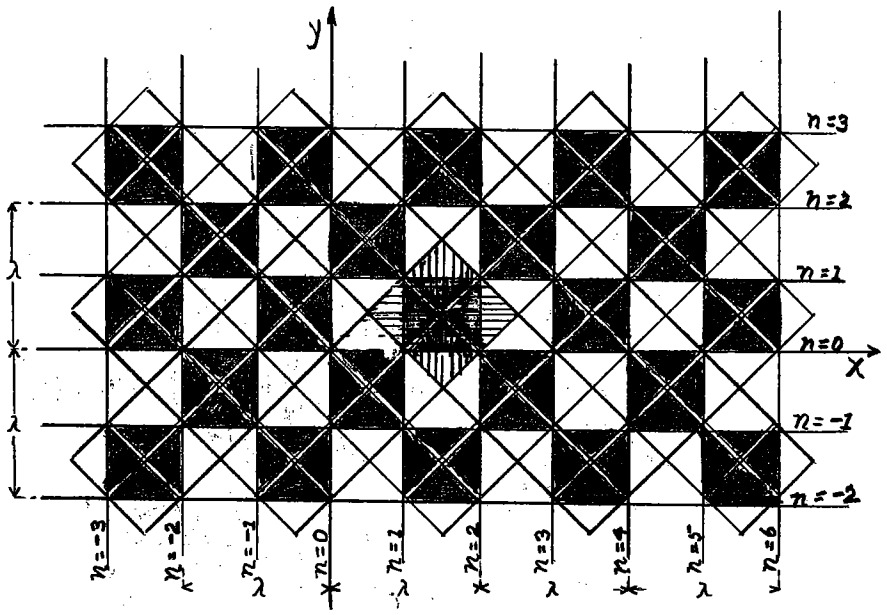

Fig. 113 Mathematic square cellular eddies: surface motion and separation of areas of ascending currents (white) and areas of descending currents (black) as one obtains them in accordance with the theory.

as that is designed in Fig. 113. In comparing the two figures 112 and 113 we observe that they differ entirely. And for this reason, the

analytical solution cannot be accepted here without reserve.

Chapter XI

Part I

Distribution of Temperatures in a Fluid Layer containing Cellular Eddies.
Thermal Field in Certain Particular Cases.

A - Theoretical Section

1. In designating by T_1 and T_2 the two extreme temperatures of the fluid layer in which cellular eddies are occurring, the temperature at any point is defined by:

$$T = T_2 + \frac{T_1 - T_2}{h} z + \Delta T, \tag{91}$$

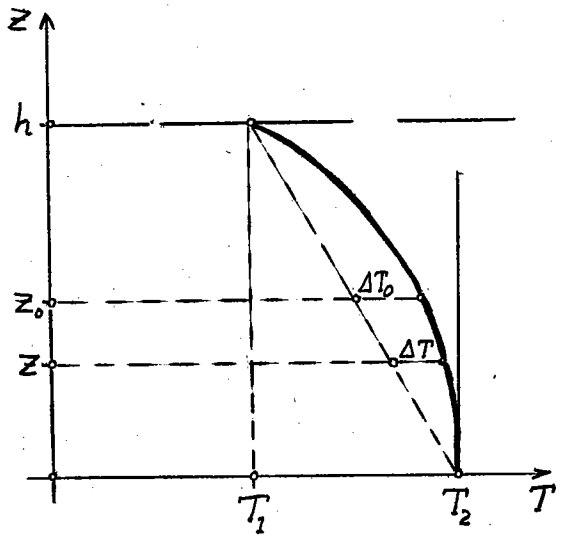

Fig. 114 Schematic diagram of the temperature distribution with depth in a fluid layer, containing thermoconvective eddies.

where $\frac{T_1 - T_2}{h}$ is the linear gradient of temperature following the vertical axis z (Fig. 114); T_2 designating the temperature of the lower

surface, this graident, which we will designate by β , if, hence, by definition, negative.

The two first terms of the second member of (91) represent the linear distribution of temperatures in an irrotational fluid layer. This distribution is modified essentially as soon as the convective currents arise. The perturbation in the linear distribution of the temperatures, occasioned by the convective currents, is represented by the additional term ΔT, which is expressed, in the theory of thermoconvective eddies by the relationship (14).

2. Determination of the amplitude ΔT_0 of the thermal perturbation.

It has been possible to determine ΔT_0 by the application of a condition at the limits or boundaries (94), not perceived by the theorists and which the experiment suggested to us.

The function Z, figuring in the expression (14), has been defined in certain particular problems (cf. Chap. X). To determine numerically the distribution of temperatures in the space occupied by the convective currents, it remains to us to find the value of ΔT_0.

It is evident that the greatest perturbations of temperature coincide with the centers of the ascending and descending currents. These centers are found at the places that satisfy the condition:

(92) $$\sin \ell x \sin my = \pm 1.$$

Then, the equation (14) simplified itself into:

(93) $$\Delta T = \pm \Delta T'_0 Z.$$

The theory supposes the constancy of the temperatures of the

two limiting partitions, (sidewalls). Hence in these places, the thermal perturbation ΔT is null, that is to say, that $Z = 0$ when $z = 0$ or h. Supposing likewise that the heat source be found solely on the bottom of the canal, the temperature T_2 os the lower surface must be maximum and the temperature T_1 of the upper surface minimum:

$$T_2 \geqslant T \geqslant T_1 .$$

Thanks to the uniform convective currents, the temperature T decreases towards the top in continuous fashion. If we admit, moreover, that the heat is transmitted to the fluid layer without discontinuity in the thermal field, there results from it the supplementary boundary condition of which we have spoken:

(94) $$\left(\frac{\partial T}{\partial z}\right)_{z=0} = 0.$$

Combining (91) and (94) and taking for ΔT the positive value of (93), since we are considering the ascending currents, we get:

(95) $$\Delta T_0 = -\frac{\beta}{\left(\frac{\partial Z}{\partial z}\right)_{z=0}} = -\frac{\beta}{\left(\frac{\partial Z}{\partial z}\right)_{z=0}} .$$

In the problem of Rayleigh we have found for the function Z the expression (83a). This last, written in the z system, which is connected to the ξ system by (21), becomes:

$$Z = \sin \pi \frac{z}{h} .$$

That being so, (95) gives us then for the amplitude:

$$\Delta T_0 = -\frac{\beta h}{\pi} .$$

In the problem of Jeffreys, the function Z has the form (85). In passing from the system ξ to the system z, the numerical solution

(85), divided by its maximum value (=18.2), becomes:

$$Z = -9.01 + 43.5\left(\frac{1}{2} - \frac{z}{h}\right)^2 - 28.9\left(\frac{1}{2} - \frac{z}{h}\right)^4 + 10 \sin\pi\frac{z}{h} + 0.01 \sin 3\pi\frac{z}{h} + 0.00033 \sin 5\pi\frac{z}{h} + \ldots \tag{96}$$

By calculating its derivative in z = 0, we find according to (95):

$$\Delta T_0 = -\frac{\beta h}{2.5} . \tag{97}$$

3. Distribution of the temperatures along the vertical.

The equation (91), where ΔT is defined by the relationship (14), gives the distribution of the temperatures in the vertical at any point. Again, it is the centers of the ascending and descending currents, defined by (92), that interest us in the first place. The variation of the temperature as a function of z is then given by:

$$T = T_2 + \beta z \pm \Delta T_0 Z. \tag{98}$$

This equation becomes particularly simple at the places that satisfy: $\sin \ell x \sin my = 0$, that is to say, at the points where the vertical velocity is null. (98) reduces itself to:

$$T = T_2 + \beta z.$$

At these places, the linear distribution of the temperatures is not modified by the thermoconvective currents: it remains as it was at the time of the stable preconvective régime.

We give two diagrams of the distribution of temperatures following the thickness of the layer of air, the one for the problem of Rayleigh (Fig. 115), the other for the problem of Jeffreys (Fig. 116). The three curves of each diagram correspond respectively to the centers

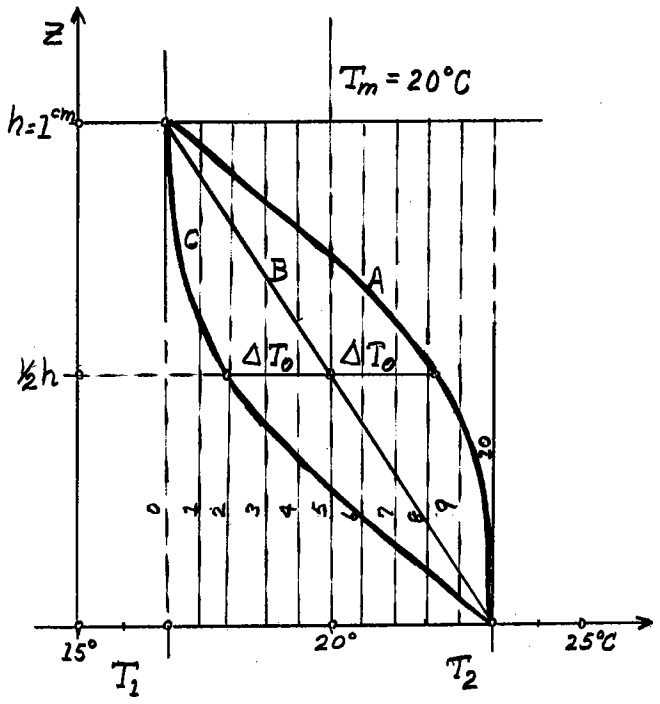

Fig. 115 Theoretical temperature distributions with depth in a layer of air with two free surfaces in the problem of Rayleigh in two dimensions.

A: following the vertical with ascending currents;
C: following the vertical with descending currents;
B: following the vertical placed between A and C.

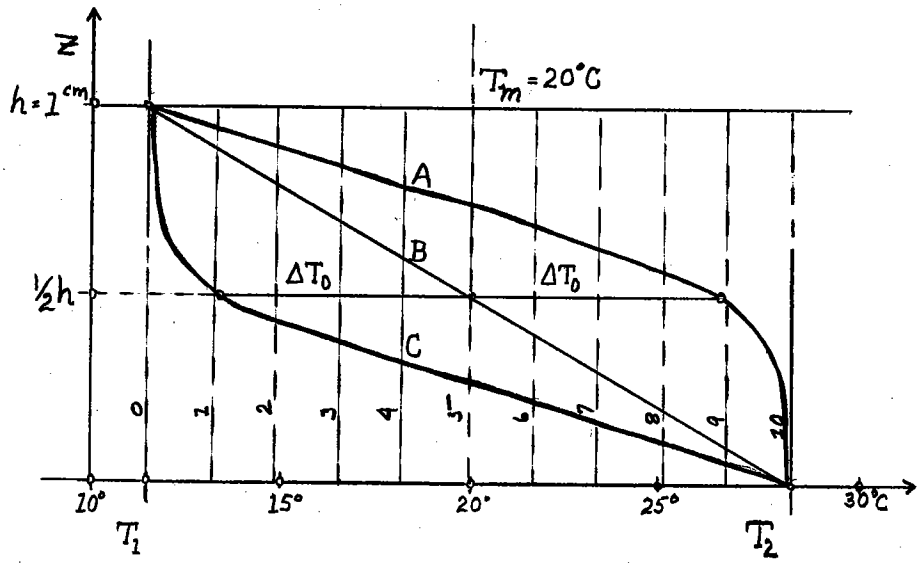

Fig. 116 Theoretical temperature distribution with depth in a layer of air contained between two rigid partitions in the problem of Jeffreys in two dimensions. A: along the vertical with ascending currents; C along the vertical with descending currents; B along the vertical placed between A and C.

of the ascending currents ($w = w_0$) and descending currents ($w = -w_0$) and at the intermediary zone where the speeds are horizontal ($w = 0$). We have given to the gradients of temperature β the critical values calculated for a layer of air 1 cm thick at an average temperature of 20°C (cf. Chap. VII, equation (67)).

4. Determination of the thermal field.

Using the relationships (14) and (95), the fundamental equation (91) is written definitively

$$T = T_2 + \beta z - \sin lx \sin my \frac{\beta}{\left(\frac{dZ}{dz}\right)_{z=0}} Z,$$

or again:

$$(99) \qquad \Theta = \frac{T - T_2}{\beta h} = \frac{z}{h} - \sin lx \sin my \frac{1}{h\left(\frac{dZ}{dz}\right)_{z=0}} Z.$$

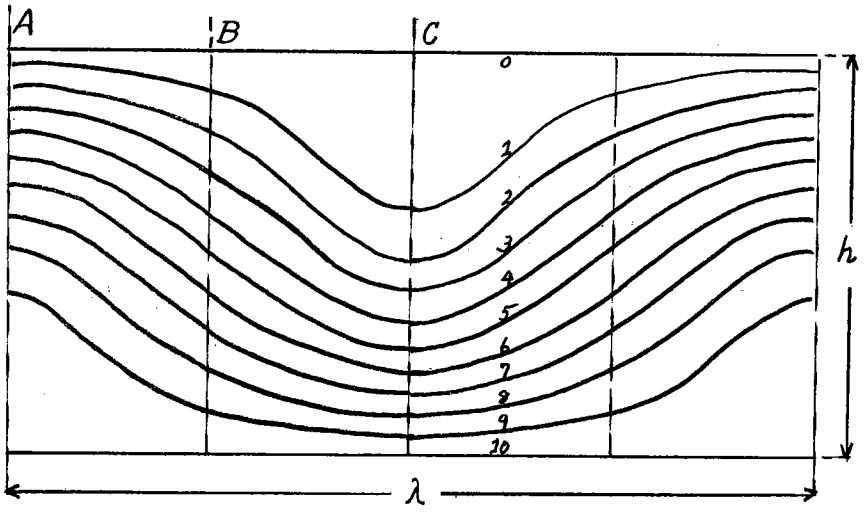

Fig. 117 Field of theoretical isotherms of eddies of two dimensions and eddies in bands in the problem of Rayleigh. (λ is not reproduced on exact scale; in reality it is equal to $2\sqrt{2}$ h.)

The thermal field, defined by (99), is, hence, independent of the gradient of temperature β and of the thickness h: the behaviour-pattern

of the isotherms is the same for all values of β and h.

The equation (99) reduces itself in the two-dimensional system to:

(100) $$\Theta = \frac{z}{h} - \sin \ell x \frac{1}{h\left(\frac{dZ}{dz}\right)_{z=0}} Z,$$

which gives for each value of Θ a line of equal temperature, situated in the plane x, z.

This result applies equally to eddies in bands, whose transversal section is identical with (that of) two-dimensional eddies.

Let us calculate the thermal fields relative to the eddies in bands, in the two previously treated problems.

Problem of Lord Rayleigh. When we introduce into the equation (100) the values of $Z, \left(\frac{dZ}{dz}\right)_{z=0}$ and ℓ, corresponding to the problem in question, it becomes

(100 a) $$\Theta = \frac{z}{h} - \frac{1}{\pi} \sin \frac{\pi}{\sqrt{2}} \frac{x}{h} \sin \pi \frac{z}{h} .$$

We have calculated, according to (100 a), eleven isotherms, in giving to Θ the successive values of 0, 0.1, 0.2, ... 0.9 and 1, and drawn on Fig. 117 the thermal field for two rectangular cellules, whose height is equal to h and the total breadth to λ. The two extreme isotherms, $\Theta = 0$ and $\Theta = 1$, are horizontal lines.

Problem of Jeffreys. ℓ is equal, nearly, to unity. Z and ΔT_0 being likewise determined by (96) and (97), the function Θ becomes

(100 b) $$\Theta = \frac{z}{h} - \sin x \left[-3.6 + 17.4 \left(\frac{1}{2} - \frac{z}{h}\right)^2 - 11.5 \left(\frac{1}{2} - \frac{z}{h}\right)^4 + 4 \sin \pi \frac{z}{h} + 0.004 \sin 3\pi \frac{z}{h} + \ldots\right] .$$

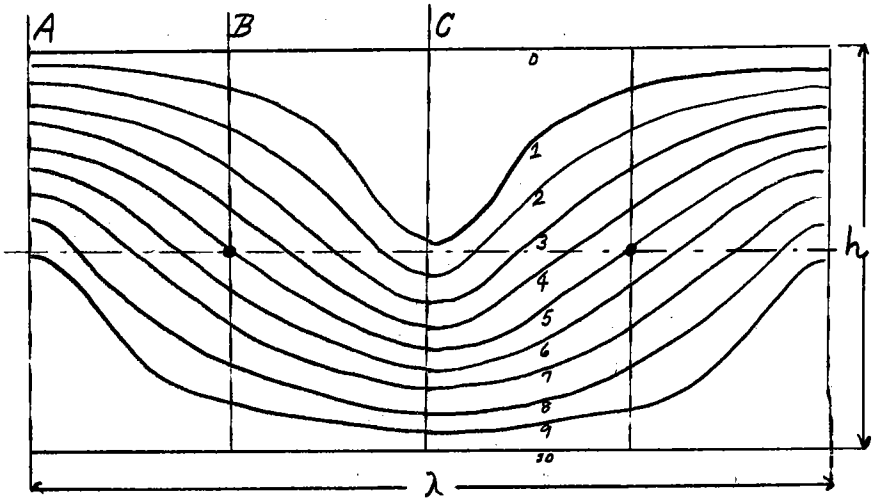

Fig. 118 Theoretical field of isotherms of eddies of two dimensions and eddies in bands in the problem of Jeffreys.

Figure 118 reproduces the thermal field, calculated according to (100 b) for eleven values of θ (0, 0.1, 0.2, ... 0.9, 1) and extended to the section of the two contiguous cellules.

In comparing the two examples examined, one sees that the thermal field of the stable preconvective régime (in which the isotherms are straight lines parallel to the x-axis) undergoes more perturbation in the problem of Jeffreys than in the problem of Rayleigh.

5. Variation of temperature normal to the axis of eddies in bands.

We shall show in Chap. XII, consecrated to the application to meteorology of the theory of thermoconvective eddies, the importance of recording of temperatures normal to the axis of a compartmented cloud system. For this recording, it is fitting to choose the horizontal level where the temperature amplitude, following a given direction, is maximum; this is evidently the median plane $z = h/2$.

In the case of eddies in bands, the variation of the temperature is defined by:

$$\Delta T = \Delta T_0 \sin \ell x \, Z_{max}$$

In the particular problem of Lord Rayleigh, it takes the form:

$$\Delta T = -\frac{\beta h}{\pi} \sin \frac{\pi}{\sqrt{2}} \frac{x}{h} = \frac{T_2 - T_1}{\pi} \sin \frac{\pi}{\sqrt{2}} \frac{x}{h} .$$

For the conditions of Jeffreys, we obtain an analogous expression:

$$\Delta T = \frac{T_2 - T_1}{2.5} \sin x.$$

Chapter XI Part II

B. Experimental Section

1. Equipment. Method of operation.

To choose a method permitting one to measure the temperatures in a layer of air containing thermoconvective eddies, it is necessary to specify the inherent characteristics of this phenomenon.

Order of magnitude of the differences of temperature to be measured. One undertakes to measure the temperatures of a layer of air whose thickness may come to 6 cm. One knows that a difference of 0.5°C between the extreme temperatures largely suffices for the production of thermoconvective eddies when h = 6 cm (cf. Chap. VII).

The measurement of these temperatures at five equidistant points along the vertical (z = 0, 0.25h, 0.5h, 0.75h and h) seems to be necessary and sufficient. Let us suppose, in first approximation, that the temperature varies linearly: the differences of temperature will be on the order of 0.1°C.

Stability of the local temperature. The preliminary endeavors show that the temperature at a given point of the fluid layer oscil-

lates incessantly between more or less wide limits.

These oscillations are the immediate consequences of the continual evolution of the form of the cellular eddies (growth of little cellules, breaking up of big cellules, alignment of polygonal cellules in chains and in bands, etc.). The causes of these transformations are very varied; we have indicated them in Chap. V. But by reason of this evolution, the measurements must be carried out:

1. Rapidly; that requires that the thermometric instrument have a small heat inertia;

2. With great precision; the readings must be made to better than one tenth of a degree C;

3. Without appreciable perturbations of the eddy system; the thermometric instruments, hence, must not be clumsy or encumbering.

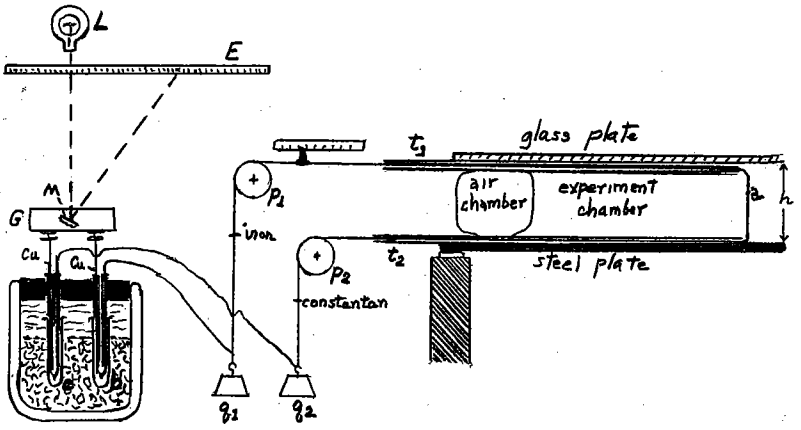

Fig. 119. Set-up of thermoelectric couple. L = lamp. E = scale.

4. At each desired point of the fluid sheet; the thermometric instrument must be very easy to move about.

The iron-constantan thermocouple possesses all these properties. The set-up that we adopted is schematically represented in Fig. 119.

Two wires, one of iron, the other of constantan, each of a diameter of 1/20 mm, are soldered at point a. The two other extremities, b and c, are soldered to the copper wires connected in their turn to a galvanometer with a mirror G. The solderings b and c, serving as a reference-point and enclosed in a thermos bottle, are maintained at a constant temperature (in our experiments, generally that of melting ice). One reads the deviations from a spot on a scale E, graduated in millimeters.

To bring the soldering a to some or other point of the experiment chamber, we worked out a very simple set-up. Two capillary tubes, t_1 and t_2, the one touching the floor, the other the ceiling of the experimental canal, guide the wires of iron-constantan in the horizontal planes, distant h mm. Two little weights q_1 and q_2 hold the wires constantly taut by means of two pulleys p_1 and p_2. Thus, one can bring the soldering a to any point according to the thickness of the layer of air, by simply raising one weight or the other. When one wishes to displace the soldering a in respect to the width of the canal, one displaces simultaneously the two capillary tubes in the same transversal plane. Finally, to explore the temperature following the length of the canal, it is necessary to displace the entire set-up. A little needle, fixed on the wire indicates on a little scale the precise location of the soldering a.

Calibration of the iron-constantan couple.

We have calibrated the couple in the interval of from 5°C to 20°C. The representative curve is rectilinear (Figure 120).

On an average, 1°C equals twenty-two divisions of scale E.

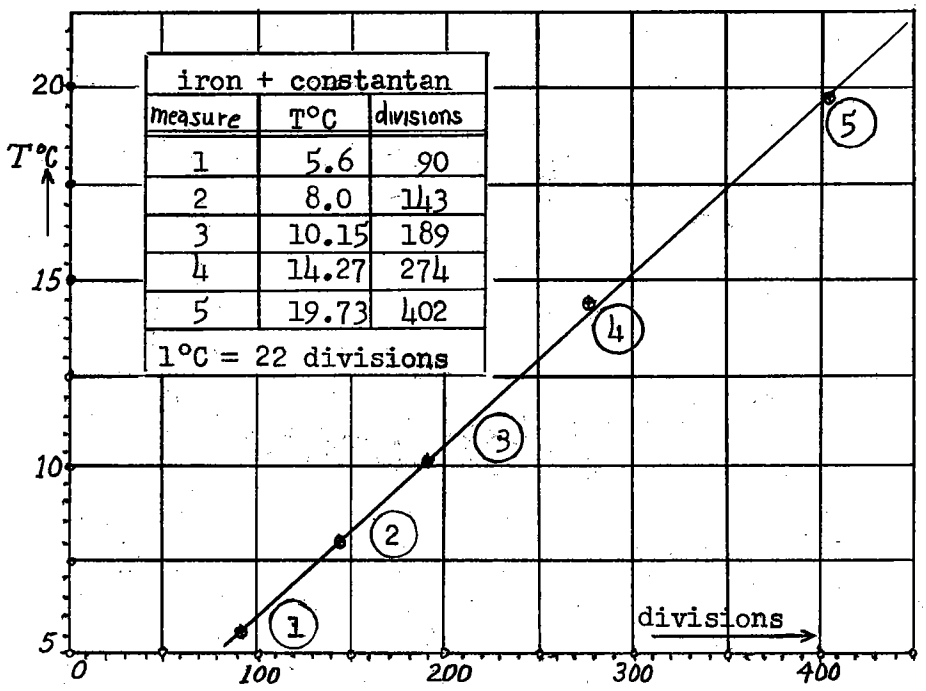

Fig. 120 Calibration curve of the iron-constantan thermoelectric couple.

The luminous pencil, being very slender, one can read nearly to a half-division, and by consequence, one can determine the temperature to 1/44°C, or close to it.

Remark. - The thickness accessible to measurement with the thermoelectric couple is slightly less than the total thickness h of the fluid layer, because one loses on each side a little thickness δ occasioned by the introduction of the capillary tubes leading the thermoelectric wires. We have marked in the figure 121 the five points where we measured the temperatures. They are uniformly separated along the reduced thickness $h_r = h - 2\delta$. (In our experiments we had $\delta = 3.5$ mm). In these conditions, all the following diagrams relate to the reduced thickness h_r. To compare more easily the results obtained at different thicknesses, we took h_r as unity. Hence, we have carried on the axis of the ordinates the values of

$$\xi_r = \frac{z-\delta}{h_r}.$$

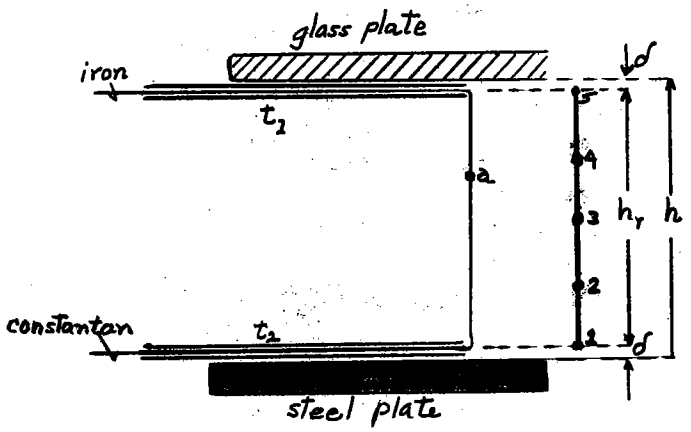

Fig. 121 Cable movement of the solder joint a of the thermoelectric couple in the experiment chamber. (h = thickness of air layer; h_r reduced thickness determining the free travel of the solder joint).

2. Distribution of temperatures in the vertical.

Unheated layer of air. At the commencement of each series of experiments, we have also measured the distribution of temperatures along the vertical before the layer was submitted to the heat. These measurements were carried out in the layer at rest and in the layer under translation-movement.

The experiments in a layer at rest have shown that the variation of temperature is sensibly linear for all the values of h. Moreover, the vertical gradient of temperature is always greater than zero. In the course of our labours, we did not find a single case where the gradient β was null, even though this case can produce itself if the conditions in the experiment chamber are favorable.

The two diagrams shown, Figs. 122 and 123, of which the first relates to h = 39 mm and the second to h = 63 mm, give several curves arising from different experiments in a layer of air at rest.

The results obtained with the same thicknesses in a layer of

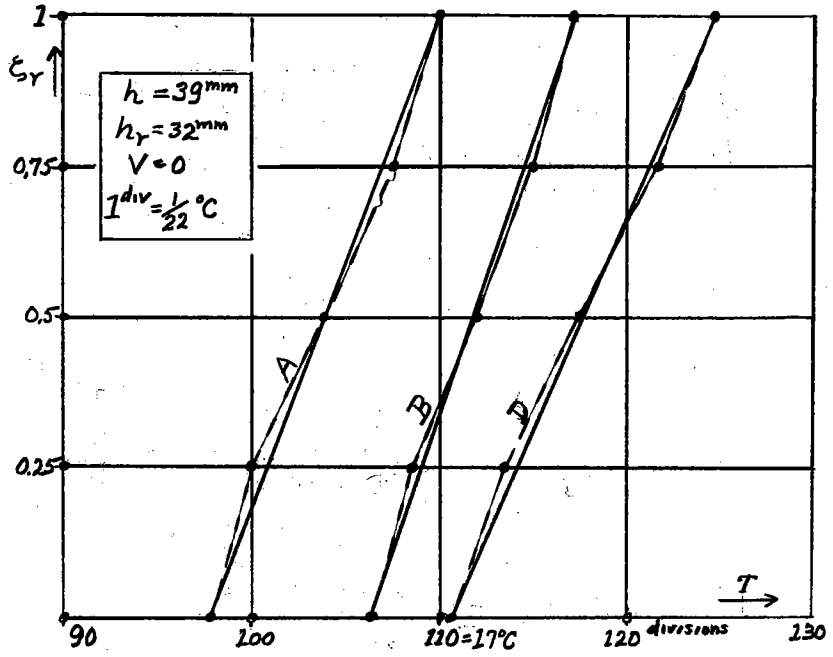

Fig.122 Distribution before the principal experiment, of temperatures along the thickness of a layer of air at rest and not heated (h=39 mm).

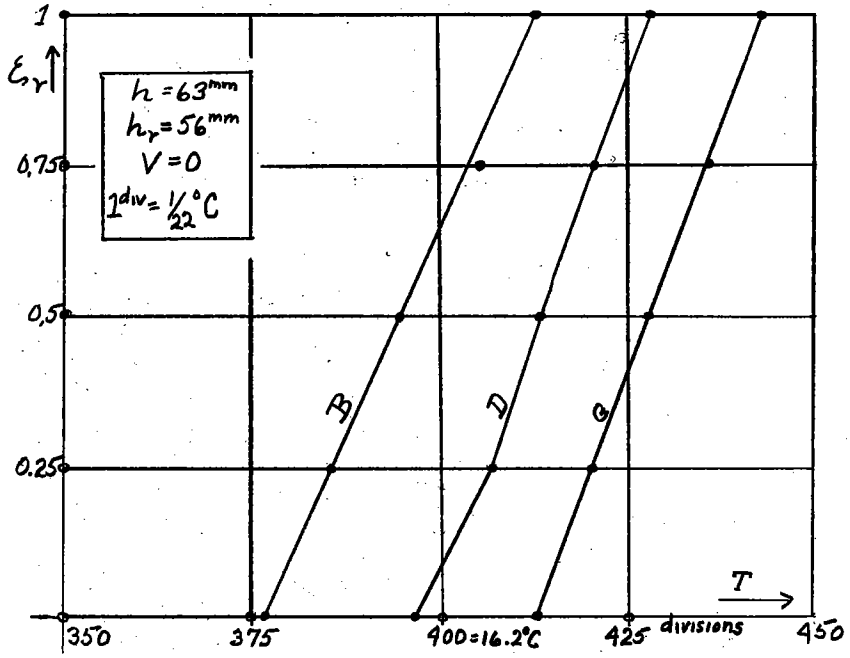

Fig. 123. Distribution, before the principal experiment, of temperatures along the thickness of a layer of air at rest and not heated. (thickness h = 63 mm).

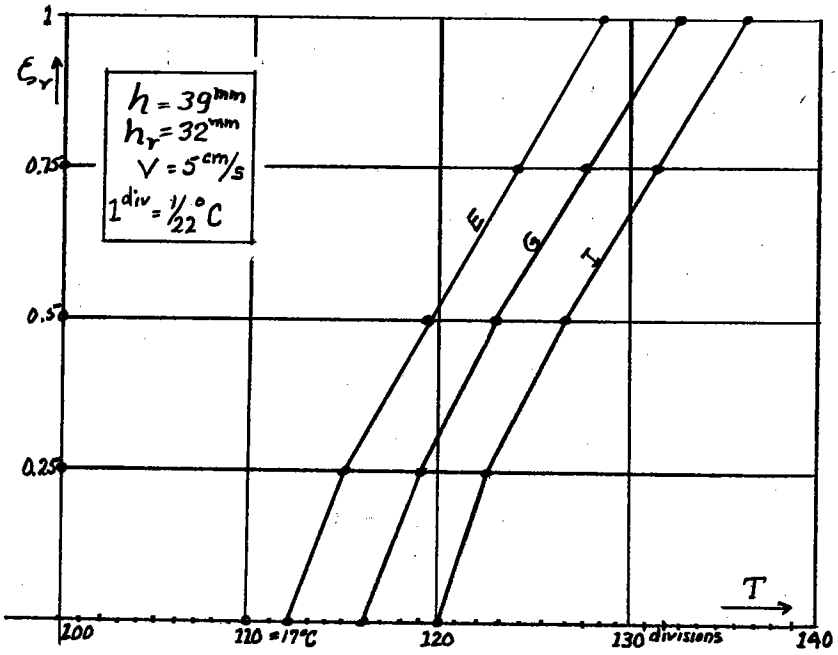

Fig. 124 Distribution, before the principal experiment, of temperatures along the thickness of an air layer in motion of translation and not heated. (thickness h = 39 mm. Speed V ≃ 5 cm/s.)

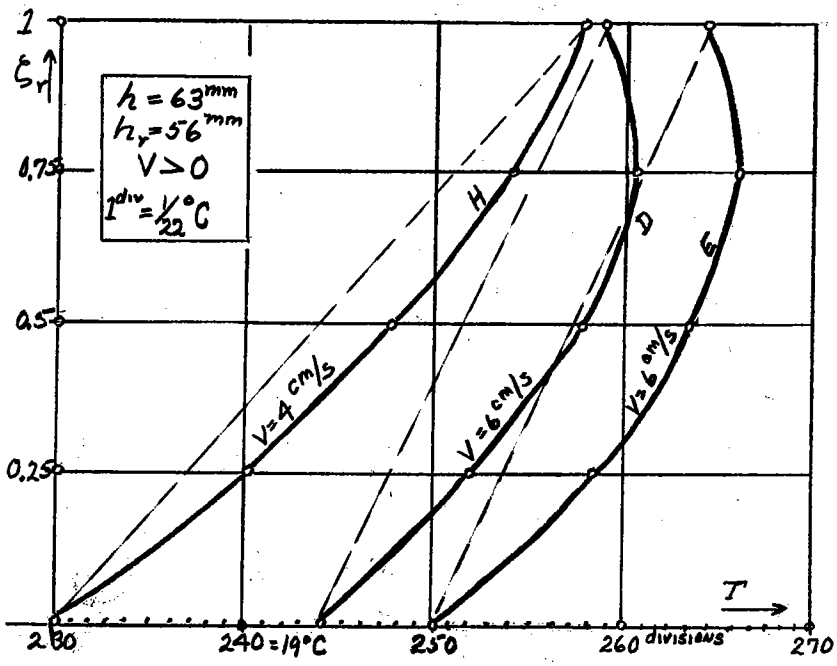

Fig. 125 Distribution before the principal experiment, of temperatures along the thickness of an air layer in movement of translation and not heated. (Thickness h = 63 mm. Speed V ≃ 6 cm/s).

air in movement of translation are shown by the diagrams of Figs.124, 125. In the case of thickness h = 39 mm and for a speed of translation

$V \simeq 4$ cm/s, the distribution stays essentially linear; it ceases visibly to be so when the thickness is greater. The departure from linear distribution becomes still more accentuated if the speed of translation V increases. This comes from the fact that the time of flowing of the fluid sheet through the canal is too short and the thickness h too great for the temperature of the air that arrives to be able to accommodate itself to the temperatures of the limiting walls.

Vertical gradient of temperature as a function of the time of application of the heat. The preceding results show that the vertical gradient of temperature in an unheated layer of air is positive and practically constant if the thickness h and the speed of translation V are relatively weak.

Now let us submit the layer of air to uniform heating, in supposing that the heat flux and translation speed are weak. The vertical gradient of temperature diminishes progressively with the time of application of the heating. At a given moment it becomes null (the temperature is uniform through all the thickness) and it passes then to negative values (the higher temperatures being on the bottom, the fluid layer becomes unstable). Here, for instance, are the results arising from two experiments made in layers of air of 43 mm and 39 mm thickness. The diagrams (Figs. 126 and 127) put in evidence the progressive change in the distribution of the temperatures along the vertical as a function of the time from first application of the heat.

Let us follow at close range the characteristic phases of the

first experiment (h = 43 mm). The first curve D has been obtained before the commencement of the heating with a layer of air animated by a translation movement of 5 cm/s. The gradient of temperature β is positive and almost constant in the entire thickness. The temperature increases continually towards the top and the layer is in perfect vertical equilibrium.

After this preliminary measure, we have submitted, at 13 h 36 mn, the layer of air to a uniform heat absorbing 2.4 watt/decimeter^2. Four minutes afterwards, we obtained the curve E. It is slightly straightened and shifted toward the right. The average temperature has increased, but that of the lower layers has increased more than that of the upper layers. To sum up, the gradient β has diminished. In the following four minutes the temperature became uniform from the bottom to the top. The curve F is a perfect vertical straight line ($\beta = 0$). Later on, the temperatures of the bottom became greater than those above. The curve G stays rectilinear even though the gradient β has passed to negative value. Nonetheless, we have made certain of a feeble oscillation of temperature at the height $\zeta_r = 0.75$. It announced, without doubt, the unleashing of the first thermoconvective currents. Hence, the criterion of Lord Rayleigh is already slightly overpassed. The curves H and I correspond to the régime where the eddies in longitudinal bands have entirely developed. The local temperatures, excepting the two extreme temperatures, oscillate between rather close limits. The heavily marked curves are the average of the extreme values which are indicated by dotted lines.

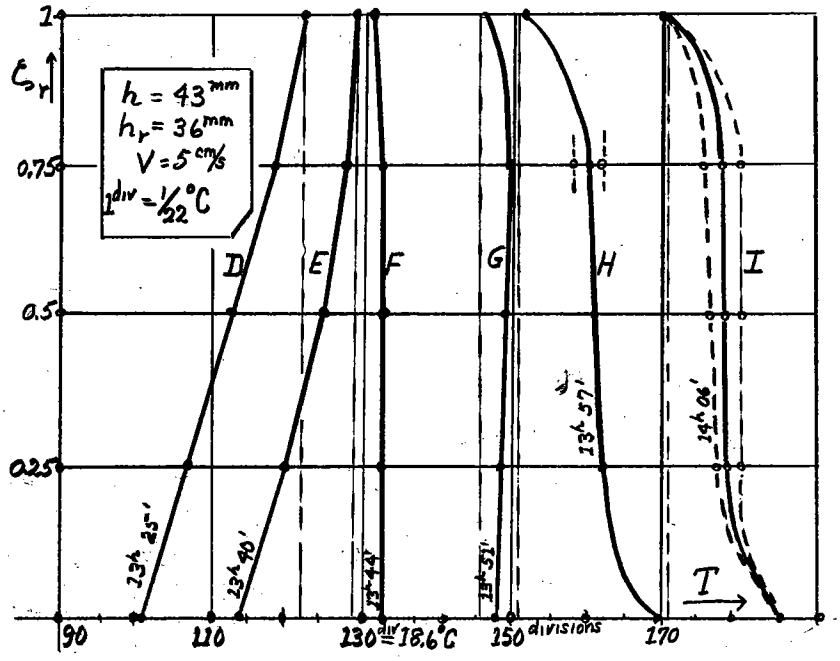

Fig. 126 Experimental distribution of temperatures along the thickness of a layer of air in motion, submitted to a progressive heating. (h = 43 mm; V ≃ 5 cm/s.)

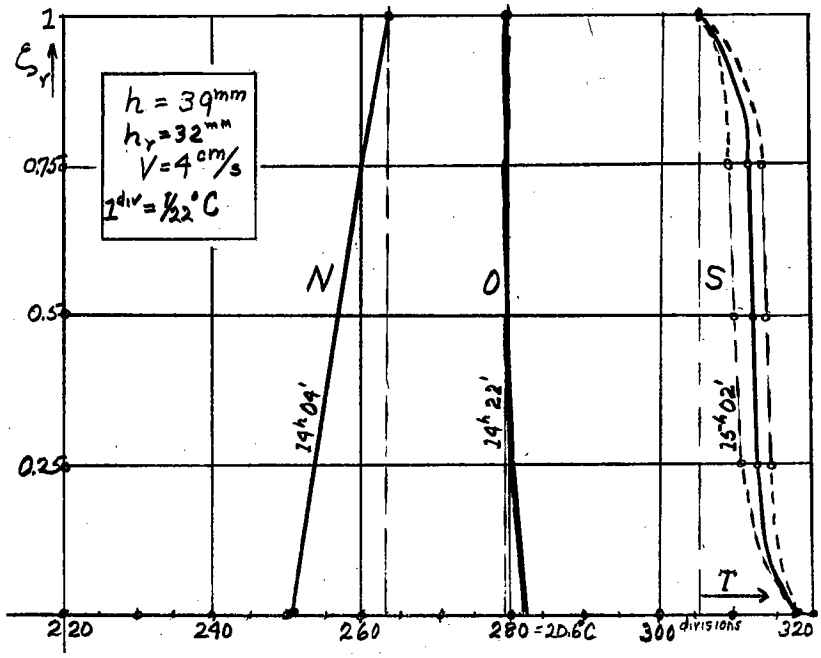

Fig. 127 Experimental distribution of temperatures along the thickness of a layer of air in motion, submitted to progressive heating. (Thickness h = 39 mm; speed V ≃ 4 cm/s.)

The results of the experiment with h = 39 mm have no need of being examined separately. One finds in the corresponding diagram all the necessary numerical data (Fig. 127).

Inversions in the distribution of temperatures along the vertical. - We have seen sometimes, and especially when the thickness of the fluid layer was great (5 or 6 cm), thermoconvective motions persistent even when the temperature of the upper wall was greater than that of the canal. This ascertainment is entirely contrary to what we know of the conditions necessary to the maintenance of convective currents. But the measurements of the temperatures along the vertical have shown that this contradiction was only an apparent one.

The air layer, 63 mm thick was put into movement of translation ($V \simeq 6$ cm/s). The first measurement, in absence of the heat, gave, as usual, a distribution of temperatures that was almost linear. The lighter layers being above the denser layers, no convective movement appeared. Next, we proceeded to the heating. 750 watts applied to a surface of 50 dm^2 during two minutes sufficed to provoke the perfect formation of eddies in longitudinal bands. At the expiration of this time, we interrupted the heating, and 10 minutes later, as shown on the diagram, the temperature at the bottom of the canal had gained its maximum.

At this critical moment, the temperatures were distributed as shown in curve J, Fig. 128. The fictitious (mean) gradient of temperature $\frac{T_1 - T_2}{h}$ is negative. The real gradient β is variable. It is negative up to the height $\zeta_r = 0.75$, where a slight inversion occurs, and passing through zero, it becomes positive.

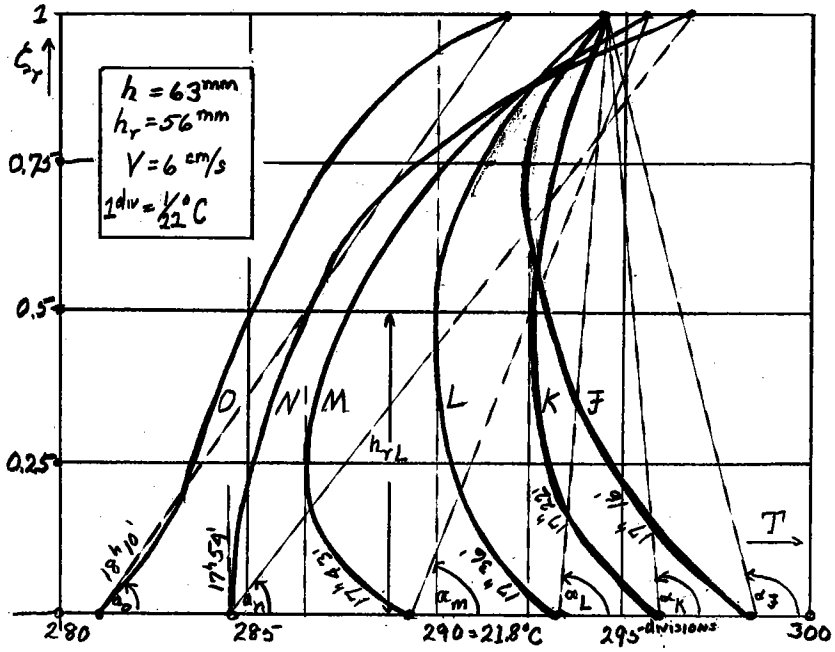

Fig. 128 Experimental distribution of temperatures following the thickness of an air layer in motion, abandoned to slow rechilling. Characteristic diagrams in respect to the inversion of the temperature gradient. (h = 63 mm $V \simeq 6$ cm/s.)

The bottom of the canal has been abandoned to slow chilling while the ceiling, which itself constituted the bottom of a tank filled with a cooling liquid, was maintained at a temperature approximately constant.

Successive measurements gave the curves K, L and M. The curve K still retains the J character of distribution. As for the curve L, its fictitious (mean) gradient has become positive ($\alpha L < \frac{\pi}{2}$).

Simultaneous observations have shown that the eddies in bands still persisted, even if the temperature of the ceiling was clearly greater than that of the bottom ($T_1 > T_2$). In examining the curve L, one sees there a strong inversion at height $\zeta_r = 0.5$. Consequently,

there is a reduced thickness (marked in the diagram by h_{rL}) where the densest layers remain above the more expanded layers. The reduced thickness is determined by the point of inversion. This layer, hence, remains the focus of thermoconvective movements up to the time when the inversion of the temperature gradient is effaced.

The curve M carries again a like inversion, but it has descended as far as the level where $\zeta_r = 0.25$. The thermoconvective currents recorded are excessively slow.

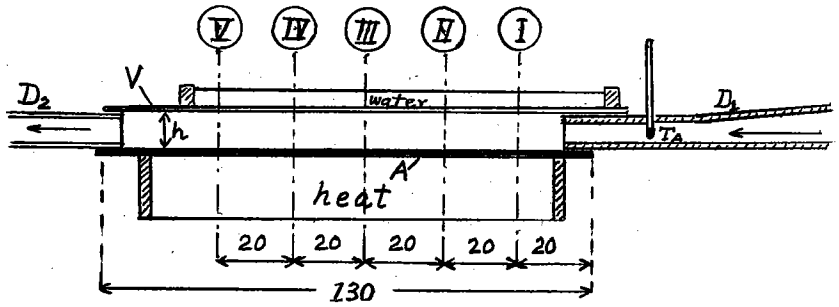

Fig. 129 Schema of the arrangement for the research or distribution of temperature along five verticals in the experiment chamber. (T_A = temperature arriving).

Finally, the two curves N and O give the distribution of temperature when the gradient β has become positive in the entire thickness. The vertical equilibrium is perfect and no vertical movement has been noted.

Now, Lord Rayleigh (13) says, in substance: "The thermoconvective currents cease to appear as soon as the difference of extreme temperatures is smaller than the critical value $(T_2 - T_1)_c$ separating the eddy regime from the stable preconvective regime." In fact, this announcement needs completing by a supplementary condition: No inversion of the temperature gradient should produce itself along the vertical.

In the experiments relative to the verification of the Rayleigh-Bénard criterion we have taken account of this fact.

Inversion of the temperature gradient is due to the air that comes in, because its temperature is higher or lower than the temperatures of the walls that limit the layer under experiment.

Here is an example where the arriving air is warmer than the bottom of the canal ($T_A > T_2 > T_1$). We have measured the vertical distribution of the temperatures in five equidistant places I, II, III, IV, V, of which the exact position is marked on Fig. 129. The curves (Fig. 130) which represent the vertical distribution of the temperatures in these places, show that the average temperature of the air penetrating the experiment chamber adapts itself progressively to that of the walls.

Being given that upon entry T_A is greater than T_2, T_A diminishes. In the upper end of the canal, the influence of T_A is considerable. The temperature of the bottom T_2 is clearly lower than the maximum temperature which occurs at a level between the floor and the ceiling. At this same level, the gradient β changes, of course, its sign (see curves I and II). It is only starting from the center of the canal that the gradient of temperature β ceases to invert itself and that it remains negative in the entire thickness (see curves III, IV, V).

If the temperature T_A is much superior to T_2 or inferior to T_1, its influence can propagate itself right to the end of the canal.

One finds in Fig. 131 some curves of this type. The measurements

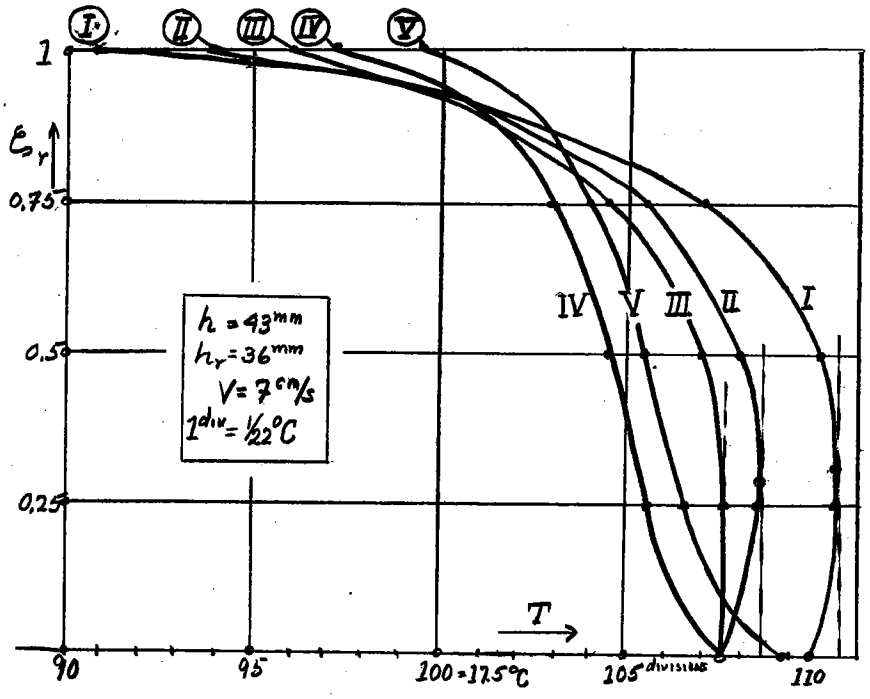

Fig. 130 Distribution of temperatures along five verticals marked in Fig. 129 in a layer of air in motion and heated from below when $T_A > T_2$. (Consequence: inversion of temperature gradient.)

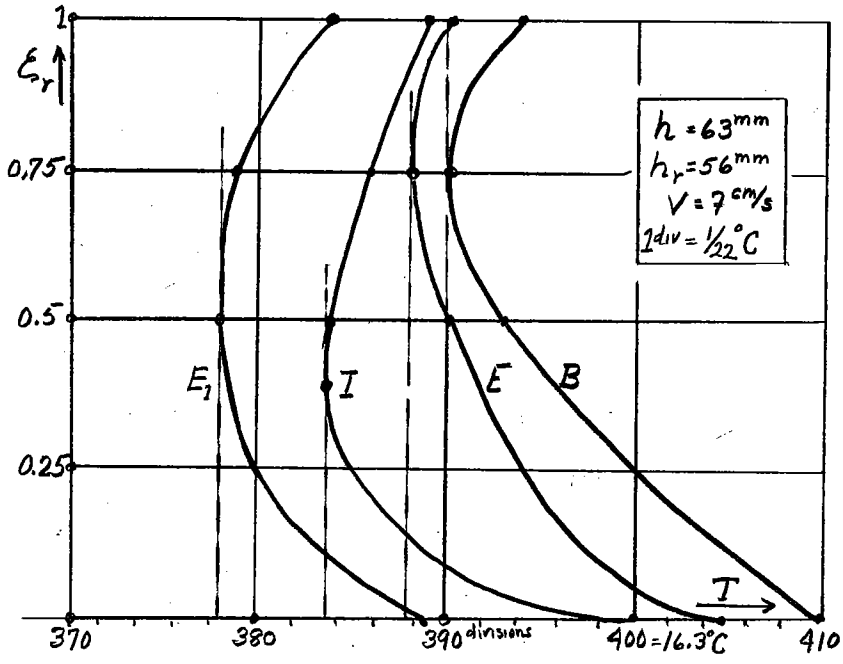

Fig. 131 Distribution of temperatures along the thickness of a layer of air in motion and heated from below when $T_A < T_1$. Consequence: inversion of temperature gradient.

were made at the outlet of the canal, whose thickness was 63 mm. They arise from different experiments where the initial temperature T_A was essentially lower than T_1. The inversions of the temperature gradient, whose values pass from the negative sign to the positive sign, are very accentuated.

To avoid inversions, it is necessary to submit the heating and chilling walls to a temperature such that the first is greater and the second lower than that of the air entering the chamber. One has then:

$$T_1 < T_A < T_2.$$

It is fitting also to carry out measurements in the lower section of the canal, where the influence of the initial temperature, T_A is less strong.

3. - Thermal field of eddies in longitudinal bands.

The determination of the thermal field in the thermoconvective eddies presents an interest of the very first order. Unhappily, great experimental difficulties beset this determination. Before all, the incessant mobility of the cellules hampers the measurements. Only eddies in bands lend themselves to this class of exploration, because they keep their place very precisely.

With a view to measuring the distribution of temperatures in the rectangular section of these eddies, we determined the exact emplacement of a longitudinal roll chosen arbitrarily. Next we proceeded to the measurement of temperatures along three verticals: the first in the plane of ascending currents, the second in the plane passing

through the axis of the roll, the third in the plane of descending currents (see Fig. 132).

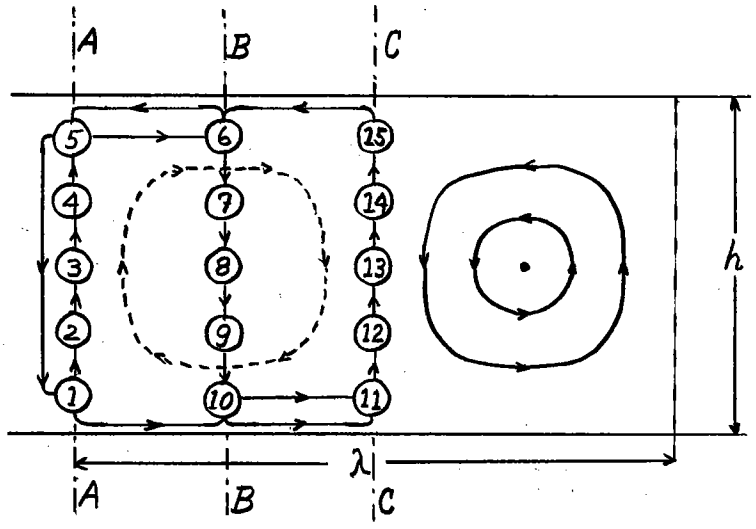

Fig. 132 The fifteen points in the rectangular section of an eddy-roll where one has made measurements of temperature distribution.

Determination of the temperatures at fifteen points (five on each of the verticals) suffices largely to establish the thermal field. Since the taking of the fifteen measurements demands a time duration of seven to ten minutes, the temperatures can change more or less at the points that have just been measured. To eliminate this variation, we had recourse to a method whereby one reduces all the temperatures to the instant of the final measurement. With this in view, one repeats rapidly the measurements at five peripheral points, near the partitions (6, 5, 1, 10 and 11). By giving to the extremities of the curves of the original temperature distribution the values obtained from the second measurement, one obtains graphically the temperatures at intermediary points.

Among the numbers of experiments we have chosen eight examples

that represent the most characteristic varieties of the thermal field as gathered in the rectangular section of the eddies in longitudinal bands.

In general, diagrams of the thermal field have been constructed with eleven isotherms, (numbered 0 to 10), the two extremes of which always reduce themselves to two points. We have drawn in dotted lines on several diagrams the intermediary isotherms to underline the particular character of the case examined. The exploration of the thermal field has been carried out in the section of one single roll, but we have likewise constructed the symmetric isotherms for the complementary roll.

We have added to each diagram of the thermal field the curves of temperature distribution along the three principal verticals (A and C are the verticals placed in the planes of currents descending and ascending respectively, B is the median vertical). The corresponding curves A', B', C' reproduce the original distribution, while the curves A", B", C" give the reduced values at the moment of the final temperature - in accordance with the method before stated. From these curves the thermal field is deduced. In effect, one divides the interval of the two extreme temperatures into ten equal parts. The intersections of the verticals (numbered from 0 to 10) with the curves A", B", C" give the points of crossing of the isotherms upon the three verticals A, B and C. The principal imposed conditions have been noted directly in the respective diagrams. Here are a few particular remarks.

Example 1 - (Fig. 133 and 134): The measurements were taken

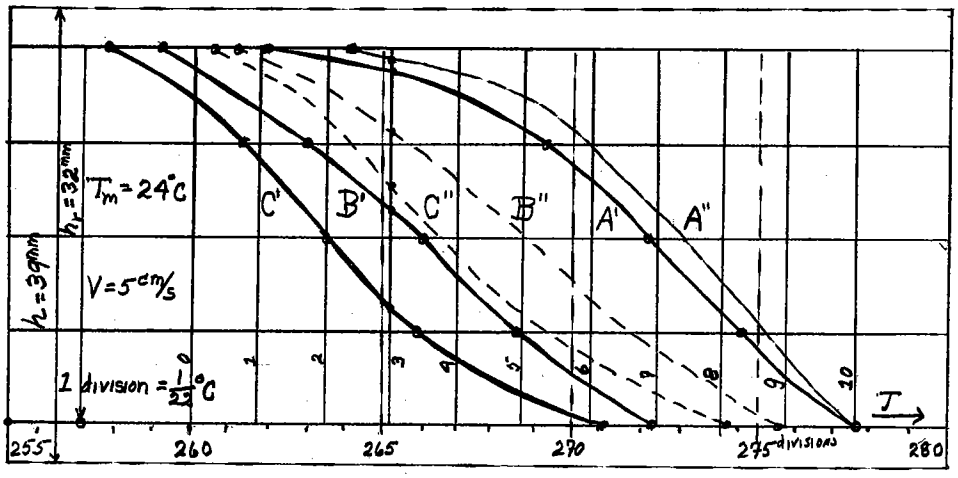

Fig. 133 Distribution of temperatures along the verticals placed in the three planes A, B and C. A: plane of ascending currents; B:plane placed between planes A and C; C: plane of descending currents. ($h = 39$ mm $V \simeq 5$ cm/s).

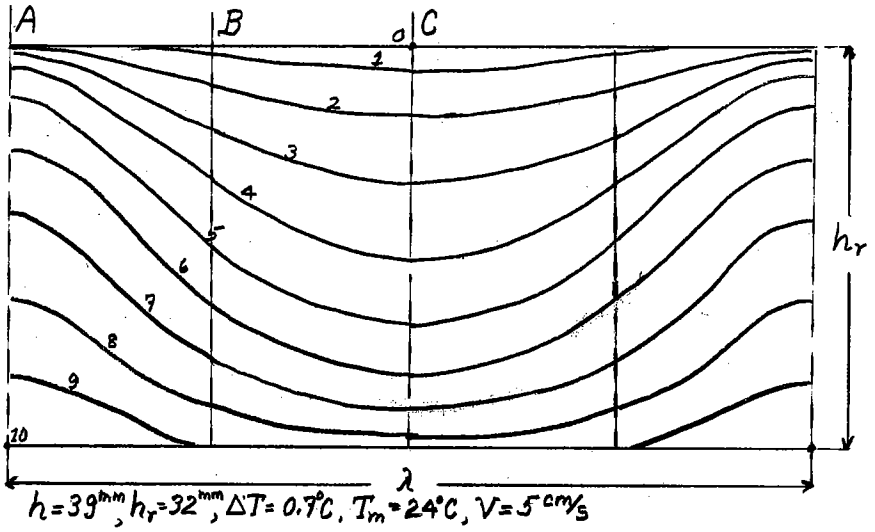

Fig. 134 Field of isotherms constructed from the diagrams of Fig.133 under a uniform heat of 63 watts on 50 dm^2. Their execution demanded eight minutes. During this time, the temperatures at the preceding points have augmented, and the curves A^{tt}, B^{tt}, C^{tt} have displaced themselves to the right. The separation, for all that, is regular.

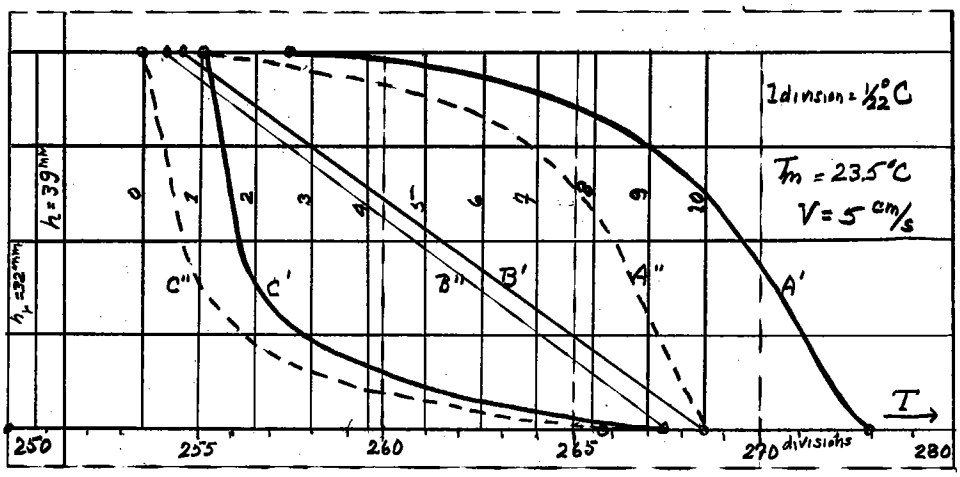

Fig. 135 Distribution of temperatures along verticals placed in the three principal planes: A, B and C. (h = 39 mm $V \simeq 5$ cm/s)

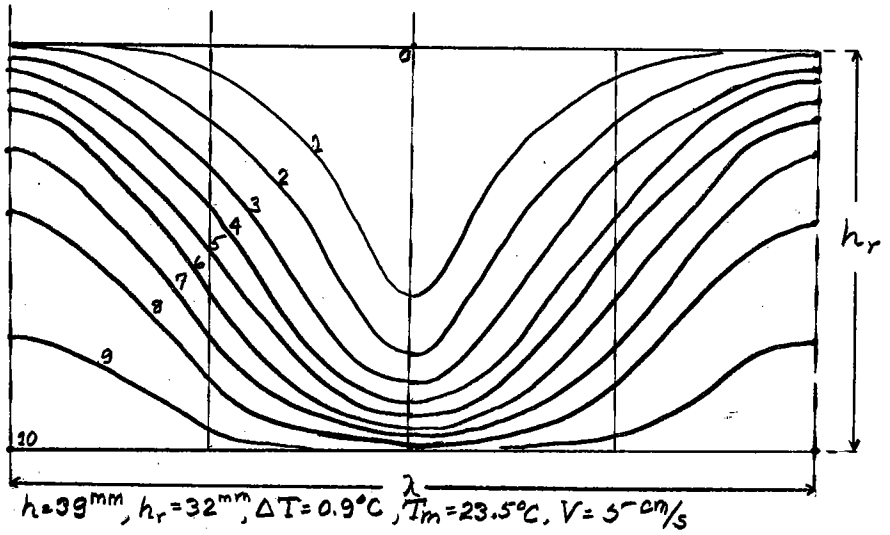

Fig. 136 Field of isotherms constructed from the diagrams of Fig. 135

Example 2. - (Fig. 135 and 136). We have repeated exactly the same experiment, but we cut off the heat. The floor of the canal was abandoned to slow chilling. As consequence, the reduced curves A", B", C" displaced themselves toward the left. Let us remark that the curve B" is perfectly rectilinear, agreeable to the theoretical result.

Example 3. - (Fig. 137, 138): The thickness was 43 mm. The apparatus was cooling off, the reduced curves, hence, shifted to the

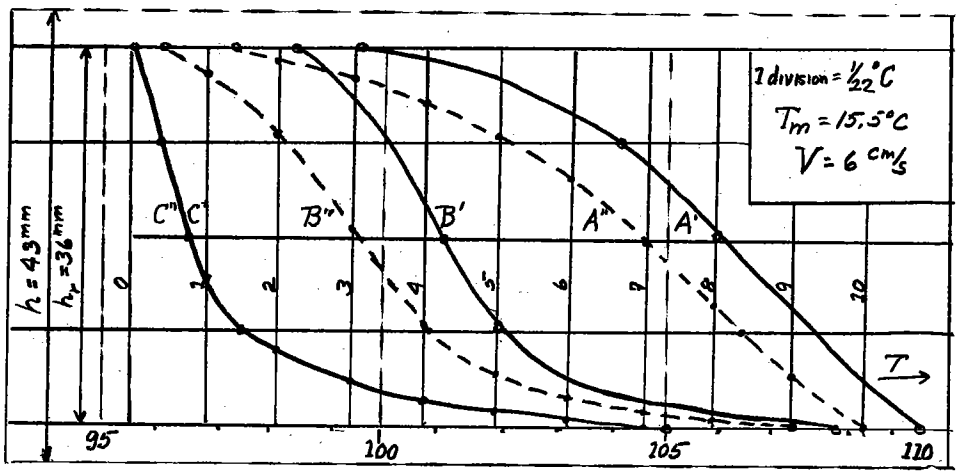

Fig. 137 Distribution of temperatures following verticals placed in the three principal planes: A, B, and C. (h = 43 mm V≃6 cm/s)

left. The character of the diagram is the same as that of the previous experiments.

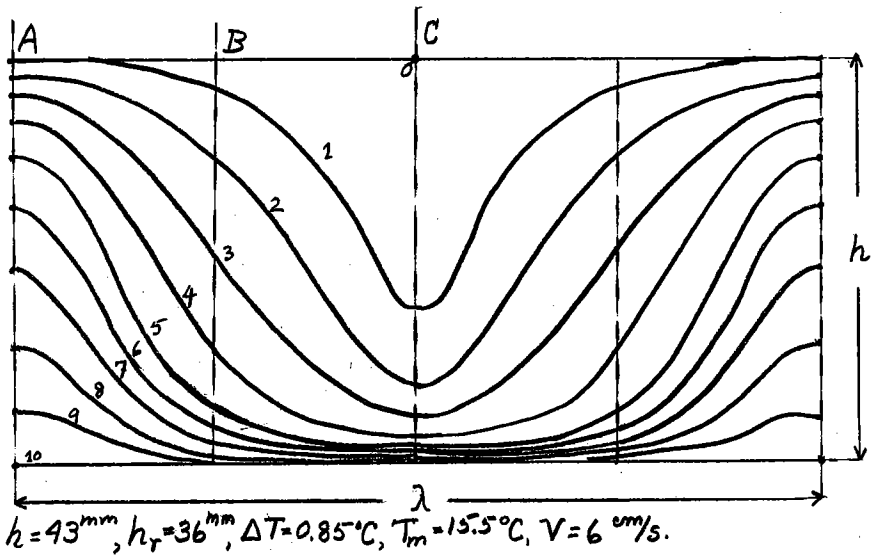

Fig. 138 Field of isotherms made from the diagrams of Fig. 137

Example 4. - (Fig. 139, 140): The temperatures having stayed constant during 7 minutes, no reduction of the values was necessary. The curve B" has a slight inversion placed between $\zeta_r = 0.25$ and 0.50. That translates itself in the thermal field by a region where

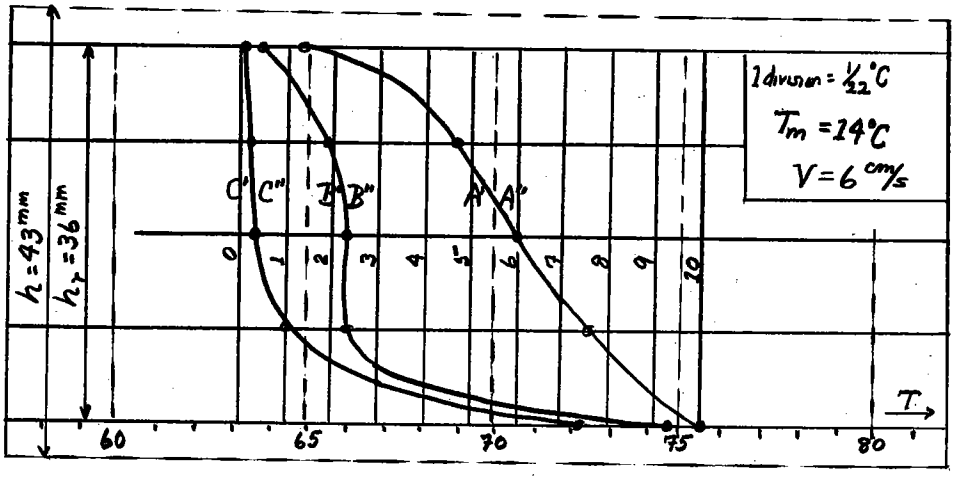

Fig. 139 Distribution of temperatures along verticals placed in the three principal planes: A, B and C. (h = 43 mm V ≃ 6 cm/s)

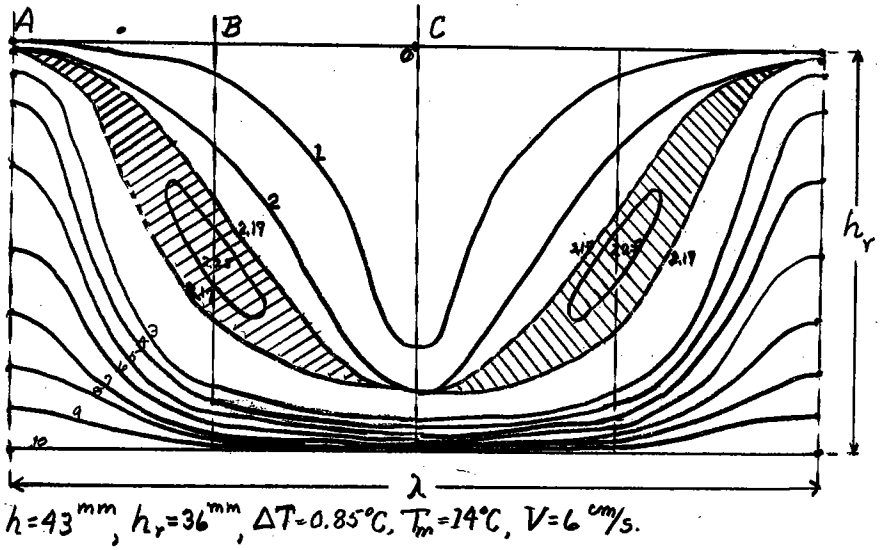

Fig. 140 Field of isotherms made from the diagrams of Fig. 139

the temperature keeps on increasing towards the interior. This region, encircled by the isotherm 2.17, pertains to the central part of the roll.

Example 5. - (Fig. 141, 142): If the incoming air has a temperature relatively low, the curves B" and C" cross over each other: there results from this special fields. In the present example, the two curves have two common points. B" is tangent to the ordinate 0. The isotherm 0,

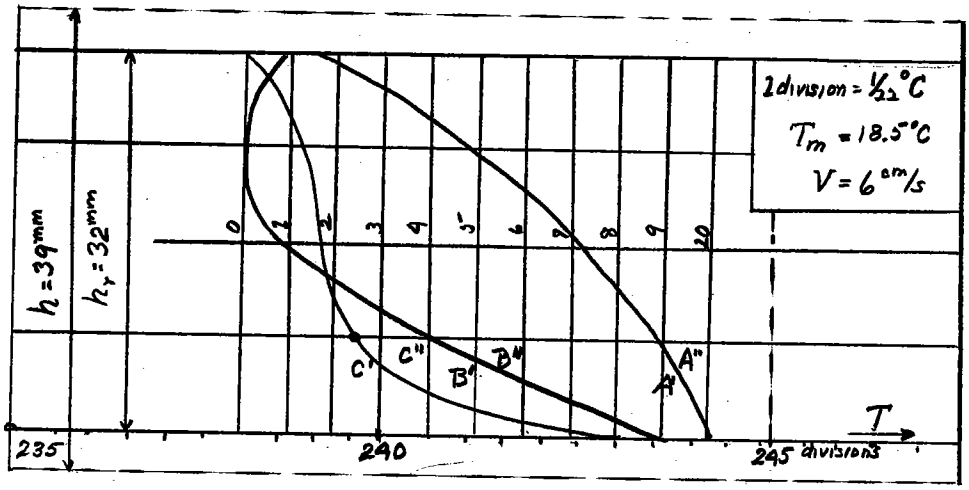

Fig. 141 Distribution of temperatures along the verticals placed in the three principal planes: A, B, and C. (h = 39 mm $V \simeq 6$ cm/s)

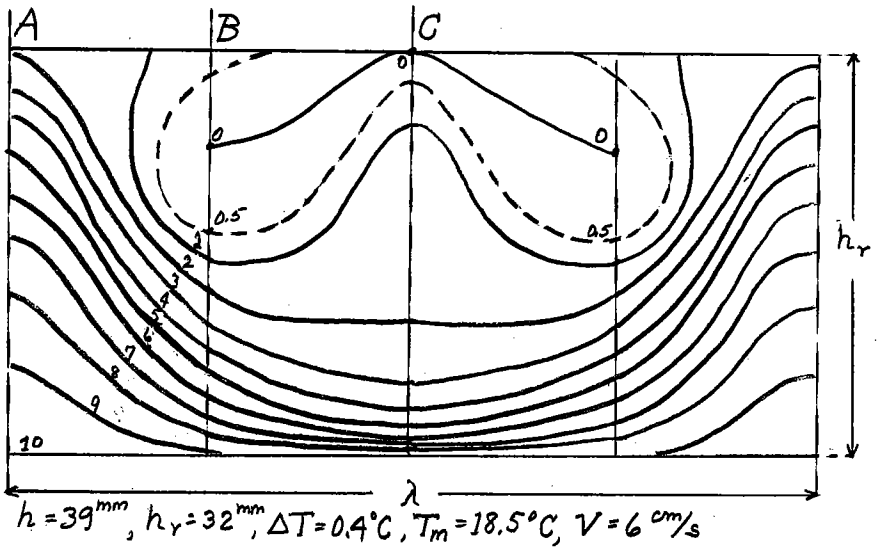

Fig. 142 Field of isotherms made from the diagrams of Fig. 141

reduced, in general, to a single point, becomes a veritable curve joining the respective points on the verticals B and C.

Example 6. - (Fig. 143, 144): It is analogous to the preceding case, but it distinguishes itself from this last by the fact that the temperature in the central region of the roll is much less than the isotherm 0. In fact, the curve B" crosses the ordinate 0

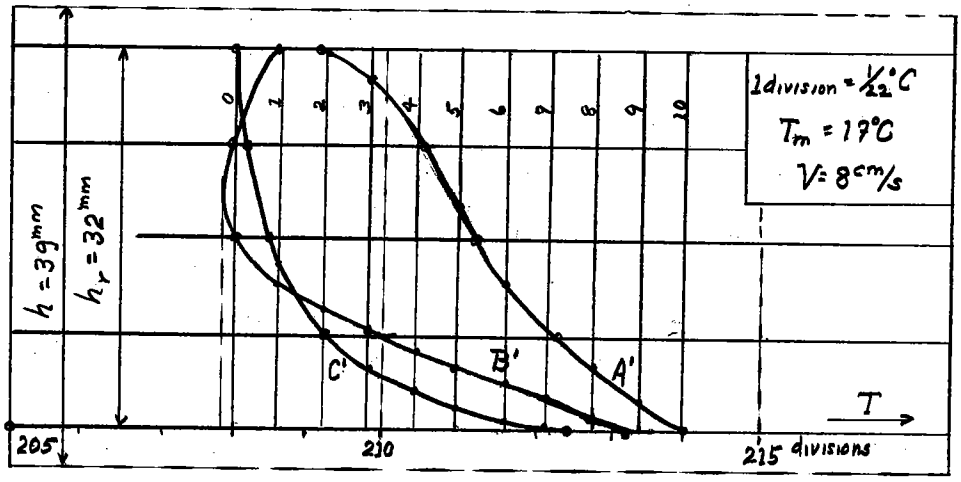

Fig. 143 Distribution of temperatures along the verticals placed in the three principal planes: A, B and C. (h = 39 mm , V ≃ 8 cm/s)

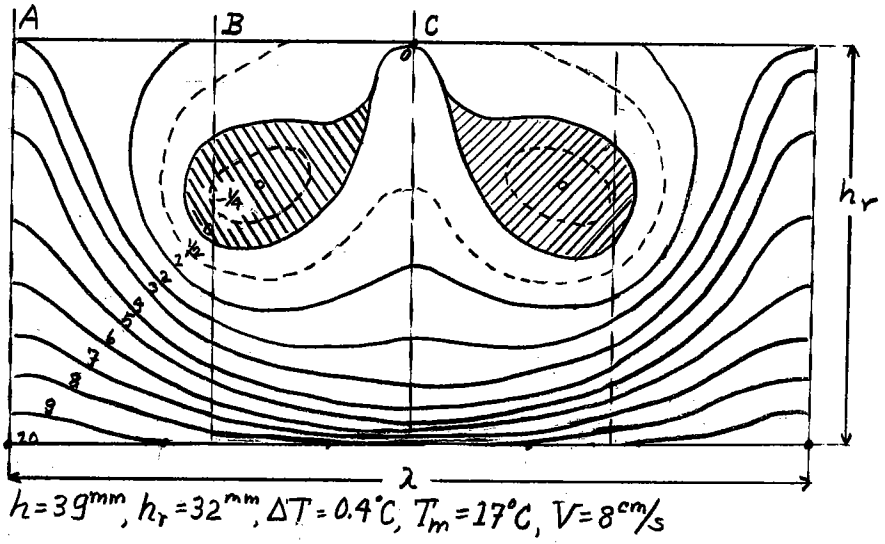

Fig. 144 Field of isotherms made from the diagrams of Fig. 143

at two points. The minimum on the vertical B is characterized by the isotherm $-\frac{1}{4}$ and the height from the datum line $\mathcal{E}_s = 63$. The center having a temperature lower than 0 is marked by crosshatching.

Example 7. - (Fig. 145, 146): The aspects of the thermal field take particular forms when the thickness h is large. In the present case, where the difference of the extreme temperatures has been weak (1/5°C at the most between points 1 and 15), the thermal field is

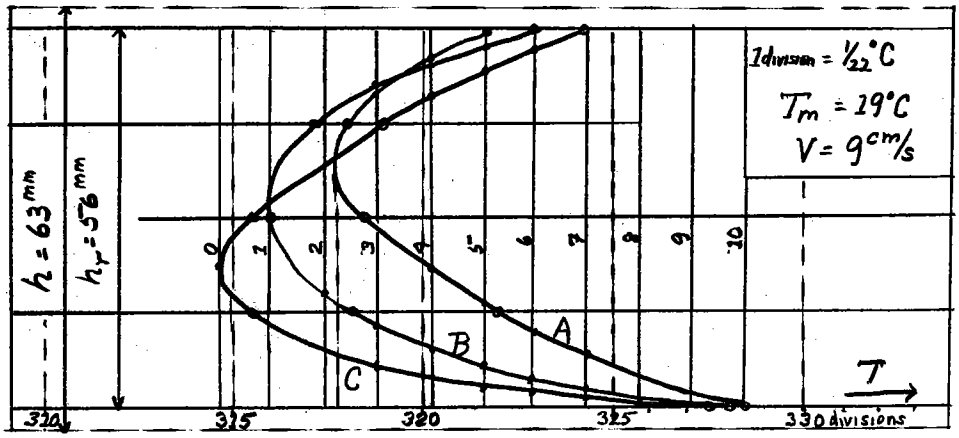

Fig. 145 Distribution of temperatures along the verticals placed in the three principal planes: A, B and C. (h = 63 mm ; V ≃ 9 cm/s)

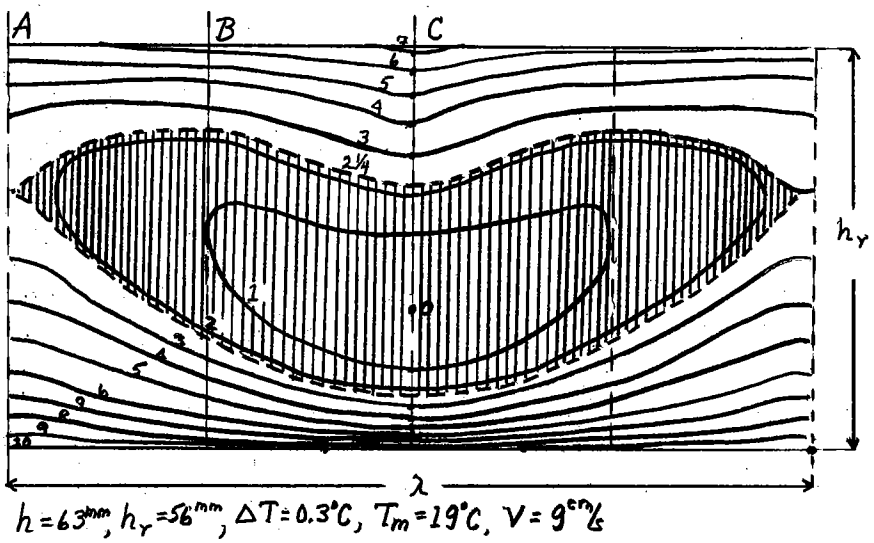

Fig. 146 Field of isotherms made from the diagrams of Fig. 145

divided by the isotherm 2.25 into two distinct parts, of which the upper part is relatively little modified. From this we conclude that the thermoconvective currents are greatly dampened off close to the ceiling, and that they do not occupy the thickness h totally.

The gaseous mass taken between the ceiling and the isotherm 7, that is, 95% of the total mass has a temperature inferior to that at the coldest point on the datum line height $\zeta_r = 1$.

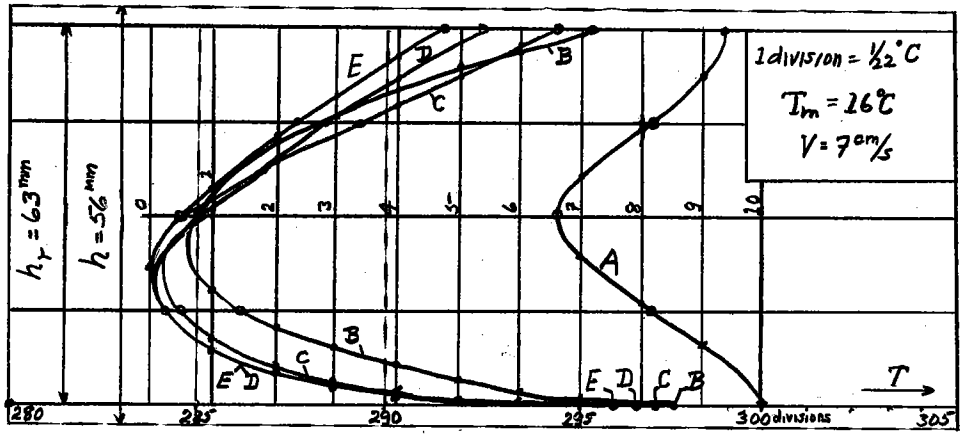

Fig. 147 Distribution of temperatures along the verticals placed in the five planes A, B, C, D, E, of a marginal roll. (h = 63 mm V ≃ 7 cm/s)

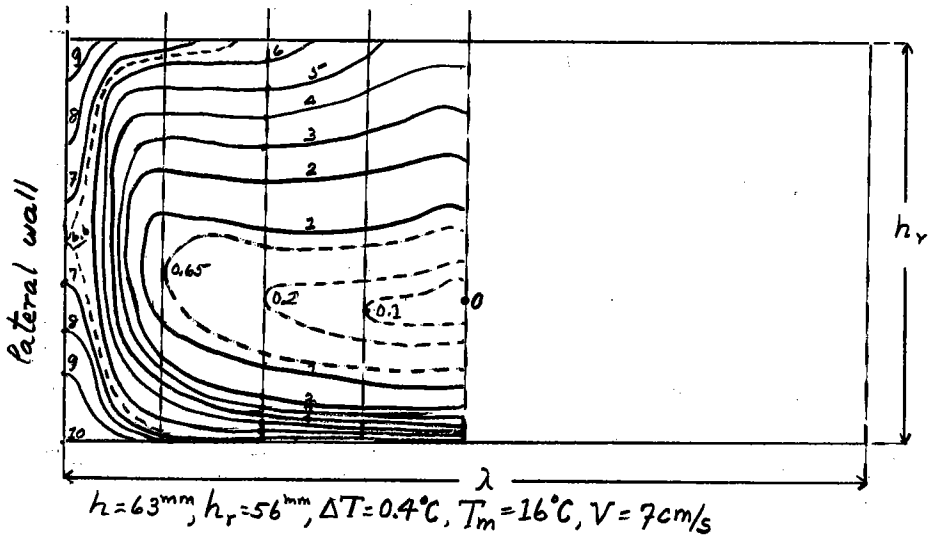

Fig. 148 Field of isotherms made from the diagrams of Fig. 147

The curve joining the point isotherm 0 on the vertical C to the point of intersection of the isotherms 2.25 on the vertical A, divides the eddy-roll into two regions. The temperature gradient of the upper field is directed toward the top, and that of the lower field toward the bottom. In consequence, if the two parts were separated by a rigid partition, the convective currents would die off in the upper region and the isotherms would become horizontal straight lines; contrarily, the

circulation would continue in the lower space. But, in reality, the currents clear this limit, thanks to their inertia, and penetrate the zone where the temperature gradient is positive.

Example 8. - (Fig. 147, 148). The thermal field considered pertains to the limiting eddy-roll of the sidewall of the canal. The measurements were taken follwoing five verticals. The vertical A is found in the plane of the sidewall, which is equally the plane of the rising currents. The presence of the sidewall modifies the thermal field and the field of speeds of the limiting roll.

4. Distribution of temperatures following the transverse section of the canal where the eddies in longitudinal bands have developed.

When we displace the thermoelectric couple in a horizontal plane following the width of the canal where eddies in bands have formed, we detect periodic oscillations of temperature. The maxima and minima indicate the locations of rising and descending currents respectively.

We made many records of temperatures following the breadth of the canal, mostly in the median horizontal plane, for theory and experiment show that the greatest thermal perturbations are seated in the central region of the fluid sheet. We measured the temperatures in (2n + 1) equidistant points, n being the number of rolls observed. Here are a few typical diagrams.

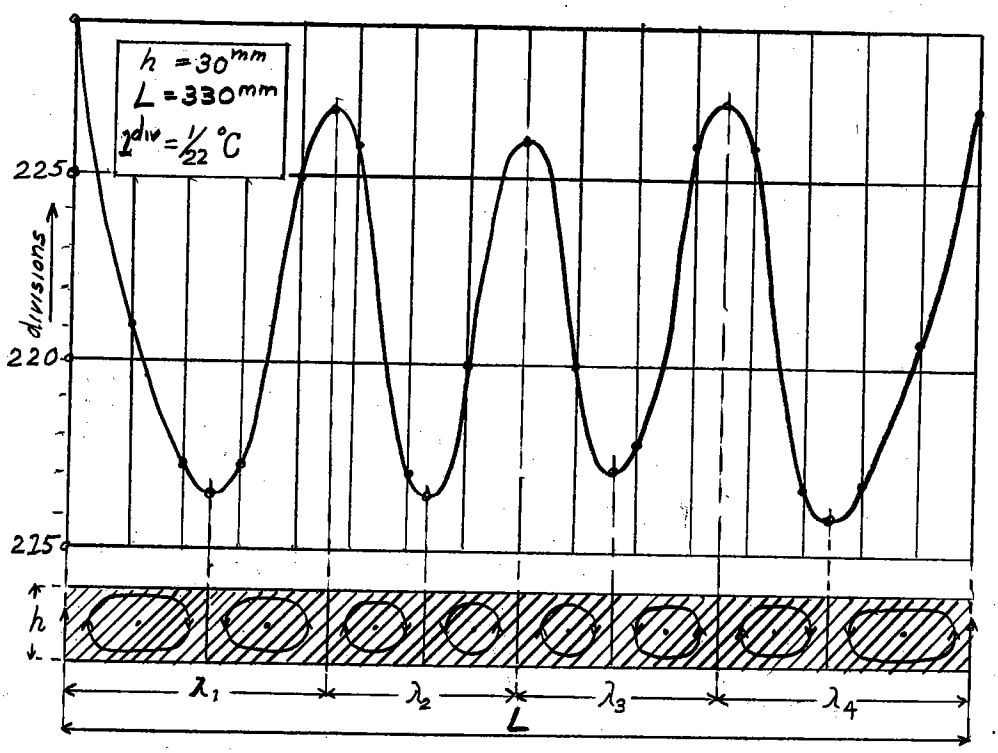

Fig. 149. Distribution of temperatures along the width of the canal, in the horizontal median plane. h = 30 mm. Width of canal L = 330 mm.

Fig. 149: The thickness of the air layer was 30 mm and the width of the canal 330 mm. Eight rolls took shape each time, and consequently, we measured the temperature at 17 points uniformly separated in the horizontal plane z = h/2. The curve, traced by the seventeen points, goes through five maxima and four minima. They coincide respectively with the ascending and descending currents.

Fig. 150: h = 43 mm and L = 300 mm. We had foreseen the appearance of six rolls; the breadth of the canal, therefore, had been divided into twelve intervals. But the result did not coincide with our preconceptions for each curve passes through five maxima and four minima, which indicates the presence of ten rolls. The curves V, VI,

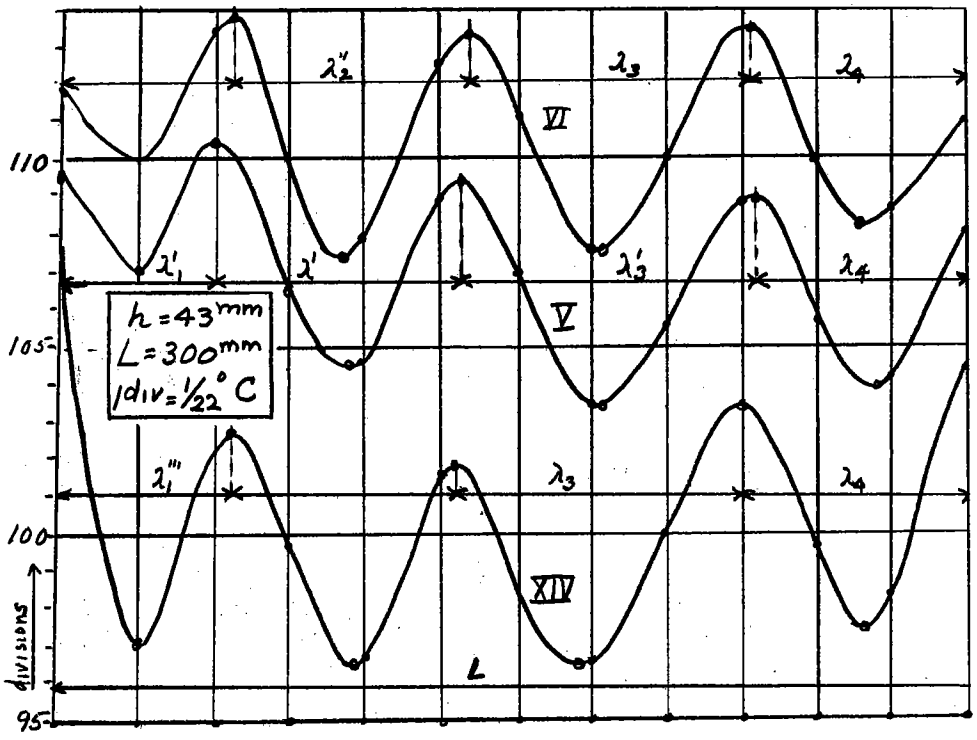

Fig. 150. Distribution of temperatures along the width of the canal, in the horizontal median plane. Three experiments: h = 43 mm Width L = 300 mm.

and XIV belong to three different experiments, but the number of maxima and minima, as also their spacing (which is irregular, moreover) remain invariable.

Fig. 151: h = 43 mm and L = 300 mm. The curves II, III and IV show the distribution of temperatures at three different heights. The curve III has been recorded in the median plane z = h/2, which explains the strong amplitude of the oscillations. Curve II shows the distribution of temperatures measured at approximately 3.5 mm from the heating floor. It conserves the oscillatory character but the amplitude is considerably reduced. Finally, Curve IV shows that the oscillations have all but died out at the height of 3.5 mm below the ceiling.

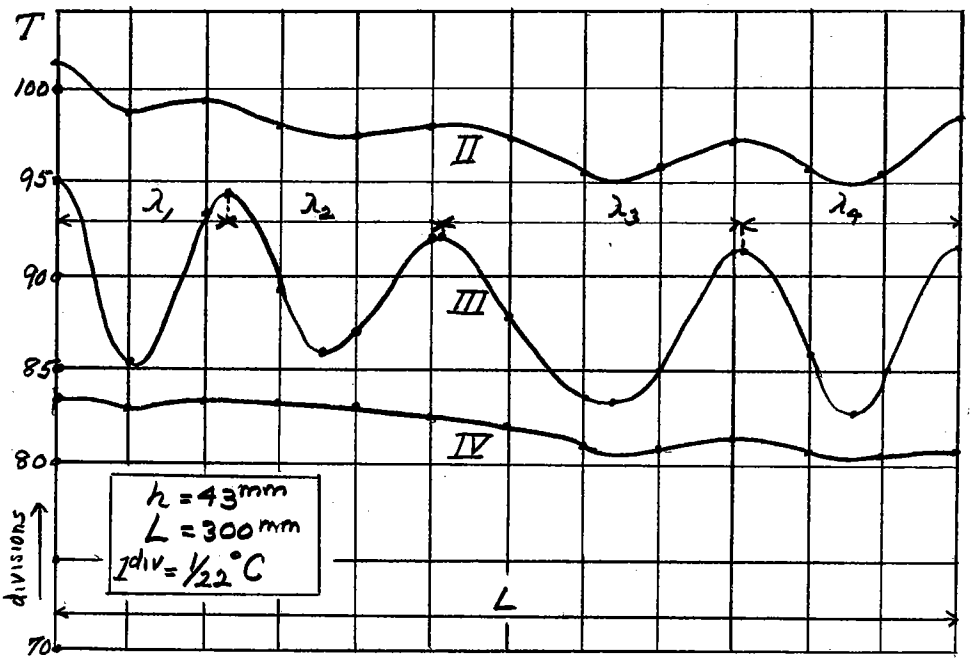

Fig. 151. Distribution of temperatures along the width of the canal. Curve II in the horizontal plane at about 3.5 mm from the bottom of the canal. Curve III in the horizontal median plane. Curve IV in the plane at about 3.5 mm from the ceiling of the canal. Thickness h = 49 mm. Width of canal L = 300 mm.

5. Comparison of theoretical and experimental results.

To terminate this chapter, we will examine at what point the theory concords with experiment. The problem reduces itself to the discussion of the practical value of the relationship $\Delta T = \Delta T_o$ sine lx sine myZ, which has been the fundamental hypothesis of the mathematical solution of the problem. As our researches on the distribution of the temperatures refer solely to eddies in longitudinal bands in air, we may limit ourselves to study the relation $\Delta T = \Delta T_o$ sine lxZ with the conditions of Jeffreys.

Substituting for Z and ΔT_o the expressions (96) and (97) respectively, the thermal perturbation ΔT following the vertical

placed in the center with <u>ascending</u> currents (sine 1x = 1), or <u>descending</u> (sine 1x = -1) takes the form:

$$\Delta T = \mp \frac{\beta h}{2.5} Z = \pm (T_2 - T_1) \left[-3.6 + 17.4 \left(\frac{1}{2} - \frac{z}{h} \right)^2 - 11.5 \left(\frac{1}{2} - \frac{z}{h} \right)^4 + 4 \sin \pi \frac{z}{h} + \ldots \right].$$

This perturbation is null in the vertical plane placed between the planes where the ascending and descending currents are maxima (sine 1x = 0). Fig. 152 gives ΔT as a function of z for the three principal planes. ΔT(sine 1x = 0) is the axis of symmetry between the two curves ΔT(sine 1x = 1) and ΔT(sine 1x = -1). Let us now compare this theoretical result with our experiments, effectuated with the view of establishing the thermal field.

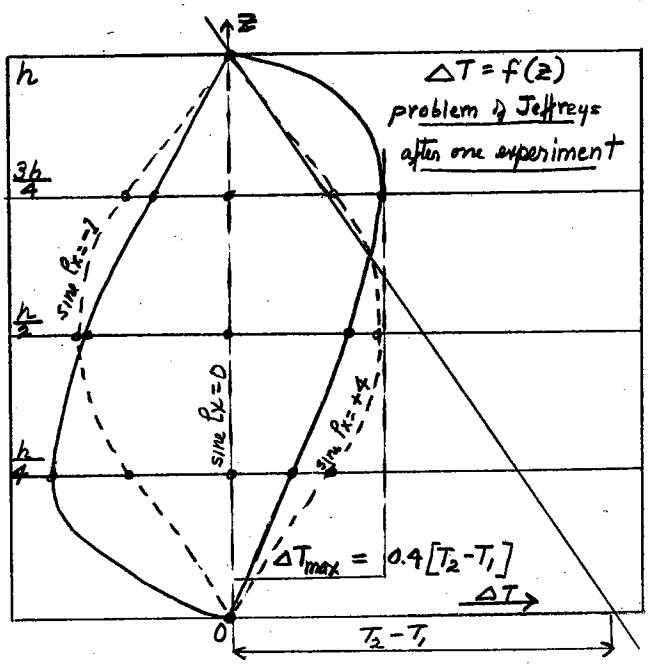

Fig. 152. Experimental and theoretical function ΔT (= kZ) (called perturbation of temperature) along the thickness of a fluid layer containing eddies in longitudinal bands.

Let us take up Example 2 first, (Fig. 135, 136), where the distribution of temperatures following the vertical B is essentially linear, which is in full agreement with the theory ($\Delta T = 0$ when sine $lx = 0$). We have reconstructed in the following diagram (Fig. 153) the curves A", B", and C" of Fig. 135. The restricted interval has been extended to the entire thickness h. The two points of intersection A_{exp}, B_{exp} and C_{exp} define entirely the difference of extreme temperatures, and consequently, we can construct the theoretical curves A_{th}, B_{th} and C_{th}. B is a straight line that connects the two extreme temperatures. One obtains A_{th} and C_{th} by carrying to left and to right of B_{th} the theoretical values of ΔT. We have entered these curves in dotted lines, while the experimental curves are drawn in heavy lines. The curves B_{th} and B_{exp} concord nicely. It does not come so for A and for C. For one thing, the maxima of C_{exp} and A_{exp} are pushed towards the top and towards the bottom respectively, and for another thing, the tangents to the curves A_{exp} and C_{exp} when z = h and 0 are not vertical. It is evident that this discordance results from the asymmetric conditions at the limiting walls and from the imperfect conductivity of the latter.

Example 3 leads to a more pronounced disagreement. One sees (Fig. 154) that the curve B_{exp} itself is far from representing the linear distribution B_{th}. One knows that this supplementary perturbation is due to the initial temperature of the incoming air. Be it as it may, overlooking particular conditions of which the simplified theory takes no account, we can say that the theoretical results

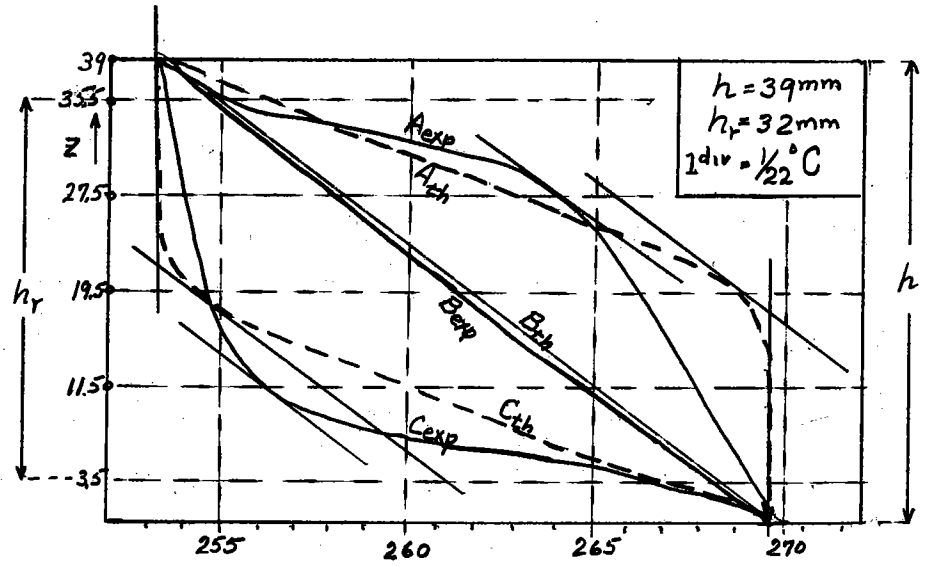

Fig. 153. Distribution of temperatures along verticals placed in the three principal planes: A, B and C. Confrontation of experimental curves and those of the problem of Jeffreys. (From example 2, Fig. 135)

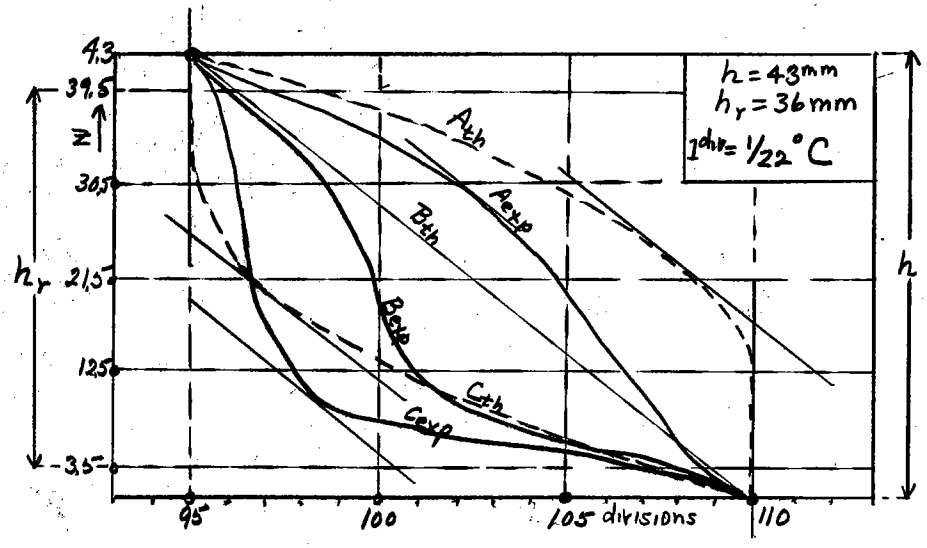

Fig. 154. Distribution of temperatures along verticals placed in the three principal planes, A, B and C. Confrontation of experimental curves and those of the problem of Jeffreys. (From example 3, Fig. 137)

reproduce very well what is essential of the phenomenon of eddies in longitudinal bands, namely, that the big perturbations of the pre-

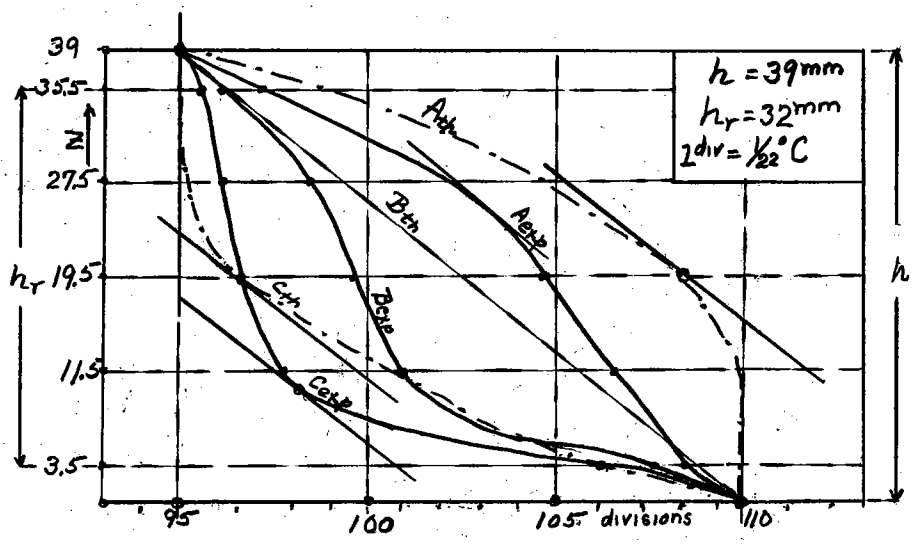

Fig. 154. Distribution of temperatures along verticals placed in the three principal planes, A. B and C. Confrontation of experimental curves and those of the problem of Jeffreys. (From example 3, Fig. 137).

convective thermal field coincide with the centers of ascending and descending currents. The qualitative resemblance of the theoretical thermal field (cf. Fig. 118) with the fields experimentally obtained (cf. Fig. 136 and 138) is clearly apparent.

It would be interesting to verify by experiments made in a canal with two metal walls (good conductors) and longer than ours (in the view of eliminating the influence of the initial temperature of the air) whether the hypothesis expressed by the equation $\Delta T = \Delta T_o$ sine 1xZ leads to results more conformant to reality.

Chapter XII

Application to Meteorology of the Theory of Thermoconvective Eddies.

1. Review of the work of Mr. P. Idrac.

It will soon be twenty years that meteorology has been desirous

to extend into the free atmosphere the results obtained by the theoretical and experimental study of Bénard upon thermoconvective eddies.

The first who had the idea of explaining the spatial periodicity of ascending and descending currents above a vast plain was Paul Idrac, a specialist in the study of vertical currents, whether occasioned by irregularities of the terrain or by differences of temperature. His first researches are dated even as far back as 1913 (4-a,b), when he observed the planing flight of seagulls near the cliffs of Dieppe and in the wake of ships. He saw that these birds using their wings as sail-planes, take advantage of ascending currents to sustain themselves in the air without need of wing-strokes. In fact, measurement showed that the ascending currents in proximity to the cliffs of Dieppe were in the order of 3 to 4 m/s, and, in the rear of steamers, in the order of 4 to 6 m/s, speeds well in excess of the minimum required to keep seagulls airborne (Idrac found for this minimum a speed of 1.2 m/s). However, these vertical currents are accidental and quite restricted in extent.

After the war, P. Idrac took up again his researches. In 1920 (4-C), he published an important Note, in which he issued for the first time the hypothesis attributing to differences of temperature the ascending and descending currents that one observed frequently in free atmosphere, and then giving to these currents the same origin as cellular eddies studied by H. Bénard. To confirm

his idea. Idrac undertook at the laboratory a series of experiments on convection currents in a layer of moving air, experiments that gave, as we know, (cf. Chap. I) the eddies in longitudinal bands (4-c,e).

Idrac thought that the conditions realized in the high atmospheric layers were favorable to the formation of regular eddies like those obtained in the laboratory. For instance, the cirrus, often disposed in bands regularly spaced, could be the upper part of convective eddies rendered visible by the condensation of water-vapor. To Helmholtz's theory of (26) atmospheric waves, that up to then was the only one to explain these forms of clouds, there now came a second theory to associate itself which we will name the "thermo-convective theory".

In the course of a sojourn in Senegal in 1921 (4-d), the same researcher discovered the spatial periodicity of ascending and descending currents in the low atmospheric layer in direct contact with flat ground. He observed the planing flight of large birds, grouped in parallel bands distant from each other some 200 or 300 meters. Recording apparatus showed that these birds were placing themselves regularly above the rising airflows that were aligned in the general direction of the wind. In these conditions, Idrac was led to suppose that the layer of air sweeping the heated soil became, by reason of the vertical instability, the seat of convective movements in the shape of gigantic rolls.

At the time of a study carried out at the lighthouse of the Jument d'Ouessant (4-f), he found that the winds above the ocean had

a similar structure. However, measurements showed the ascending speeds to be very small, in the order of 0.25 to 0.5 m/s.

Finally, let us recall that P. Idrac likewise recognised all the practical interest of the ascending currents for motorless sailplane gliders. In a special study he investigated (4-g) the favorable conditions of ascendance for glider flight. After the examination of the ascending currents caused by variation of the groundplan, he passed on to that of the currents provoked by temperature differences. This last study, carried out in the Sahara in June, 1923, showed the average speed of ascending currents is the order of 1 m/s; but the maxima, which generally occur from eleven o'clock to half-past twelve, very often attain 2 m/s and even 3 m/s. Let us note, by the way, that in regions with moderate climate the thermal currents are more feeble. Therefore, long evolutions of sailplane glider flight are impossible.

We have already told in the general historical part of Chapter 1 that after Idrac, the study of ordered convective currents was pursued very actively by the English meteorologists, sometimes in collaboration with physicists. Taking account of their work, of that of P. Idrac, and of the complementary results acquired in the course of our own experiments, we are now going to undertake a systematic resumé of the present state of the theory of convective eddies in the terrestrial atmosphere.

2. Equilibrium and instability along the vertical in free atmosphere.

The free atmosphere finds itself in stable vertical equilibrium if the less dense layers are above the denser ones.

The equation of vertical equilibrium is written:

$$\frac{\partial p}{\partial z} = -\rho g \tag{101}$$

In supposing that the gravitational acceleration g of a geographic place is a constant and that the two other variables p and ρ (pressure and density) depend only upon the height above the datum line z(101) becomes a differential equation:

$$\frac{dp}{dz} = -\rho g. \tag{102}$$

Being given that the equation of perfect gasses:

$$p = RT\rho \ , \tag{103}$$

applies integrally to atmospheric air (even humid) the integration of the differential equation (102) gives with (103):

$$\log \frac{p}{p_o} = -\frac{g}{R} \int_o^z \frac{dz}{T} \ , \tag{104}$$

where p_o is the pressure at the ground.

It concerns us to know the law of variation of the temperature T with the altitude. Observations show that the temperature decreases linearly in the tropopause, which extends approximately to an altitude of 11,000 meters. If we designate by T_o the absolute temperature at the ground and by β the linear gradient of temperature, which is about 1°C for each 100 meters elevation, the empirical law, hence, is written:

(105) $$T = T_o - \beta z.$$

That being so, we obtain after integration of the equation (104) the law of variation of pressure in function of the altitude:

(106) $$p = p_o \left(\frac{T}{T_o}\right)^{\frac{g}{R\beta}} = p_o \left(\frac{T_o - \beta z}{T_o}\right)^{\frac{g}{R\beta}}$$

From this, one deduces easily the analogous law relative to the density of the air:

(107) $$\rho = \rho_o \left(\frac{T}{T_o}\right)^{\frac{g}{R\beta} - 1} = \rho_o \left(\frac{T_o - \beta z}{T_o}\right)^{\frac{g}{R\beta} - 1}$$

The curves (105), (106) and (107) are represented by Fig. 155. We have carried the variables T, p, and ρ upon the x axis, and the altitude, going up to 10,000 meters, on the z axis.

In the problem studied the density and the pressure decrease towards the top in a continuous fashion. However, in the low atmospheric layers, discontinuities of the temperature and of the density are not rare. These discontinuities are in direct correlation with the superposition of layers of different densities.

First of all, let us examine the case where a layer of warm air reposes upon one more chill: the masses so staged remain in perfect equilibrium. Being given that the conductivity of gasses is weak, the thermal exchanges between the two masses are extremely slow. In consequence, the distributions of temperature and density are represented by discontinuous curves (Fig. 156). Only after a certain lapse of time, the discontinuities grow fainter, giving on the diagram the short incurved portions in dotted lines. If the layer of warm air has

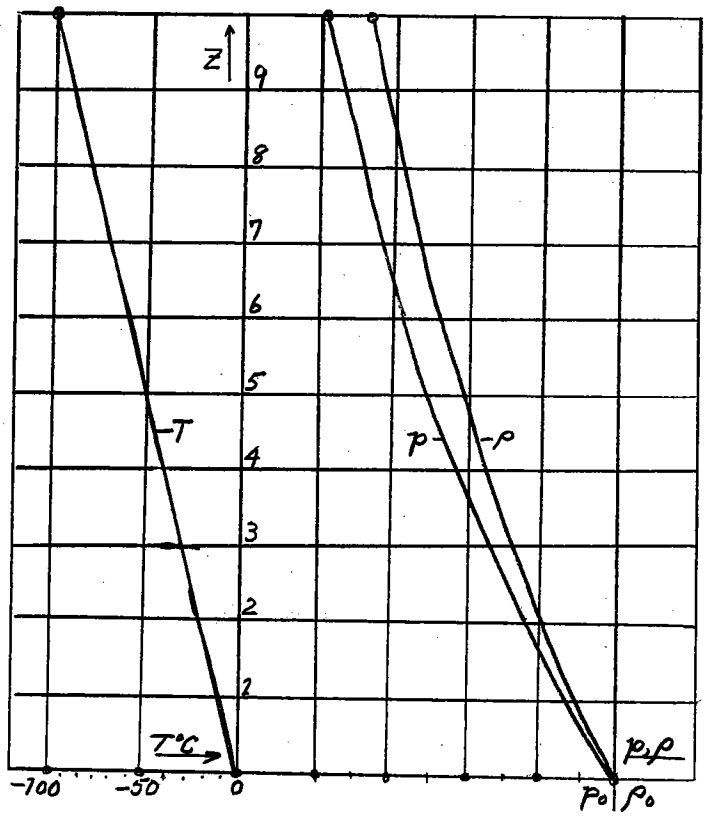

Fig. 155 Pressure, density and temperature in free atmosphere as functions of altitude.

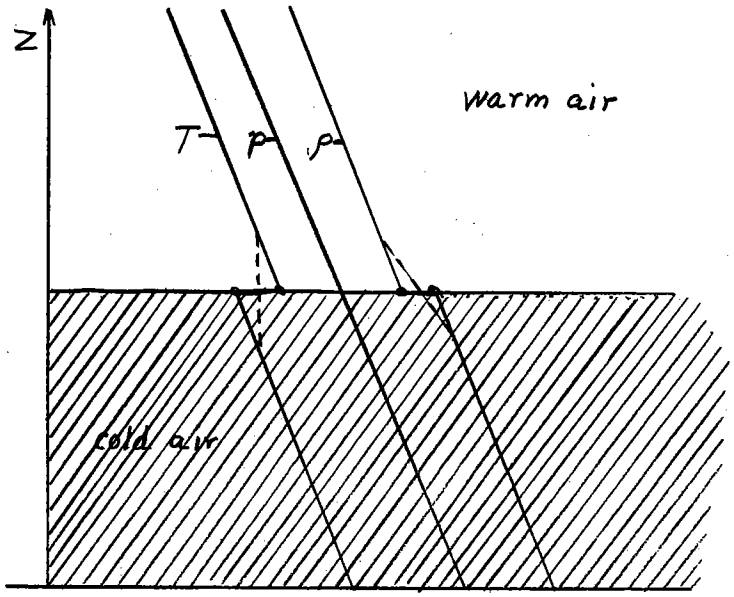

Fig. 156 Discontinuity of temperature and density when a layer of hot air is found above a layer of cold air. (Stable stratification).

a translation speed V, the turbulent movement produced at the separation-surface accelerates the effacement of the sharp discontinuities.

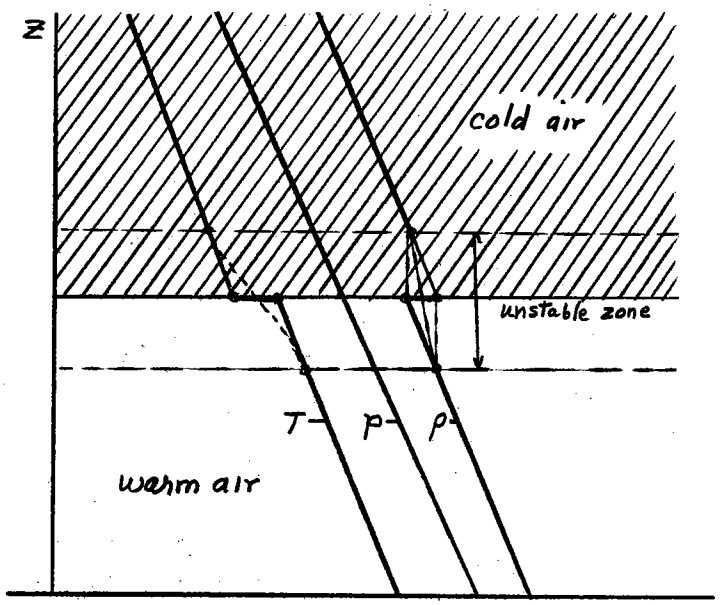

Fig. 157 Discontinuity of temperature and density if a layer of cold air is found above a layer of hot air (Unstable stratification).

The inverse case where the density of the upper layer exceeds the density of the lower layer, is also frequent. Naturally, this system is not stable: vertical motions must necessarily show up. If such a system could remain in equilibrium, the vertical distribution of temperature and density would be represented by the discontinuous curves of Fig. 157. But the eddy-motion, occupying the unstable zone that one can determine graphically (see Fig. 157), assures continuous transition.

As for the causes that bring on inversions of the temperature gradient, and consequently of the density gradient, they are very numerous. Mr. S. Mal (9) mentions two of them, well known to

meteorologists anyway:

1st. If a cloudy layer rises, limited above by dry air, there results an instability. This last is produced at the separation surface, because during the adiabatic elevation the temperature of the dry air diminishes. The dry air, therefore, will descend to recover the initial conditions. If the cloud layer is thick, the eddy motion will occupy only the uppermost portion of the layer. On the other hand, if the layer is thin, the movement is able to pierce it, and occupy a certain thickness of the moist air beneath the clouds.

2nd. Another cause capable of provoking vertical instability is radiation. The lower atmosphere beneath a cloud layer is heated by the radiation of the sun, whereas the air above the clouds is chilled off by radiation towards empty space. The lower mass of air becomes less dense than the superposed mass: hence, the system is unstable. Some very interesting works on this subject are presently being done by G. Sartori (18).

3. Convection currents in the atmosphere provoked by vertical instability.

We have just shown, firstly, that following the vertical, the atmosphere is very frequently made up of layers more or less heterogeneous, a fact that brings on discontinuities in the distribution of humidity and temperature and consequently, in that of the density. Then secondly, we have noted that the corresponding vertical gradients very often undergo strong inversion. This last fact leads to vertical instabilities that resemble those realized in the experiments on thermoconvective eddies in a fluid horizontal layer, heated from

beneath or heated from above. And so it is quite logical to suppose that the currents of convection, that must of necessity produce themselves, manifest the same organization of circulation as the cellular eddies obtained at the laboratory on a much smaller scale.

We know that P. Idrac, author of the theory of organized currents in free air, succeeded in demonstrating practically the existence of such currents. This researcher effectuated the greater part of his researches in moist air. He was not able to observe any phenomenon of an optical nature such as to permit him to distinguish the regions of rising or descending currents. He had to take recourse at one time to special apparatus recording the vertical component of the wind, the temperature and pressure, and at another to the observation of birds flying by planing and gliding. None the less, he expressed the idea that the clouds that presented themselves in the aspect of regularly-spaced bands could be the upper part of eddy elements rendered visible by the condensation of water vapor.

We have confirmed, partially, this original hypothesis by a series of experiments on thermoconvective eddies in air saturated with water vapor, experiments we have described at the end of Chap. II (21-g). In supposing that the cellular eddies in two dimensions are the transversal section of eddies in bands, one can compare the deposits of condensed water vapor upon the panes of the vat with the section of analogous clouds. If it is a question of clouds in bands, they are the result of the condensation of water vapor between two contiguous rolls, turning oppositely. In making reference to the

same laboratory experiment, we conclude that the cloud rolls should cover the regions where ascending currents produce themselves. As a consequence, the descent should effectuate itself in the spaces separating the cloud bands. As for clouds in balls (or polygonal), they would be so many hats, capping the cellular eddies: their centers, then would indicate the columns of rising air, and the clear spaces the places where descending currents were found. (Figs. 158, 159, 160 in back).

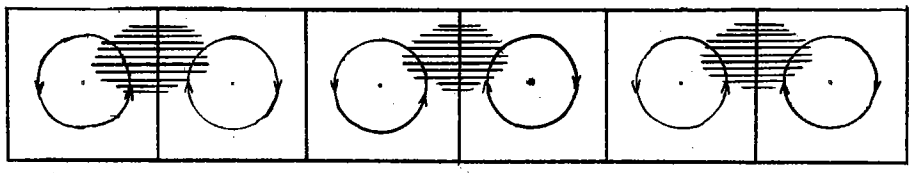

First phase

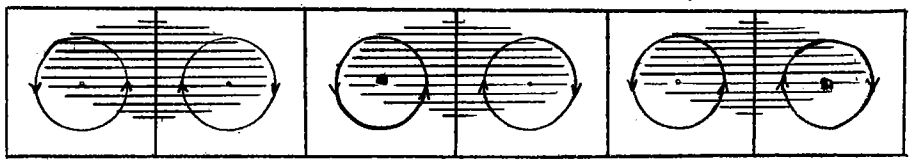

Second phase

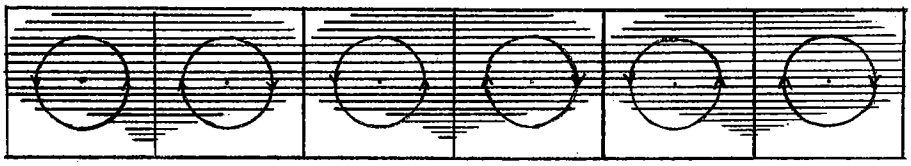

Third phase

Fig. 161 Schematic transformation of a cloud layer fractionated into one continuous layer.

After Idrac, all the meteorologists who have adopted the principle of the theory of thermoconvective eddies have adapted the primitive hypothesis to all the other forms of fragmented clouds, hypothesizing, (to sum it up) that the clouds in equidistant bands could reveal analo-

gous eddies. This category of clouds, present, in effect, superb formations, possessing all the geometric characteristics of thermoconvective eddies. One finds as well among them clouds in balls, clouds in rectangular cellules, and polygonal cellules, as clouds in bands longitudinal or transversal.

4. Clouds in balls and in polygonal cellules.

These clouds must form themselves in consequence of the vertical instability in a horizontal layer that is in relative rest in reference to the bounding layers.

The altocumulus translucidus, shown in Fig. 158 (27), is the typical example of clouds in balls. In conformance with our experiments in humid air, the cloud-balls would be hats indicating summits of the eddies in polygonal cellules.

We reproduce again two other photos from our collection (Fig. 159, 160). While in the second photograph the cloud elements retain clearly their individuality (one sees there some of them very strongly illuminated) they are in the first photograph very pressed together and form one layer almost unified.

If one refers to the two last series of experiments in humid air (cf. Chap. II), the one carried out under a moderate heating (feeble evaporation), and the other under a more forced heat (strong evaporation), one is led to apply the mechanism of the growing islets to the transition of segmented clouds into a continuous layer. If indeed this is so, the cloud elements will keep their individuality if the inversions of density (temperature) and their content of water

vapor be small. On the other hand, in presence of strong inversions, and if the mass of air is abundantly saturated with water vapor, the cloud elements will grow and confound themselves into one continuous layer.

Figure 161 represents schematically three successive phases of this transition. Evidently, this mechanism is but an approximate image of that which produces itself in the atmosphere; for the physical conditions change profoundly as soon as the condensation of water vapor intervenes. And this change cannot be without consequences for the original circulation.

Let us recall even here that the mechanism of this transition, which applies just as well to clouds in balls as to the clouds in bands, can produce itself in the inverse sense, the continuous layer fracturing itself into separate elements.

5. Clouds in bands

Referring to the Atlas Internationale des Nuages (27), one sees there two principal varieties of clouds in bands, the first designated "undulatus" and the other "radiatus".
(Figs. 162, 163 in back).

By definition, the designation "undulatus" applies to clouds composed of elongated elements, mutually parallel, resembling waves of the sea. Figs. 162 and 163 show two altocumulus undulatus.
In the first case, the rolls are very close-pressed and their edges are tattered out in a direction perpendicular to their axes. On the other hand, in the second photograph, the big rolls are separated by

intervals of blue sky. As a result of perspective, only two or three of these clear bands are visible consecutively.
(Figs. 164, 165 in back)

For another point, the designation "radiatus" is applied to clouds composed of parallel bands which, by perspective effect, seem to converge towards one point on the horizon. Fig. 164 gives a typical cirrus radiatus, whose convergent bands are made up of a very thick mass of cloud. In Fig. 165, which shows an altocumulus undulatus radiatus, one sees an analogous convergence. The big converging bands are undulated in the perpendicular sense, but the undulation-length of the transversal waves is sensibly smaller than that of the principal waves.

We know that two separate theories attempt to explain the origin of these clouds in regularly-spaced bands; the first, dating from 1888, due to H. von Helmholtz (22-b,c), attributes them to atmospheric waves, the other dated from 1920, due to P. Idrac, considers them as thermoconvective eddies. To be able, in each given case, to decide between the two theories, it is necessary to set in relief the essential points that characterize the two possible origins.

Atmospheric waves and clouds in transversal bands. - One can demonstrate by the principle of mechanical similitude that the rôle of the viscosity diminishes in proportion as the space occupied by the fluid is the greater. The numerical example of H. von Helmholtz gives a good idea of the slowness of propagation of the motion by friction. Let us suppose, to simplify the problem, an atmosphere of constant

density, giving by consequence to the temperature 0°C a reduced height of 8000 m. Next let us admit that this atmospheric layer moves with a uniform speed of translation V. At the level of ground contact, the speed is necessarily null. The upper layers are braked also, but as much the less so as they are the more distant from the ground. Helmholtz (26-b) shows that it would require more than 42,000 years for the speed at the upper surface to be reduced to half its initial value. One would find a still longer duration, if one took account of the fact that in reality, the density of the air diminishes with the altitude.

If one studies by analogous processes the propagation of heat by ordinary conductivity the calculation gives, for the lowering of the temperature, durations of the same order of magnitude (36,000 years).

Let us now consider the case of a fluid layer in translational motion and sliding above another fluid layer at rest. H. von Helmholtz has already shown in 1868 (26-a) that such discontinuous motions may well exist during some moments. But in consequence of the unstable equilibrium at the surface of discontinuity, the eddying is not slow to start. If the two masses are homogeneous, there comes about an integral wholesale mixture. On the contrary, if the superposed layer is lighter than the lower mass, the conditions are then favorable to the formation and propagation of regular waves, as is proven, to push the matter to the extreme, by the existence of regular swells on the free surface of the ocean.

Being granted that in the free atmosphere, stratification in heterogeneous layers exists, Helmholtz estimated that analogous waves

must be produced very frequently at the surface of discontinuity separating two air layers of different densities. Evidently, we cannot observe them directly, unless the lower layer of air is charged enough with water vapor, for then the summits of the waves, where the pressure has dropped, can become opaque by reason of condensation. In the sky, then, clouds in parallel bands regularly spaced would appear. The schema of their transversal section is shown in Fig. 166. The spacing of the bands is governed by the wave length λ, which depends upon the relative speed of translation between the two layers, and upon the difference of their densities. As for the breadth and opacity of the cloud bands, they are in direct correlation with the humidity and with the amplitude and the length of wave. By the terms of the calculation, the wave length between two layers of air, respectively at 0° and 10°C and of which the difference of the speeds of translation is 10 m/s, is equal to 550 m. But one can imagine likewise cases where the atmospheric waves could attain a wave length of 30 km, as also lengths of some dozens of meters, merely.

Clouds in bands oriented in the direction of the wind. The theory of atmospheric waves and of clouds in bands that one would think of as resulting from them is, incontestably, very reasonable. And yet, withal, it is not always applicable to the clouds in bands. If one notes the disposition of cloud bands in respect to the general wind stream, one can discover that they are not always perpendicular to the speed of translation, and, yet it is the principal characteristic of waves of dynamic origin. How then can we explain the waves in bands oriented in the direction of the wind, and whose frequency appears even

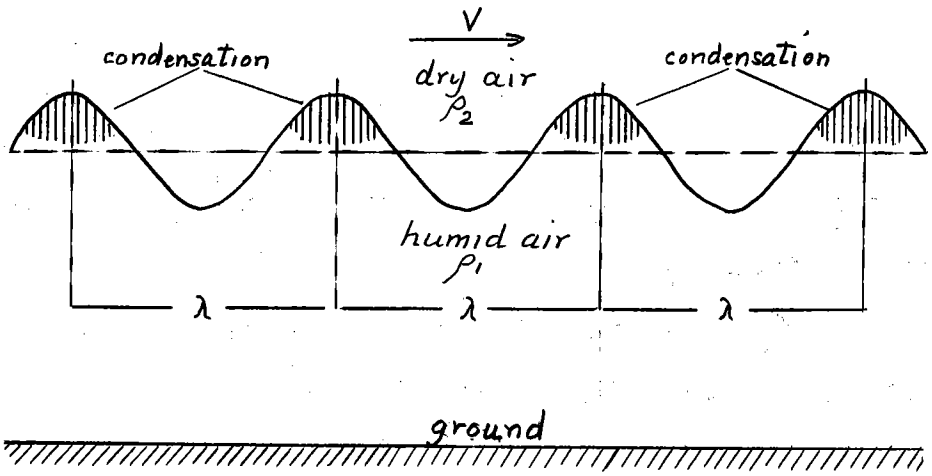

Fig. 166 Condensation at the summit of waves that arise at the surface of discontinuity of a layer of humid air and a layer of dry air in relative motion.

greater than the frequency of transversal bands (4-c,e; 28)?

Idrac showed experimentally that their origin must be attributed to thermoconvective currents, which organize, as we know, in rolls, parallel and elongated in the general wind direction. According to him, the direction of the cloud bands in respect to the general wind would be the deciding criterion between the two theories; if the bands are parallel to the speed of translation, they would be of thermoconvective origin; on the contrary, if the bands are perpendicular to the wind, they proceed from atmospheric waves.

Clouds in transversal bands of thermoconvective origin. - The thermoconvective theory has been entirely approved and actively developed by many other meteorologists and physicists, sometimes to the detriment, even, of the theory of atmospheric waves.

We have already said in the historical part, that Sir G. I. Walker and A. C. Philipps (10) produced thermoconvective eddies in their laboratory experiments, in bands disposed perpendicularly to the speed of translation. Walker even estimates that the clouds of

Telmholtz would produce themselves very rarely, and consequently, that the transversal bands would themselves also be of thermoconvective origin.

A probable conciliation between the theory of the atmospheric waves and the thermoconvective theory.

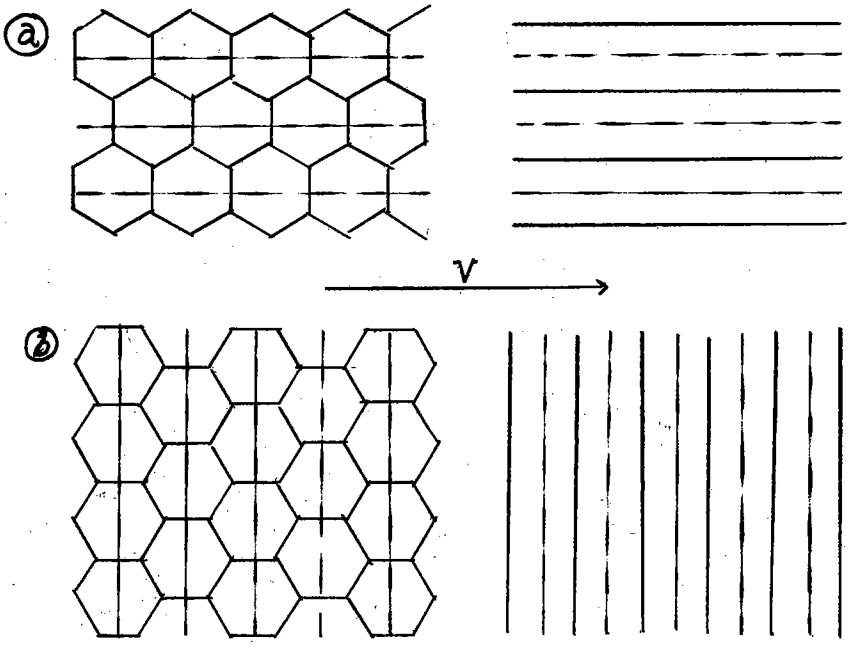

Fig. 167 Orientation of hexagonal cellules and their transformation into longitudinal bands (a), and into transversal bands (b).

According to Philipps and Walker, the eddies in transversal bands are the intermediary form between the polygonal cellules that produce themselves in a layer of air at rest, and the square cellules whose diagonals are directed in the direction of the current of translation. The rate of the speed of translation, comprised between zero and the value corresponding to the formation of square cellules, would be the sole factor deciding their appearance.

Elsewhere, A. Graham (11) has found that the production of the

transversal rolls does not always come off. According to him, the original arrangement of the hexagonal cellules plays a capital rôle in the later development. If the hexagons are oriented in such fashion that their sides are perpendicular to the movement of translation (Fig. 167-a), they cannot ever arrange themselves in transversal rolls, but they transform themselves easily into longitudinal bands. On the other hand, if the diagonals of the hexagons are parallel to the general current, (Fig. 167-b), the eddies in transversal bands may well come about as a result.

The initial orientation of these hexagons being due to hazard, one could not hope that transversal bands could produce themselves frequently. But, all the same, we have shown that it has been possible to provoke eddies in transversal bands without their being preceded by hexagonal cellules.

In point of fact, according to our experiments, eddies in bands perpendicular to the movement of translation are the result of two superposed phenomena -, to wit:

1. Formation of waves at the separation surface between the two fluid layers of different densities;

2. The development of the thermoconvective currents which must adapt themselves to the valleys and the crests of the successive waves. By consequence, it is very probable that the clouds in transversal bands are of the same origin as the eddies in transversal bands: for one thing, the separation surfaces, so frequent in the atmosphere, are favorable to the appearance of the waves, and for another thing, the inversions of the temperature gradient, which one can almost always detect in those

places, must give birth to convective currents. In these conditions, the theory of atmospheric waves remains perfectly valid, but completed, when it is necessary, by the thermoconvective theory.

6. Dimensions of fragmented clouds.

Quantitative measurements on the dimensions of clouds in bands and clouds in balls are far from numerous. However, those we know of show that the horizontal dimensions are generally very much greater than the vertical dimension. Otherwise said: the ratio λ/h is very large.

For example, S. Mal (9) has observed a cumulus arrangement in bands that were separated from each other by 4000 m and were 600 m thick, and a stratocumulus whose bands were distant 250 m and only 70 m thick. And so, the relationships of distance of the two bands and their thickness were respectively 6.6 and 3.5.

When we consider our theoretical and experimental results on eddies in longitudinal bands where the ratio λ/h varies in normal conditions between 2 and 3, the high values found in the atmospheric phenomenon appear surprising.

For the sake of elucidating this question, let us reconsider our experiment with thermoconvective eddies in air saturated with water vapor, conditions more nearly approximating those realized in the free atmosphere (21-g). We note, Figs. 12, 13, 14, that the foggy smears are very flattened and that they occupy only a portion of the total height of the layer of air in eddy motion. In these conditions, one should not identify the relationship λ/h of the eddy cellules with the relationship attached to the principal dimensions of the deposits of

condensed vapor. (Fig. 168 in back).

Here, among others, is a numerical example, drawn from Fig. 168: The λ/h ratio of two central cellules is equal to 2, which is exactly the theoretical value, whereas λ/h_r relative to the foggy smear of the center goes as high as 4.3.

By analogy with this experiment, one can say that the cloudy layer divided into isolated compartments is not necessarily equal to that occupied by thermoconvective currents: in general, it will be less, and the relationship of the distance of two neighboring bands and of their thickness will be able to exceed more or less the ratio λ/h relative to eddy movements.

7. Criterion of Rayleigh and atmospheric thermoconvective currents.

Compartmented clouds attain in their dimensions hundreds of meters - more than one thousand times the linear dimensions of artificial eddies. Nature, despite conditions apparently unfavorable to her, gives birth to some phenomena the production of which in the laboratory exacts a great many precautions.

D. Brunt (7,8) tried to explain this paradoxical particularity by a complex viscosity and conductivity in the atmosphere, which (qualities) would be much greater than they were in the calm air in an experimental chamber. An approximate analysis of the criterion of Lord Rayleigh will confirm that Brunt's explanation is well founded.

According to the classic definition, the atmosphere is in vertical equilibrium if the less dense layers overlie the denser layers, or at least, if the density along the vertical remains constant. However, it is not rare to find temperature lapse rate sensibly greater

than the adiabatic decrease (proof, indirectly, that the denser air remains on top of the more expanded air), without any destruction of the vertical equilibrium. In these conditions, it is logical to suppose that the system remains in stable preconvective equilibrium, and to apply Rayleigh's criterion to the atmospheric phenomenon.

Let us consider again the inequality (66-bis), that we found for perfect gasses and let us suppose the pressure constant. If the thickness of the layer of atmospheric air is not great, this inequality can aid us efficaciously in the approximate estimation that we propose to make.

Let us suppose the boundary conditions of Rayleigh's problem and an average temperature of 0°C. We have calculated that the difference of extreme temperatures of a layer of air of 1 cm thickness should exceed 4.42°C if the stable preconvective equilibrium is to be broken. But, in virtue of the inequality (66-bis), this critical difference of extreme temperatures diminishes in inverse relationship to the third power (cube) of the thickness h. In these conditions, a suradiabatic temperature gradient β_s only a very little greater than the adiabatic gradient β_a would suffice to release convective movements in a layer of air 100 meters thick. In fact, the calculation gives:

$$\beta_s = (\beta_a + 4.42 \times 10^{-8})°C \text{ per 100 meters.}$$

But currently observed gradients in the atmosphere are clearly greater than the above value. If we suppose that the criterion of Lord Rayleigh be approximately exact, we must justify the strong superadiabatic

gradients by the hypothesis that the product $\varkappa\nu$ of the atmospheric air is much greater than the product of the molecular conductivity and of the kinematic viscosity in the small experiments.

If one knows the temperature gradients β_s and β_a and the thickness h of the air layer in stable preconvective equilibrium at the moment when the convective currents are on the point of being released, one can calculate the product $\varkappa\nu$ by the formula:

$$= \frac{\beta_s - \beta_a}{T + 273} \frac{g\, h^4}{\Lambda} ,$$

drawn from the inequality (66-bis) where one has put:

$$T_2 - T_1 = h(\beta_s - \beta_a) .$$

In this way one finds values of $\varkappa$ and ν from 10^3 to 10^4 times greater than those encountered in the experiments in the laboratory.

8. Directives for researches on thermoconvective eddies in the free atmosphere.

As yet, researches in flight upon convective currents in the free atmosphere are few in number. This is why the Commission de la Turbulence Atmospherique proposes to extend its activity also in this field.(1) And so it seems to us needful to mark out certain directives that might guide future explorations in the atmosphere.

Simultaneously recording motions occupying the vast space of the humid atmosphere is practically an impossibility. But on the other hand, if the sky is covered with clouds, and above all, with clouds having clean-cut contours, one can seize these currents with a single glance. But it is important, with J. Kampe de Feriet (30), that the

(1) One can find the detailed program of the work envisaged by the Commission on Atmospheric Turbulence in the preface by M.Ph.Wehrlé in the excellent memoirs of M.Paul Dupont (29).

presence of clouds disturbs the atmosphere, for the physical conditions are considerably changed, and by consequence, the motions are also. Be it as it may, in the study of ordered convective currents, clouds offer the most convenient means of visualization, and often, even, the only means applicable. The photography of these clouds whether taken from the ground below or from above by airplane, sailplane or balloon, constitutes the most important document, which will serve essentially for study of the forms of the elements of clouds and for measurements of the transversal dimensions of these clouds.

Evidently, the simple geometrical similitude of compartmented clouds to cellular eddies is not sufficient proof of their thermoconvective origin. And, to confirm the hypothesis that the segmentation of the cloudy layer is the result of vertical instability, one has to prove that the conditions in which this phenomenon is produced are identical with those that one realizes in laboratory experiments upon thermoconvective eddies.

With these points now rendered precise, the verifications effectuated in the free atmosphere must bear upon the following questions:

1. Do these fragmented clouds coincide with the places where strong inversions of the vertical temperature gradient are produced?

2. Does the temperature oscillate periodically when one traverses the stratified clouds, and that in such fashion that the maxima and minima coincide respectively with the centers of the cloud-elements and with the localities of clearing?

3. Does the vertical component of speed oscillate with the same periodicity as the temperature when one traverses the stratified clouds

in the horizontal plane?

4. Are the forms of compartmented clouds in correlation with their speed of translation in respect to the bounding layers?

Let us again consider these diverse points.

1. The principal condition for the appearance in free atmosphere of thermoconvective currents is the reversal of the adiabatic temperature gradient in the vertical.

Automatic recording of the temperature as function of the altitude is, of course, indispensable. Since the discontinuities of the vertical temperature distribution and the inversions of the vertical temperature gradient are correlative to the distribution of humidity, it is necessary to take records also of the specific humidity at the same time as that of the temperature.

The use of the meteorograph, registering the pressure (altitude), the temperature and the humidity, becomes, hence, a necessity. By scrutinizing the diagrams, one will be able to glean the required data to reconstitute the altitude and the thickness of the unstable layer.

2. On the other hand, the recording of temperatures and humidity in a horizontal plane situated in the midst of the cloudy layer is equally important, because the character of the temperature diagram will allow us to <u>determine whether the layer of stratified clouds is in eddy movement or not.</u>

In fact, the diagram of recorded temperature at the time of a traverse of clouds in bands will have the same character, if these clouds are really of thermoconvective origin, as that which we found in our experiments (cf. diagrams of Figs. 149, 150, 151), which have

shown that the temperature oscillates and that its maxima and minima coincide respectively with ascending and descending currents.

3. According to our experiments on thermoconvective eddies in humid air, one must seek the maximal ascending speeds in the central column of clouds in balls, and in the vertical plane of symmetry in the case of clouds in longitudinal bands. Consequently, one should find the maximal descending speeds in the clearings of the clouds. However, certain meteorologists said that they had sometimes seen a circulation in the opposite sense, that is, descent at the centers of compartmented clouds, and ascent along their partitions. Such cases are going to require research.

The instruments employed in these studies in the horizontal traverse of clouds in bands will have, of course, to record periodic oscillations of the vertical component of speed.

But, first one will have to find appropriate measuring procedures. The kite-flying method connected with special recording apparatus, used with full success in the low layers of the atmosphere by P. Idrac (4-c), seems impracticable for higher altitudes. We will have to take recourse to the airplane with its inconveniences: it flies too fast - with vibrations, etc. - or to the glider, with its advantages: slowness, air-sensitivity, no vibrations, and we will need to be equipped with recording apparatus.

4. Experiments show that the principal forms of thermoconvective eddies depend, in the first place, upon the speed of general translation with which the fluid layer moves. Pursuantly, one will investigate the question as to whether there exists the same correlation

between compartmented clouds and their speed of translation in respect to the limiting stable layers.

By the terms of our theory, one should find, first, that clouds in polygonal cellules do form themselves when the unstable layer is in relative repose, and, secondly, that the clouds in bands appear when they move with greater translation speed than do those of the limiting layers.

In view of the fact that cloud bands can form, at the general speed, every angle comprised between 0° (longitudinal bands) and 90° (perpendicular bands) the observer will determine likewise their orientation.

The actual taking of measurements of speeds of translation and of orientation of clouds in bands in relation to the ground is very simple.

But one must carry out, above all, the measurements of relative speed between the layer of stratified clouds and the stable layers, a speed which alone is decisive for the form of convective eddies. Therefore, a satisfactory method will need first to be worked out. (Figs. 169, 170 in back).

9. Remark on electroconvective eddies. (Fig. 171 in back).

For the sake of obtaining for laboratory experiments conditions as closely as possible approximating those realized in free atmosphere, it has seemed to us that the physical causes of the formation of clouds in balls and in bands ought not to be studied exclusively in the thermal state of the atmosphere, but that one could also conjecture analogous eddy motions of electrical origin. With a view of confirming this

hypothesis upon a presumed existence of eddies of electric origin, we undertook with Mr. M. Luntz, in 1936-7, a series of experiments(2).

We have succeeded in producing:

1. In an insulating layer of oil, submitted to an intense electric field, polygonal electroconvective eddies, similar to the thermoconvective eddies of Bénard (Figs. 169, 170);

2. Electroconvective eddies in longitudinal bands in a layer of oil in motion;

3. Electroconvective eddies of two dimensions contained either between two rectilinear and parallel electrodes, or between two circular concentric electrodes. (Figs. 171, 172).
(Figs. 172, 173 in back).

4. Toroidal electroconvective eddies between two coaxial cylindrical electrodes (Fig. 173), that resemble those that G. I. Taylor (18), obtained between two turning cylinders.

Let us extend our conclusions to the atmosphere; it is probable that besides the thermoconvective currents, and above all at elevated altitudes, there exist movements of electroconvective origin. In fact, the ionization of the atmosphere augments rapidly with altitude, whereas the temperature gradient becomes very uniform and without inversions. To confirm these predictions, which render still more complex the exploration of aerological phenomena, the meteorologist will find it necessary to interest himself still more, and more methodically, in the dynamic consequences of the electricity of the atmosphere.

Conclusion

By reason of the present lack of inclusive expositions concerning thermoconvective eddies, it seemed to us that a general monograph on the subject could, perhaps, render some service. This conception of the present memorandum has necessitated in the first place that we should relate certain results already classic in meteorology, but which perhaps are not very widely known outside of specialized circles, and, in the second place, that we should incorporate our own labours with the conclusions obtained by other authors. And so, we wish to indicate upon just which points we believe we have contributed personally.

1. To interpret more readily the problem of the convective movements in an indefined layer of air, we worked out three experiments on organized movements in two dimensions (Chap. II).

a) By operating with a layer of oil surmounted by a layer of water, we have given the simplest example of organized movements.

b) The second experiment with thermoconvective eddies of two dimensions in dry air permitted us to observe and photograph the partitioning and the trajectories in the vertical plane in a flat tank.

c) The third experiment has for its object thermoconvective eddies of two dimensions in humid air. We were able thus to study the condensation of water vapor in relation to the convective currents and to clear up several questions concerning the study of compartmented clouds.

2. Contrary to what several authors have stated who had experimented in gasses (Philipps, Walker, Graham), we have established that

eddies in longitudinal bands are produced as well in thick as in thin layers. This experimental result was of capital importance for the researches we intended, for, the thickness interval being considerably augmented, we have been able to carry out some very systematic measurements (see in what follows).

3. We have described the characteristic phases of the development of eddies in gasses (Chap. IV). In particular, we have demonstrated that the eddies in bands perpendicular to the general current result, first, from the formation of waves at the surface of the denser fluid layer (heavy tobacco smoke), and secondly, from the appearance of convection currents that engage themselves in the hollow of two succeeding waves. This clarification modifies the original hypothesis of Philipps and Walker.

4. We have proven the existence of eddies in longitudinal bands with undulated partitions, and we have indicated several of the causes that can provoke this undulation (Chap. V, Paragraphs 6 and 7).

5. We have observed and described numerous cases of mutual transformation of eddies (Chap. V, Paragraphs 1, 2, 3, and 4), and proven the coexistence of eddies of differing forms (Paragraph 5 of the same chapter).

6. We have demonstrated experimentally that the little accidental perturbations, practically unavoidable, cause more or less important variations of the transversal dimension of eddies in bands. We have eliminated the influence of accidental perturbations by artificially provoking regular perturbations, whose amplitude was greater than the first, and in this fashion we have provoked a predetermined number of rolls (Chap. IX).

7. By injecting into eddies in longitudinal bands tobacco smoke in little doses, we have succeeded in making visible the helicoidal trajectories, which, in the photographs, present themselves as sinusoidal lines. (Chap.X, Experimental Section). This method of visualization of the internal movement, completed by the photography of the trajectories in the vertical plane of the eddies in two dimensions, will be able to serve efficaciously in the quantitative study of speeds in function of temperature extremes and of the thickness of the layer of air.

8. We have measured the transversal dimensions of the eddies as a function of the thickness of the layer of air. The results relating to eddies in longitudinal bands are particularly developed. (Chap.VIII. Experimental Section).

9. We have confirmed experimentally that the régime of thermoconvective currents is preceded by a stable preconvective régime, a fact foreseen by Lord Rayleigh's theory (Chap.VII, Experimental Sec.)

10. We have effectuated systematic measurements on the distribution of temperatures following the thickness and the width of eddies in longitudinal bands. By making vary the thickness of the air layer, the intensity of the heat, and the speed of translation, we have established several varieties of thermal field (Chap.XI, Experimental Sec.)

11. We have confronted the theoretical results and the results arising from our own experiments. Starting with the original theory of H. Jeffreys, we have worked out the following generalizations and calculations:

a) After having shown that the theory of Jeffreys contains as many multiple solutions as that given later on by A. R. Low, we have developed the calculation of the Rayleigh-Bénard criterion for any number of empiled circuits (Chap. VII, Theoretical Part).

b) We calculated the theoretical values of the λ/h relationship in several simple cases (Chap. VIII, Theoretical Part).

c) We have determined the Z function of perturbation in the problems of Rayleigh and of Jeffreys, in both cases for one and for two stages of eddies (Chap. X, Paragraph 2).

d) The function Z being known, we have been able to determine the stream function in the same special problems (Chap. X, Paragraph 3).

e) We have given a detailed analysis of the distribution of temperatures in the rectangular section of two-dimensional eddies and of eddies in bands (Chap XI, Theoretical Part).

12. To complete the theory of convective currents organized in free air, (Chap. XII), we have drawn upon our own results relative to thermoconvective eddies in air.

a) In applying the mechanism of our eddies in transversal bands, we have tried to reconcile the atmospheric waves theory and the thermoconvective theory.

b) Our experiments upon eddies in air saturated with water vapor have allowed us to propose an explanation:

α) of the mechanism by which compartmented clouds transform themselves into an extended cloudy layer and inversely;

β) of the formation of clouds above columns of rising humid air;

γ) of the differences of thickness between the cloudy layer and that occupied by the convective currents:

c) We have raised the question of organized currents of an origin attributable to atmospheric electricity.

d) We have given finally some directives which might guide future researches upon convective eddies in the free atmosphere.

Bibliography

(1) H. Bénard:

(a) Cellular eddies in a liquid sheet (First part: General description of phenomena. Second part: Mechanical and optical procedures of testing; numerical laws of the phenomena). Revue générale des Sciences pures et appliquées, t.11, 1900, p.1261-1271 and p.1309-1328.

(b) Cellular eddies in a liquid sheet propagating heat by convection, in a steady régime. Thèse de Doctorat, Paris, 1901.

(c) On the formation of lunar circles, according to the experiments of C. Dauzère. Comptes rendus de l'Académie des Sciences de Paris, t.154, 1912, p.260.

(d) On cellular eddies and the theory of Rayleigh. Comptes rendus de l'Académie des Sciences de Paris, t.185, 1927, p.1109.

(e) On eddies in bands and the theory of Rayleigh. Comptes rendus de l'Académie des Sciences de Paris, t.185, 1927, p.1257.

(f) Eddies of the developing baths. Bulletin de la Société française de Physique, no.266, 1928, p.112S.

(g) Is the superficial solar photosphere a layer of cellular eddies? Comptes rendus de l'Académie des Sciences de Paris, t.201, 1935, p.1328, and Livre jubilaire de M. Marcel Brillouin, p.125, Paris, 1935.

(h) P. Idrac and the theory of clouds in bands. La Météorologie, Paris, no.3, May-June, 1936.

(2) D. Avsec, M. Luntz:

(a) Electroconvective eddies. Comptes rendus de l'Académie des Sciences de Paris, t.203, 1936, p.1140.

(b) Electroconvective eddies in a fluid sheet. Comptes rendus de l'Académie des Sciences de Paris, t.204, 1937, p.470.

(c) Some new forms of electroconvective eddies. Comptes rendus de l'Académie des Sciences de Paris, t.204, 1937, p.757.

(d) Thermoconvective and electroconvective eddies. La Météorologie, Paris, no.3, May-June 1937.

(3) C. Dauzere:

(a) On the stability of cellular eddies. Comptes rendus de l'Académie des Sciences de Paris, t.154, 1912, p.974.

(b) On the changes that cellular eddies undergo when the temperature rises. Comptes rendus de l'Académie des Sciences de Paris, t.155, 1912, p.394.

(c) On isolated cellular eddies. Comptes rendus de l'Académie des Sciences de Paris, t.156, 1913, p.218.

(d) On a new kind of cellular eddies. Comptes rendus de l'Académie des Sciences de Paris, t.156, 1913, p.1228.

(e) On the crystallization of the oxide of phenyl. Comptes rendus de l'Académie des Sciences de Paris, t.162, 1916, p.385.

(f) On the formation of a cellular network during the crystallization. Comptes rendus de l'Académie des Sciences de Paris, t.162, 1916, p.597.

(g) On the formation of columns of basalt. Comptes rendus de l'Académie des Sciences de Paris, t.169, 1919, p.76.

(h) Cellular solidification. Thèse de Doctorat, Paris, 1919.

(4) P. Idrac:

(a) Experimental researches upon planing flight. Comptes rendus de l'Académie des Sciences de Paris, t.157, 1913, p.635.

(b) Observations on the flight of gulls astern of ships. Comptes rendus de l'Académie des Sciences de Paris, t.157, 1913, p.1130.

(c) On convection currents in the atmosphere in respect to their

relation to planing flight and to certain cloud formations. Comptes rendus de l'Académie des Sciences, Paris , t.171, 1920, p.42.

(d) Experimental studies on planing flight. Comptes rendus de l'Académie des Sciences de Paris, t.172, 1921, p.1161.

(e) Experimental studies on planing flight. Thèse de Doctorat, Paris, 1921.

(f) On the structure of the winds on the high seas and their utilization for planing flight. Comptes rendus de l'Académie des Sciences de Paris, t.177, 1923, p.747.

(g) Study on the conditions of updraft winds favorable to flight by sailplane. Mémorial de l'O.N.M., Paris, first year, no.7, 1923.

(5) T. Terada and Second Year Students of Physics:

Some experiments on periodic columnar forms of vortices caused by convection. Report of the Aeronautical Research Institute, Tôkyô Imperial University, t.3, 1928, no.31, p.3.

(6) T. Terada, M. Tamano:

Further researches on periodic columnar vortices produced by convection. Report of the Aeronautical Research Institute, Tôkyô Imperial University, t.4, 1929, no.53, p.448.

(7) A.R. Low, D. Brunt:

Instability of viscous fluid motion. Nature, t.115, 1925, p.289.

(8) D. Brunt:

Convective circulations in the atmosphere. The Meteorological Magazine, t.60, 1925, no.709.

(9) S. Mal:

Forms of stratified clouds. Beiträge zur Physik der freien Atmosphäre, Leipzig, t.17, 1930, no.1

(10) A.C. Philipps, Sir G.T. Walker:

The forms of stratified clouds. Quarterly Journal of the Royal Meteorological Society, t.58, 1932, p.24.

(11) A. Graham:

Shear patterns in an unstable layer of air. Philosophical Transactions of the Royal Society of London, ser.A, t.232, 1933, p.285.

(12) Sir G.T. Walker:

(a) Recent work by S. Mal on the forms of stratified clouds. Quarterly Journal of the Royal Meteorological Society, t.57,1931,no.242.

(b) Cloud formation and its effect upon gliding. The Royal Aeronautical Society, conference of Feb. 16, 1933.

(c) Cloud and cells. Quarterly Journal of the Royal Meteorological Society, t.59, 1933, no.252.

(d) Clouds in the sky and in the laboratory. Science progress, 1935, no.115.

(13) J.W. Strutt, baron Rayleigh:

On convection currents in a horizontal layer of fluid, when the higher temperature is on the under side. Philosophical Magazine, 6th series, t.32, 1916, p.529.

(14) H. Jeffreys:

(a) The stability of a layer of fluid heated below. Philosophical Magazine, 7th ser., t.2, 1926, p.833.

(b) Some cases of instability in fluid motion. Proceedings of the Royal Society of London, ser.A, t.118, 1928, p.195.

(15) A.R. Low:

(a) On the criterion for stability of a layer of viscous fluid heated from below. Proceedings of the Royal Society of London, ser.A, t.125, 1929, p.180.

(b) Multiple modes of instability of a layer of viscous fluid, heated from below, with an application to meteorology. Proceedings of the 3rd International Congress for Applied Mechanics, Stockholm, t.1, 1930, p.109.

(16) P. Vernotte:

(a) Bénard's theory of cellular eddies. Comptes rendus de l'Académie des Sciences de Paris, t.202, 1936, p.119.

(b) The general laws of natural convection. Conditions of the appearance of the first regime. Comptes rendus de l'Académie des Sciences de Paris. t.202, 1936, p.733.

(c) The theoretical dimensions of the cellular eddies, by H.Bénard. Comptes rendus de l'Académie des Sciences, Paris, t.202, 1936, p.1764; t.203, 1936, p.43; t.203, 1936, p.985.

(d) Convection and cellular eddies. Bulletin de la Société française de Physique, no.391, 1936.

(17) V. Volkovisky:

(a) On eddies in festoons. Comptes rendus de l'Académie des Sciences de Paris, t.200, 1935, p.1285.

(b) On eddies in bands in liquids. Comptes rendus de l'Académie des Sciences de Paris, t.204, 1937, p.1461.

(c) On certain properties of the vertical trajectories in the plane problems of convection. Comptes rendus de l'Académie des Sciences de Paris t.207, 1938, p.1166.

(d) Study on thermoconvective eddies in liquids. Thèse de Doctorat, Paris, 1939, and Publications Scientifiques et Techniques du Ministère de l'Air, no.151, 1939.

(18) G. Sartory:

Formation of thermoconvective ascendances above a region uniformly heated by radiation. Comptes rendus de l'Académie des Sciences, Paris, t.208, 1939, p.327.

(19) V. Romanovsky:

Eddies in heavy muds. Application to arctic polygonal terrains. Comptes rendus de l'Académie des Sciences, Paris, t.208, 1939, p.621.

(20) M. Luntz:

Alternating thermoconvective eddies in a slender layer. Comptes rendus de l'Académie des Sciences de Paris, t.204,1937, p.547.

(21) D. Avsec:

(a) On the formation of convection eddies in a layer of gas with thicknesses of the order of several centimeters. Comptes rendus de l'Académie des Sciences, Paris, t.203, 1936, p.532.

(b) On the experimental verification of the fact, forseen by the theory of Lord Rayleigh, of the existence of the stable preconvective regime, and on the mechanism of the appearance of convective currents in a gaseous layer, heated uniformly from beneath. Comptes rendus de l'Académie des Sciences de Paris, t.203, 1936, p.556.

(c) On the λ/h ratio of eddies in longitudinal bands. Comptes rendus de l'Académie des Sciences de Paris, t.203, 1936, p.1318.

(d) On undulated forms of eddies in longitudinal bands. Comptes

rendus de l'Académie des Sciences de Paris, t.204, 1937, p.167.

(e) Thermoconvective eddies in superposed layers. Comptes rendus de l'Académie des Sciences de Paris, t.204, 1937, p.549.

(f) Eddies in transversal bands in a layer of air heated from beneath. Comptes rendus de l'Académie des Sciences de Paris, t.206, 1938, p.40.

(g) On thermoconvective eddies and the condensation of water vapor. Comptes rendus de l'Académie des Sciences de Paris, t.207, 1938, p.565.

(22) G.I.Taylor:

Stability of a viscous liquid contained between two rotating cylinders. Philosophical Transactions of the Royal Society of London, ser.A, t.223, 1923, p.289.

(23) J. Boussinesq:

Analytic theory of heat, t.2, 1903, p.172 and following(Gauthier-Villars, editor).

(24) C. Woronetz:

Perturbations provoked in the motion of a fluid by variations of the temperature. Thèse de Doctorat, Paris, 1934, and Publications Scientifiques et Techniques du Ministère de l'Air. No.60, 1934.

(25) K. Chandra:

Instability of fluids heated from below. Proceedings of the Royal Society of London, ser.A, t.164, 1938, p.231.

(26) H. von Helmholtz:

(a) Concerning discontinuous fluidity movements. Helmholtz Scientific Treatises, t.1, p.146.

(b) Concerning atmospheric movements. Report of the Sessions of the Royal Prussian Academy of Science at Berlin. Jan-May 1888, p.647.

(c) Concerning atmospheric motions: On the theory of wind and waves. Report of the Sessions of the Royal Prussian Academy of Sciences at Berlin, June-December 1889, p.761.

(27) International meteorological Committee - Commission for study of clouds:

International Atlas of clouds and the states of the sky,t.1,Paris, 1932.

(28) M. Besson:

On the alignments of the clouds. Annals of the Meterological Society of France. April, 1909.

(29) P. Dupont:

Contribution to the study of flight in agitated atmosphere. (Studies conducted by the Commission of Atmospheric Turbulence and by the Aeronautical Service of Techniques and Scientific Researches). Report on the campaign of the "Potez 540" at the Banne d'Ordanche, of the 19th to the 30th of September, 1936. Publications Scientifiques et Techniques of the Ministry of Air, Bulletin of Technical Services. no.77, 1938.

(30) J. Kampe de Feriet:

Atmospherical Turbulence. Compte rendu des Journées techniques internationales de l'Aéronautique, Paris, November 1936.

(31) R.J.Schmidt, S.W. Milverton:

On the instability of a fluid when heated from below. Proceedings of the Royal Society of London, ser.A, t.52, 1935, p.586.

Titles of Illustrations

Fig. 2. Spontaneous cellular eddies in a layer of spermaceti heated from below. (Bénard's experiment, 1900: method using graphite powder in suspension in the liquid; squares drawn = 1 cm^2.)

Fig. 3. Cellular eddies in a layer of spermaceti. (Bérnard's experiment, 1900: clear liquid; optical method; diameter of observed field = 32 mm.)

Fig. 7. Solidifies cellules at the surface of a plate of wax. (Experiment of C. Dauzère).

Fig. 8. Spontaneous eddies in chains in a layer of spermaceti in a movement of translation. (Bénard's experiment).

Fig. 11(a,b,c,d,e). Development of eddies of two dimensions in a layer of air. (Visualisation by tobacco smoke).

Fig. 12 (a,b) Eddies of two dimensions in a layer of air saturated with water vapor. (Visualisation by deposits of condensed water vapor).

Fig. 13. Development of deposits of condensed water vapor under moderate heating.

Fig. 14. Development of condensed water vapor under more active heating. (Continuous cloudy layer).

Fig. 23-a. Light depressions at the surface of the layer of smoke.

Fig. 23-b. Tobacco smoke forming a network of polygons. This and the preceding show the appearance of cellular eddies in gasses.

Fig. 26. Experimental transformation of polygonal eddies into eddies in vermiculated bands in a layer of air heated from below. (The smoke concentrated in crests with sharp edges shows the places of rising currents.)

Fig. 27. Eddies in vermiculated bands in air. (The smoke concentrated in sharp crests indicates the places of ascending currents.)

Fig. 28. Eddies in vermicular bands in air. (The smoke is diffused.)

Fig. 29. Spontaneous cellular eddies in a layer of spermaceti heated from below. Bénard: method using heavy particles deposed in little heaps at the center of each cellule; square = 1 cm^2.

Fig. 30. Cellular eddies in a layer of smoke heated from below. Thickness of layer h = 20 mm; width of the pictured area: 320 mm.

Fig. 31. Cellular eddies in a layer of smoke heated from below. Thickness of layer h = 20 mm. Width of area viewed 410 mm.

Fig. 34. Eddies in transversal bands in the midst of a smoke layer moving uniformly and heated from beneath. Commencement of their appearing.

Fig. 35. The same eddies in transversal bands; more advanced development.

Fig. 37. A dense layer of smoke penetrates the experiment chamber. The front, at first straight, (a) becomes indented (b) and (c); from each hammock between the teeth a pair of eddy-rolls derives (d).

Fig. 39. Experimental development of eddies in longitudinal bands. 1st phase: lengthwise depressions appear on the surface of the smoke.

Fig. 40. Development of longitudinal eddies. 2nd phase: The smoke accumulated in sharp crests shows where currents ascend.

Fig. 41. Development of longitudinal eddies in bands, 3rd phase: The smoke has diffused inside the rolls; their aspect becomes opaque.

Fig. 42. Development of longitudinal eddies in bands. 4th phase, thanks to the progressive dispersion of the smoke the rolls become transparent.

Fig. 43. Eddies in longitudinal bands. Initial phase; an injection of smoke makes the internal helicoidal movement again visible; the number of gimlets penetrating is that of the eddy-rolls in the layer of pure air.

Fig. 44. Eddies in longitudinal bands. Later phase; The smoke fills the rolls; they are opaque and enveloped in sheaths of pure air.

Fig. 46. Experimental transformation of polygonal cellules into longitudinal bands, by the setting in motion of a layer of air heated from below. Thickness of the layer h = 20 mm.

Fig. 47. Experimental transformation of polygonal cellules into longitudinal bands. The trajectories inside the rolls are plainly visible. Thickness of layer; h = 20 mm.

Fig. 50. Cellular eddies in very slow translation. Thickness of the layer h = 20 mm.

Fig. 51. Unstable cellular eddies in slow translation. Downstream one sees the cellules transforming into longitudinal bands. Thickness of layer, h = 30 mm.

Fig. 52. Experimental transformation of polygonal cellules into transversal bands in a gaseous layer in motion ahd heated beneath. Thickness of the layer h = 20 mm.

Fig. 53. Same transformation of polygonal cellules into transversal bands, same conditions. Thickness of layer h = 25 mm.

Fig. 54. Coexistence of longitudinal bands and transversal bands in a gaseous layer in motion heated from below. Thickness of layer h = 10.5 mm.

Fig. 56. Eddies in undulated bands obtained by slowing-up of the eddies in straight bands. The partitions where currents ascend stay straight, those where currents descend become undulated. Thickness of layer h = 40 mm.

Fig. 57. Another case of eddies in undulated bands obtained by slowing up. Two rolls, 4 and 7 intercalate themselves, having constant width, between the rolls of the preceding case. Thickness of the layer h = 30 mm.

Fig. 58. Another variety of eddies in undulated bands; alternative succession of sinusoidal bands of equal width and bands that consist of a succession of alternated swollen and shrunken regions. Thickness of layer h = 30 mm.

Fig. 59. Another case of eddies in undulated bands; group of 8 straight rolls accompanied by a group of 8 undiluted rolls. Thickness h = 30 mm.

Fig. 62. Eddies in twisted columns; undulation provoked by a very high difference of temperature extremes of the gaseous layer heated beneath. Concentrated smoke. Speed of translation: $V \simeq 6$ cm/s. Thickness of layer h = 30 mm.

Fig. 64. Eddies in twisted columns: undulation provoked by a high difference of temperature extremes. Smoke almost used up. Speed of translation $V \simeq 8$ cm/s. Thickness of layer h = 30mm.

Fig. 65. Eddies in twisted columns: undulation provoked by a very high difference of temperature extremes. Smoke all but exhausted; speed of translation $V \simeq 3$ cm/s. Thickness h = 35 mm.

Fig. 70. Eddies in longitudinal bands. Geometric measurements: Thickness of layer h = 20 mm. Width of canal L = 352 mm. Number of rolls n = 16.

Fig. 71. Eddies in longitudinal bands. Geometric measurements: Thickness h = 30 mm. Width L = 308 mm. Number of rolls n = 6.

Fig. 72. Eddies in longitudinal bands. Geometric measurements: Thickness h = 40 mm. Width L = 335 mm. Number of rolls n = 6.

Fig. 73. Eddies in longitudinal bands. Geometric measurements:

Fig. 73(cont) Thickness h = 50 mm. Width L = 285 mm. Number of rolls n = 4.

Fig. 74. Eddies in longitudinal bands: case of an odd number of rolls (21). One of the two marginal rolls presents a structure significant of progressive disappearance. Thickness of layer h = 15 mm. Width L = 330 mm. Number of rolls n = 21.

Fig. 75. Same experiment of eddies in longitudinal bands; one sees here disappearing the last trace of the superfluous roll. The system of 20 rolls will reestablish itself. Thickness h = 15 mm. Width L of canal = 330 mm. Number of rolls n = 20.

Fig. 76. Variant of the experiment of the eddies in longitudinal bands; at the start, 19 rolls took shape. The twentietn is now taking shape. Thickness h = 15 mm. Width L = 330 mm. Number n = 19.

Fig. 79. Normal production of 4 longitudinal rolls in a layer of air in translation heated from below. Thickness h = 40 mm. Width of canal L = 200 mm.

Fig. 80. By placing at the entry of the experiment chamber two little obstacles, a and b, one provokes six longitudinal rolls. Thickness h = 40 mm. Width L = 200 mm.

Fig. 81. By placing at the entry of the experiment chamber three little obstacles, a, b and c, one provokes first 8 longitudinal rolls which transform themselves into 6. Thickness of the layer h = 40 mm. Width L = 200 mm.

Fig. 83. One contrives by imposing particular initial conditions, to reduce the normal number of rolls. In the figure, production of two rolls instead of four. Thickness h = 40 mm. Width L = 200 mm.

Fig. 86. Experimental augmentation of the number of rolls by bifurcation. Thickness h = 40 mm. Width L = 335 mm.

Fig. 87. Experimental imposition, at the entry of the experiment chamber, of a number of rolls greater than the natural number of rolls. Thickness h = 30 mm. Width L = 308 mm.

Fig. 106. Helicoidal trajectories of eddies in longitudinal bands: smoke was injected in small doses. Thickness h = 35 mm. Width of canal L = 345 mm.

Fig. 108. Experimental helicoidal trajectories of eddies in longirudinal bands. Visualization by a filament of smoke injected in small doses. Thickness h = 50 mm. Width L = 345 mm.

Fig. 109. Experimental helicoidal trajectories of the marginal rolls: visualized by a filament of smoke injected in small doses. Thickness h = 50 mm. Width L = 330 mm.

Fig. 158. Altocumulus translucidus in balls.

Fig. 159. Cloudy layer fractionated into compartments. Cloud elements are in contact.

Fig. 160. Cloud layer fractionated into compartments. The cloud elements are separated by intervals of blue sky.

Fig. 162. Altocumulus undulatus. The big rolls, that one may judge to be at right angles to the general current, are tattered. Taken at 10:30 at angle of 60°.

Fig. 163. Altocumulus undulatus. The big rolls, that one may judge to be parallel to the general wind, are separated by intervals of blue sky. They jam together towards the horizon under the effect of the perspective. Taken 9:15 N.W. Angle 15°.

Fig. 164. Cirrus radiatus. The bands converge towards the horizon.

Fig. 165. Altocumulus undulatus. Simultaneous cloud organizations along two perpendicular directions! (Pendulum bivalens!) Taken towards the S.W.

Fig. 168. Dimensions of cellular eddies in relation to the dimensions of the deposits of water vapor condensed on the glass panes.

Fig. 169. Electroconvective eddies in a layer of oil submitted to an electric field. Intense current. Thickness of layer h = 2 mm.

Fig. 170. Electroconvective eddies in a layer of oil submitted to a very intense electric field. Thickness of layer h = 5 mm. Distance between the 2 electrodes : d = 28 mm.

Fig. 171. Electroconvective eddies of two dimensions in a layer of oil between two electrodes of straight surfaces.

Fig. 172. Two-dimensional electroconvective eddies in a layer of oil between two concentric circular electrodes. (The picture contains an error 90 mm should be 180 mm.) (Diameter of the electrodes: Exterior $2R_2$ = 250 mm. Interior $2R_1$ = 180 mm.)

Fig. 173. Toroidal electroconvective eddies in oil between two coaxial cylinders. (Cut of the phenomenon visible by a plane of shadow.)

The difference d of the radii of the two cylindrical electrodes: d = 45 mm.

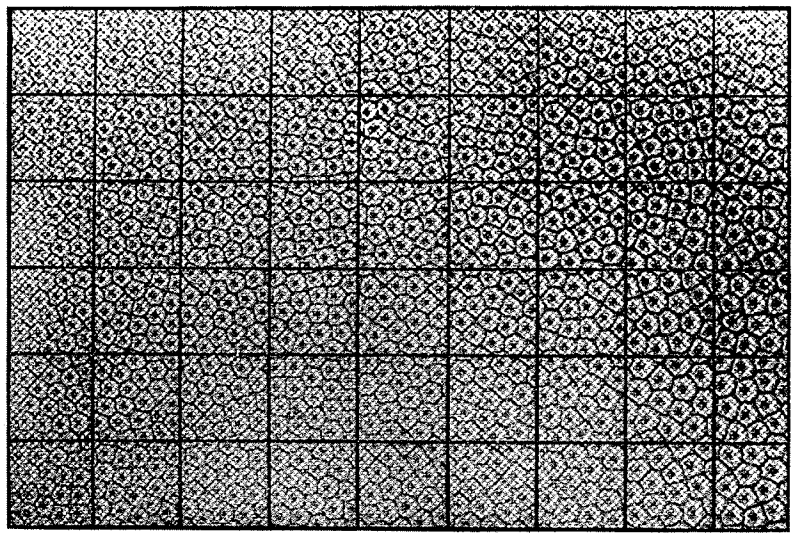

Fig. 2.

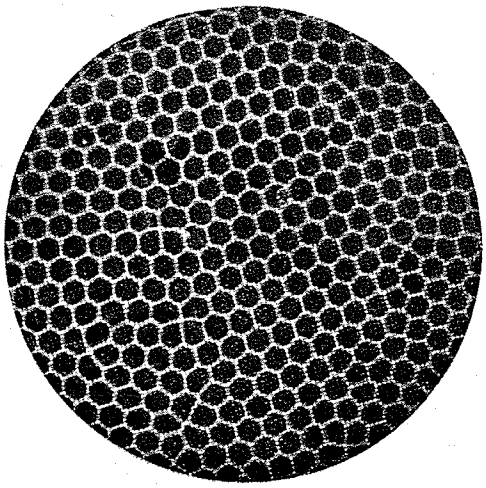

Fig. 3.

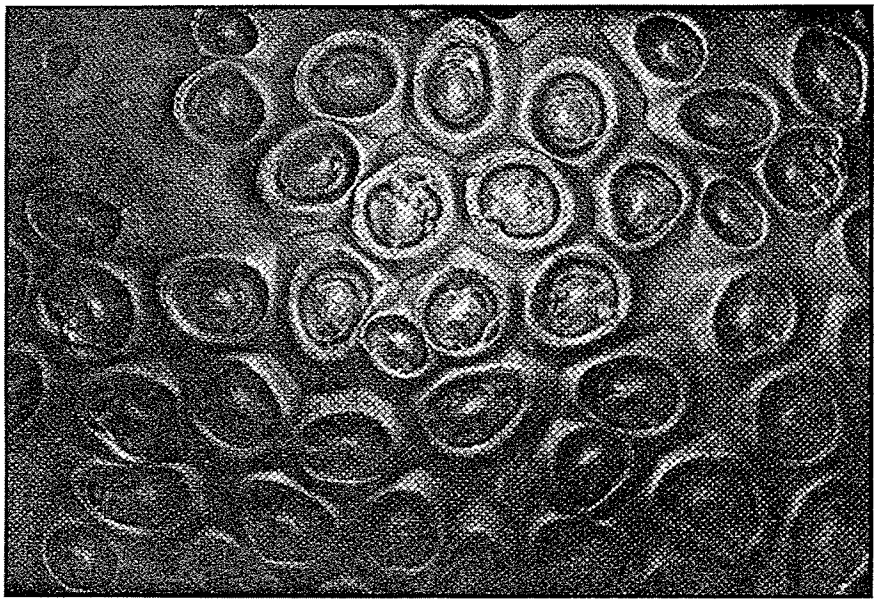

Fig. 7.

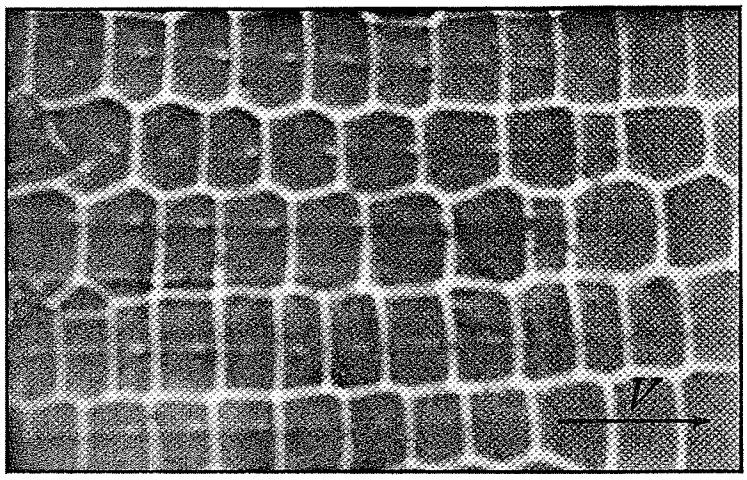

Fig. 8.

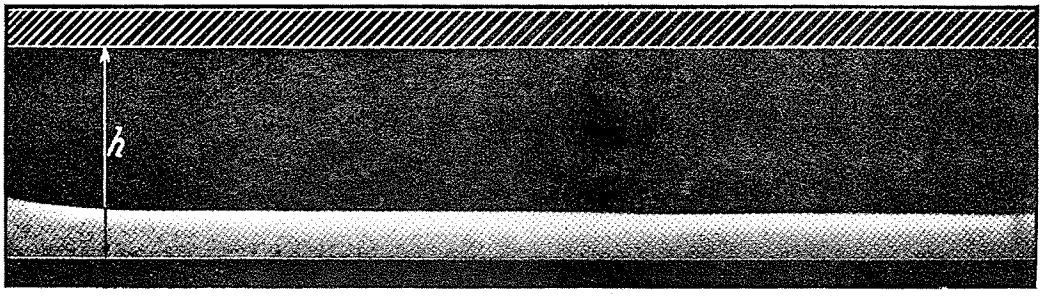

Fig. 11-*a*

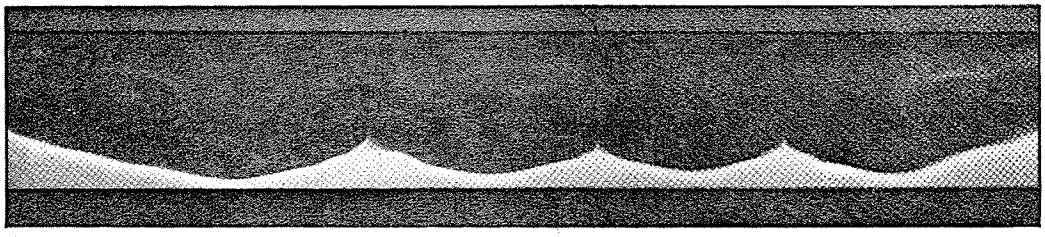

Fig. 11-*b*

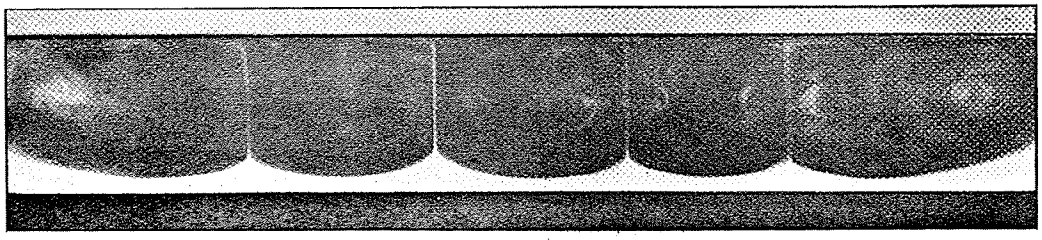

Fig. 11-*c*

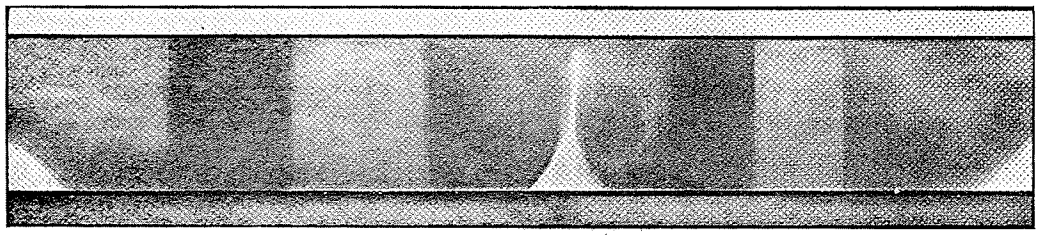

Fig. 11-*d*

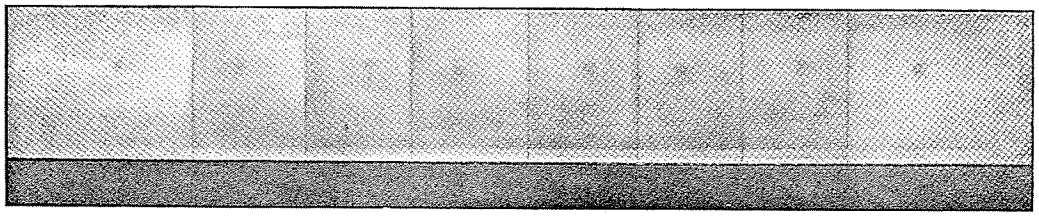

Fig. 11-*e*

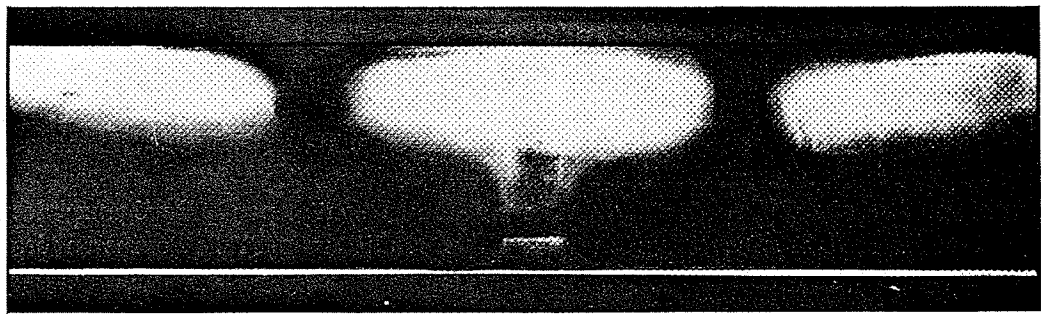

Fig. 12-*a*

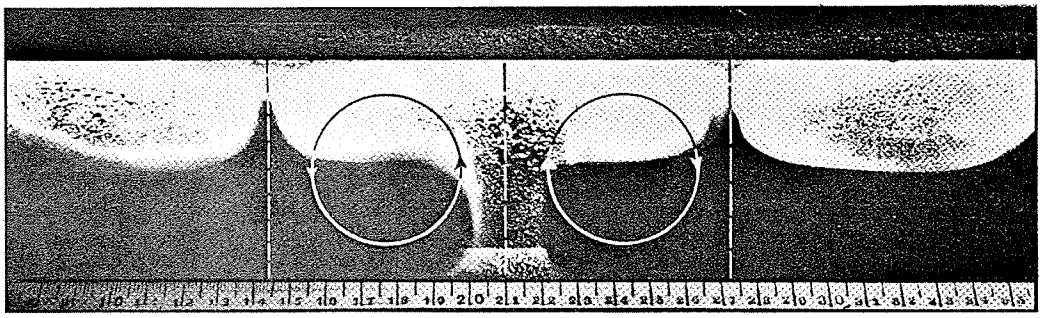

Fig. 12-*b*

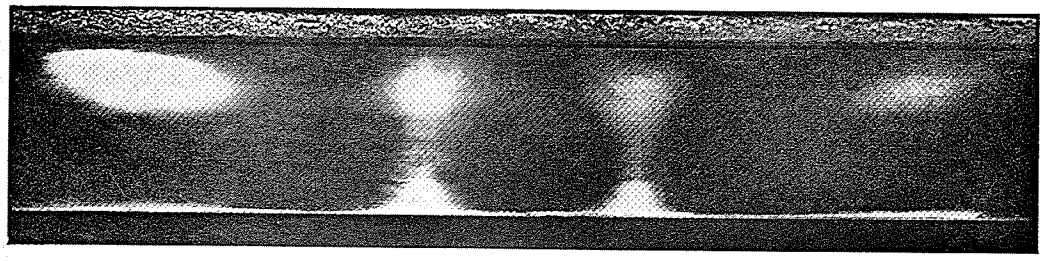

Première phase

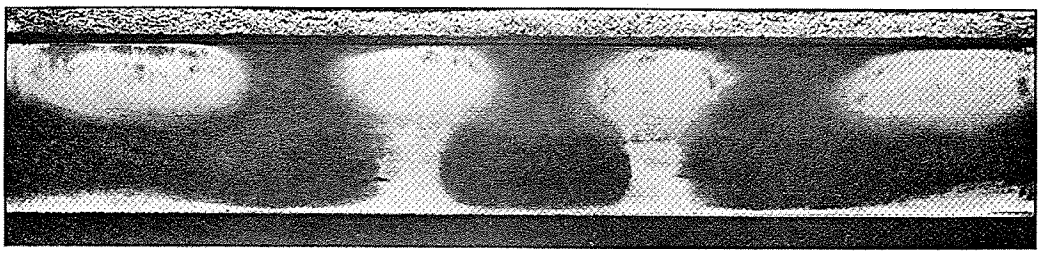

Deuxième phase

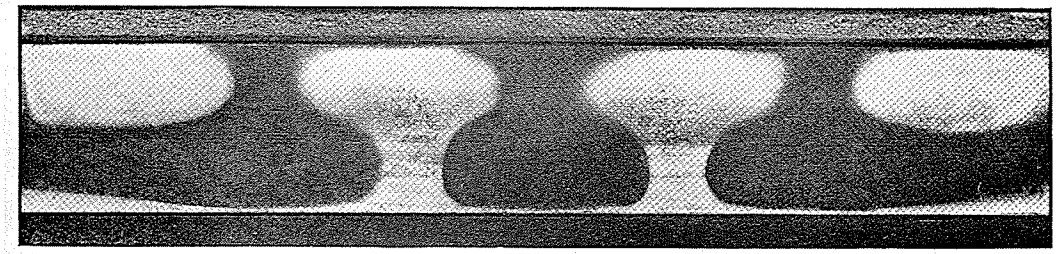

Troisième phase

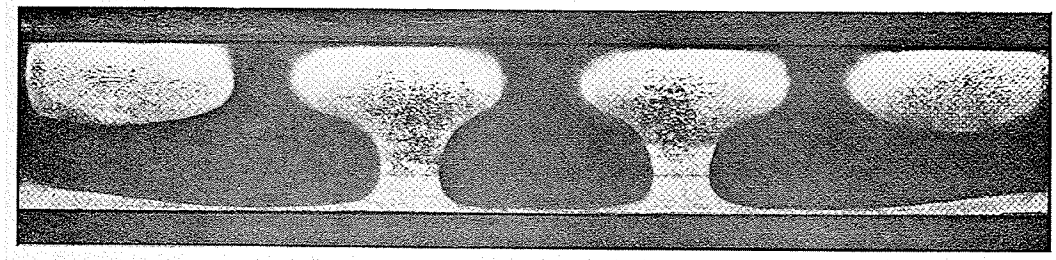

Quatrième phase

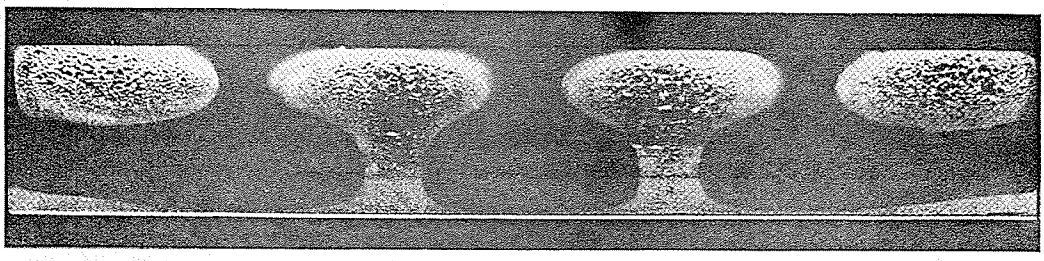

Cinquième phase

Fig. 13.

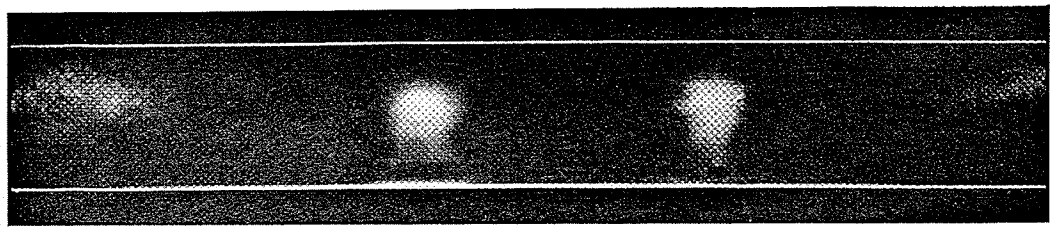

Première phase

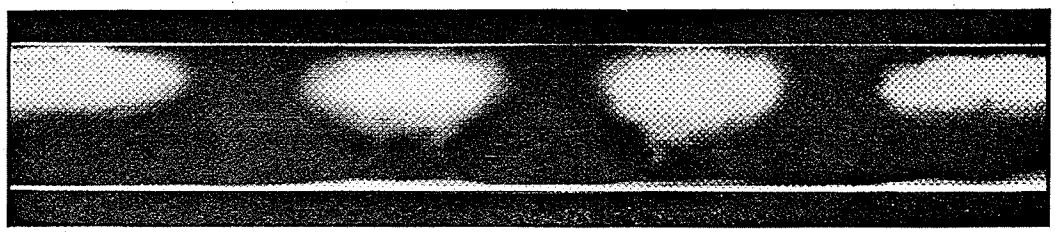

Deuxième phase

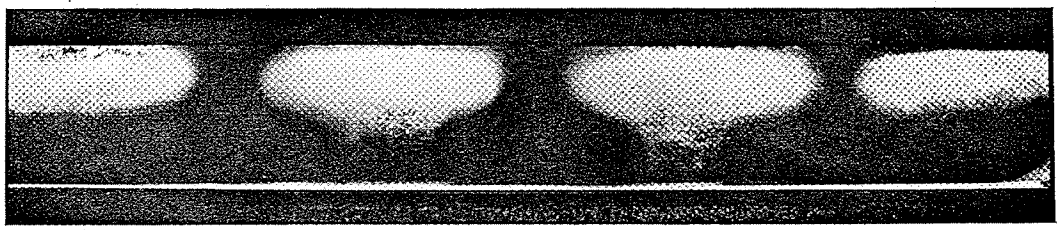

Troisième phase

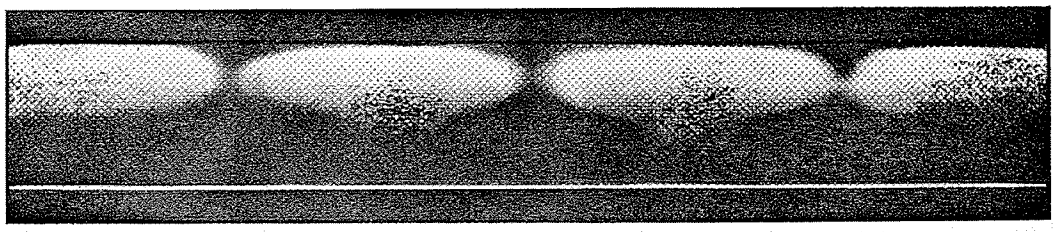

Quatrième phase

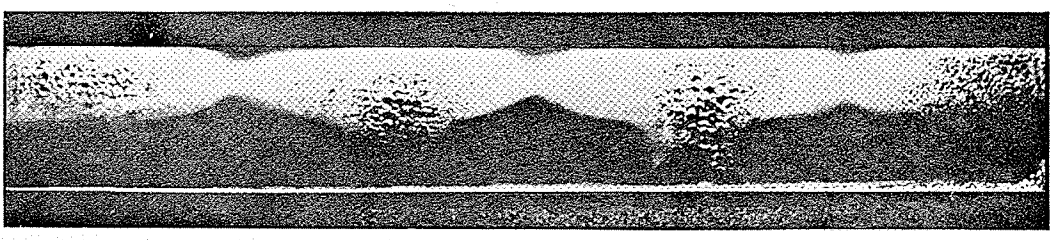

Cinquième phase

Fig. 14.

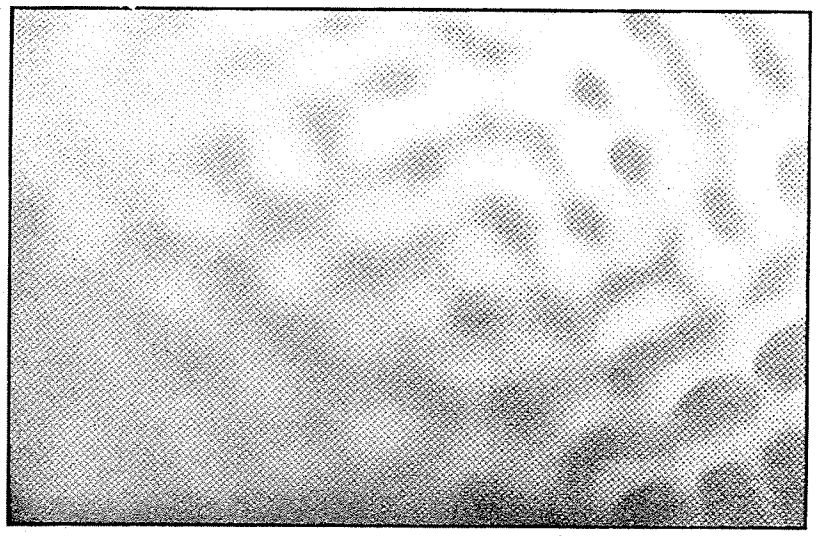

Fig. 23-*a*.

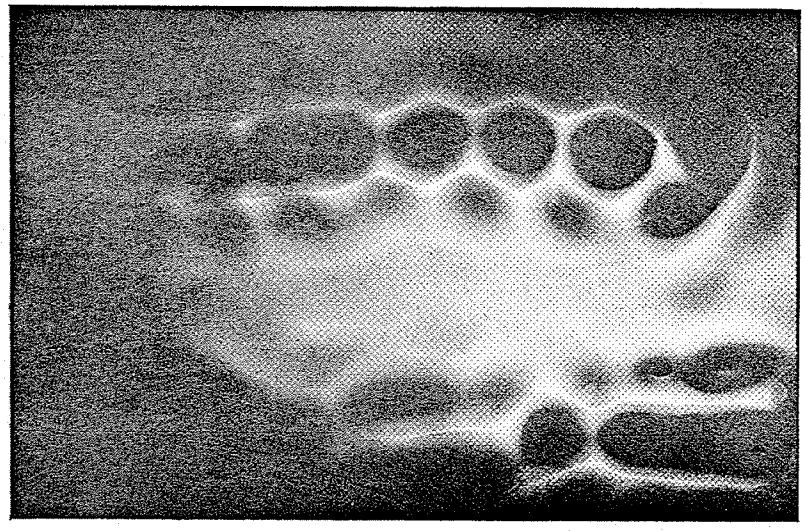

Fig. 23-*b*.

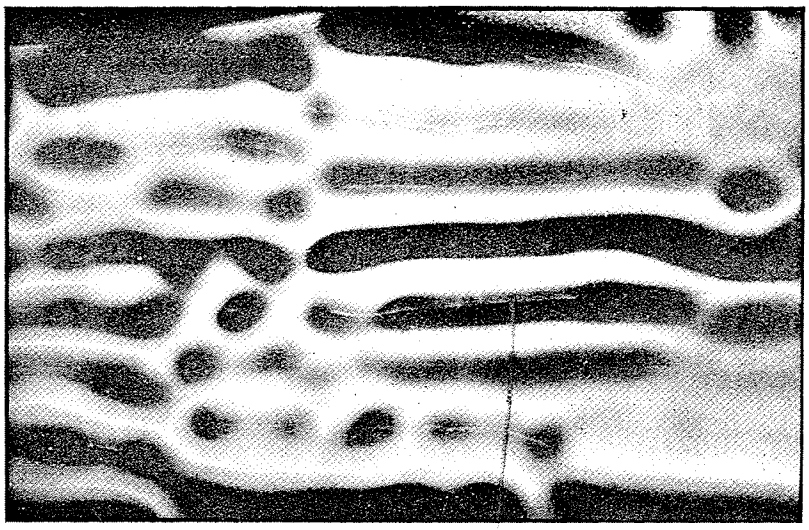

Fig. 26.

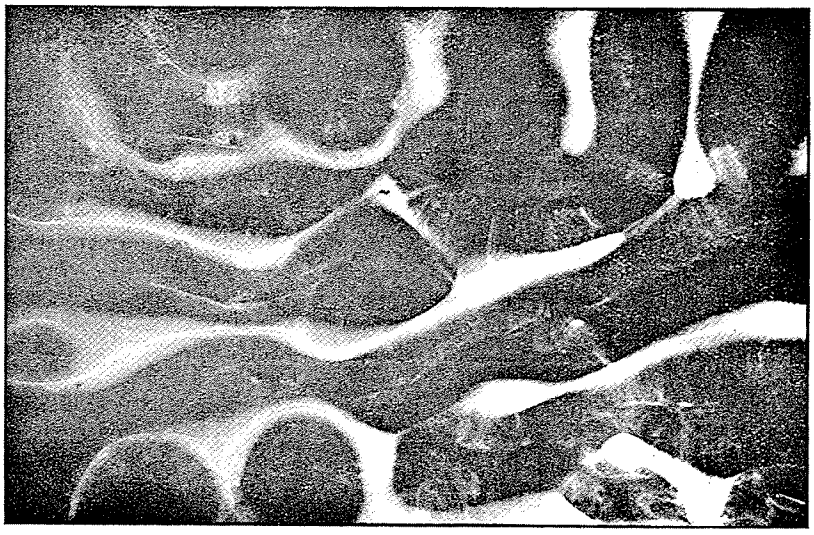

Fig. 27.

Fig. 28.

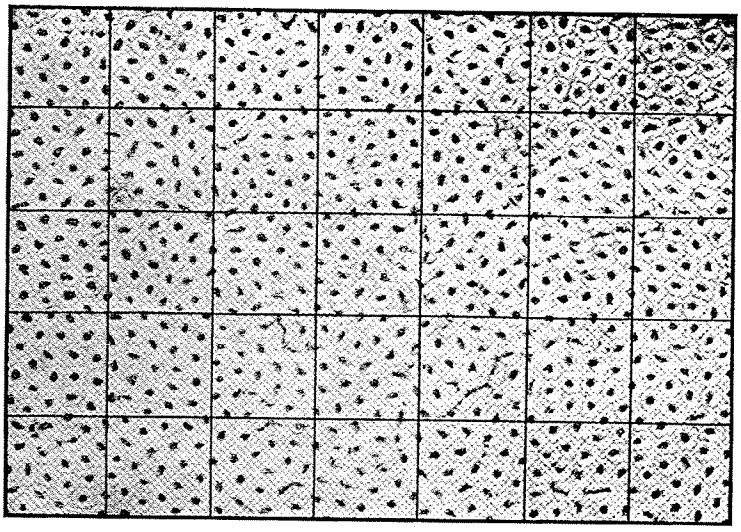

Fig. 29.

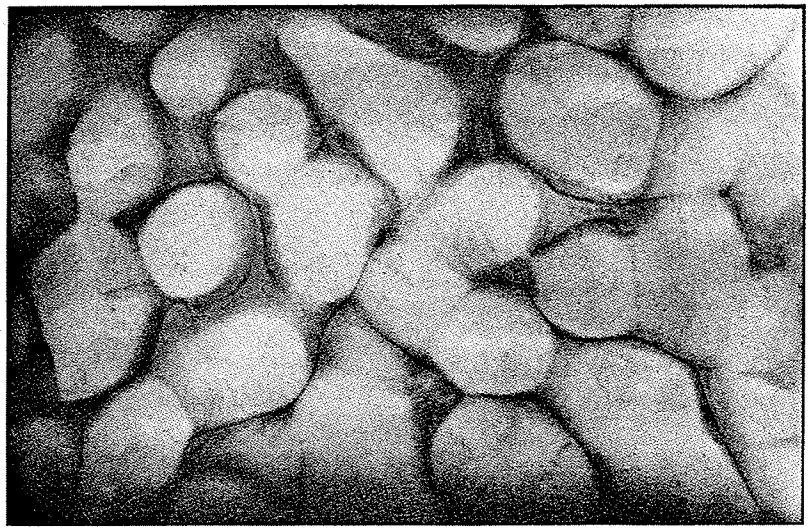

Fig. 30.

Fig. 31.

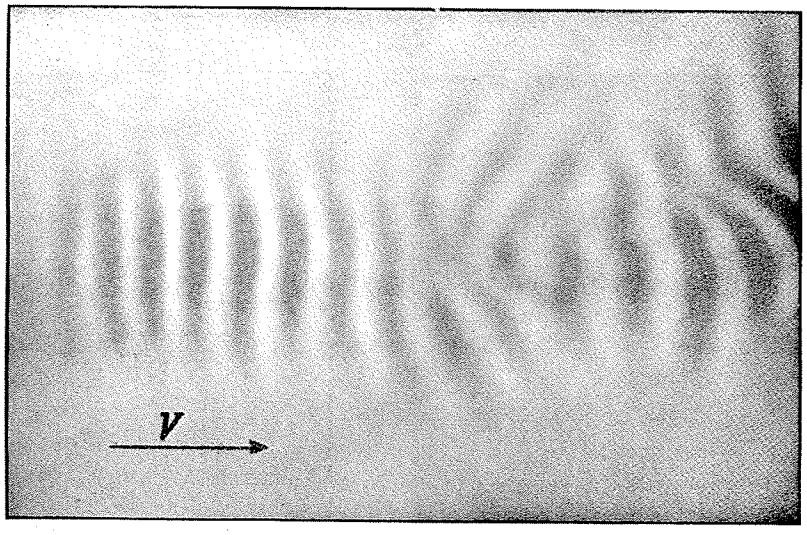

Fig. 34.

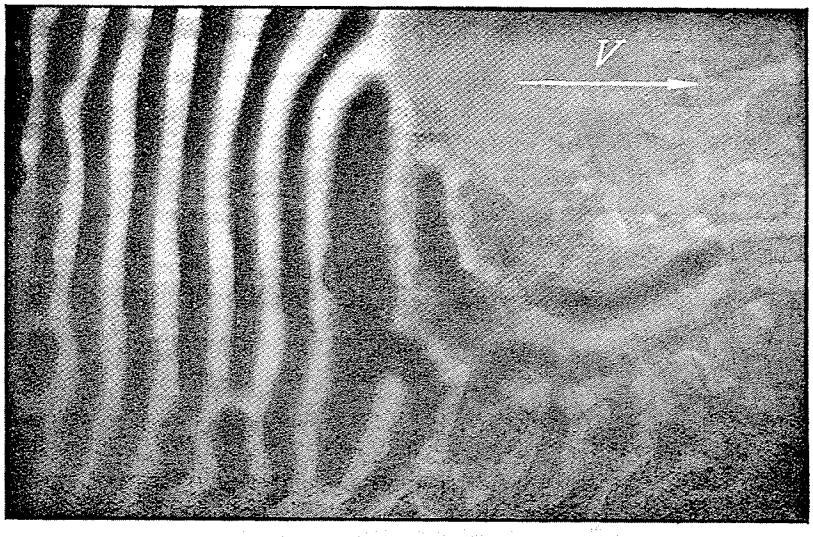

Fig. 35.

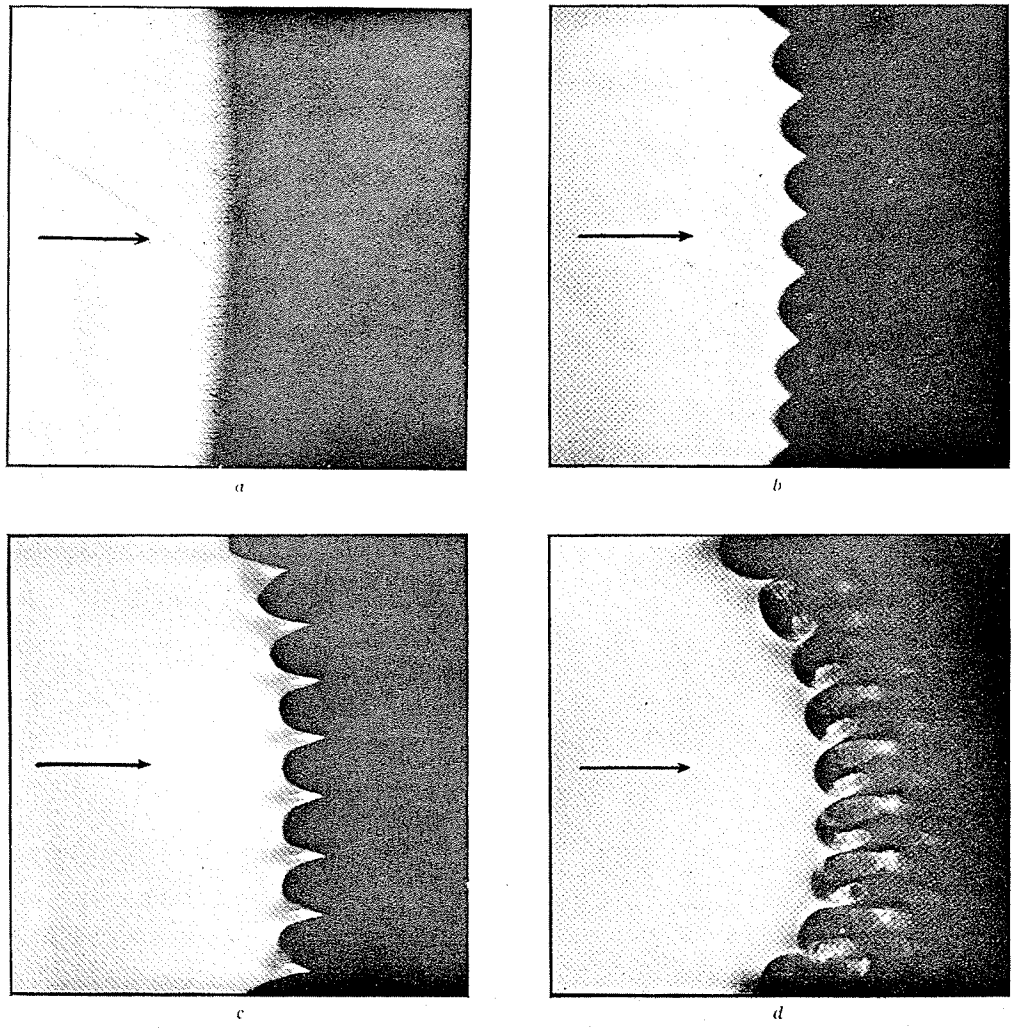

Fig. 37.

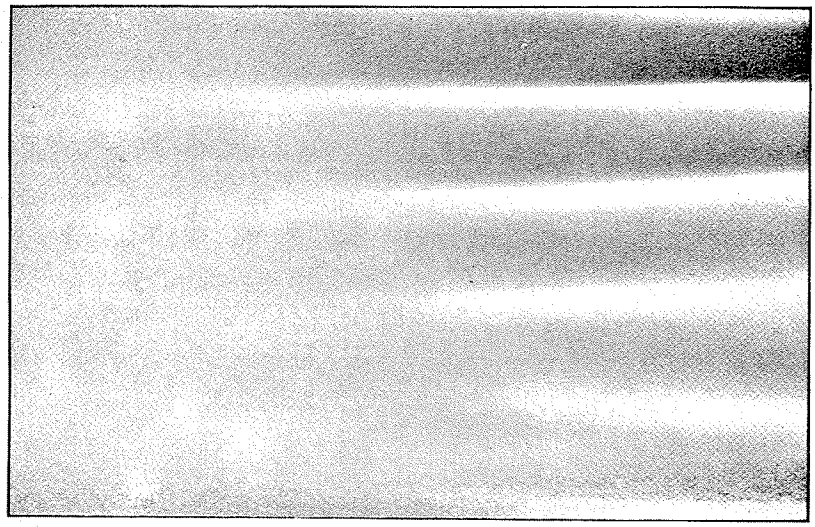

Fig. 39.

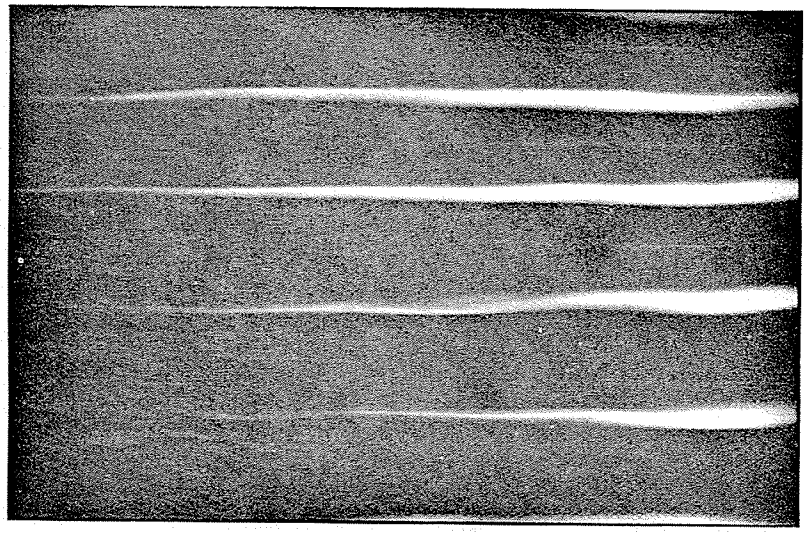

Fig. 40.

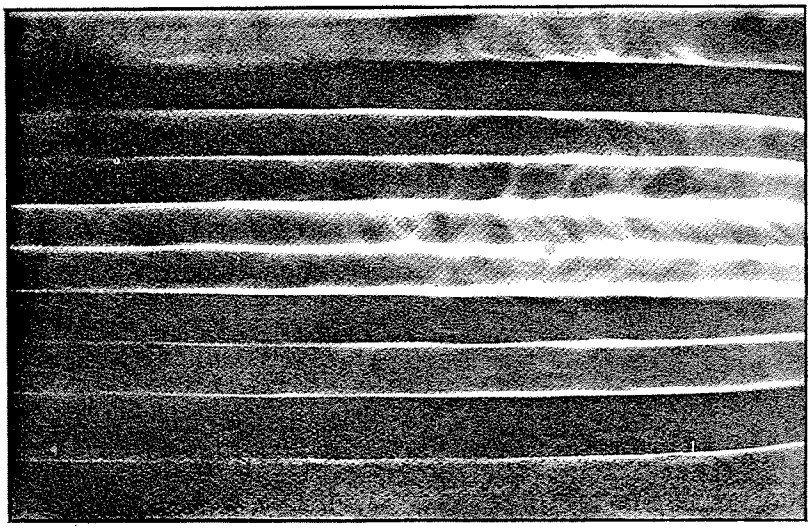

Fig. 41.

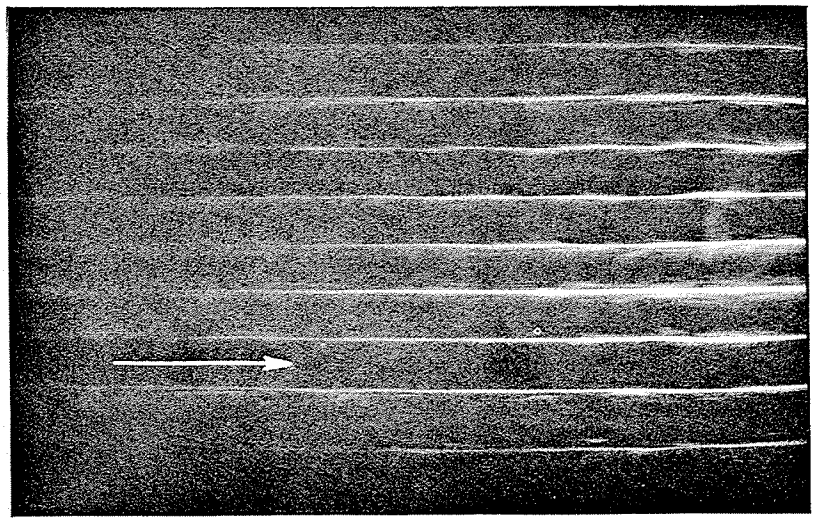

Fig. 42.

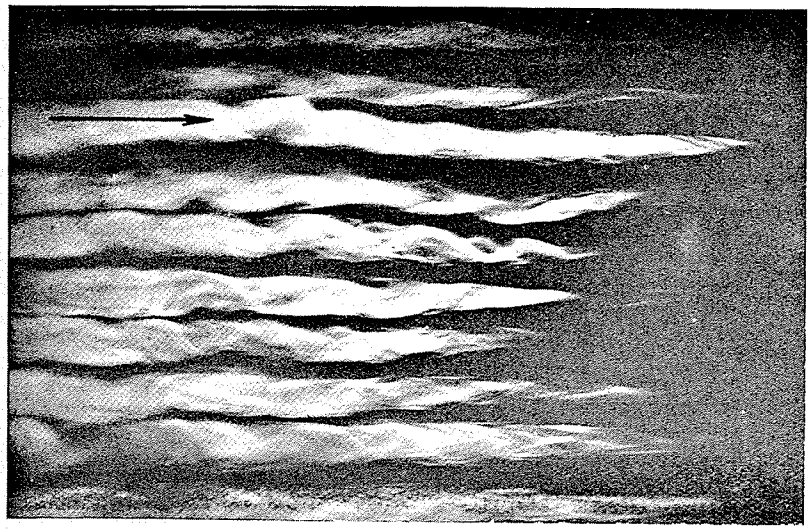

Fig. 43.

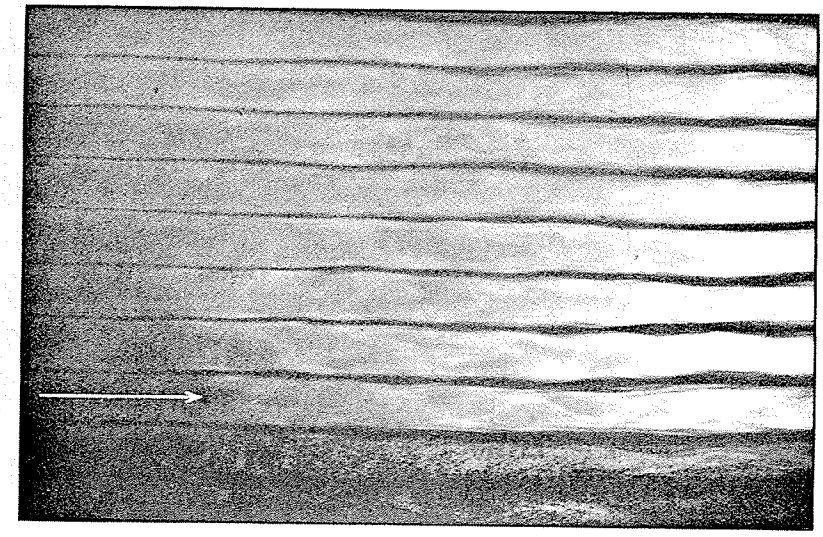

Fig. 44.

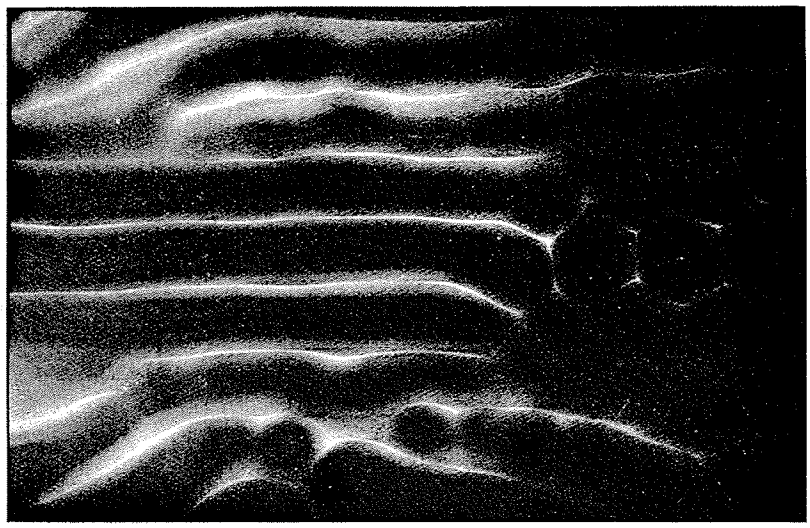

Fig. 46.

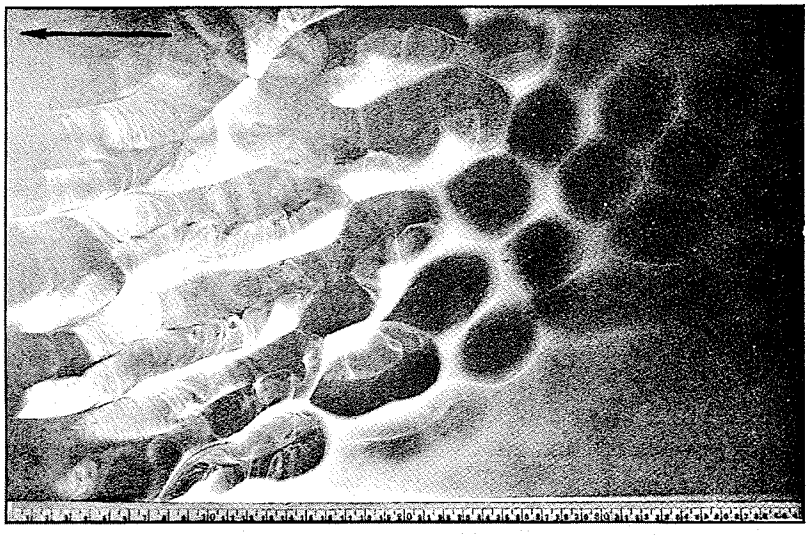

Fig. 47.

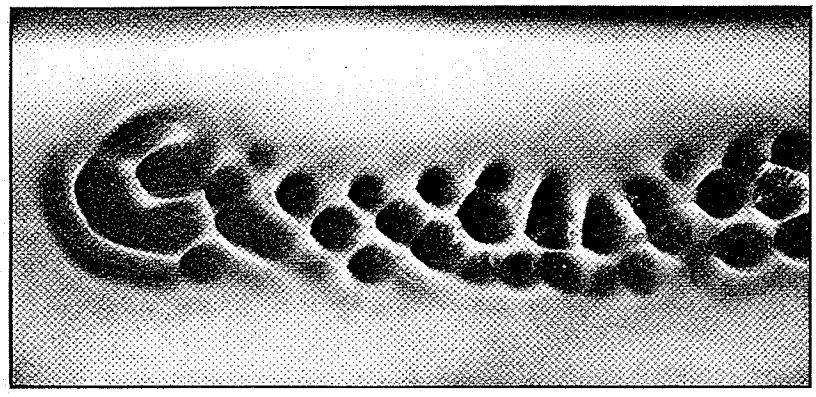

Fig. 50.

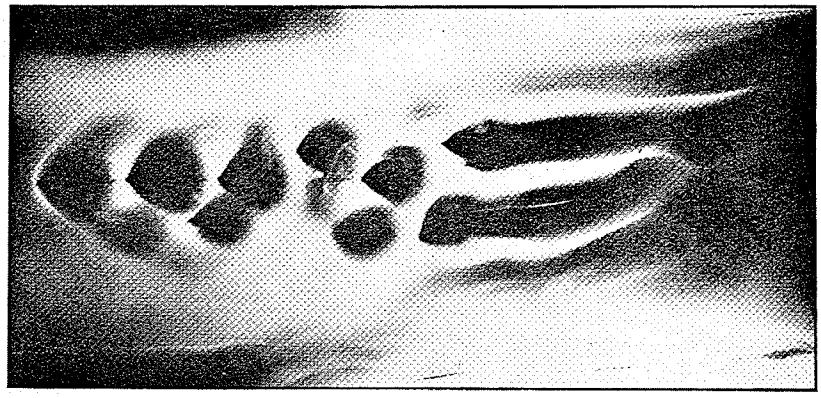

Fig. 51.

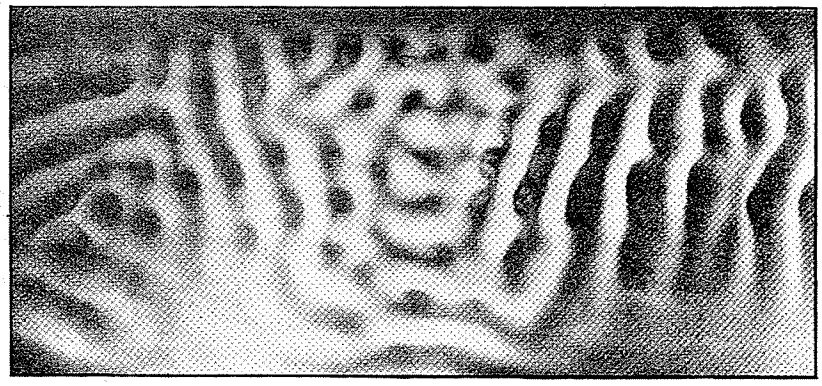

Fig. 52.

Fig. 53.

Fig. 54.

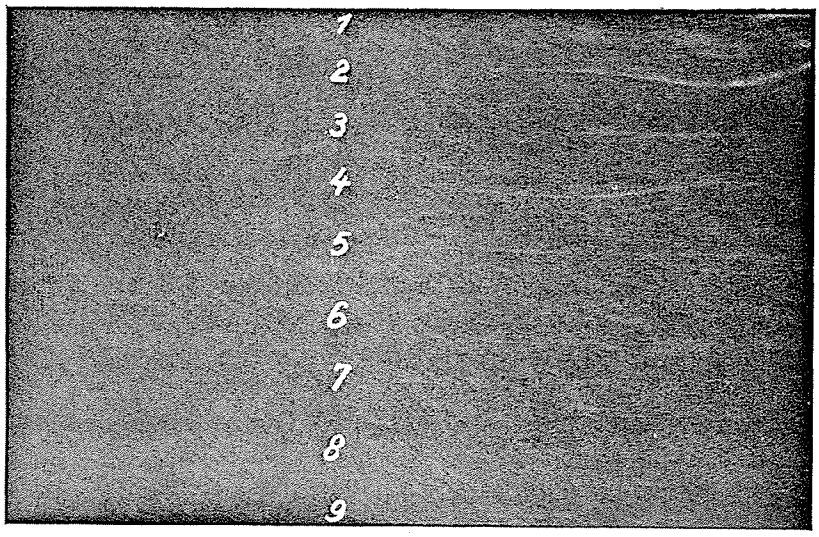

Fig. 56.

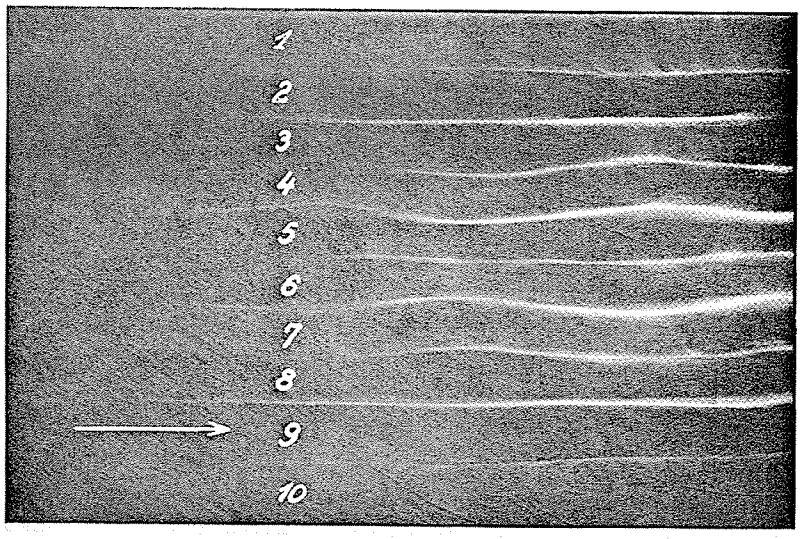

Fig. 57.

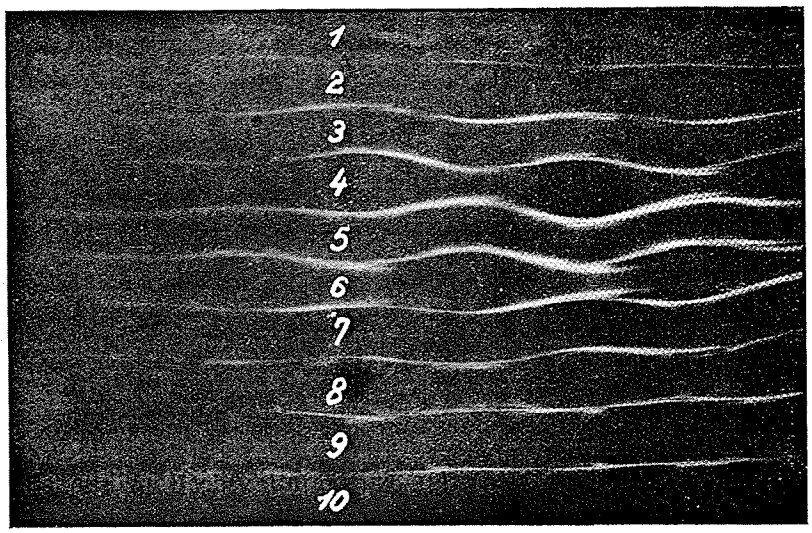

Fig. 58.

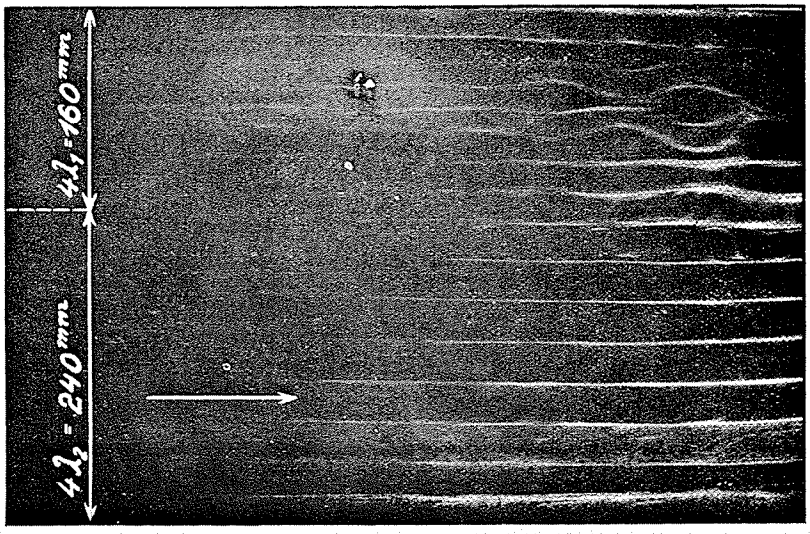

Fig. 59.

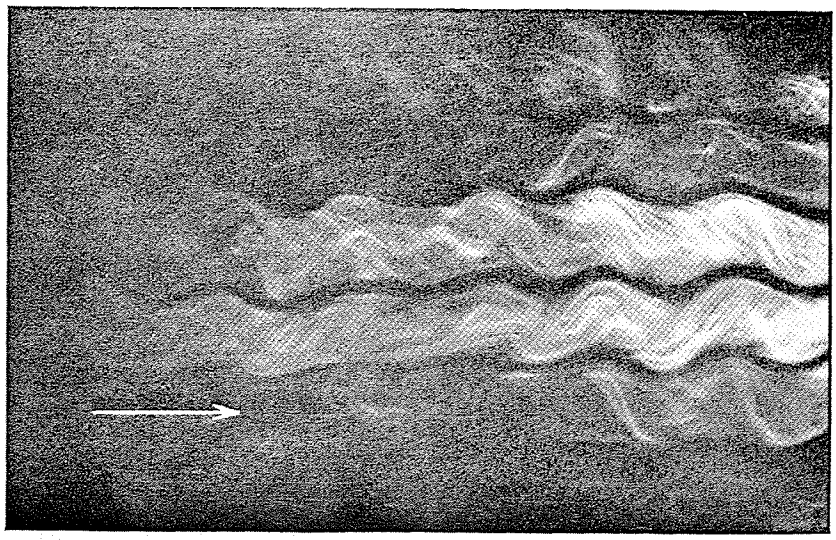

Fig. 62.

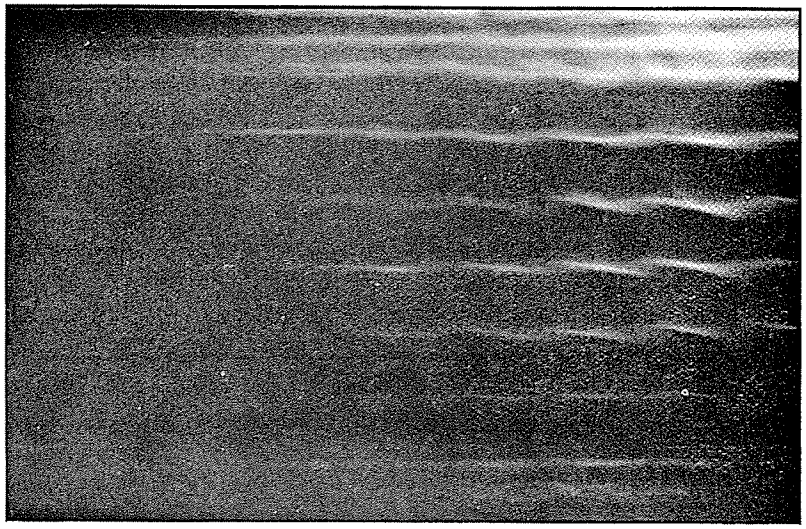

Fig. 61.

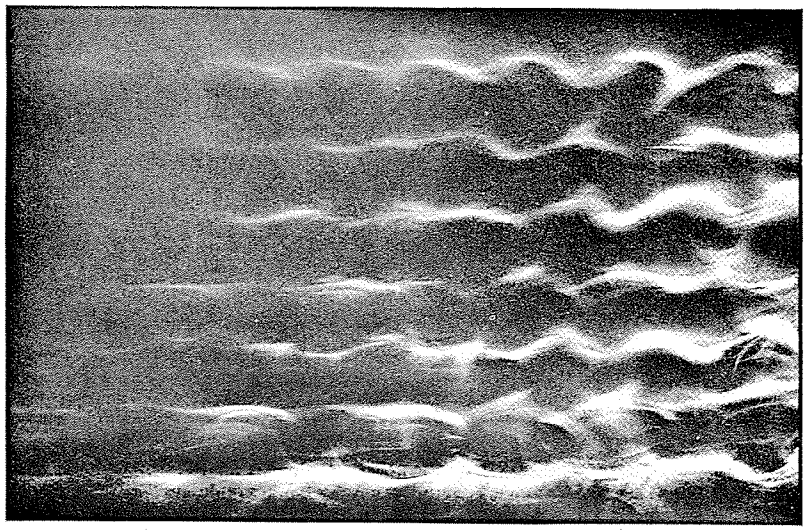

Fig. 65.

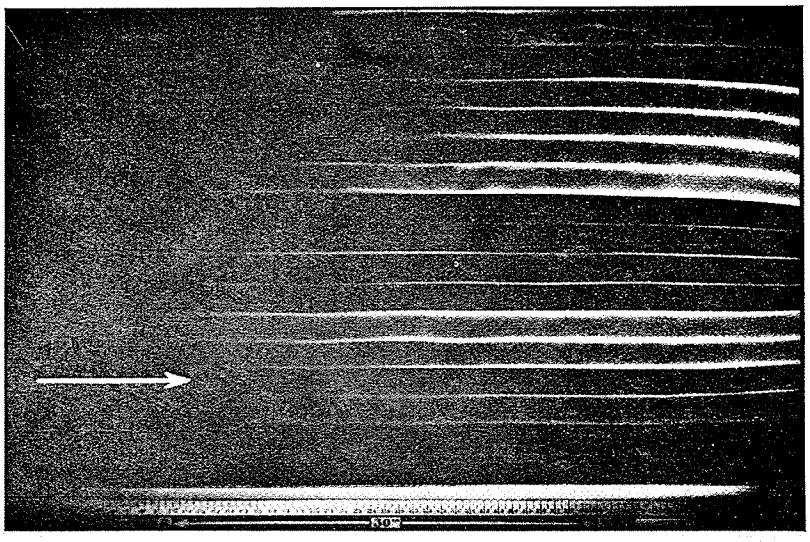

Fig. 70.

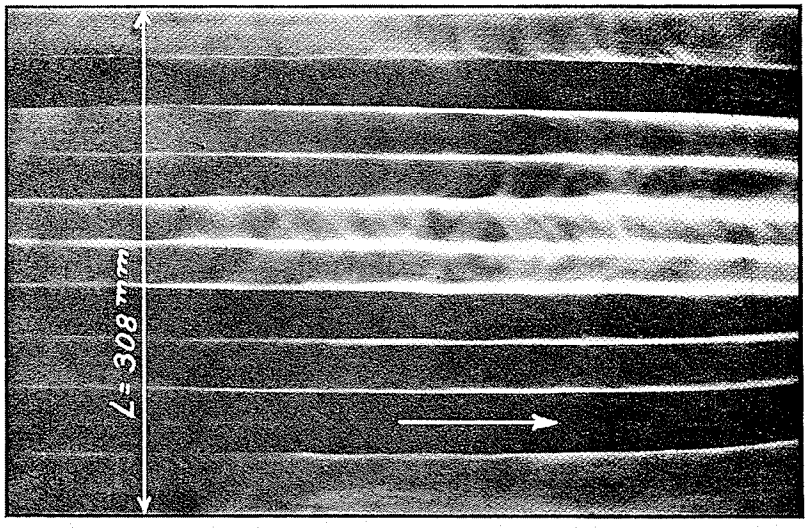

Fig. 71.

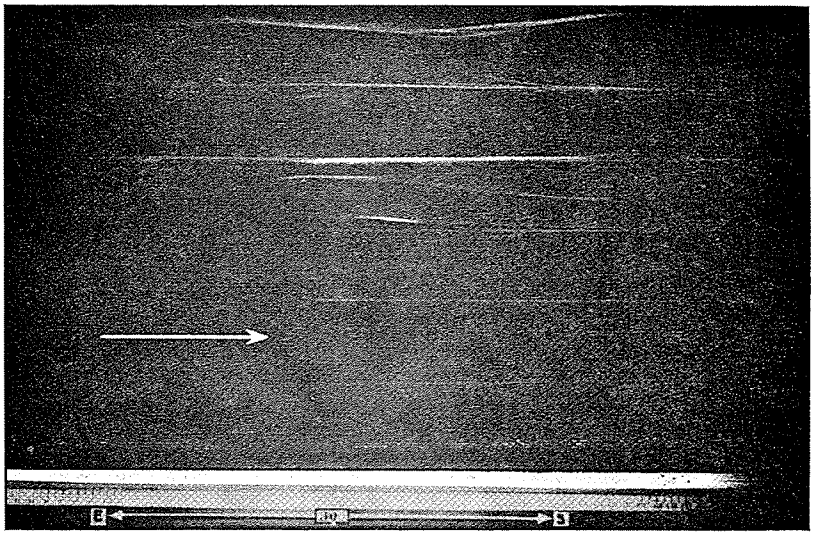

Fig. 72.

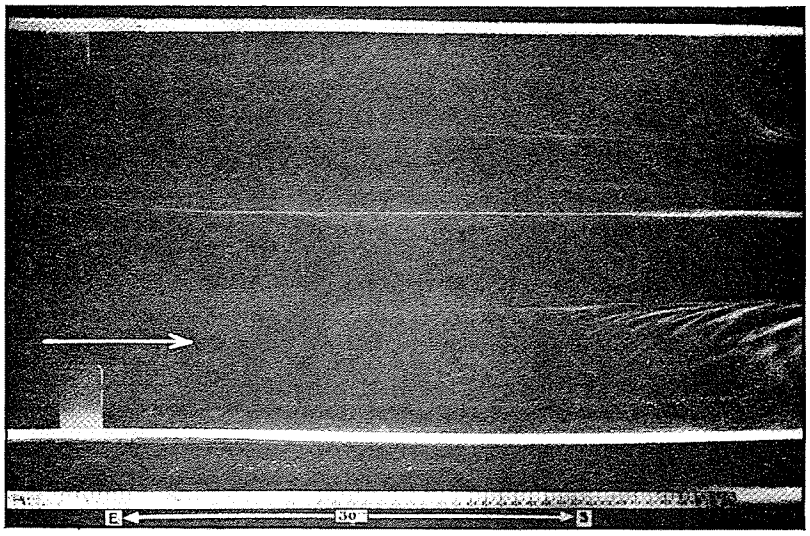

Fig. 73.

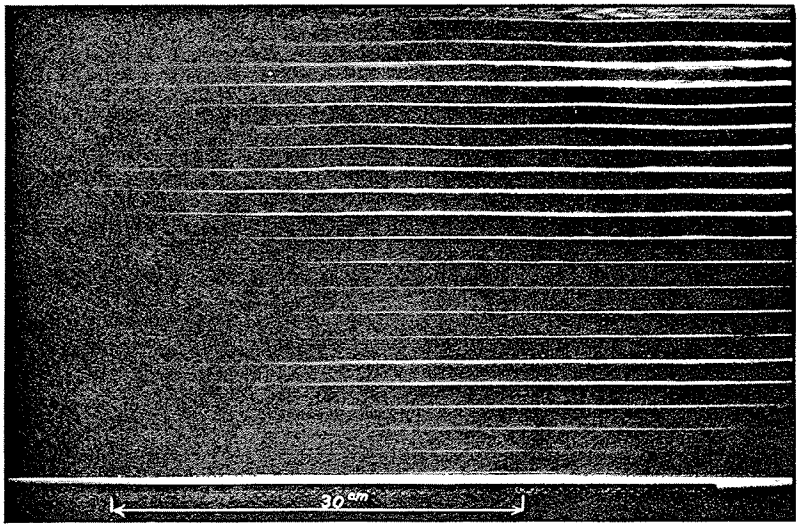

Fig. 74.

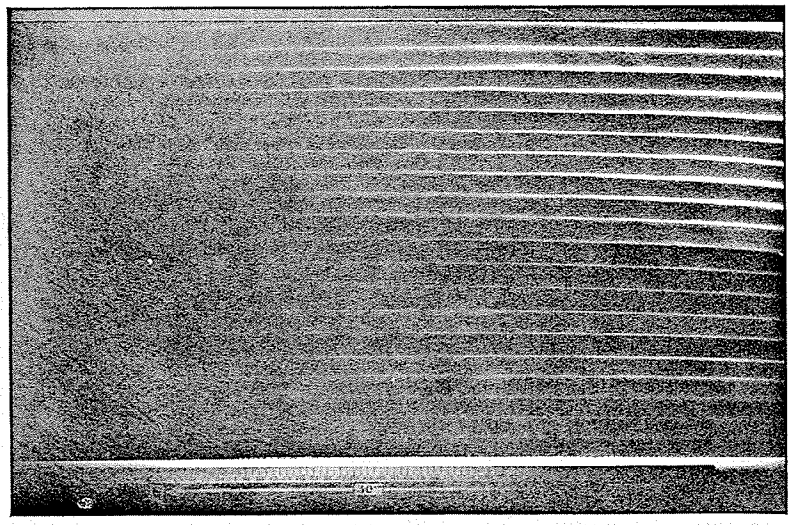

Fig. 75.

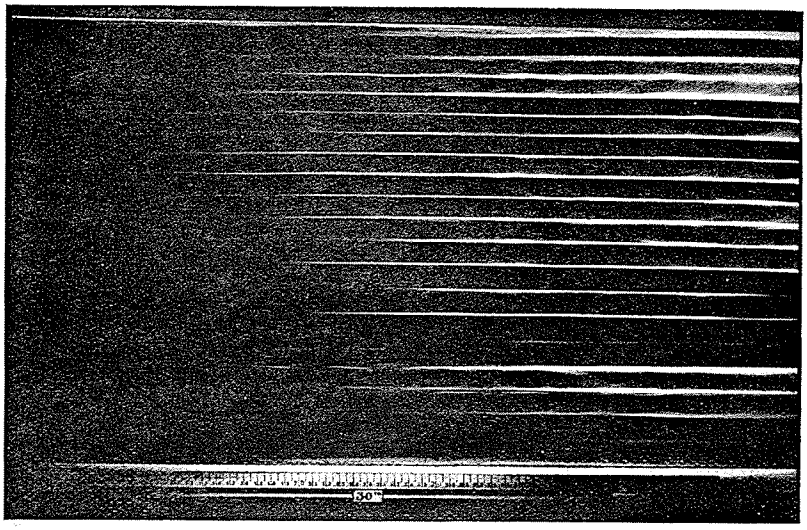

Fig. 76.

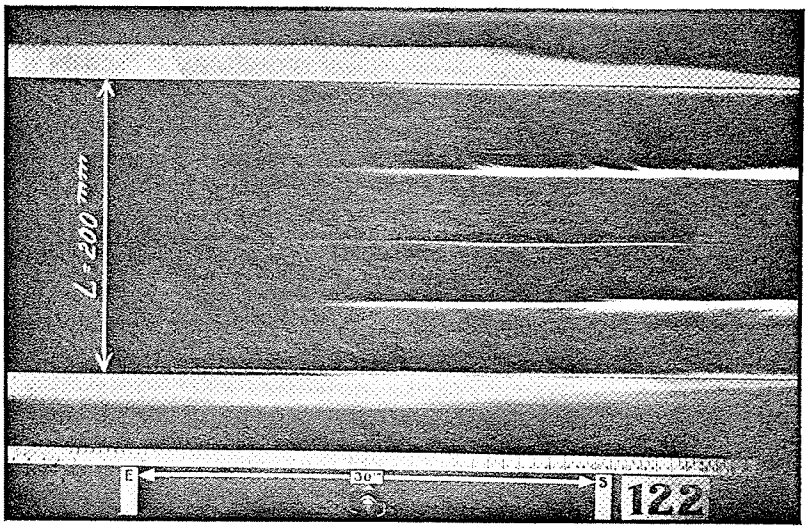

Fig. 79.

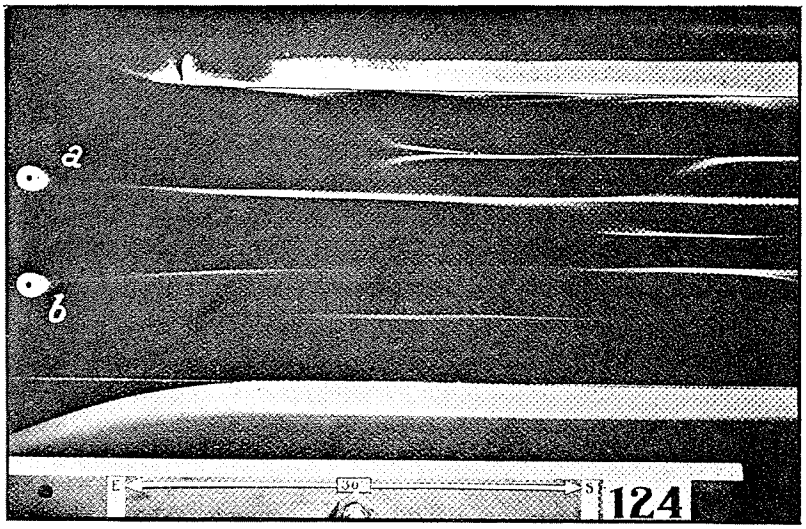

Fig. 80.

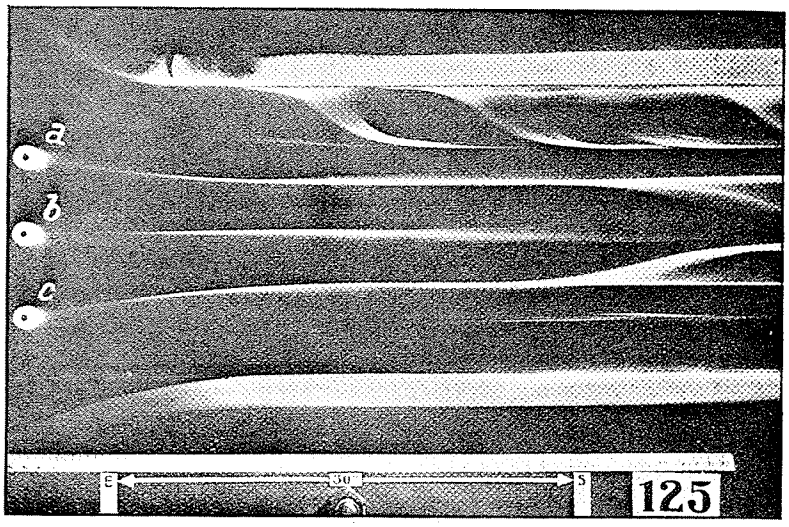

Fig. 81.

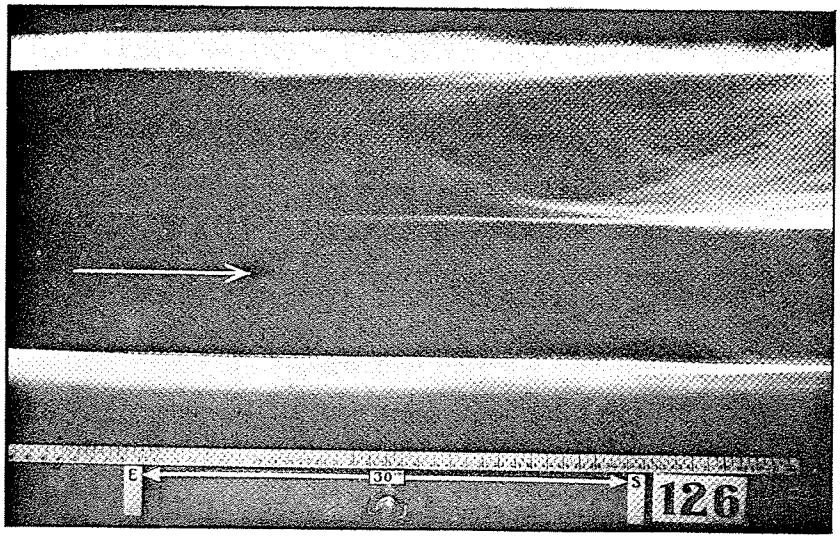

Fig. 83.

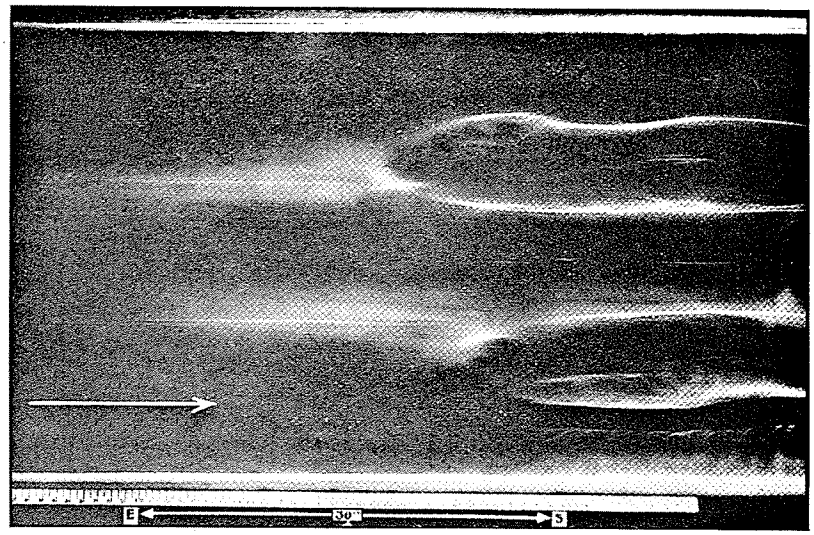

Fig. 86.

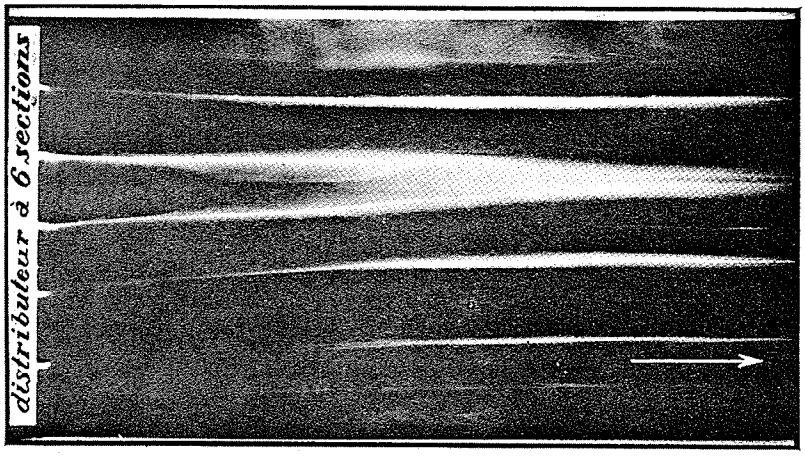

Fig. 87.

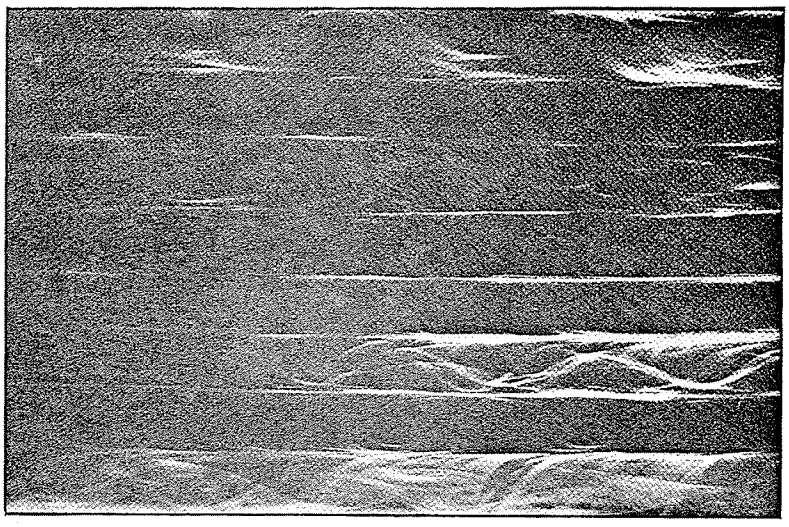

Fig. 106.

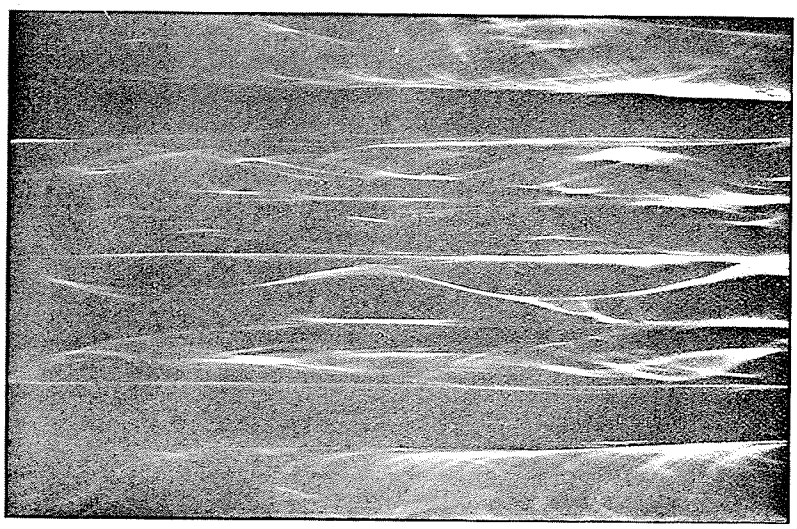

Fig. 108.

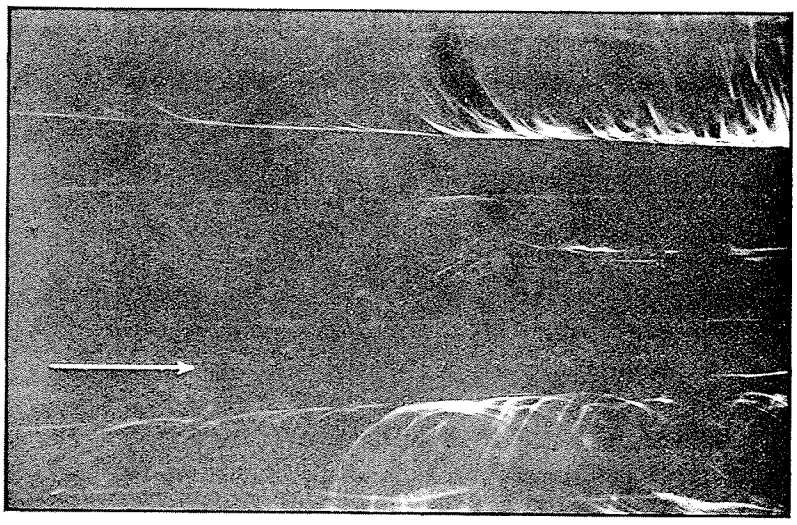

Fig. 109.

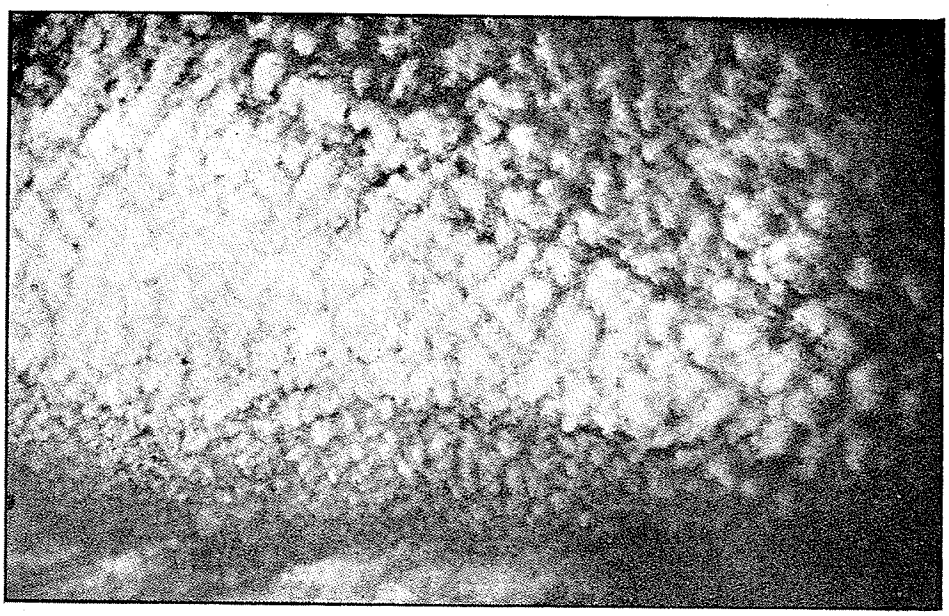

Fig. 158.

Fig. 159.

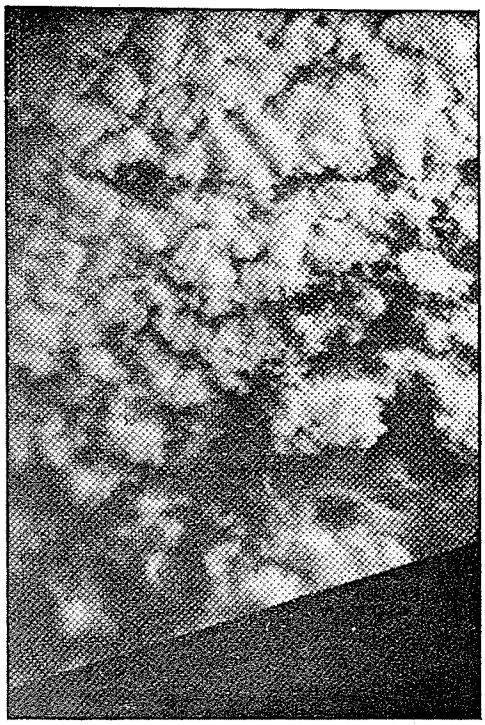

Fig. 160.

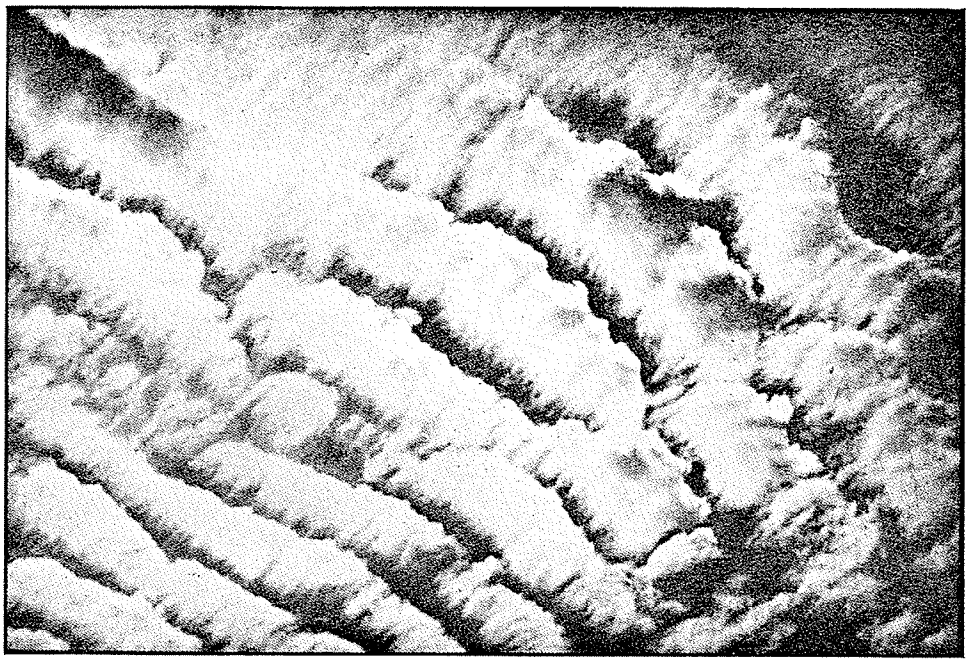

Fig. 162.

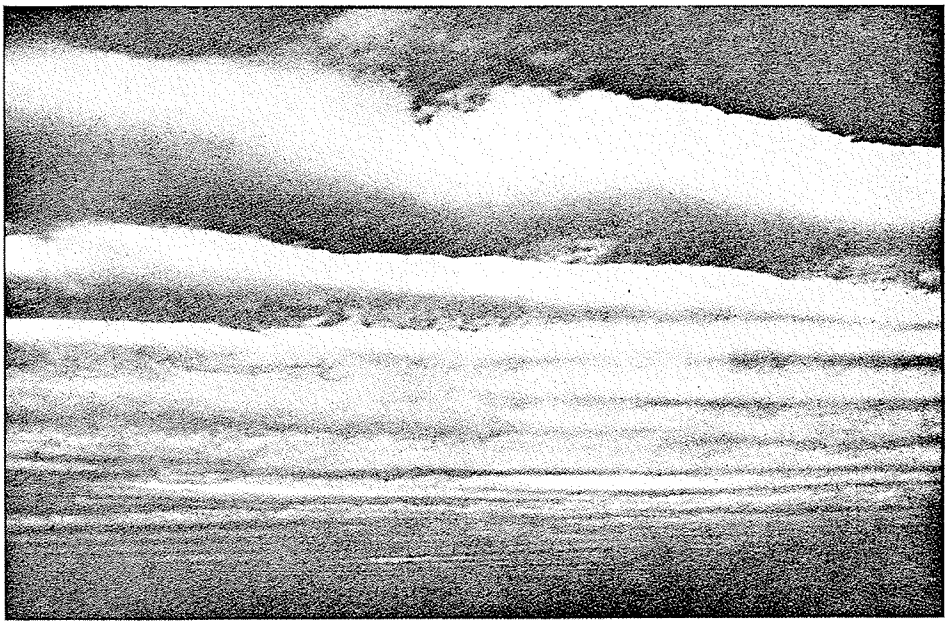

Fig. 163.

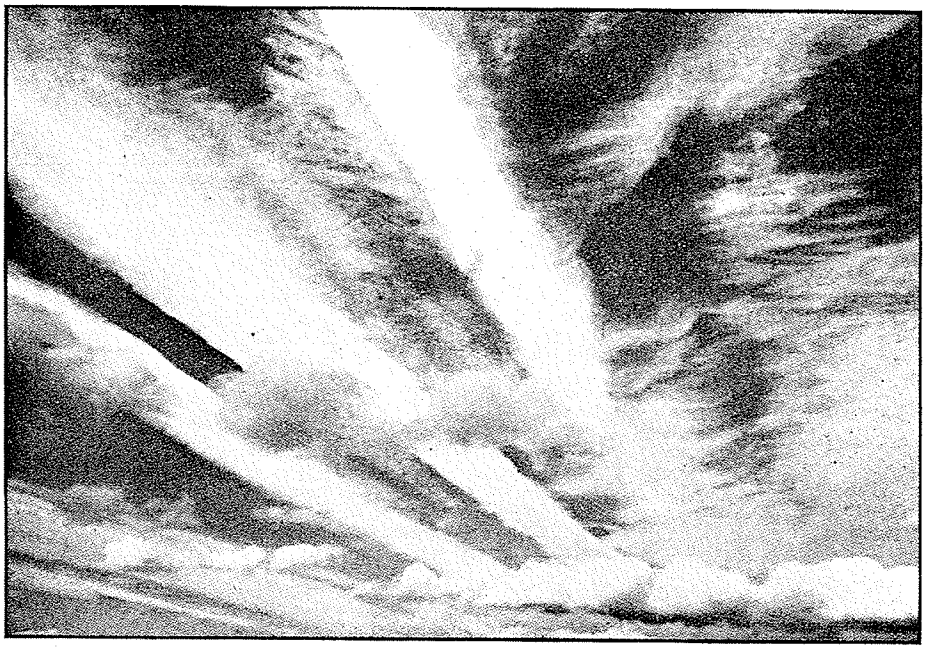

Fig. 164.

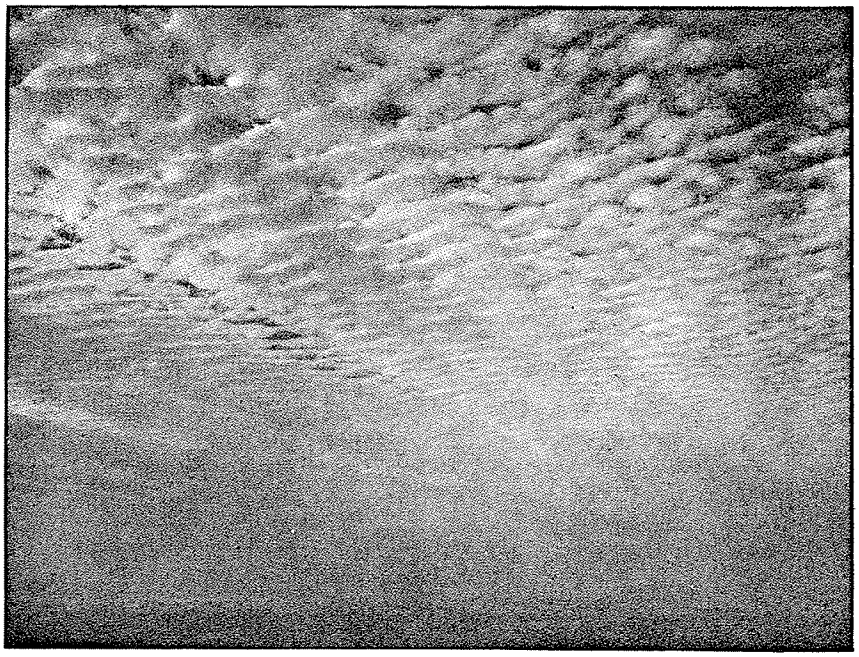

Fig. 165.

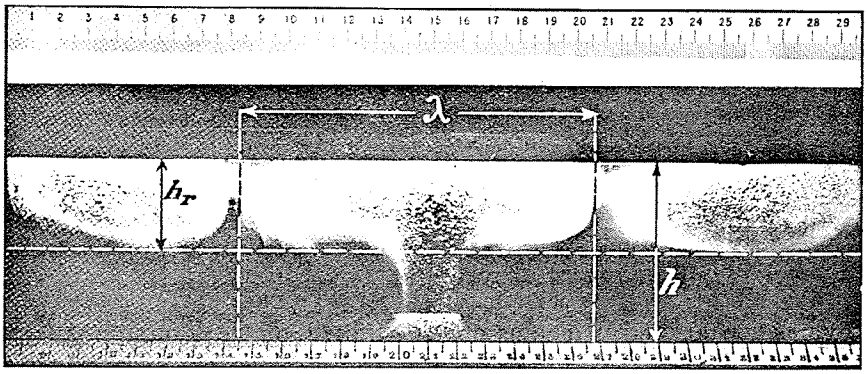

Fig. 168.

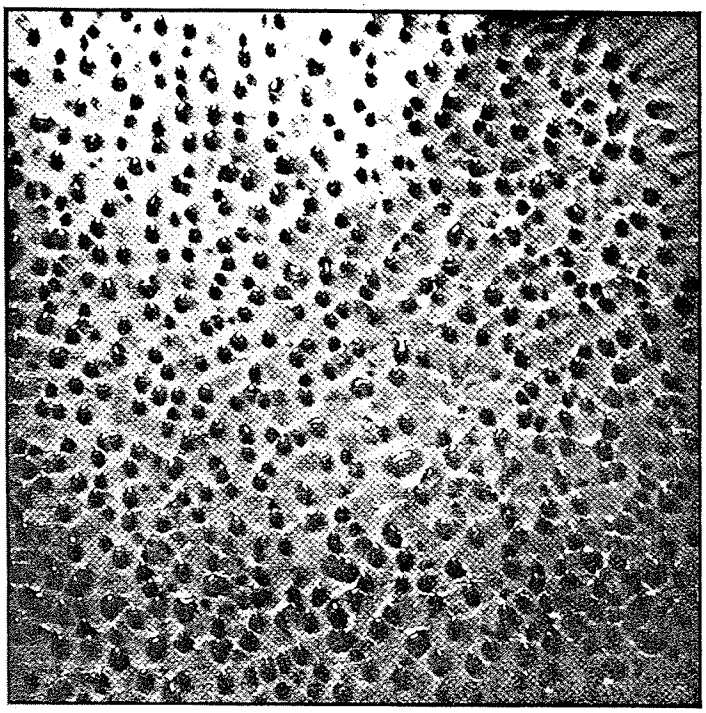

Fig. 169.

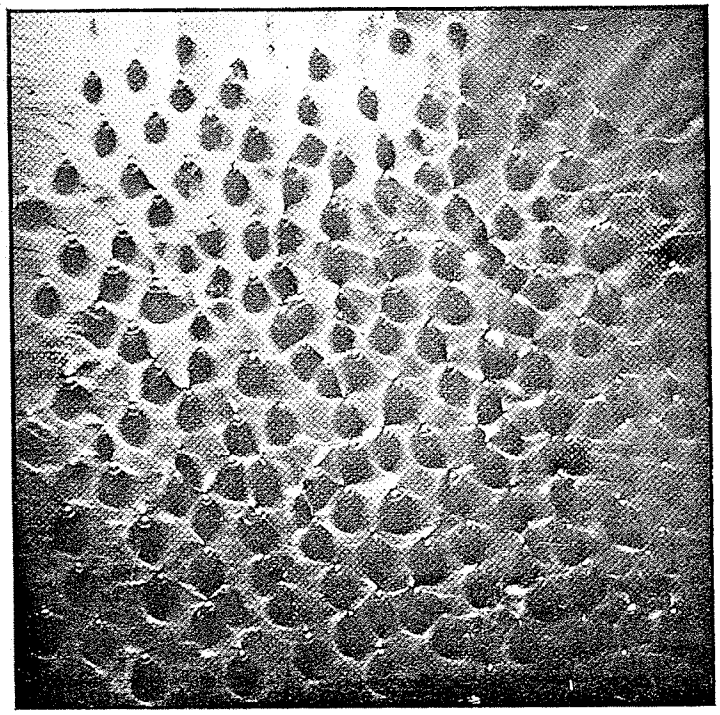

Fig. 170.

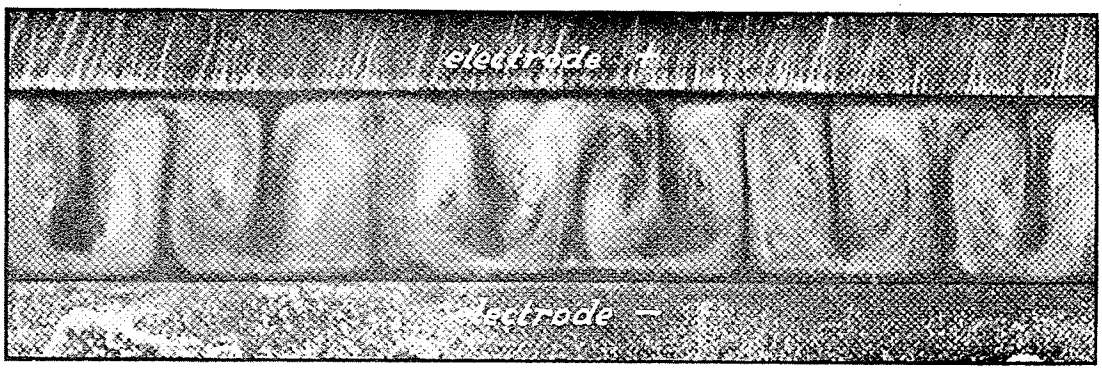

Fig. 171.

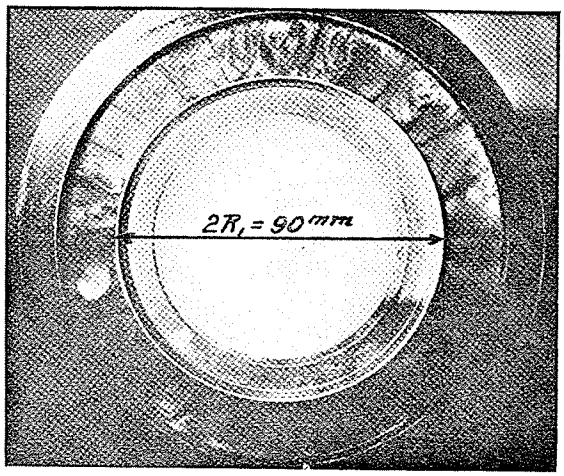

Fig. 172.

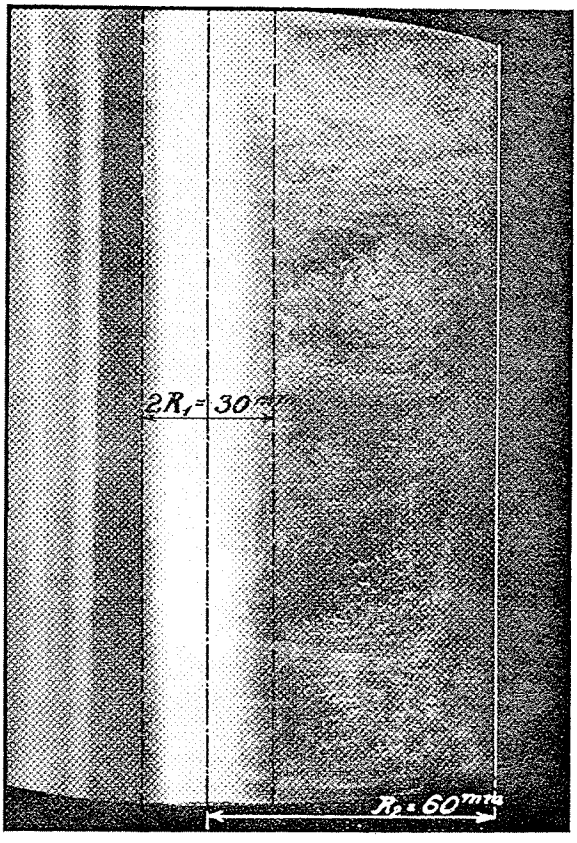

Fig. 173.